Structural Fire Performance of Steel Portal Frame Buildings

by

Ming Wei Bong

Supervised by

Professor Andrew H. Buchanan

Assoc. Professor Peter J. Moss

Dr. Rajesh Dhakal

Fire Engineering Research Report 05/4
August 2005

A thesis submitted in partial fulfilment of the requirements for the degree of Master of Engineering in Fire Engineering

Department of Civil Engineering
University of Canterbury
Private Bag 4800
Christchurch, New Zealand

For a full list of reports please visit http://www.civil.canterbury.ac.nz/fire/fe_resrch_reps.shtml

Abstract

This report investigates the behaviour of steel portal frame buildings at elevated temperatures using the finite element programme SAFIR. The finite element analysis carried out in this report is three dimensional and considers several different locations and severities of fires within the building, different support conditions at the column bases, the presence of axial restraints provided by the end walls, different levels of out-of-plane restraint to the columns and the effect of concrete encasement to the columns. This report also provides recommendations for the design of steel portal frame structures for fire resistance.

Steel portal frame buildings are a very common and popular form of construction used in New Zealand, usually with reinforced concrete precast wall panels attached to the steel frames. In the past, concrete boundary wall panels were required to remain standing after a fire, but it is now considered acceptable for the panels to collapse inwards provided that they remain connected to each other. However there remains concern that under fire conditions, the concrete panels may collapse outwards, creating a danger to fire-fighters and to adjacent property.

The analysis of this report was conducted using SAFIR, a non-linear finite element program developed at the University of Liege, Belgium. The analytical models consisted of a 410UB54 section forming the steel portal frames, with steel purlins and brace channels forming the roof structure and supported on the rafters. The concrete panels themselves were not included in the models, but they were represented by appropriate boundary conditions for the steel members. The ISO 834 Standard Fire and the Eurocode External Fire with and without a decay phase were used in this report.

From a large number of analyses, it has been shown that the bases of the steel portal frames at the foundations must be designed and constructed with some level of base fixity to ensure that the structure will deform in an acceptable way during fire, with no outwards collapse of the walls. The analyses also show that it is not necessary for steel portal frame columns to be fire-protected unless the designer wishes to ensure that the columns and the wall panels remain standing, during and after the fire.

Acknowledgements

I wish to acknowledge my deepest appreciation for the generous help and encouragement given to me by the following people and organisations:

- My supervisors, Professor Andrew Buchanan, Associate Professor Peter Moss and Dr. Rajesh Dhakal for their enthusiasm for the topic, encouragement, ideas and guidance thorough the course of this project.

- Professor Jean-Marc Franssen of the University of Liege in Belgium for his invaluable ideas regarding three dimensional finite element modelling using beam elements and the use of the finite element programme, SAFIR.

- Jerry Chang for his guidance with the SAFIR programme and his overall support.

- Geoffrey Banks of StructeX Limited for his technical advice on the design of steel portal frame buildings.

- Warren Lewis of Lewis & Barrow Ltd and Grant Coombes of Alan Reay Consultants Ltd for their precious information and comments on the fire incidents.

- Dr. Linus Lim for his brilliant research in the fire performance of industrial buildings with concrete cantilever walls and steel roof frames.

- The New Zealand Fire Service and the Todd Foundation for the financial assistance you provided this year.

- Finally, to my family (especially Xie Ying) for their unwavering support and guidance over the years. Without their help this research would not have been possible.

Table of Contents

List of Figures

List of Tables

1 INTRODUCTION

1.1 Steel Portal Frame Buildings in New Zealand

Steel portal frame buildings with concrete tilt panels are a very common form of industrial building in New Zealand. They are formed by a series of parallel steel portal frames as the major framing elements which support the roof structure. Large clear spans of up to approximately 40 metres can be achieved economically using steel Universal Beams (UB). Concrete tilt-up wall panels are commonly used as boundary walls due to their fast erection method and on-site fabrication of the panels.

From a fire resistance perspective, the concrete walls must act as effective compartmentation to prevent fire spread to adjacent property. In addition, they must not collapse outwards which may endanger the lives of the fire-fighters undertaking rescue and fire fighting operations in close vicinity to the building. The concrete panels are commonly pinned at the base and to the steel portal frames. Under fire conditions, the collapse mechanisms of these walls are in turn dependent on the performance of the supporting frames under elevated temperatures, providing the connections between the walls and the frame do not fail.

This project is carried out on the type of portal frame building described above. There is a recent trend to construct industrial buildings in New Zealand utilising tall and slender concrete tilt panels which are cantilevered from the ground and directly support the roof structure. The concrete panels do not have a supporting structure attached to them and is connected to each other with an eaves tie member at the top. This type of building has been previously studied by Lim (2000) and the results are described in Chapter 4.

1.2 Impetus for the research

Steel portal frame industrial buildings with concrete tilt panels are a popular method of construction in New Zealand. It has been observed in many real fire incidents that such buildings collapse or deform excessively when fires occur. The outwards collapse of the concrete walls has also been observed and has raised a serious concern

amongst the owners of adjacent property and fire fighters. The lives of the fire fighters could be endangered if one of these wall panels falls outwards onto them while undertaking fire operations.

This project is initiated to investigate the behaviour of steel portal frame buildings at elevated temperatures and to give design recommendations which will promote the inwards collapse of the structure.

1.3 Objectives of this research

The primary objective of this research is to investigate the structural fire behaviour of steel portal frame buildings using three dimensional structural finite element models.

The secondary objective of this research is to propose design recommendations on the following:

- Support conditions of the steel portal frames
- Passive fire protection to the column legs
- Connections between the side wall panels and the supporting frames

1.4 Scope of this research

A typical steel portal frame building has been designed in accordance with the New Zealand Loading Code NZS 4203:1992 and the New Zealand Steel Structures Standard NZS 3404:1997. Three dimensional finite element models consisting of the steel elements of the building are then constructed and the structural fire behaviour of the structure is investigated under various conditions as summarised below:

1. *Support conditions.* Steel portal frame buildings are usually designed by assuming pinned support conditions at the column bases of the steel portal frames. This represents the lower bound of the performance of the frames. However, there is usually some degree of fixity for the connections used in practice. Fully fixed, partially fixed and fully pinned support conditions are investigated in this project.

2. *Location and severity of the fire.* A fire occurs at a particular location and may grow and spread outwards to other areas of the building over a certain time period. Both localised and fully developed fires are investigated for pinned and fixed support conditions at the column bases. For a localised fire, the fire is assumed to be confined in a small area and occurs either near the centre or near the end of the building; for a fully developed fire, all the steel structural elements are exposed to the fire.

3. *Various boundary conditions or restraints.* The steel components of the building are modelled using beam elements in the finite element models and these models do not include the concrete boundary walls. The side walls are usually attached to the top and mid-height of the steel columns and the end walls are connected to the purlins near the top. The connections between the steel elements and the walls are represented by appropriate boundary conditions or restraints for the steel elements and are used to simulate the presence of the concrete walls on the fire behaviour of the structure. These restraints may not be a real representation of the actual situations and the effects of changing the restraints to the overall fire behaviour are also included.

4. *Passive protection to the column legs.* Passive protection is sometimes applied to two-thirds height of the column legs. This can be economically achieved by encasing the columns in cast *in-situ* concrete. The effect of providing concrete encasement to the column legs are investigated in this project.

5. The ISO 834 standard fire has been used in most of the analyses in this research project. However, an Eurocode External fire with and without a decay phase has also been included in the analysis.

The analysis in this project is conducted with SAFIR, a non-linear finite element programme developed at the University of Liege, Belgium, by Jean-Marc Franssen.

1.5 Organisation of this report

This report consists of nine chapters.

Chapter 2 provides a review of the literature from various design codes and standards. It also summarises the previous research carried out on the performance of steel portal frame buildings, concrete walls and connections between the walls and the supporting structure under elevated temperatures.

Chapter 3 provides a review of the material properties at elevated temperatures.

Chapter 4 provides an overview of the behaviour of industrial building and concrete walls under elevated temperatures. The design of connections between the concrete panels and supporting structure is also included. This chapter also describes the results from the research conducted in this field by previous researchers as well as the observed structural behaviour in real fire incidents.

Chapter 5 describes the finite element programme, SAFIR, used in this research project.

Chapter 6 provides an overview of the design of a typical industrial building according to the New Zealand Loading Code NZS 4203:1992 and the New Zealand Steel Structures Standard NZS 3404:1997. The building is then used for the analyses in this project.

Chapter 7 covers the finite element modelling of parts of the building, and includes the discretisation of the cross-sections of the steel elements and the structure, the fire curves and the applied loading in the finite element models. The discrepancy between static and dynamic algorithms in SAFIR has also been described in this chapter.

Chapter 8 discusses the analytical results of the structural fire behaviour of the whole building under various conditions. This includes different locations and severities of the fires, different support conditions at the column base, the presence of axial restraints in the purlins provided by the surrounding structure, different levels of out-

of-plane restraint to the columns and the effect of concrete encasement to the columns. The results from using an External fire are also included in this chapter.

Chapter 9 describes the conclusions and findings of this report and makes recommendations for design and future research.

2 LITERATURE REVIEW

2.1 Introduction

This chapter gives an overview of the literature relevant to this project and contains extracts from various design codes and standards. This chapter also summarises the previous research carried out on the fire behaviour of industrial buildings, concrete walls and connections between the walls and the supporting structure.

2.2 Design Codes and Standards

2.2.1 New Zealand Building Code

Clauses C1, C2, C3 and C4 in the New Zealand Building Code contain the fire safety requirements in buildings. The primary objectives in fire safety design are to ensure that occupants can evacuate from a burning building safely and that fire-fighters can undertake rescue operations safely. The code also requires that the adjacent units and other property are protected from damage from the spread of fire by thermal radiation or structural collapse and the environment is safeguarded from adverse effects of fire. However, the code does not consider protection for the owner's property.

The possibility of fire spread is highly dependent on the active fire protection systems and fire rated building systems. For limiting fire spread to adjacent properties, boundary walls become the most important structural elements, where these in turn are dependent on the primary supporting structures. These walls must not collapse outwards given the fire load within the building, which will endanger the lives of fire-fighters undertaking rescue and fire fighting operations or occupants escaping from the building, and damage the adjacent property by the means of fire spread.

2.2.2 Approved Document for New Zealand Building Code

The Approved Document for New Zealand Building Code (Building Industry Authority, 2000) has clear performance requirements for maintaining fire safety depending on the building use and fire hazard category. This section reviews the

design of external boundary walls, with due regard to the S rating system as outlined in Part 5 of the Approved Document. The benefits of providing sprinklers in industrial buildings are also described. Part 7 of the Approved Document requires buildings located closer than a given limiting distance to the relevant boundary to have a fire resistance rating (FRR) for the external walls to prevent fire spread. The area of openings should also be checked to make sure fire spread by radiation is not possible.

The Approved Document requires structural members to achieve various levels of fire resistance depending on the function of the member. The fire resistance of each member is dependent on purpose group, occupant level, height and other fire safety precautions taken. Fire resistance is determined by subjecting the member to standard fire test conditions (International Organisation for Standardisation 834, 1985) and measuring the time to failure. The Approved Document specifies the fire resistance ratings of any member by three criteria: stability, integrity and insulation. Each criterion is described in more detail below:

- The stability criterion applies to primary members and is concerned with the ability of the member to support applied loads without collapsing during a fire.
- The integrity criterion applies to secondary members. These members are required to prevent hot gases and flames from transmitting through the member by means of cracks, fissures and the like.
- The insulation criterion applies to both primary and secondary members. This criterion is concerned with the ability of a building member to provide an adequate barrier between a fire compartment and an adjacent compartment to ensure that the average temperature rise does not exceed 140^{o}C or a local maximum of 180^{o}C is not reached on the unexposed face.

Note: Primary member is defined as a building element providing the basic loadbearing capacity to the structure (i.e. columns, beams). Secondary member is defined as a building element not providing load bearing capcity to the structure (i.e. non load-bearing fire separation walls).

Two fire ratings are used to classify the fire resistance rating of a primary or secondary element as stated in Part 5 of the Approved Document, which depends on the function of the building element (refer to Table 2-1).

Table 2-1 Classification of F and S ratings (Building Industry Authority, 2000)

Function	Term used	Symbol
Prevent internal spread of fire	Firecell rating	F
Prevent structural collapse close to a relevant boundary and fire spread through external walls	Structural fire endurance rating	S

In the case of boundary walls, the S ratings must be determined from equation (2-1) as they pose a threat of fire spread to the adjacent properties.

$$S = k\, t_e \qquad \textbf{(2-1)}$$

where,

k = 0.5 for sprinklered firecells (i.e. benefits of providing sprinklers)
= 1.0 for unsprinklered firecells

t_e = Equivalent time of fire exposure in minutes

The Approved Document includes a table for determining the S ratings for external walls based on fire hazard category and ventilation characteristics (see Table 2-2). The Approved Document specifies different fire hazard categories to buildings with different fuel loads. Fire hazard categories 1, 2 and 3 represent fuel load energy densities (FLED) of a building with 400, 800 and 1200 MJ/m^2 floor area, respectively.

For industrial buildings, the minimum acceptable design solution outlined in the Approved Documents is usually restrictive due to the high combustible loading. Design for boundary walls requires specific fire engineering design if the fire hazard category is '4' (i.e. the fuel load energy density, FLED, is greater than 1500MJ/m^2). Cosgrove (1996) has suggested a 4 hour fire rating which is considered a suitable value based on buildings containing goods exceeding a fire load energy density of 1500 MJ/m^2 and not containing active fire protection. Clifton and Forest (1996) have suggested methods for estimating the required fire resistance rating for each of the fire hazard categories based on the approved document and the fire engineering design guide (Buchanan, 1994).

Table 2-2 Equivalent fire severity, t_e, for calculating the S ratings (Building Industry Authority, 2000)

	Fire Hazard Category 1 (FLED = 400 MJ/m²)					Fire Hazard Category 2 (FLED = 800 MJ/m²)					Fire Hazard Category 3 (FLED = 1200 MJ/m²)				
	A_h/A_f					A_h/A_f					A_h/A_f				
A_v/A_f	0.00	0.05	0.10	0.15	0.20	0.00	0.05	0.10	0.15	0.20	0.00	0.05	0.10	0.15	0.20
0.05 or less	90	60	50	40	40	180	120	100	80	80	240	180	140	140	120
0.06	80	50	50	40	40	160	110	90	80	80	240	160	140	120	110
0.07	70	50	40	40	40	150	100	80	80	70	220	160	140	120	110
0.08	70	50	40	40	30	140	90	80	70	70	220	140	120	110	100
0.09	60	40	40	30	30	140	90	80	70	70	200	140	110	110	100
0.10	60	40	40	30	30	120	80	70	70	70	180	140	110	100	100
0.11	50	40	30	30	30	110	80	70	70	60	160	120	110	100	100
0.12	50	40	30	30	30	100	70	70	60	60	160	110	100	100	90
0.13	50	40	30	30	30	100	70	70	60	60	160	110	100	90	90
0.14	50	30	30	30	30	90	70	60	60	60	140	100	100	90	90
0.15	40	30	30	30	30	80	70	60	60	60	120	100	90	90	90
0.16	40	30	30	30	30	80	60	60	60	60	110	100	90	90	90
0.17	40	30	30	30	30	80	60	60	60	60	110	90	90	90	90
0.18	40	30	30	30	30	70	60	60	60	60	110	90	90	90	80
0.19	30	30	30	30	30	70	60	60	60	60	110	90	90	80	80
0.20	30	30	30	30	30	70	60	60	60	60	100	90	80	80	80
0.25 or greater	30	30	30	30	30	60	60	50	50	50	90	80	80	80	80

where,

A_v = Area of vertical openings in boundary walls (m^2)

A_f = Floor area (m^2)

A_h = Area of horizontal openings (m^2)

Alternatively, the equivalent time of fire exposure, t_e, can be obtained from the Eurocode time equivalent formula (EC1, 1994). It should be noted that Table 2-2 is derived from the Eurocode time equivalent formula. A firecell height of 3.0 m has been assumed and a thermal inertia factor corresponding to the most severe conditions for typical construction materials (i.e. k_b = 0.09). Therefore, S ratings can also be obtained from the Eurocode time equivalent formula shown below, which is mandatory for fire hazard category '4'.

$$t_e = e_f \, k_b \, w \qquad \textbf{(2-2)}$$

where,

e_f = Fuel load (MJ/m^2 of floor area)

k_b = Parameter to account for different compartment linings (Table 2-3)

w = Ventilation factor

Table 2-3 Values of k_b in the Eurocode time equivalent formula

Typical construction	$\sqrt{k\rho c}$ **(Ws$^{0.5}$/m^{2}K)**	**k_b (min m^2/MJ)**
Insulating material	<720	0.090
Normal and lightweight concrete	720-2500	0.055
Steel	>2500	0.045

where,

k = Thermal conductivity (W/mK)

ρ = Density (kg/m^3)

c = Specific Heat (J/kgK)

The ventilation factor (w) is given by:

$$w = \left(\frac{6.0}{H_r}\right)^{0.3} \left\| 0.62 + \frac{90(0.4-\alpha_v)^4}{1+b_v a_h} \right\| > 0.5 \qquad \textbf{(2-3)}$$

where,

α_v = A_v/A_f $\quad 0.025 \leq \alpha_v \leq 0.25$

α_h = A_h/A_f $\quad \alpha_h \leq 0.20$

b_v = $12.5(1 + 10\alpha_v - \alpha_v^2)$

A_f = Floor area of firecell (m^2)

A_v = Area of horizontal openings in the walls (m^2)

H_r = Height of the firecell (m)

Limitations

As mentioned above, Table 2-2 extracted from the Approved Document has been produced using the Eurocode formula. Therefore, it is important that users of Table 2-2 or Eurocode time equivalent formula should be aware of the derivation, significance and limitations as outlined below:

- The equivalent time of fire exposure, t_e, is the equivalent time of exposure to the ISO 834 standard fire that would produce the same maximum temperature in a protected structural steel member given a complete burnout of the firecell.

However, it is also considered reasonable for materials other than steel (Buchanan, 2001). Therefore, the value of t_e is an equivalent time for comparing real fires with the ISO 834 standard fire, and it is not an estimate of the duration of the time.

- The Eurocode time equivalent formula was developed from small room tests. There is no validation in large compartment with a ceiling height greater than 3 m.
- The Eurocode time equivalent formula applies to compartments where the roof and walls remain intact for a complete burnout. The formula may not be appropriate for buildings where roof and walls may collapse during the fire.

Therefore, it can be seen that the time equivalent formula is totally inappropriate for single storey industrial buildings. However, due to the lack of better design tools, Cosgrove (1996) suggests that the Eurocode equivalent time formula is probably a conservative estimate of the required fire resistance.

Benefits of Sprinklers

Sprinklers are expected to extinguish or to at least control the fire to the growth area at the time of activation. In a sprinkler controlled fire the compartment temperature is not expected to exceed 300^oC. Cosgrove (1996) suggests that if sprinklers are present in an industrial building, a fire resistance rating of 60 minutes for boundary walls would be sufficient. However, sprinkler systems have been overcome by some manufacturing and warehouse fires due to the following reasons:

a) Incorrect sprinkler installation resulting in inadequate protection
b) Incorrect storage for the sprinkler hazard classification
c) Failure of sprinkler system such as blockage in pipelines
d) Explosion being the cause of fire, either resulting in an excessive number of heads to operate or causing critical damage to the sprinkler system.

It is beyond the scope of this study to investigate the issues of whether sprinklers should be provided in industrial buildings.

2.2.3 Building Code of Australia

The Building Code of Australia (Australian Building Codes Board, 2004) specifies the requirements for the performance of concrete external walls that could collapse as complete panels, in a building of not more than 2 storeys high. This clause was added to the code because fires have occurred in single storey warehouse buildings and external walls panels have been observed to fall outwards. The panels become detached due to poor design and detailing of the connections between the supporting structure and the panels (Bennetts and O'Meagher, 1995). Specification C1.11 of the Building Code of Australia states the following:

"SPECIFICATION C1.11 PERFORMANCE OF EXTERNAL WALLS IN FIRE

1. Scope

This Specification contains measures to minimise, in the event of fire, the likelihood of external walls covered by Clause 2 collapsing outwards as complete panels and the likelihood of panels separating from supporting members.

2. Application

This Specification applies to buildings having a rise in storeys of not more than 2 with concrete external walls that could collapse as complete panels (eg. tilt-up and precast concrete) which -

(a) consists of either single or multiple panels attached by steel connections to lateral supporting members; and

(b) depend on those connections to resist outward movement of the panels relative to the supporting members and

(c) have height to thickness ratio not greater than 50.

3. General requirements for external wall panels

(a) Cast-in inserts and fixings must be anchored into the panel with welded bars or be fixed to the panel reinforcement.

(b) Cast-in inserts for top connections and fixings acting together must be able to resist an ultimate load of two times the larger of the forces required to develop:

(i) the ultimate bending moment capacity of the panels at its base; or

(ii) the overturning moment at the base of the panel arising from an outwards lateral displacement at the top of the panel equal to one tenth of the panel height.

(c) Top connections of the panel exposed to fire, such as clips and drilled-in insets, acting together must be able to resist an ultimate load of six times the larger of the forces required to develop the moment specified in (b)(i) or (ii).

(d) Lateral supporting members and their connections must be designed to resist the connection forces specified in (b) and (c) and in the case of an eaves tie member the force in the member must be determined assuming that it deforms in a manner compatible with the lateral displacement of the wall panels, and that it acts in tension only.

(e) External wall panels that span vertically must have at least two upper connections per panel to the supporting member, except that where a number of panels are designed to act as one unit, (eg. tongue and groove hollow-core panels), only two upper connections are required for each unit.

(f) External wall panels that span horizontally between columns must have at least two connections at each column."

Note.

The increased forces specified by the use of the multiplier of two or six in (b) and (c) above are to take account of the lower strength of the connections and members at the higher than ambient temperatures expected in a fire.

4. Additional requirements for vertically spanning external panels adjacent to columns

(a) Where vertically spanning external wall panels are located adjacent to columns, connections to the panels must be located and/or detailed to minimise forces that may develop between the panels and columns arising from the restraint of differential displacements.

(b) The requirements of (a) are satisfied by –

(i) detailing the connections and/or the supporting member to sustain a relative outward displacement of d(m) between the panels and columns at the connection height where d(m) is calculated as –

(A) the square of the connection height (m) divided by one hundred and twenty-five, when the connection height is less than 5 m; or

(B) the connection height (m) divided by twenty-five, when the connection height (m) is greater than or equal to 5 m; or

(ii) in situation where an eaves tie member is used to provide lateral support to external wall panels, the tie member is connected to the panels no closer than a distance s(m) from the column where s(m) is taken as one quarter of the panel height (m).”

2.2.4 Steel Structures Standard NZS 3404

Fire resistance ratings for steel portal frame

The steel portal frames in industrial buildings are only required to fulfil the stability criterion in the Approved Document to satisfy the fire resistance requirements of the New Zealand Building Code. The behaviour of steel structures exposed to a fire depends on the steel temperatures increase, strength and stiffness of the steel, the applied loads and the support conditions (Buchanan, 2001). The increase in steel temperatures depends on the severity of the fire, the area of steel exposed to the fire and the amount of applied fire protection. The New Zealand Steel Structures Standard NZS 3404:1997 sets out the design requirements for steel structures but with no special requirement for portal frame buildings. Section 11 of NZS 3404:1997 contains the fire design requirements for steel building elements required to have a fire resistance rating (FRR), and requires the calculation of the period of structural adequacy (PSA) for steel members and connections and must equal to the required FRR. The period of structural adequacy (PSA) can be determined using one of the methods outlined below:

a) By calculation:

i) By determining the limiting temperature of the steel (T_1) using the equation shown below, and then

$T_1 = 905 – 690r_f$

where r_f is the load ratio and is the ratio of the expected loads on the structure during a fire to the loads that would cause collapse at normal temperatures.

ii) By determining the PSA at which the limiting steel temperature is attained. The PSA at which the limiting temperature is attained for unprotected

members can be found using relatively simple formulae. However, the PSA at which the limiting temperature is attained for protected members is calculated based on regression analysis with certain limitations and conditions; or

b) By direct application of a single standard fire test; or

c) By structural analysis using the variations of the mechanical properties of steel with temperature as shown in Section 3.5. Calculation of the steel temperature should be done by using a rational method of analysis which has been confirmed by test data.

2.2.5 Concrete Structures Standard NZS 3101

Fire resistance ratings for walls

The tilt-up precast walls in industrial buildings are required to fulfil the integrity and insulation criteria to satisfy the fire resistance requirements in the Approved Document. The stability criterion is required in the case where the wall perform as a load-bearing structural member. The New Zealand Concrete Structures Standard NZS 3101:1995 sets out the design and detailing requirements for reinforced concrete structures and their elements. Section 6.7 of NZS 3101:1995 contains requirements for fire resistance ratings of walls.

Insulation

The average temperature rise must not exceed 140^{o}C and must not have a local maximum temperature of 180^{o}C on the unexposed surface of the wall. The insulation rating is satisfied by providing a sufficient effective thickness, which is the actual minimum thickness of the wall. Any joint sealants used must have at least the same insulation performance as the wall itself. The minimum effective wall thicknesses for fire resistance ratings for insulation according to NZS 3101:1995 are shown in Table 2-4.

Integrity

The standard states that the wall will have the stated fire resistance rating for integrity if it meets the requirements for both insulation and stability for that rating.

Stability

The standard specifies the following requirements in order to satisfy the stability criterion for the required fire resistance rating:

a) The thickness of wall panels should follow the dimensional limitations given in Clause 12.3.2 of NZS 3101:1995, which contains the following minimum thickness limits:
   - 1/25 of the unsupported height when the ultimate limit state axial load ratio N*/ $f_c^{'}A_g$ is greater than 0.2.
   - 100 mm for the top 4 m of height, increasing by 25 mm for each 7.5 m of height.
   - The lesser of 100 mm and 1/30 of the distance between supporting or enclosing member for non-loadbearing walls.

b) The effective thickness of the wall should not be less than the thickness required by the insulation criterion;

c) If $N^* \leq 0.03f'_cA_g$, h_{we}/t_w should not be greater than 50;
   Note: h_{we}/t_w is the effective height/wall thickness ratio (the effective wall slenderness ratio)

d) If $N^* \geq 0.03f'_cA_g$,
   i) h_{we}/t_w should not be greater than 20; and
   ii) The cover fro the fire-exposed face to the vertical reinforcement or tendons is not less than the corresponding cover given in Table 2-5.

Clause 6.7.4 of NZS 3101:1995 states that N* is the design axial load for the ultimate limit state (exclusive of self weight) at the mid-height of the wall. Clause 6.7.4 also gives the following effective height (h_{we}) in relation to the unsupported height (h_{wu}) for walls which are laterally supported at top and bottom only:

i) 1.0 h_{wu} if neither support is rotationally restrained;
ii) 0.85 h_{wu} if one support is rotationally restrained; or
iii) 0.70 h_{wu} if both supports are rotationally restrained,

where if any rotational restraint at the support is provided, it should be provided by a member outside the fire compartment (including a continuation of the wall itself). The effective height for rotationally restrained walls is treated as a column and Euler buckling theory is applied.

Table 2-4 Minimum effective wall thickness for fire resistance ratings for insulation (Table 6.1 of NZS 3101:1995)

Fire resistance rating (minutes)	Effective thickness (mm) for different aggregate type		
	Type A aggregate	Type B aggregate	Type C aggregate
30	50	45	40
60	75	70	55
90	95	90	70
120	110	105	80
180	140	135	105
240	165	160	120

Aggregate types:

A - quartz, greywacke, basalt and all others not listed

B - dacite, phonolite, andesite, rhyolite, limestone

C - pumice and selected lightweight aggregates

Table 2-5 Minimum cover to vertical reinforcement and tendons for stability of walls (Table 6.4 of NZS 3101:1995)

Fire resistance rating (minutes)	Cover, c (mm)	
	To reinforcement	To tendons
30	20	30
60	20	30
90	35	30
120	40	30
180	45	35
240	50	50

Steel Reinforcement and Spacing

Restrepo *et al.* (1996) and McMenamin (1999) state that it is commonly observed in the design of tilt-up buildings that stresses induced by the seismic forces are usually low and the walls only require minimum reinforcement according to NZS 3101:1995. Similarly, in terms of preventing fire spread to adjacent property, the wall panels in the industrial buildings must act as fire separation functions and the amount of reinforcement can also be based on the minimum amount of reinforcement allowable in Section 7 of NZS 3101:1995. Clause 7.3.31.2 gives the minimum ratios of horizontal and vertical reinforcement to the gross cross-sectional area as 0.0025 and 0.0015, respectively; these values may be reduced to 0.0020 and 0.0012 respectively if 16 mm or smaller bars with characteristic yield strength of at least 430 MPa are used.

Similarly, the spacing of the reinforcing bars is based on the minimum and maximum allowable spacing in Section 7 of NZS 3101:1995. Clause 7.3.5.1 requires the clear distance between reinforcing bars to be at least the larger of the diameter of the bar and 25mm. This clause is always satisfied and the reinforcement in tilt-up walls is usually more concerned with the maximum allowable spacing of the bars. Clause 7.3.5.5 sets the maximum spacing in walls as the lesser of twice the wall thickness and 450 mm. Clause 7.3.31.3 requires two layers of reinforcement to be used when the thickness of the wall is greater than 200 mm. The reinforcing bars must be at least 10 mm in diameter, and the maximum spacing is the lesser of 2.5 times the wall thickness and 250 mm.

2.2.6 New Zealand Loading Code NZS 4203

The New Zealand Loading Code NZS 4203:1992 gives the loading requirements on structures which are subjected to elevated temperatures. Clause 2.4.3.4 of the standard states the following:

"*2.4.3.4.*
Strength and stability in fire emergency conditions and afterwards shall comply with (a) and (b) following:

(a) For that period of time during fire emergency conditions when the structure is subject to elevated temperatures and designated members are required to remain stable, the affected members shall be designed for the following combination of factored load:

$$(7)\ G\ \&\ Q_u$$

(b) The stability of elements which could collapse onto adjacent household units or other properties shall be ensured:

Either by designing the element and supporting structure to resist the loads in combination (7) above, using a detailed stress analysis which considers elevated temperatures and appropriate structural deformations throughout the fire.

Or, as an approximation, by designing the element and an appropriately fire rated supporting structure so that after a fire the residual structure at ambient temperatures is able to resist the loads in combination (7) above, plus a uniformly distributed face load on the residual structure of 0.5 kPa."

2.2.7 Australian/New Zealand Loading Standard AS/NZS 1170.0

The new joint Australian/New Zealand loading standard AS/NZS 1170.0:2002 states the loading requirements on structures during fire in part 0 of the standard (i.e. Part 0: General Principles). Clause 4.2.4 of the standard states the following:

"*4.2.4 Combinations of actions for fire*

The combination of factored actions used when confirming the ultimate limit state for fire shall be as follows:

[G, thermal actions arising from the fire, $\psi_l Q$]

NOTE: Where it is appropriate to consider the stability of remaining walls that may collapse outwards after a fire event, other ultimate limit states criteria are given in Section 6."

Note: ψ_l is defined as the factor for determining quasi-permanent values (long-term) of actions.

2.2.8 Revision of the Concrete Structures Standard NZS 3101

The current New Zealand Steel Structures Standard NZS 3404:1997 and Concrete Structures Standard NZS 3101:1995 do not contain any design requirements with regard to external wall panels which could collapse outwards in fire. The Concrete Structures Standard NZS 3101:1995 is currently being revised and will contain specific design requirements for external wall panels which are commonly found in industrial buildings. Unlike the Building Code of Australia, the design requirements are not restricted to external wall panels with a slenderness ratio (i.e. height to thickness ratio) of less than 50.

The traditional approach to external walls in industrial buildings with an unprotected steel roof structure has been to ensure that the walls remain standing in place and attached to the supporting structures (i.e. columns) after a fire even if the roof structure collapses. According to the Loading Code NZS 4203:1992, this can be met by ensuring the free-standing external walls are designed to resist a face load of 0.5 kPa after the fire. However, the joint Australian/New Zealand loading standard AS/NZS 1170:2002 does not include this face load. The new Concrete Structures Standard NZS 3101 has included this face load for the design of walls and connections and to ensure some degree of stability for this type of building. The new standard also requires the face load to be applied during the fire and not just after the fire as stated in the Loading Code NZS 4203:1992. This face load is intended to give the external walls some resistance to wind or earthquake load after the fire.

The new standard is based on a more recent approach which allows external walls to be pulled inwards by the collapsing steel frame and collapse into the building. In this case, the walls must remain connected to each other so that they remain acting as compartmentation to the fire and prevent fire spread to adjacent property. The inwards collapse of the walls can increase the fire separation distance to the relevant boundary and reduce the likelihood of horizontal fire spread by radiation. This approach is described in more detail in Chapter 4.

The following are extracts from the draft New Zealand Concrete Structures Standard DZ 3101.1 (SNZ, 2005a).

"4.8 External walls that could collapse outwards in fire.

4.8.1 Application

This Section applies to external walls which could collapse outwards from a building as a result of internal fire exposure. All such walls shall:

a. *be attached to the building structure and to adjacent wall panels by steel connections;*
b. *be restrained by these connections, when subject to fire, from outward movement of the wall relative to the building structure; and*
c. *comply with the appropriate provisions of this Standard for walls.*

4.8.2 Forces on connections

During fire exposure, the connections between each wall and the supporting structure shall be designed to resist all anticipated forces. In the absence of a detailed analysis, the connections shall be designed to resist the largest of:

a. *For all walls, the force resulting from a face load of 0.5 kPa,*
b. *For walls fixed to a flexible structure of unprotected steel, the force required to develop the ultimate bending moment of the wall at its base,*
c. *For walls fixed to a rigid structure such as reinforced concrete columns or protected steel columns or another wall at right angles, the force required to develop the ultimate bending moment of the wall at mid-height.*

4.8.3 Design of connections

To allow for reduced capacity in fire conditions, the fixings in the wall shall be designed as follows:

a. *Components made from unprotected mild steel shall be designed using 30% of the yield strength of the steel in ambient conditions.*
b. *Components made from other types of steel shall be designed using the mechanical properties of the steel at 680℃.*

c. *Proprietary inserts shall be designed for a fire resistance rating of at least 60 minutes for unsprinklered buildings and 30 minutes for sprinklered buildings.*

4.8.4 Fixing inserts

a. *Proprietary cast-in or drilled-in inserts with an approved fire resistance rating shall be installed in accordance with the manufacturers specifications.*
b. *Cast-in inserts without an approved fire resistance rating shall be anchored into the wall by steel reinforcement or fixed to the wall reinforcement.*
c. *Adhesive anchors shall only be used if they have an approved fire resistance rating and are used in accordance with the manufacturers specifications.*

4.8.5 Walls spanning vertically

Walls that span vertically shall have at least two upper connections per wall panel except where several narrow panels are connected to each other to act as a single unit in which case there shall be two upper connections per unit.

4.8.6 Walls spanning horizontally

Walls that span horizontally between columns shall have at least two connections per column."

The commentary clauses (SNZ, 2005b) are also extracted for completeness:

*"**C4.8 EXTERNAL WALL PANELS THAT COULD COLLAPSE OUTWARDS IN FIRE***

C4.8.1 Application

Section 4.8 applies to external walls which could collapse outwards from a building as a result of a fire inside the building. This section is not restricted to those buildings close to a property boundary where it is necessary to prevent spread of fire to adjacent property,

because it is also necessary to provide protection to fire fighters who could be killed or injured if walls fall outwards, in accordance with the New Zealand Building Code.

The traditional approach to external walls in buildings with non-fire-rated roofs has been to ensure that the walls remain standing in place after a fire, even if the roof collapses. This Standard is based on a more recent approach which allows walls to be pulled inwards by the collapsing steel frame, ensuring that the walls remain attached to the steel frame and to each other, to avoid large gaps between the walls which would allow spread of fire to adjacent property. This approach is summarised in reference [3].

C4.8.2 Forces on connections

The process of design for fire conditions will depend on the design philosophy used for ambient conditions. It is impossible to predict the behaviour accurately, so the forces given in this section are rough estimates of the possible forces which could develop under various scenarios.

A detailed analysis must consider all likely forces, including the face load on the wall, the forces resulting from thermal bowing of the concrete panels, the forces resulting from deformation or collapse of a steel roof structure, and the self weight of the walls due to deformations away from the vertical position.

C4.8.2 a. *The loadings standard (NZS 4203:1993) requires free-standing external walls to be designed to resist a face load of 0.5kPa in the "after fire" condition. The value of 0.5kPa was derived from previous code requirements for a nominal level of wind or earthquake load in the after-fire condition. This requirement is not included in the joint New Zealand/Australian standard NZS 1170, but is retained in this document in order to provide a nominal level of force for design of walls and connections, and to ensure some degree of robustness for this type of building. A significant change from NZS 4203:1993 is that the face load is now required to be applied during the fire, not just after the fire. This is because:*

- *The primary concern of the New Zealand Building Code is with collapse of walls and possible fire spread <u>during</u> a fire.*
- *Walls able to resist this load during a fire will, in most cases, be able to resist a similar load if they are still standing after the fire.*
- *It is considered acceptable for walls to be pulled inwards during the fire, hence not remain standing after the fire.*

A wall connected to a very weak or flexible roof structure will need to be designed to cantilever from its base, resisting a face load of 0.5 kPa during fire exposure. Flexural design at the base of the wall should include the effects of thermal bowing and the resulting P-Δ forces which will cause much larger base moments than assumed in the cold design. Note that the relevant reinforcing will either be central in the wall where it will remain relatively cool, or near the fire exposed face in which case the properties at elevated temperatures should be considered. Guidance on thermal bowing of cantilever walls is given in [4] and [5].

C4.8.2 b. *For a wall with a cantilever base, which also relies on the roof structure to prevent outwards collapse of the wall, it is necessary to check the forces required at the top of the wall to develop a plastic hinge at the base of the wall. This bending moment will develop as the roof structure prevents thermal bowing in the outwards direction, or as the wall is pulled inwards by the unprotected steel roof structure as it collapses. Note that the relevant reinforcing will usually be central in the wall or near the outer face, so it is unlikely to have reduced mechanical properties due to elevated temperatures.*

C4.8.2 c. *Additional requirements are necessary for walls which are not free to deform as thermal bowing occurs. This applies to a wall connected to reinforced concrete columns or protected steel columns, or connected to another wall at right angles. This section also applies to walls connected to half height concrete columns or half height protected steel columns which will restrict thermal bowing. Large forces will develop at the connections when such walls attempt to deform due to thermal bowing, which may be in two directions (horizontal and vertical).*

Clause 4.8.2 c provides a rough approximation of the connection forces which could develop in walls which are restrained against thermal bowing deformations. The relevant reinforcing will usually be central in the wall or at the outer face, so it is unlikely to have reduced mechanical properties.

For highly restrained walls bowing in double curvature, the connections should also be able to resist the forces associated with flexural yielding in the wall at 45° across the corners of the walls. It is not easy to predict the precise location of the yield-line across the corner of a wall. If a nominal distance of, say, 1 metre is assumed, the force required to develop a 45° yield line is largely independent of its location because the lever arm increases in direct proportion to the length of the line (the width of the cracked cross section).

Some Australian documents allow for connections to be designed specifically for large relative displacements between the walls and the supporting columns or adjacent corner walls. To satisfy this condition, the connections should be detailed to allow a relative outward displacement of $H_c/25$ between the wall and the supporting structure, where H_c is the height of the connection above the foundations. A problem with this approach is that the reduction in the connection force due to the lack of restraint may be offset by large P-Δ forces. Some details for connections allowing large relative displacements are provided in reference [3].

C4.8.3 Design of connections

***C4.8.3 a**. The reduction to 30% of the yield strength in ambient conditions is based on an expected temperature of unprotected steel of approximately 680°C, which is the maximum temperature reached in the Eurocode "external" fire [6]. In a real fire in a typical industrial building, it is likely that higher temperatures will be reached in the early stages of the fire before the roof burns through, but 680°C is an estimate of the likely temperature if the fire continues to burn for some time after the roof has collapsed.*

***C4.8.3 b**. For steel other than normal mild steel, the connections can be designed using the mechanical properties of the steel at 680°C.*

A higher level of design stress can be used if the steel in the connection is protected using approved fire protection materials, in which case specific calculations of steel temperatures will be necessary.

***C4.8.3 c**. Proprietary anchors will have fire resistance ratings based on standard fire resistance tests in accordance with AS 1530 Part 4 or a similar national or international standard. The required rating of 60 minutes for unsprinklered buildings is an estimate of the worst likely fire severity in a typical industrial building with a non fire-rated roof structure. The reduction to 30 minutes for sprinklered buildings reflects the much lower probability of a severe fire in such buildings. These values have been prescribed because it is impossible to accurately predict the severity of a fire in a single storey building with non-fire-rated roof construction.*

C4.8.4 Fixing inserts

There are a number of proprietary adhesive anchors which have been tested under fire conditions. Manufacturers of such systems specify design loads depending on the required fire resistance rating (ref 7). Fire-rated adhesive connections rely on synthetic organic resins with or without inorganic fillers or active ingredients such as cement. Epoxy grouted inserts without an approved fire resistance rating must not be used for connections which are required to carry loads during a fire, because most epoxy resins lose strength at temperatures over about 60℃."

2.2.9 Eurocode

Eurocode 2 (EC2, 2002) and Eurocode 3 (EC3, 2002) provide relationships on the thermal and mechanical properties of concrete, reinforcing steel and structural steel when they are subjected to elevated temperatures. The relationships given in the Eurocode are recommended to be used for analysis with structures submitted to fire in Europe. The properties of structural steel given in Eurocode 3 (EC3, 2002) have not been changed from the previous version of Eurocode 3 (EC3, 1995). The details of the properties of structural steel from the Eurocode 3 (EC3, 1995) are described in detail in Chapter 3 and will be used in the analyses of this project.

It should be noted that the concrete properties defined in Eurocode 2 (EC2, 1995) are not entirely consistent to the properties defined according to the new version of Eurocode 2 (EC2, 2002). Bernhart (2004) has compared the relationships given in both versions of the Eurocode 2.

2.3 Behaviour of Steel Portal Frames and Concrete Walls subjected to elevated temperatures

This section summarises the research carried out by previous researchers to investigate the behaviour of steel portal frames, concrete walls and connections between the walls and the supporting structures when exposed to elevated temperatures. The details of their analyses are described in more detail in Chapter 4.

2.3.1 Steel Portal Frames

Newman (1990), O'Meagher *et al.* (1992) and Wong (2001) have investigated the behaviour of industrial buildings incorporating steel portal frames subjected to fires and provided design recommendations for such buildings. The details of their analyses are described in Section 4.4. Wong *et al*. (2000) derive simple formula for estimating the failure temperature of a steel portal frame with pinned supports using plastic theory and is described further in Section 4.4.4.

2.3.2 Concrete Walls

Cooke (1987), Cooke and Morgan (1988), O'Meagher (1994) and Lim (2000) have investigated the behaviour of concrete walls subjected to elevated temperatures on one side. Lim (2000) has also investigated the behaviour of cantilever walls attached to an unprotected steel roof similar to that shown in Figure 4-5. They have shown that thermal bowing of concrete walls are significant especially for tall concrete walls. Unless otherwise summarised in this section, the details of their analyses are discussed in Section 4.5.

Wickström (1986) gives a simple hand calculation method for estimating the temperature profiles in a concrete section. Cooke (1987) has derived some simple formulae to predict the deflection of structural members due to thermal bowing effects. The formulae have been validated for steel elements with both linear and curvilinear thermal distributions but not for materials with low thermal conductivity such as concrete and brickwork.

O'Meagher and Bennetts (1987) have developed FIREWALLS, a computer programme capable of analysing the structural behaviour of concrete walls with pin supports at both ends and exposed to elevated temperatures on one side. FIREWALLS takes into account the P-delta effects and the variation of material properties with temperature. The programme was later modified by Munukutla (1989) to include various boundary conditions at the top and bottom of the wall. O'Meagher and Bennetts (1991) later analysed the behaviour of concrete walls pinned at the ends based on different slenderness ratios (H_w/t_w), amount and locations of reinforcement,

and axial loads applied at the top of the walls. The details of their analyses are discussed in Section 4.5.2

The only experiment performed to investigate the phenomenon of thermal bowing of walls was at the Building Research Establishment in the United Kingdom by Cooke and Morgan (1988). Two brick wall specimens were built and acted as vertical cantilevers so that they were free to move vertically and horizontally when exposed to heat on one side. One wall was 225 mm thick and the other was 337 mm; both walls were 1 m wide by 3 m high. The brick walls were subjected to the standard fire test conditions (International Organisation for Standardisation 834, 1985) on one side and horizontal deflections at the top were measured. The results are shown in Figure 2-1 and the horizontal deflections at the top of the walls were 110 mm and 120 mm for the 215 mm and 337 mm thick walls respectively after 1.5 hour exposure.

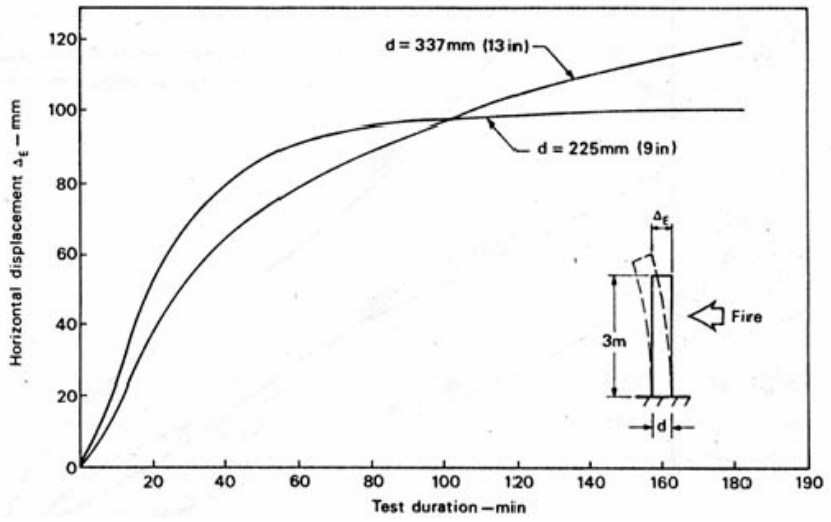

Figure 2-1 Thermal bowing of solid masonry walls (Cooke and Morgan, 1988)

The results obtained from Cooke and Morgan (1988) imply that large horizontal deflections at the top could occur for very tall cantilever walls. They have made some recommendations to minimise the thermal bowing deflections as follows:

- Use construction materials with low coefficients of thermal expansion
- Increase the thicknesses of the walls
- Use simply supported walls instead of cantilever walls

Cooke *et al*. (1996) have used a finite difference computer programme to simulate the two brick walls tested by Cooke and Morgan (1988). The programme makes the assumption that the material properties are independent of temperature and results in inconsistent results for the 337 mm thick wall.

Cooke *et al*. (1996) also derive a simple relationship to extrapolate from test data to obtain the thermal bowing deflections of walls which are higher than those tested. The horizontal deflections (Δ_P) at the top of a cantilevered wall with a height of H_P, can be predicted from the measured deflection (Δ_M) of a tested wall with a height of H_M using the relationship shown below. The limitations of this simple formula are that the walls must be identical and the relationship does not consider the P-delta effects of the self weight of the walls, which may become the dominant factor governing the deflections of tall walls.

$$\Delta_p = \Delta_M \left(\frac{H_P}{H_M} \right)^2 \qquad \textbf{(2-4)}$$

2.3.3 Connections between Wall Panels and the Supporting Structure

Bennetts and O'Meagher (1995) and Bennetts and Poh (2000) have proposed the use of deformable column ties for the connections between the wall panels and the steel frames which may satisfy the requirements of the Building Code of Australia. The ties allow for relatively large relative deflection to occur between the panel and the supporting structure and have been experimentally verified. Clifton and Forrest (1996) have proposed an eaves channel restraint which is more appropriate to be used in New Zealand due to seismic requirements. The details of their connections are described in Section 4.6.

Lim and Buchanan (2003) have suggested that the wall panels must always be well connected to the steel frames. The connection may have to withstand very high pull-out forces due to thermal bowing of the walls. Steel rafters and eaves ties are normally

bolted to inserts cast into the wall panels and the behaviour of these inserts at elevated temperatures are not well known.

Experimental studies on the failure of steel anchors at elevated temperatures have been recently carried out by Reick (2001). The steel anchors are located at the underside of a loaded concrete floor slab. The common failure modes of anchorage system are bolt failure, pullout failure (refer to Figure 2-2) and concrete cone failure.

Figure 2-3 shows bolt failure of either rupture at weak cross section or failure of threads. It has been found that the failure of a bolt is dependent on the type and diameter of the bolt. The presence of water from the concrete also has profound effects on the failure time of the bolt. It has also been found that the concrete cone failure is due to the reduction of concrete strength at elevated temperatures and the local heat flow through the anchor in addition to the normal heating of the slab. Spalling of concrete in fire can also cause concrete cone failure. However, the compressive stresses induced around the anchor due to concrete expansion are beneficial and work well for anchor with large embedment depth.

Figure 2-2 A typical pull-out failure (Reick, 2001)

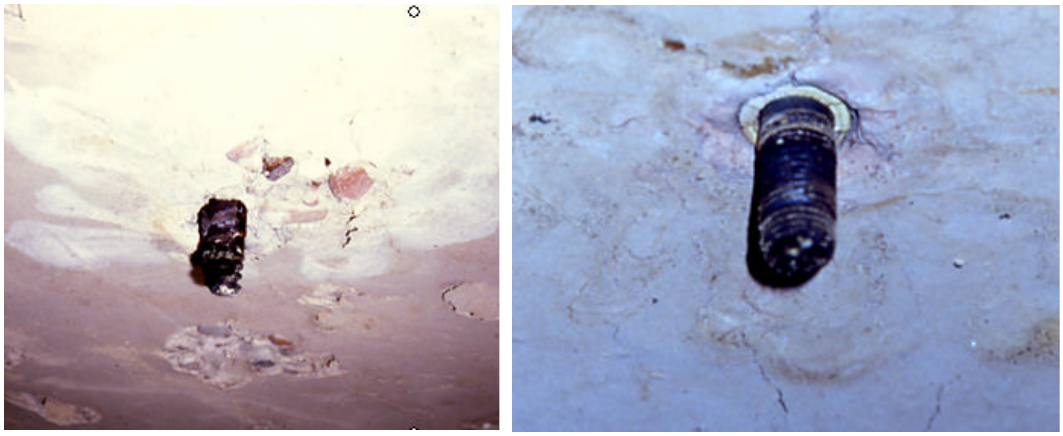

Rupture at cross section *Failure of threads*

Figure 2-3 Bolt failure under elevated temperatures (Reick, 2001)

3 PROPERTIES OF MATERIALS AT ELEVATED TEMPERATURES

3.1 Introduction

The main material that is used in the construction of steel portal frame buildings is structural steel. This chapter covers extracts of properties of structural steel at elevated temperatures. This chapter also covers the thermal and mechanical properties of steel used in SAFIR when they are subjected to elevated temperatures. SAFIR uses the non-linear relationships suggested in the Eurocode 2 and 3 (EC2, 1995 and EC3, 1995) to simulate the temperature dependent properties of the materials. The mechanical properties of structural steel at elevated temperatures according to the New Zealand Steel Structures Standard NZS 3404:1997 are also included.

3.2 Properties of Structural Steel at elevated temperatures

This section covers extracts of structural steel properties at elevated temperatures.

3.2.1 Components of Strain

The deformation of steel at elevated temperatures is described by assuming that the change in the total strain $\Delta\varepsilon$ consists of the thermal strain, stress related strain and creep strain. The transient strain is absent in steel.

$$\Delta\varepsilon = \varepsilon - \varepsilon_i = \varepsilon_{th}(T) + \varepsilon_{\sigma}(\sigma,T) + \varepsilon_{cr}(\sigma,T,t) \quad \textbf{(3-1)}$$

where,

ε is the total strain at time t

ε_i is the initial strain at time t = 0

ε_{th} is the thermal strain and is a function of temperature

ε_{σ} is the stress-related strain and is a function of applies stress and temperature

ε_{cr} is the creep strain and is a function of stress, temperature and time

For simple structural members, it is only required to consider the stress-related strain, allowing the reduced strength at elevated temperatures to be calculated without reference to the deformations. For more complex structures and especially when members are restrained by surrounding structures, the thermal strain and the creep strain must be considered using a computer programme (Buchanan, 2001).

3.2.2 Thermal Strain, $\varepsilon_{th}(T)$

The thermal strain of steel is the thermal expansion that occurs when it is heated. Its behaviour under elevated temperatures is described in the Eurocode 3 (EC3, 1995) and can be found in Section 3.4.3. As mentioned above, it is not necessary to include the effects of thermal strains and thermal restraint forces developed are usually beneficial to the fire performance, although the axial load in the member may increase (Buchanan, 2001).

3.2.3 Creep Strain, $\varepsilon_{cr}(\sigma,T,t)$

Creep strain in structural steel only becomes significant at temperatures over 400°C or 500°C. Kirby and Preston (1988) have shown that the creep is highly dependent on temperature and stress level of the steel (Figure 3-1). The creep strains increase rapidly where the curve becomes nearly vertical at higher temperatures. Therefore, creep deformations are important when the steel members approach their collapse loads. The Eurocode 3 (EC3, 1995) describes that the stress-strain relationships used for design implicitly include the likely deformations due to creep during the fire exposure.

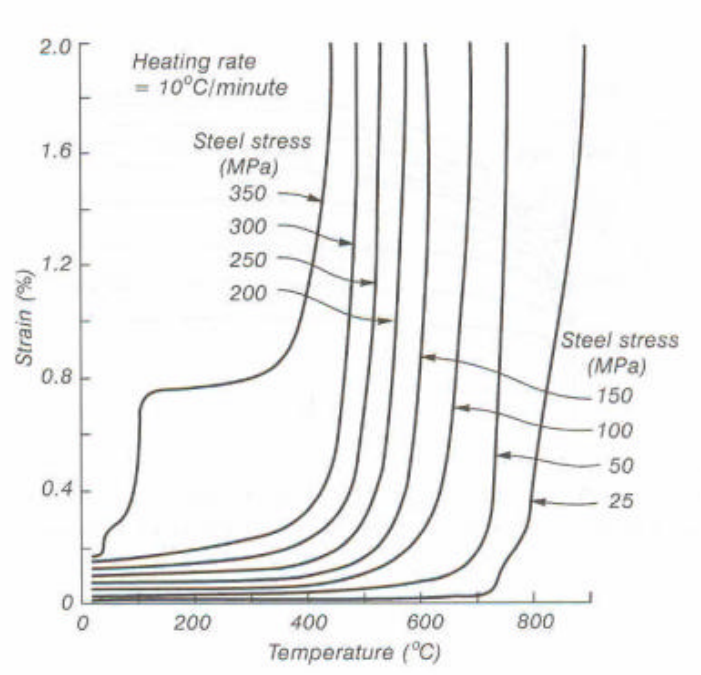

Figure 3-1 Creep of steel tested in tension (Kirby and Preston (1988)

3.2.4 Stress-related Strain, $\varepsilon_\sigma(\sigma,T)$

Harmathy (1993) has obtained typical stress-strain relationships for structural steel at elevated temperatures (Figure 3-2). The figure shows that yield strength and modulus of elasticity both decrease with increasing temperature. However, the ultimate tensile strength increases slightly in the temperature range of 180°C to 370°C before decreasing at higher temperatures. Figure 3-3 shows the stress-strain relationships of hot-rolled structural steels at elevated temperatures given in the Eurocode 3 (EC3, 1995) for designing steel members subjected to elevated temperatures.

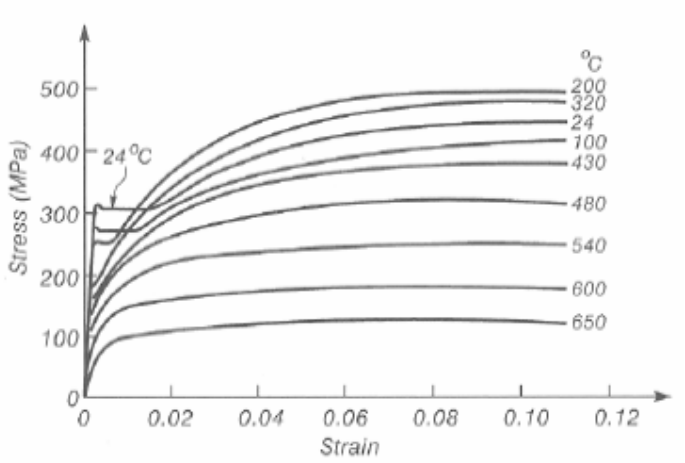

Figure 3-2 Stress-strain curves for typical hot-rolled steel at elevated temperatures (Harmathy, 1993)

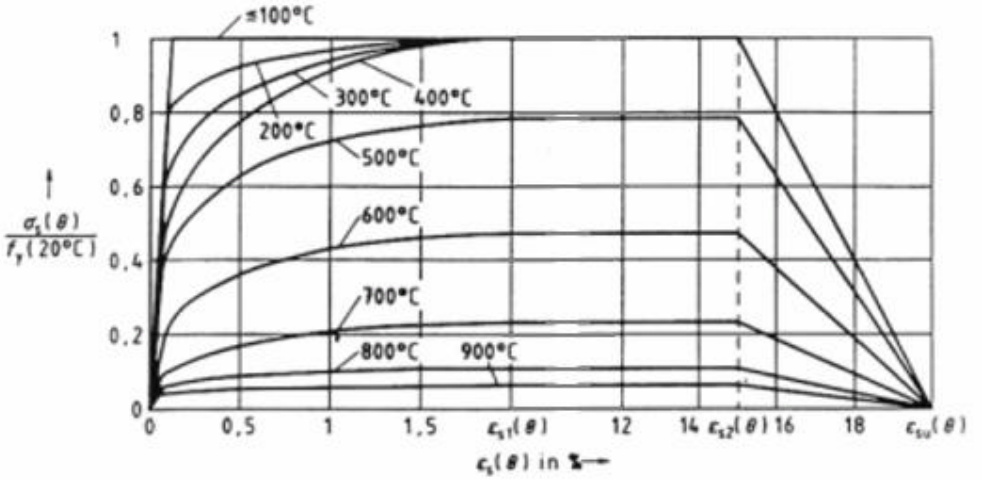

Figure 3-3 Stress-strain curves for typical hot-rolled steel at elevated temperatures according to Eurocode 3 (EC3, 1995)

Ultimate and Yield Strengths

Most normal construction steels have well-defined yield strength at normal temperatures. However, this disappears at elevated temperatures (Buchanan, 2001). Kirby and Preston (1988) recommend using the 1% proof strength as the effective yield strength in the design of structures subjected to elevated temperatures. Harmathy (1993) reviewed a large amount of published research and found that there is a significant amount of scattering in the reduction of the ultimate and yield strengths of hot-rolled and cold-worked steel (refer to Figure 3-4). The dotted lines are the suggested values for design by The Institution of Structural Engineers (1978). It

should be noted that the suggested relationship for hot-rolled structural steel is different to that shown in Figure 3-7 as suggested in the Eurocode 3 (EC3, 1995).

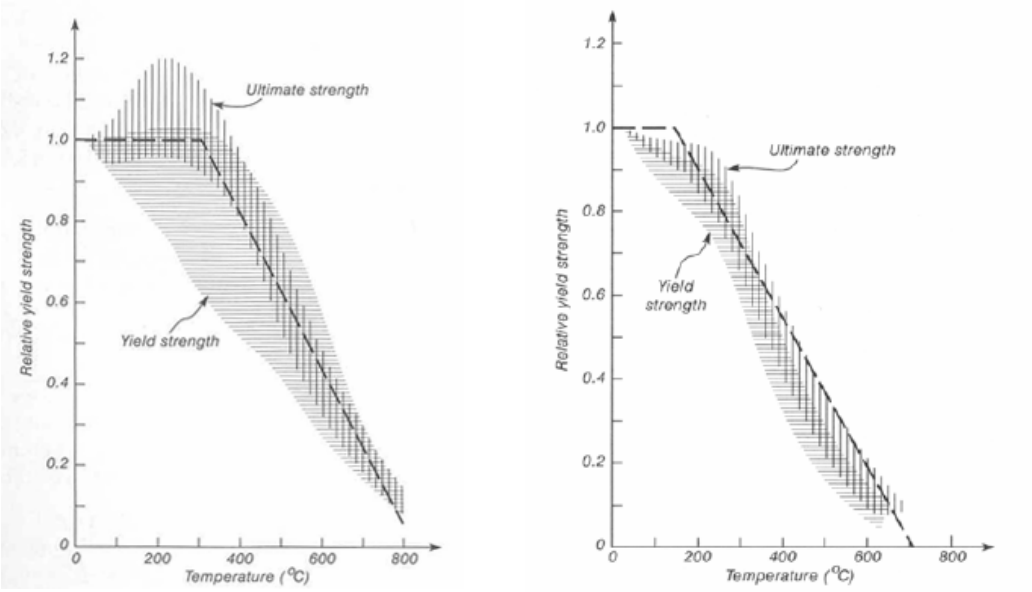

Figure 3-4 Variation of ultimate and yield strengths of hot-rolled (left) and cold-worked (right) steels at elevated temperatures (Harmathy, 1993)

Modulus of Elasticity

The reduction of the ratios of modulus of elasticity at elevated temperatures over the ambient modulus of elasticity for structural steel, prestressing steel and reinforcing steel is shown in Figure 3-5. The figure shows that modulus of elasticity of the steels decreases with increasing temperatures. Similarly, the relationship shown in the figure is different to that shown in Figure 3-7 as given in the Eurocode 3 (EC3, 1995).

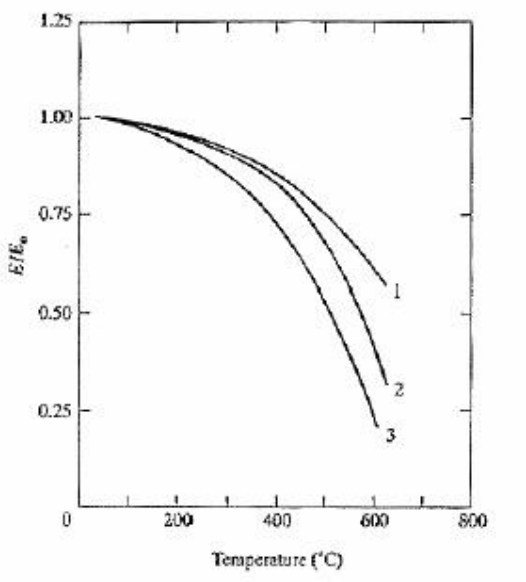

Figure 3-5 Variation of modulus of elasticity of structural steel (curve 1), prestressing steel (curve 2) and reinforcing steel (curve 3). (Harmathy, 1993)

3.3 Steel Mechanical Properties in SAFIR

This section describes the ambient and temperature dependent mechanical properties of the structural steel model used in the SAFIR analysis. SAFIR uses the non-linear temperature dependent relationships of the material based on the Eurocode 3 (EC3, 1995).

3.3.1 Ambient Properties of Steel

The ambient properties of all the steel sections used in this research project are summarised and tabulated in Table 3-1. These values have been entered directly into the structural analysis input files in SAFIR. The design yield stresses of Dimond Hi-Span (DHS) purlins and brace channels are obtained from the Hi-Span design manual (Dimond Industries, 1995).

The density of steel can be considered to be independent of the steel temperature (EC3, 2002) and remains essentially constant at 7850 kg/m^3 (Buchanan, 2001). The initial strain resulted from the manufacturing of steel has been assumed to be negligible.

Table 3-1 Ambient steel properties

Property	**Nomenclature**	**Value**	**Unit**
Portal Frame -- 410UB54 yield stress	f_y	320	MPa
Purlin -- DHS 250/15 yield stress	f_y	500	MPa
Brace Channel -- DB89-10 yield stress	f_y	250	MPa
Elastic Modulus	E_{steel}	210	GPa
Poisson's Ratio	ν	0.3	-
Density	ρ_s	7850	kg/m^3

3.3.2 Steel Properties at elevated temperatures

Eurocode 3 (EC3, 1995) states that the strength and deformation properties of steel at elevated temperatures shall be obtained from the stress-strain relationship shown in Figure 3-6. Table 3-2 gives the reduction factors, relative to the appropriate values at 20^{o}C, for the stress-strain relationship (i.e. effective yield strength, proportional limit and elastic modulus) of structural steel at elevated temperatures given in the figure. These reduction factors are used to determine the structural resistance to tension, compression, moment or shear and are shown graphically in Figure 3-7. For temperatures below 400^{o}C, although not considered in SAFIR, strain hardening can be included into the stress-strain relationship provided local or overall buckling does not lead to premature collapse.

The reduction factors are defined as follows:

- Effective yield strength, relative to yield strength at 20^{o}C: $k_{y,\theta} = f_{y,\theta} / f_y$
- Proportional limit, relative to yield strength at 20^{o}C: $k_{p,\theta} = f_{p,\theta} / f_y$
- Modulus of elasticity, relative to the elastic modulus at 20^{o}C: $k_{E,\theta} = E_{a,\theta} / E_a$

where θ is the steel temperature (^{o}C).

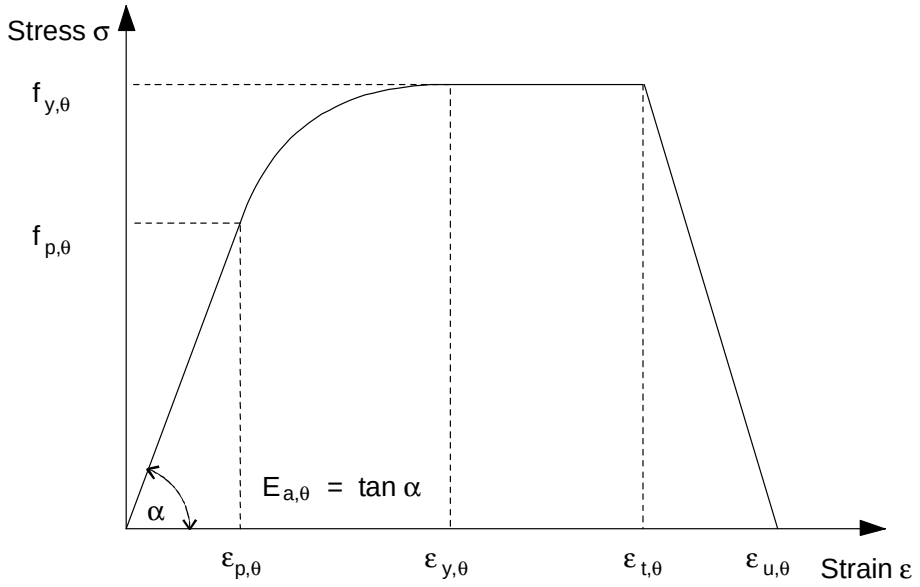

Strain range	Stress σ	Tangent modulus
$\varepsilon \le \varepsilon_{p,\theta}$	$\varepsilon E_{a,\theta}$	$E_{a,\theta}$
$\varepsilon_{p,\theta} < \varepsilon < \varepsilon_{y,\theta}$	$f_{p,\theta} - c + (b/a)\left[a^2 - (\varepsilon_{y,\theta} - \varepsilon)^2\right]^{0,5}$	$\frac{b(\varepsilon_{y,\theta} - \varepsilon)}{a\left[a^2 - (\varepsilon_{y,\theta} - \varepsilon)^2\right]^{0,5}}$
$\varepsilon_{y,\theta} \le \varepsilon \le \varepsilon_{t,\theta}$	$f_{y,\theta}$	0
$\varepsilon_{t,\theta} < \varepsilon < \varepsilon_{u,\theta}$	$f_{y,\theta}\left[1 - (\varepsilon - \varepsilon_{t,\theta})/(\varepsilon_{u,\theta} - \varepsilon_{t,\theta})\right]$	-
$\varepsilon = \varepsilon_{u,\theta}$	0,00	-
Parameters	$\varepsilon_{p,\theta} = f_{p,\theta}/E_{a,\theta}$ $\varepsilon_{y,\theta} = 0,02$ $\varepsilon_{t,\theta} = 0,15$ $\varepsilon_{u,\theta} = 0,20$	
Functions	$a^2 = (\varepsilon_{y,\theta} - \varepsilon_{p,\theta})(\varepsilon_{y,\theta} - \varepsilon_{p,\theta} + c/E_{a,\theta})$ $b^2 = c(\varepsilon_{y,\theta} - \varepsilon_{p,\theta})E_{a,\theta} + c^2$ $c = \frac{(f_{y,\theta} - f_{p,\theta})^2}{(\varepsilon_{y,\theta} - \varepsilon_{p,\theta})E_{a,\theta} - 2(f_{y,\theta} - f_{p,\theta})}$	

Figure 3-6 Mathematical model for stress-strain relationship for structural steel at elevated temperatures (EC3,1995)

Table 3-2 Reduction factors for the stress-strain relationship of steel at elevated temperatures (EC3:1995)

Steel Temperature θ	**Reduction factors at temperature θ_a relative to the value of f_y or E_a at 20°C**		
	Reduction factor for effective yield strength $k_{y,\theta} = f_{y,\theta}/f_y$	Reduction factor for proportional limit $k_{p,\theta} = f_{p,\theta}/f_y$	Reduction factor for the slope of the linear elastic range $k_{E,\theta} = E_{a,\theta}/E_a$
20°C	1.000	1.000	1.000
100°C	1.000	1.000	1.000
200°C	1.000	0.807	0.900
300°C	1.000	0.613	0.800
400°C	1.000	0.420	0.700
500°C	0.780	0.360	0.600
600°C	0.470	0.180	0.310
700°C	0.230	0.075	0.130
800°C	0.110	0.050	0.090
900°C	0.060	0.0375	0.0675
1000°C	0.040	0.0250	0.0450
1100°C	0.020	0.0125	0.0225
1200°C	0.000	0.0000	0.0000

Note:
For intermediate values of steel temperature, linear interpolation may be used.
Strain hardening is not included.

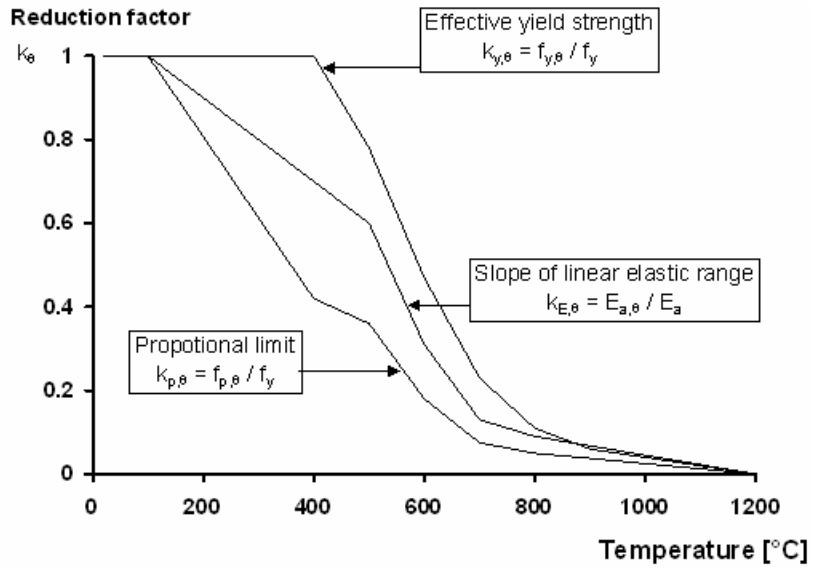

Figure 3-7 Reduction factors for the stress-strain relationship of steel at elevated temperatures (EC3, 1995)

3.4 Steel Thermal Properties in SAFIR

This section describes the thermal properties of the structural steel model used by SAFIR from the Eurocode 3 (EC3, 1995).

3.4.1 Thermal Conductivity, λ_a

Thermal conductivity is the ability of a material to conduct heat and is defined as the ratio of heat flux to the temperature gradient. For steel materials, it is dependent on steel composition as well as the steel temperature. Figure 3-8 shows that the EC3 steel model has a linear reduction in thermal conductivity from 20 to 800°C and is constant at higher temperatures. The equations for thermal conductivity, λ, from the Eurocode 3 (EC3, 1995) are shown below.

$$\lambda_a = 54 - (0.0333 \times \theta_a) \quad \text{(W/mK)} \quad 20^oC \leq \theta_a < 800^oC \qquad \textbf{(3-2)}$$

$$\lambda_a = 27.3 \quad \text{(W/mK)} \quad 800^oC \leq \theta_a < 1200^oC \qquad \textbf{(3-3)}$$

where θ_a is the steel temperature (°C).

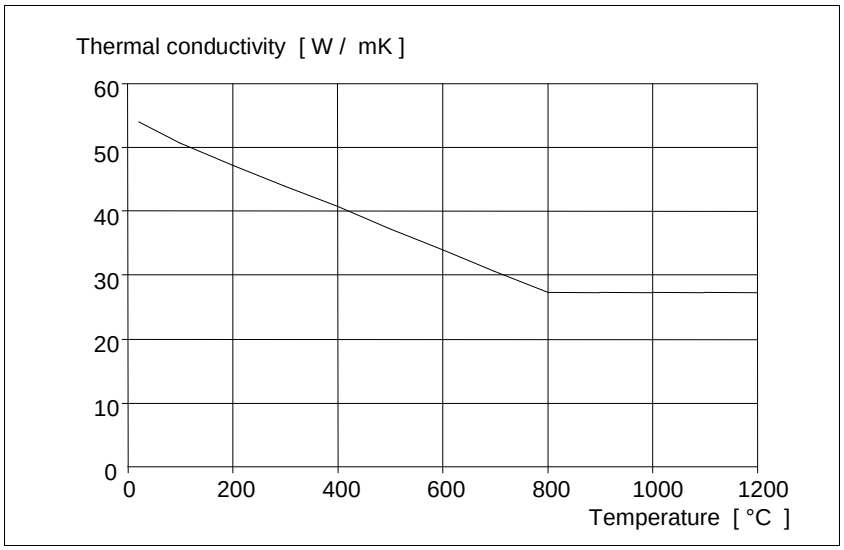

Figure 3-8 Thermal conductivity of steel as a function of temperature (EC3, 1995)

3.4.2 Specific Heat, c_a

Specific heat is the ability of a material to absorb heat. The specific heat of steel is independent of steel composition and varies only with the temperature. Figure 3-9 shows the relationship of specific heat and temperature of steel according to the Eurocode 3 (EC3, 1995). At 730°C there is a metallurgical change in the steel crystal structure that causes a peak specific heat. The equations from the Eurocode 3 (EC3, 1995) for the specific heat relationships are shown below.

$$c_a = 425 + 0.773 \bullet_a - 1.69x10^{-3} \bullet_a^2 + 2.22x10^{-6} \bullet_a^3 \quad \text{(J/kgK)} \quad 20^oC \leq \bullet_a < 600^oC \quad \textbf{(3-4)}$$

$$c_a = 666 + 13002/(738 - \bullet_a) \quad \text{(J/kgK)} \quad 600^oC \leq \bullet_a < 735^oC \quad \textbf{(3-5)}$$

$$c_a = 545 + 17820/(\bullet_a - 731) \quad \text{(J/kgK)} \quad 735^oC \leq \bullet_a < 900^oC \quad \textbf{(3-6)}$$

$$c_a = 650 \quad \text{(J/kgK)} \quad 900^oC \leq \bullet_a \quad \textbf{(3-7)}$$

where θ_a is the steel temperature (°C).

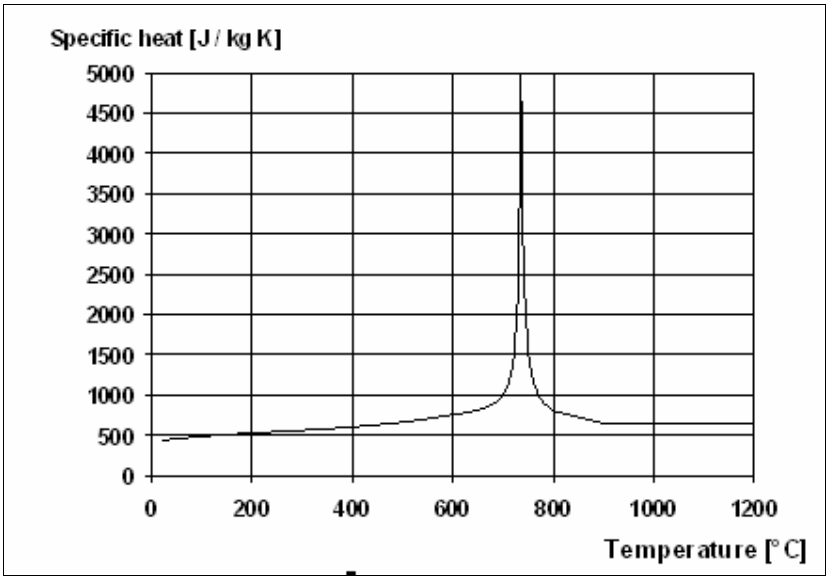

Figure 3-9 Specific heat of steel as a function of temperature (EC3, 1995)

3.4.3 Thermal Elongation, $\Delta l/l$

The thermal elongation of steel, $\Delta l/l$, is the increase in the length of a member caused by heating divided by the initial length. Figure 3-10 shows the relationship of elongation and the temperature of steel according to the Eurocode 3 (EC3, 1995). The discontinuity in the thermal elongation between 750°C and 860°C is due to a phase transformation in the steel. The following equations from the Eurocode 3 (EC3, 1995) describe the thermal elongation relationships in steel.

$$\Delta l/l = 1.2\times10^{-5} \bullet_{a} + 0.4\times10^{-8} \bullet_{a}^{2} - 2.416\times10^{-4} \qquad 20^{o}C \leq \bullet_{a} < 750^{o}C \qquad \textbf{(3-8)}$$

$$\Delta l/l = 1.1\times10^{-2} \qquad 750^{o}C \leq \bullet_{a} < 860^{o}C \qquad \textbf{(3-9)}$$

$$\Delta l/l = 2\times10^{-5} \bullet_{a} - 6.2\times10^{-3} \qquad 860^{o}C \leq \bullet_{a} < 1200^{o}C \qquad \textbf{(3-10)}$$

where θ_a is the steel temperature (°C).

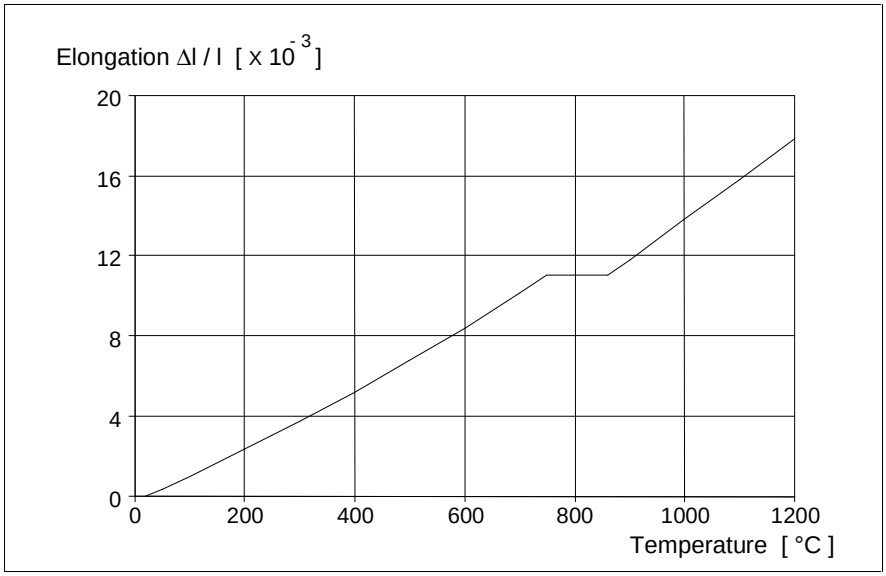

Figure 3-10 Thermal elongation of steel as a function of temperature (EC3, 1995)

3.5 Steel Structures Standard NZS 3404:1997

The New Zealand Steel Structures Standard NZS 3404:1997 requires structural analysis of steel structures at elevated temperatures according to the variation of yield stress and modulus of elasticity ratios of steel with temperature as shown in Figure 3-11. The relationships given below are used to describe the curves shown in the figure. It should be noted that the relationships given in the NZS 3404:1997 are slightly different to those suggested in the Eurocode 3 (EC3, 1995).

$$f_y(T)/f_y(20) = 1.0 \qquad 0^oC < T \leq 215^oC \qquad \textbf{(3-11)}$$

$$f_y(T)/f_y(20) = (905-T)/690 \qquad 215^oC < T \leq 905^oC \qquad \textbf{(3-12)}$$

$$E(T)/E(20) = 1.0 + T/(2000(Ln(T/1100))) \qquad 0^oC < T \leq 600^oC \qquad \textbf{(3-13)}$$

$$E(T)/E(20) = 690(1-T/1000)/(T-53.5) \qquad 600^oC < T \leq 1000^oC \qquad \textbf{(3-14)}$$

where T is the steel temperature (^oC).

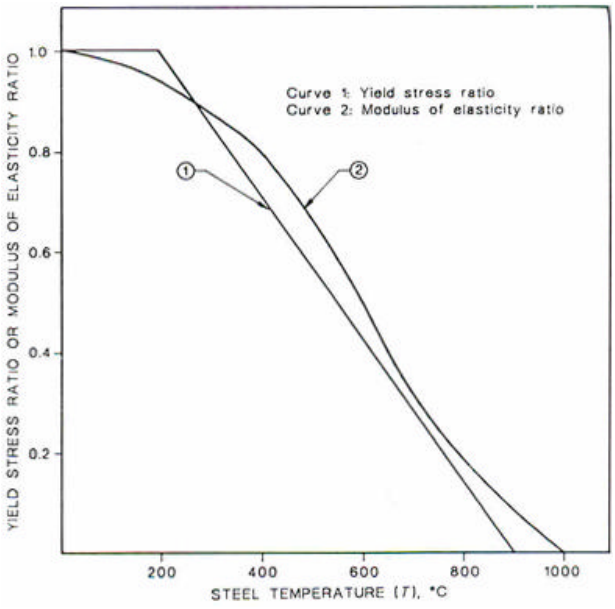

Figure 3-11 Variation of mechanical properties of steel with temperature according to NZS 3404:1997

4 BEHAVIOUR OF INDUSTRIAL BUILDINGS AND CONCRETE WALLS IN FIRES

4.1 Introduction

This chapter describes the two forms of industrial buildings constructed in New Zealand. The work carried out by previous researchers to investigate the behaviour of steel portal frames, concrete walls and connections between these frames and the walls attached at elevated temperatures are also described. This chapter also reviews the results of the analyses obtained by previous researchers on the performance of industrial buildings. Observed building behaviour in recent fires has been included.

4.2 Industrial Buildings in New Zealand

Single storey warehouses and industrial buildings are very common in New Zealand. They are usually used for manufacturing purposes, storing materials with high fuel loads or commercial uses. These types of buildings have large unpartitioned spaces and high ceilings due to handling requirements. The most common form of construction in New Zealand is first described, followed by a more recent construction form in which the steel rafter is supported on internal columns. Tilt-up precast concrete panels are used for the boundary walls of the building.

4.2.1 Typical Industrial Buildings

Single-storey warehouse and industrial buildings are commonly constructed from structural steel portal frames with steel, masonry or concrete cladding. The steel portal frames are formed by a steel rafter spanning between two steel columns. It is common to encase all or part of the steel portal frame column leg with concrete, or to use a reinforced concrete column for the lower part of the portal frame leg (Figure 4-1 and Figure 4-2). The portal frames are usually spaced at 5 to 10 metres apart and the steel columns are fixed or partially fixed at the base. The roofs of such buildings are always constructed using corrugated steel sheeting with 5% to 15% translucent plastic skylights, supported on steel purlins which are in turn supported by the rafters. This

project is aimed at investigating the behaviour of these frames when they are subjected to elevated temperatures.

In terms of fire protection to the adjacent buildings, masonry and concrete walls are used as fire-resistant walls. Concrete walls in the form of cast-on-ground “tilt-up” panels are commonly used in New Zealand. These concrete walls are considered as pinned at the base, although they may be partially fixed in practice. Four commonly used connection details at the base are shown in Figure 4-3. These precast concrete panels are attached to the portal frames and are sometimes connected to each other by an eaves tie member.

In the corners of the buildings, the side wall panel and the end wall panel intersect each other at right angles. For most situations a column will not be present at the junction and the side wall panel is connected to the end wall panel. Similarly, the end walls are not cantilevered from the ground and are attached to steel columns or cast *in-situ* concrete columns. These walls are essentially pinned at the base, with no or little moment resistance (Figure 4-4). The steel columns are sometimes encased in concrete for additional fire resistance.

As mentioned above, the steel columns are sometimes encased in concrete to provide additional fire resistance rating to satisfy the fire resistance rating requirements in the Approved Document. However, this will generate additional forces in the connections between the wall panels and the supporting structure when the walls are prevented from deforming away from the fire due to the steep temperature gradients across the wall known as thermal bowing effects (Cooke, 1988, Bennetts and O’Meagher, 1995). This also raises the issue of how well the steel columns are protected by the concrete encasement when exposed to very high temperatures or when the steel portal frames are starting to deform excessively. Evidence from real fire incidents has shown that concrete encasement can fall off when exposed to high temperatures (Figure 4-67).

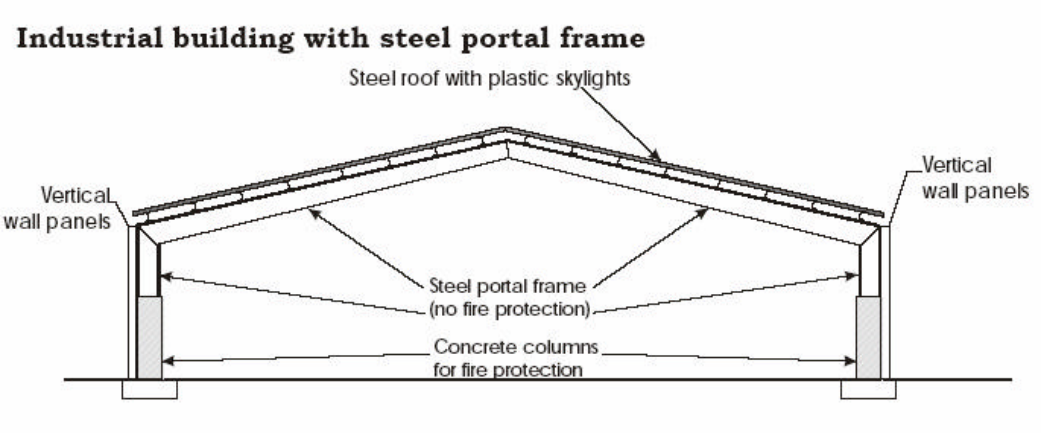

Figure 4-1 Typical industrial buildings in New Zealand (Lim, 2000)

Figure 4-2 Industrial buildings with non load-bearing walls

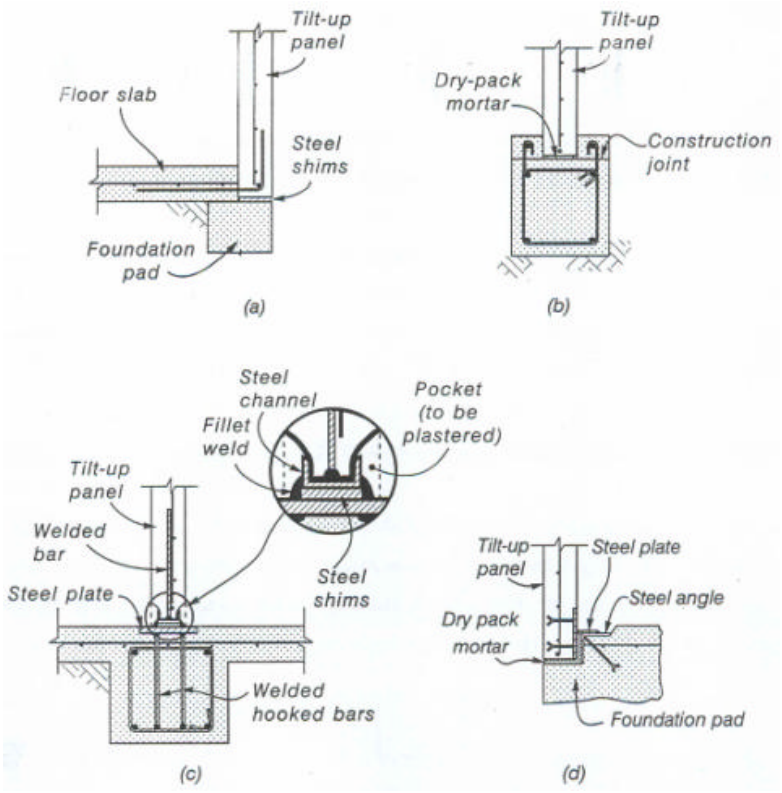

Figure 4-3 Typical base connection details for tilt-up walls pinned at the base (Restrepo *et al.*, 1996)

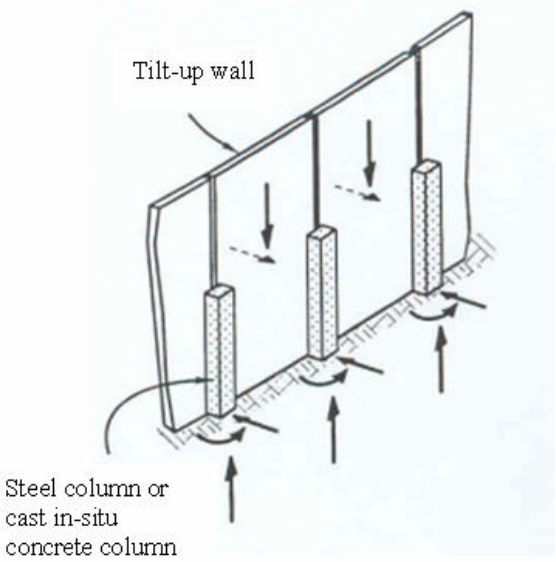

Figure 4-4 Typical end walls attached to steel columns or cast *in-situ* concrete columns (Restrepo *et al.*, 1996)

4.2.2 Recent Industrial Buildings

There have been some industrial buildings recently constructed in the form of steel rafters supported on internal steel columns and cantilevered tilt-up precast panels at the perimeter of the building (Figure 4-5 and Figure 4-6). These load-bearing walls do not have columns attached to them and no intermediate lateral support is provided (Bull, 1998). The walls are connected to each other at the top by an eaves tie with steel clips or bolt anchored into cast-in inserts (Figure 4-7). The roof is braced to act as a diaphragm to resist wind loading and provide stability to the top of the concrete walls. The wall panels also provide in-plane resistance to lateral loads such as earthquake or wind induced forces. The steel rafters are typically attached to every second or third wall panel. These modern industrial buildings are intended to be built with long span steel rafter and high ceiling to maximise the building space. The clear spans range between 15 m to 30 m. The rafters usually have a spacing of 6 to 12 metres (Lim, 2000).

The performance of cantilevered concrete panels with high slenderness ratios (height/thickness ratios) is the main concern from fire resistance and seismic stability perspectives. Tall and slender cantilever wall panels have been constructed with slenderness ratios ranging from 50 to in excess of 80 and some of these walls are very thin with thicknesses ranging from 125 mm to 150 mm (Brown, 1999, Lim, 2000). The walls are only reinforced with one central layer of reinforcing steel. The effective slenderness ratios of these walls exceed the maximum allowable effective ratios stated in the New Zealand Concrete Structures Standards NZS 3101:1995 (refer to Section 2.2.5). Lim (2000) has carried out extensive modelling of slender concrete walls and frames incorporating slender cantilevered walls similar to that shown in Figure 4-5 using SAFIR (refer to Section 4.4.3 and Section 4.5.2).

Various types of connections are used to connect the cantilever walls panels at the base to the cast *in-situ* slab and foundations. Restrepo *et al*. (1996) and Lim (2000) conducted surveys on the typical connections details used in New Zealand (Figure 4-8). These connections are required to provide full fixity at the base of the cantilever walls to resist overturning moments. The connection methods used range from simple reinforcing steel connections to proprietary connection details.

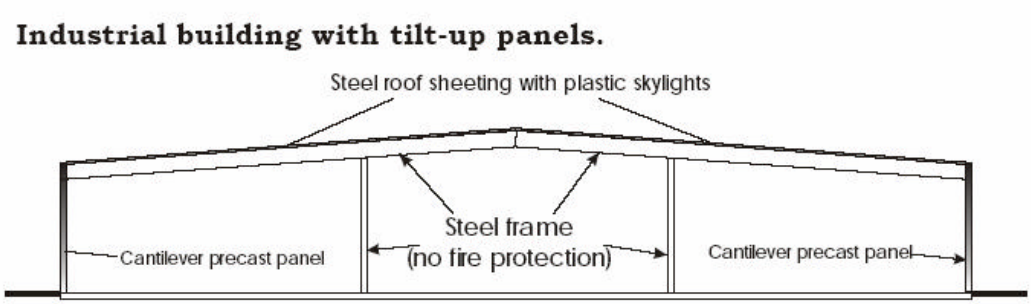

Figure 4-5 Industrial buildings recently constructed in New Zealand (Lim, 2000)

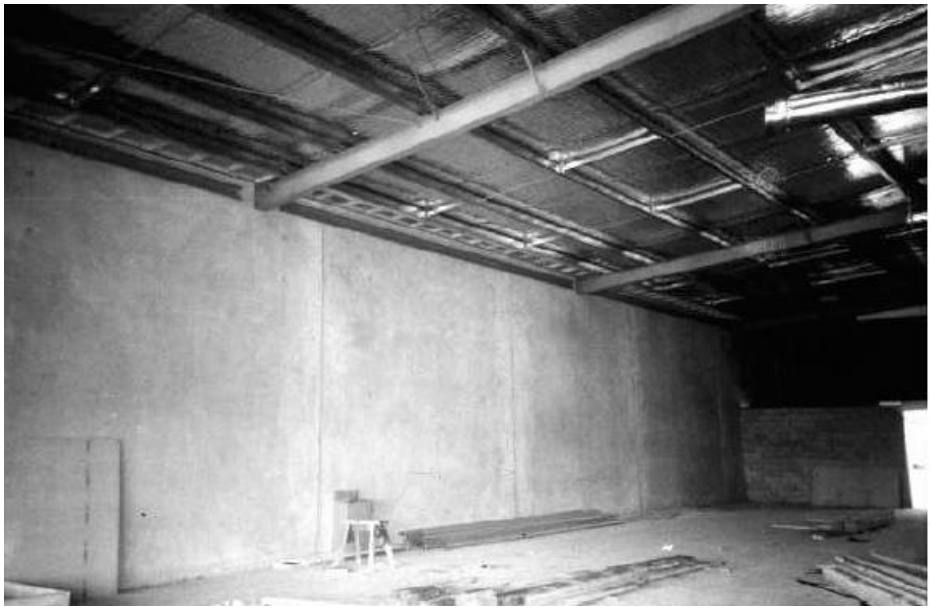

Figure 4-6 Industrial buildings with load bearing cantilever walls (Lim, 2000)

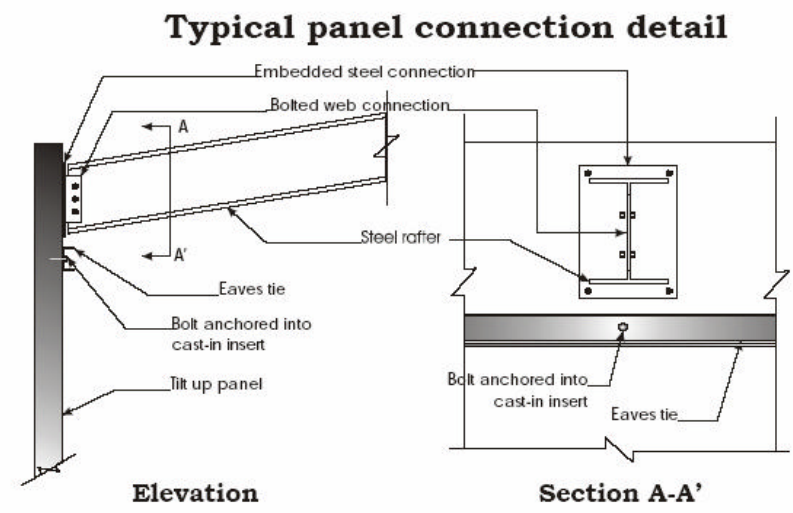

Figure 4-7 Typical steel rafter to concrete panel connection (Lim, 2000)

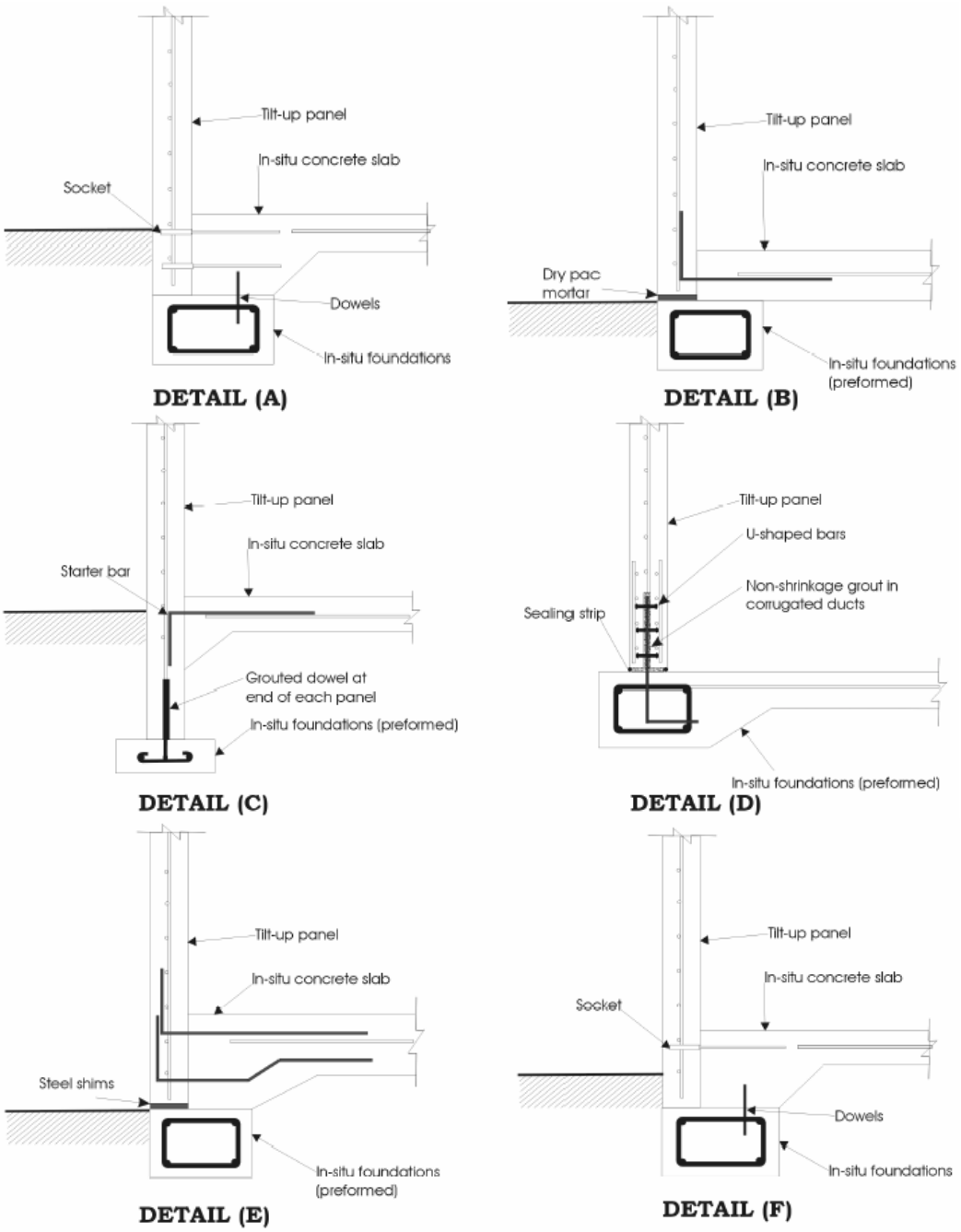

Figure 4-8 Typical base connection details for cantilever walls (Lim,2000)

4.2.3 Connections between Tilt-up Walls at vertical joints

It is common to have more that one tilt-up panel between the supporting elements. Multiple wall panels must act as a complete unit in the event of a fire and an eaves tie member connecting these panels is recommended by Lim and Buchanan (2003). Various connections are currently used in connecting the wall panels at vertical joints

and these can be divided into four groups: welded connections, bolted connections, monolithic joints and connections to adjacent columns (Restrepo *et al.*, 1996). The descriptions of each connection type are given below. The performance of these connections at elevated temperature is not very well understood at this stage. After the erection of the wall panels, except when monolithic vertical joints are used, it is common to place two backing strips between the walls to form a vertical gap of approximately 10 mm which is then blocked with fire proofing materials (Figure 4-9).

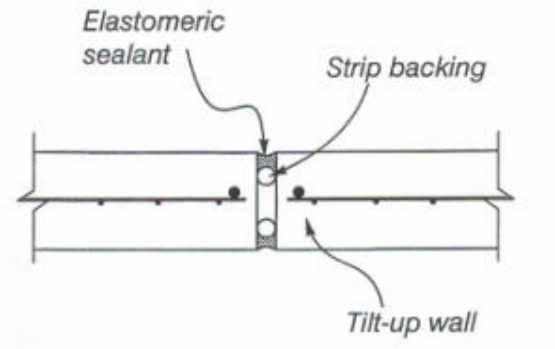

Figure 4-9 Typical sealing of the vertical gap between tilt-up wall panels (Restrepo *et al.*, 1996)

Welded Connections

Typical welded connections are illustrated in Figure 4-10. The concrete panels are connected by welding a steel plate to either steel angles or other plates embedded in the precast panels. Figure 4-11 shows similar connections for connections of tilt-up panels located in a corner.

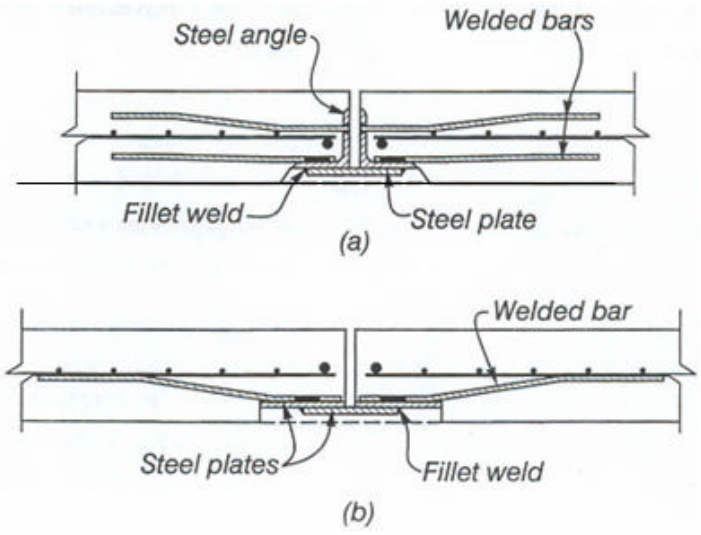

Figure 4-10 Typical welded connections for joining wall panels (Restrepo *et al.*, 1996)

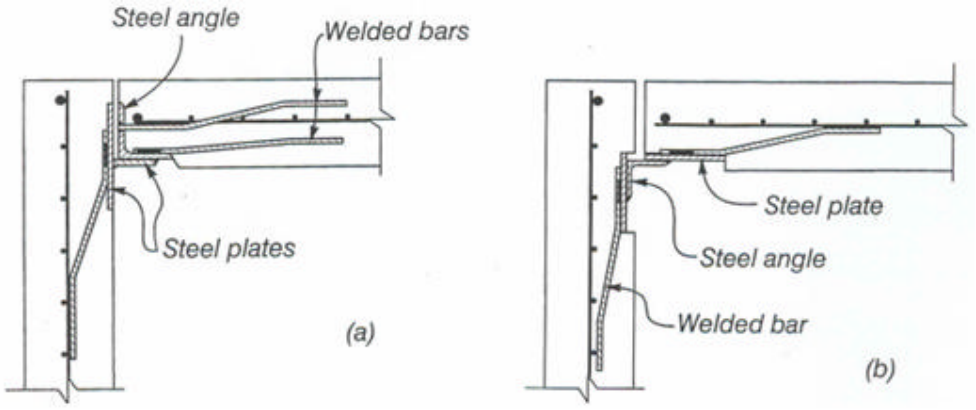

Figure 4-11 Typical welded connections for joining panels located in a corner (Restrepo *et al.*, 1996)

Bolted Connections

The use of bolted connections with oversized holes is very common to take account into the erection tolerances of the walls. This is especially true in the cases where fast construction is important. Figure 4-12 (a) and (b) shows similar connection details in which bolted steel angles or plates are used to connect the wall panels. The bolts are fixed to the steel inserts embedded in the walls panels. Figure 4-12 (c) is an alternative connection for joining walls at right angles. The connection detail shown in Figure 4-12 (d) is applicable to corner connections. The bolts pass through one of the panels and are then fixed into couplers embedded in the other wall panel. It is also convenient to provide additional reinforcing bar to the steel inserts to resist any moment resulting from accidental eccentricities that may occur during construction (Figure 4-13).

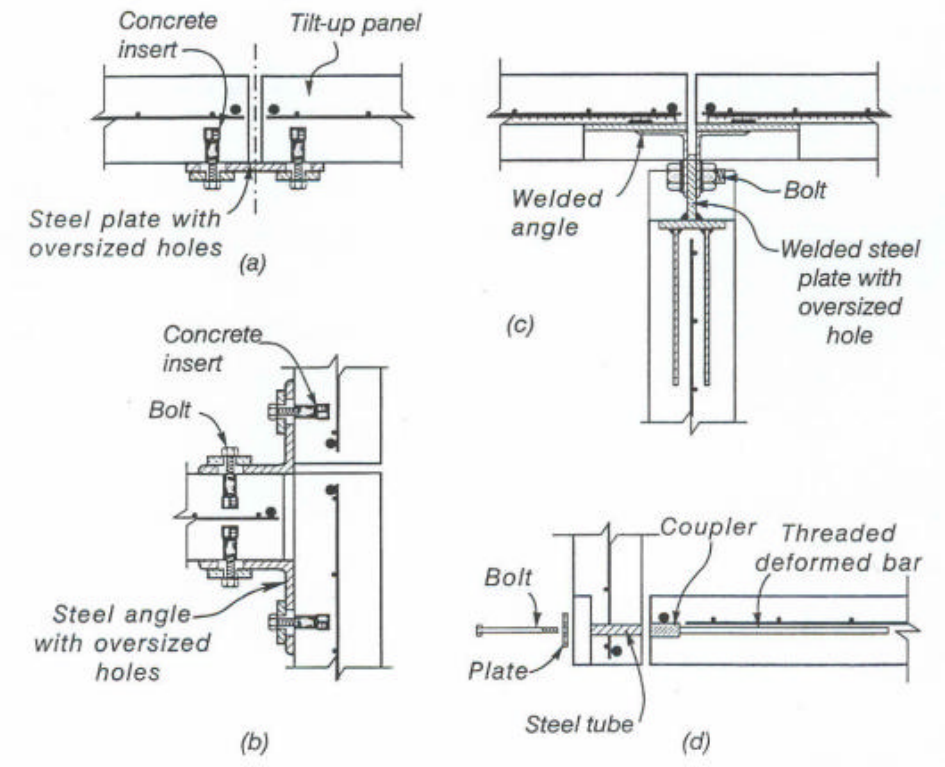

Figure 4-12 Typical bolted connections between tilt-up walls (Restrepo *et al.*, 1996)

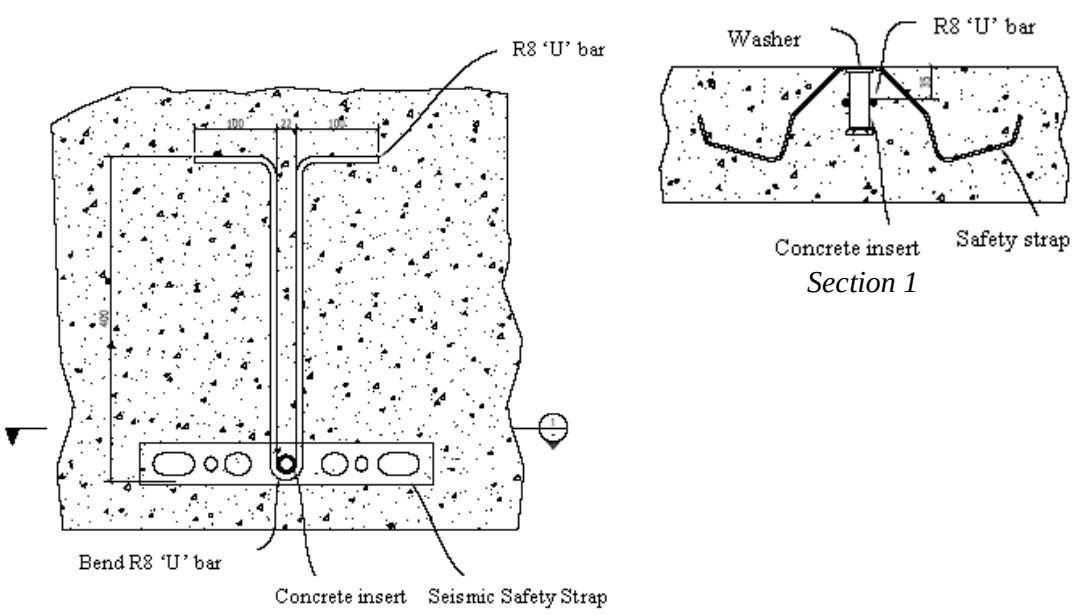

Figure 4-13 Additional reinforcing 'U' bar to concrete insert (Courtesy of Structex Limited)

Monolithic Vertical Joints

Monolithic vertical joints are constructed using cast *in-situ* concrete. Horizontal reinforcing bars protruding from the wall panels are lapped and combined with vertical reinforcing to form a connection capable of resisting the stresses transmitted from adjacent wall panels. The construction of monolithic vertical joints is more labour intensive than bolted or welded connections between walls.

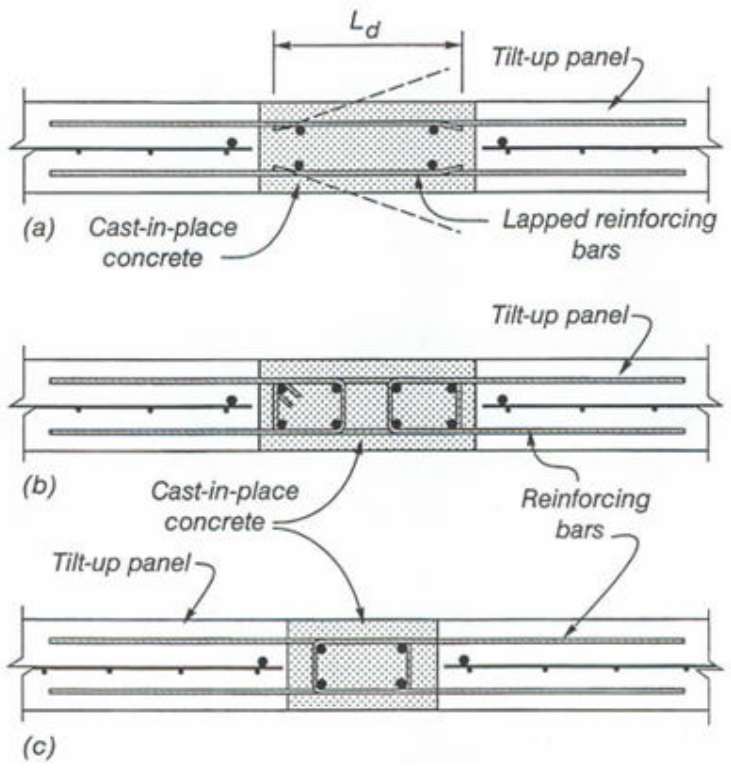

Figure 4-14 Typical monolithic vertical joints using cast *in-situ* concrete and lapped bars (Restrepo *et al.*, 1996)

Connections to Adjacent Columns

These types of connections are commonly used to attach tilt-up walls to the adjacent steel or cast *in-situ* concrete columns which act as the main supporting elements for the walls. The connections are required to provide moment resistance against lateral face forces acting on the panels. Figure 4-15 shows the typical connections between concrete panels and columns used in practice. In Figure 4-15 (a), the connection is formed by hooked deformed bars protruding from both panels, which are anchored in the cast *in-situ* concrete column. Figure 4-15 (b) and (c) show connections using bolts. Figure 4-15 (d) illustrates a very common detail for connecting end wall panels

to universal steel columns using bolts and small steel plates. A more recent approach is to replace the steel plates with steel angles which are bolted to the web of the column (Lewis, W., *personal communication*).

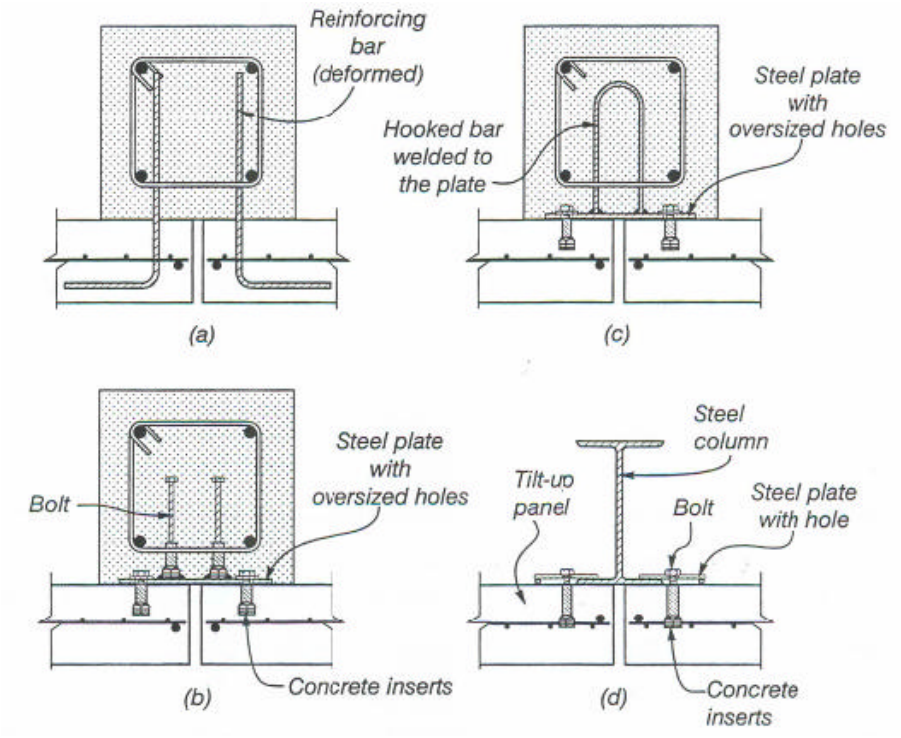

Figure 4-15 Typical connection details between wall panels and steel or reinforced concrete columns (Restrepo *et al*., 1996)

4.2.4 Connections between Tilt-up Walls and Roof

A common connection detail used in New Zealand for the connection between steel purlins and wall panels is shown in Figure 4-16. The steel purlin is supported by a cleat which is fixed to the wall panel using expansion anchors. The bolts connecting the purlin and the steel angle are designed to resist shear forces, whereas the expansion anchors must resist shear forces and also axial forces resulting from the bending moment produced by the gravity load.

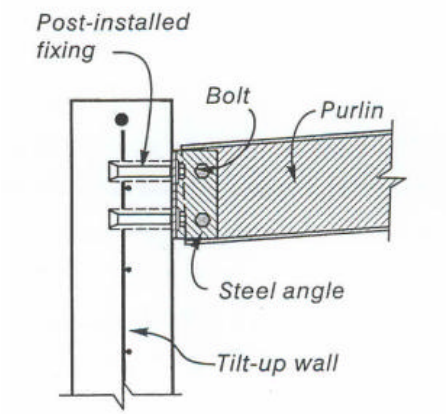

Figure 4-16 Typical connection detail between end wall and steel purlin (Restrepo *et al*., 1996)

4.3 Fires in Industrial Buildings

4.3.1 Small Enclosure Fire

A fire in an enclosure can develop in a large number of different ways, mostly depending on the enclosure geometry and ventilation and the fuel type, amount, and surface area (Karlsson and Quintiere, 2000). After ignition, the fire grows and releases increasing amounts of energy. Initially, the enclosure has no effect on the fire, which then is fuel-controlled. The fire will form a convective plume of hot gas which will rise and impinge on the ceiling of the fire compartment. As the fire plume rises, cold air will be entrained into the plume. As a result of this entrainment, the total mass flow in the plume increases, and the average temperature decreases with height.

The gases will then spread across the ceiling as a momentum-driven circular jet, called the ceiling jet. As the ceiling jet moves radially outward, cold air is entrained into the jet and the flow will be cooled. However, the gases in the jet area are still warmer than the surrounding ambient air, and the flow will turn upward due to buoyancy and a layer of hot gases will be formed under the ceiling (see Figure 4-17) . Heat from the hot layer is also radiated toward the floor and the lower walls. Additionally, heat is transferred to the fuel bed by radiation from the hot layer and the hot enclosure boundaries. This leads to an enhanced burning rate of the fuel and the heating up of other fuel packages in the enclosure.

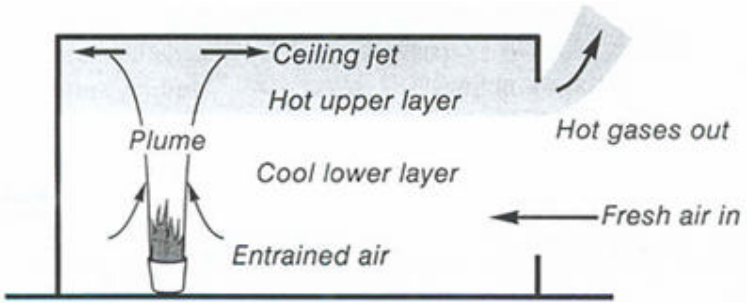

Figure 4-17 Early stages of fire in a room (Buchanan, 2001)

The fire may continue to grow provided there is enough fuel load and ventilation openings in the fire compartment. The upper layer increases in temperature and as a result of radiation from the hot layer toward other combustible material in the enclosure, there may be a stage where all the combustible material in the enclosure is ignited, with a very rapid increase in energy release rates. This sudden transition from a growing fire to a fully developed fire is called flashover.

4.3.2 Large Compartment Fire

The behaviour of a fire in a large compartment, such as warehouses or industrial buildings, is not the same as a small enclosure fire. These buildings usually have very high ceilings and large open spaces. The fire plume will have entrained a large amount of cold air when it impinges on the ceiling. The hot gases will continue to spread across the ceiling and similarly, cold air will be entrained into the ceiling jet. Therefore, the radiant heat flux from the upper hot layer may not be high enough to cause flashover.

Initially, the fire in this large compartment would be a fuel-controlled fire. The temperatures of the fire may get sufficiently high at areas of fire origin such that local structural failure may occur due to local buckling of the purlins and rafters. It may also cause melting of skylights and collapse of the roof resulting in the venting of the fire releasing the accumulated hot gases into the atmosphere. Therefore, the temperatures of the in the building may be lower when compared to a small enclosure fire.

Cosgrove (1996) has produced a simplified fire development sequence in an industrial building, as measured by the heat release rate (see Figure 4-18). The figure shows that the fire grows as a t-squared fire in the very early stages. A steady state will be reached and this can be ventilation or fuel controlled depending on whether the burning rate of the fuel packages is greater or less than the relative burning rate possible due to the available ventilation openings in the building. The melting of skylights and the collapse of roof will increase the available ventilation and will result in an increase in heat release rate given that the fire is ventilation controlled. Once the available fuels have been consumed, the heat release rate will decrease resulting in a decay phase.

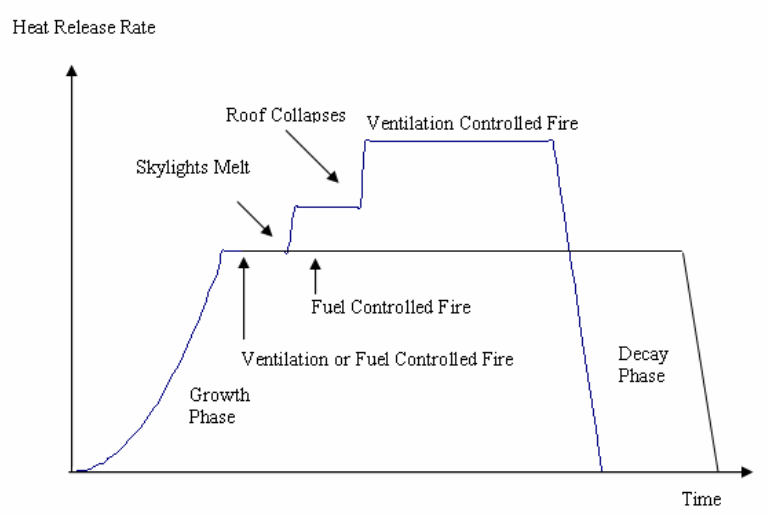

Figure 4-18 A typical fire development in a single storey industrial building

4.3.3 Fire Concepts

The concept of a developing fire was introduced by O'Meagher *et al*. (1992) regarding the likely nature and characteristics of fire in industrial buildings. A fire occurs at a particular location and may spreads outwards to other parts of the building over a certain time period (see Figure 4-19). It is therefore considered reasonable to assume that the heating is non-uniform throughout the building at any point in time. As the fire spreads, it is possible that an increasing number of structural elements will be affected by the fire if high fuel loads are present.

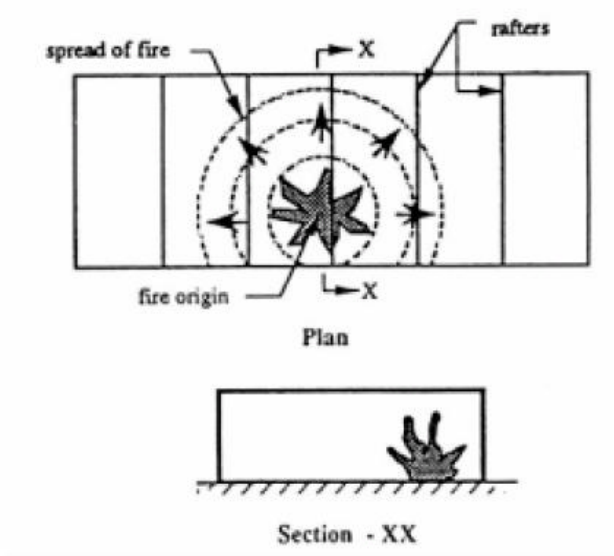

Figure 4-19 Developing fire in single storey large compartments (O'Meagher *et al.*, 1992)

The developing fire concept suggests that the parts of the structure not in the immediate vicinity of the fire may only be exposed to low temperatures such that the structural performance will not be significantly impaired. This is particularly true during the early stages of the fire. Clifton and Forrest (1996) have adopted the same concept and suggested that at the point of fire origin, the fuel will soon be consumed and the fire will decay. If the fire is able to spread to other areas, those areas will be subjected to high temperature, while other regions may only be subjected to relatively low temperatures.

For storage occupancies in such buildings, the development of fire is related to the burning characteristics of the material stored, combustibility of packaging, method of storage and packaging, quantity stored, and as well as fire protection systems (Hisley, 2003). Horizontal air spaces formed by the pallets in palletised storage can cause fast spreading fires. Rapid fire spread can also be expected in rack storage areas due to the rack height and narrow aisle width typically present when automatic materials-handling equipment is used. Modern developments in material handling have brought rapid change to storage occupancies, including high-rack storage areas as tall as 15 metres to 30 metres.

It is clear that the temperatures of the structural elements of industrial buildings in fires are much harder to predict. To obtain accurate temperature profiles for all the

structural members, sophisticated computer programmes which use computational fluid dynamics (CFD) to model fires using a large number of discrete zones in a three-dimensional grid must be used. The time at which critical temperatures in the steel members are exceeded can be determined and thereby imply roof collapse. This process may require a substantial amount of information to be collected regarding the type of fuel, the location and configuration of the fuel packages, the geometry of the buildings and the thermal properties of the building elements. It is beyond the scope of this study to discuss this issue further. For the purpose of the analysis in this project, an ISO 834 standard fire curve and an Eurocode External fire curve are used.

4.4 Behaviour of Industrial Buildings at elevated temperatures

4.4.1 Structural Fire Behaviour by Newman (1990)

From a study of fires in a number of industrial buildings with steel portal frames in the U.K. by Newman (1990), it has been found that as the fire develops, the portal rafter begins to heat up and expand, which causes an outward deflection of the eaves together with an upward deflection of the apex. The initial outward movement can cause masonry or precast concrete walls to collapse outwards (Buchanan, 2001). Both of these deflections are very small.

As the fire continues to burn, the rafter temperature rises and the moments due to thermal expansion increase. It is assumed that the columns are not severely affected by the fire and the columns stay relatively straight throughout the duration of the fire. Because of the increasing temperature, hinges start to form in the rafter. These hinges are caused principally by plastic yielding of the rafter as the yield stress falls with increasing temperatures. The moment of resistance of a plastic hinge caused by a fire is considerably less than the corresponding value at normal temperature.

Axial thrusts are induced in the rafter from the very early stages of fire. With the formation of the hinges, the rafter is unable to resist the axial thrusts from the relatively stiff columns and begins to collapse and falls below eaves level. The overturning moment induced at the base of the columns by thermal expansion of the rafter quickly reduces to zero and then builds up in the opposite sense (refer to Figure

4-20). At the same time an inwards tensile force is developed as the rafters droop into a catenary. Torsional instability may occur as the purlins lose their strength and the rafter may rotate so that it sags with its web horizontal as it loses stiffness. As the rafter further loses strength it will deflect further and cause the columns to lean inwards.

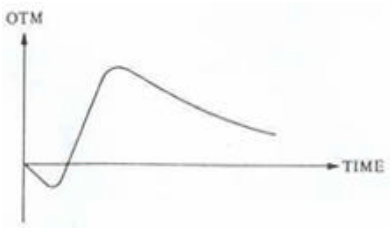

Figure 4-20 Variation of base overturning moment with time (Newman, 1990)

Newman (1990) emphasises that the design of the base at this stage is very important. Bases with a large resistance moment will be capable of supporting the column in a reasonably upright position but nominally pinned bases are likely to prove inadequate thus allowing the collapsing rafter to pull the columns invariably inwards. Newman (1990) describes that a portal frame with fixed bases will usually have adequate base fixity to resist rafter collapse provided the ratio of the span divided by the height to eaves is less than two. The methods for calculating the overturning moment at the column bases and designing the column bases to resist rafter collapse are presented in Newman (1990). The methods are based on the collapse mode such that sufficient strength and ductility is available to allow the column to lean inwards to an equilibrium position (Figure 4-21) and the columns will then remain static while the rafter continues to collapse. It should be noted that these methods are only suitable for the case where the strength and stiffness of the columns are not severely affected by the fire and collapse of the walls is not allowed.

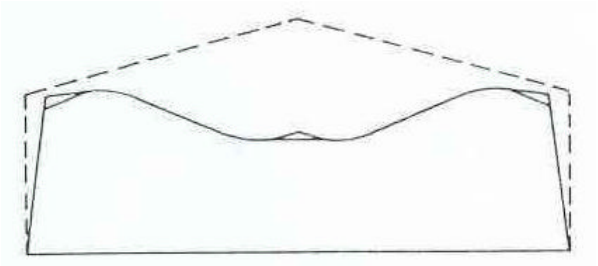

Figure 4-21 Rafter sags until an equilibrium position is reached (Newman, 1990)

Multi-bay Frames

Newman (1990) describes the behaviour of multi-bay frames and suggests that the frames will deform in very similar ways to that of single-bay frames. Collapse of the rafter will occur in a similar manner but the behaviour of the columns will be slightly different. For a fire occurring in end bay, as the rafter collapses, the external column is pulled slightly inwards. The internal column stays almost vertical (Figure 4-22). For a fire occurring in the internal bay, the rafter collapses but the columns stay upright being stabilised by the adjacent frames. In certain circumstances an unprotected internal column may partially collapse.

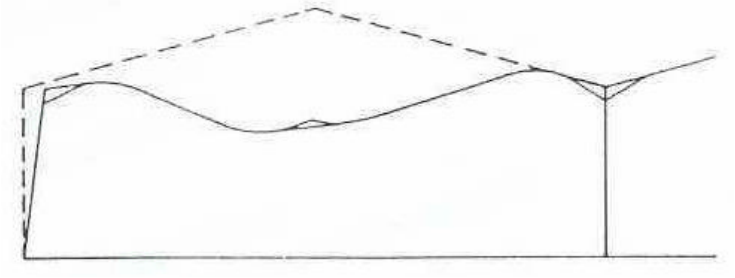

Figure 4-22 The collapse mode of a multi-bay frame (Newman, 1990)

4.4.2 Structural Fire Behaviour by O'Meagher *et al*. (1992)

O'Meagher *et al*. (1992) have done extensive modelling using ABAQUS, a finite element programme to study the behaviour of single-bay industrial buildings under fire condition. Their analyses were two dimensional and took account into the self weight of the structure and the effects of displacements on the overall behaviour (i.e. P-delta effects).

The structural models analysed are shown in Figure 4-23. The first model is a representation of a typical industrial building with steel portal frames. The concrete walls are attached to the eaves of the frame by a pin. The second model is a building with non-cantilevered walls which also act as load-bearing walls to support the roof. The model is a four pin mechanism, stabilised by the presence of the roof system represented as a spring. The last model consists of a building with cantilevered load-bearing walls. Since this project is mainly focussing on the behaviour of typical steel

portal frame buildings found in New Zealand, particular attention will be paid to the detail of the analysis of the first model.

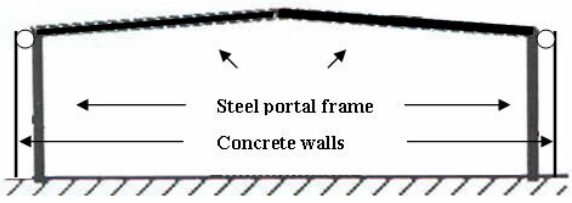

Typical industrial buildings (Model 1)

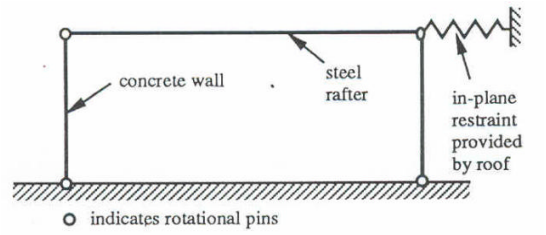

Buildings with non-cantilevered walls (Model 2)

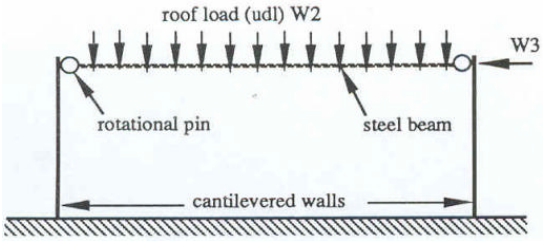

Buildings with cantilevered walls (Model 3)

Figure 4-23 Structural models as representation to the real buildings (O'Meagher *et al*., 1992)

Acceptable and Unacceptable Modes of Failures

The deformation mode is either acceptable or unacceptable as shown in Figure 4-24 below. For the frames collapsing into the building, it can be seen that the resulting deformation will not endanger adjacent property or person located outside the building provided that the boundary walls are tied together and fall inwards as a complete unit. This collapse mechanism will still maintain an adequate separation distance as the resulting horizontal separation will now be increased by the wall height, which is usually at least 5 metres. The inwards collapse may also extinguish the fire directly beneath the walls. This mechanism is contrasted with frames that collapse outwards and may lead to adjacent property being damaged or persons outside the building being endangered.

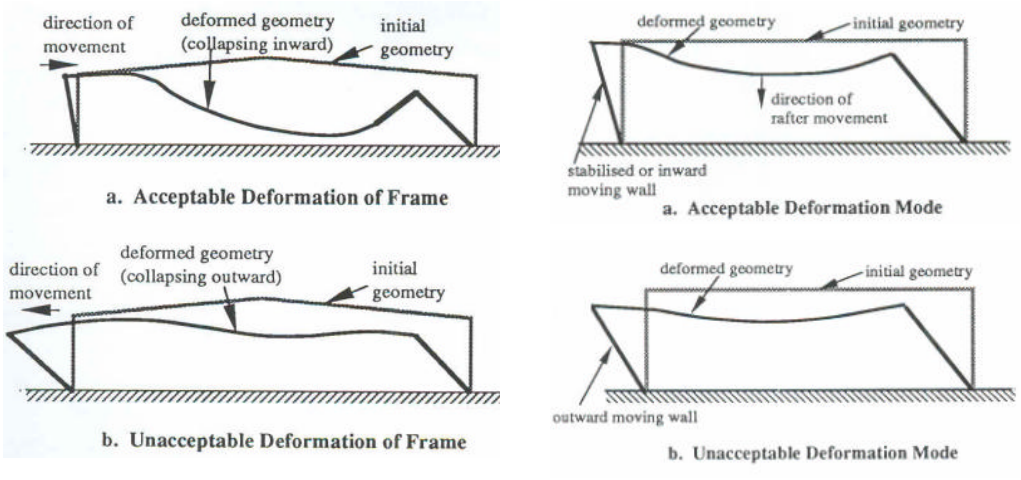

Figure 4-24 Acceptable and unacceptable deformation modes (O'Meaghter *et al.*, 1992)

Structural Model for Buildings with Steel Portal Frames (Model 1)

Various frame geometries, wind loadings, in-plane restraint to the rafter from cooler parts of the roof and the restraint provided by the column base connection were included in the study by O'Meagher *et al.* (1992). The heating situations considered are shown in Figure 4-25. The results show that for portal frames with typical restraint at the base of the column, the inwards collapse mechanism occurs irrespective of whether:

1. the steel column is fire protected or not;
2. the entire frame is heated; and
3. the steel frame is restrained against in-plane lateral movement by the cooler parts of the roof or not.

Potter (1994) supports this concept, but emphasises the importance of designing the connections between panels and structure to ensure they do not fail in the early stages of fire. As the wall panels are heated they tend to move outwards. The pulling of the panels inwards will only occur once the fuel load is high enough and sustained for a sufficient period. This allows the frame to soften and result in a plastic hinge mechanism which pulls the frame into the building.

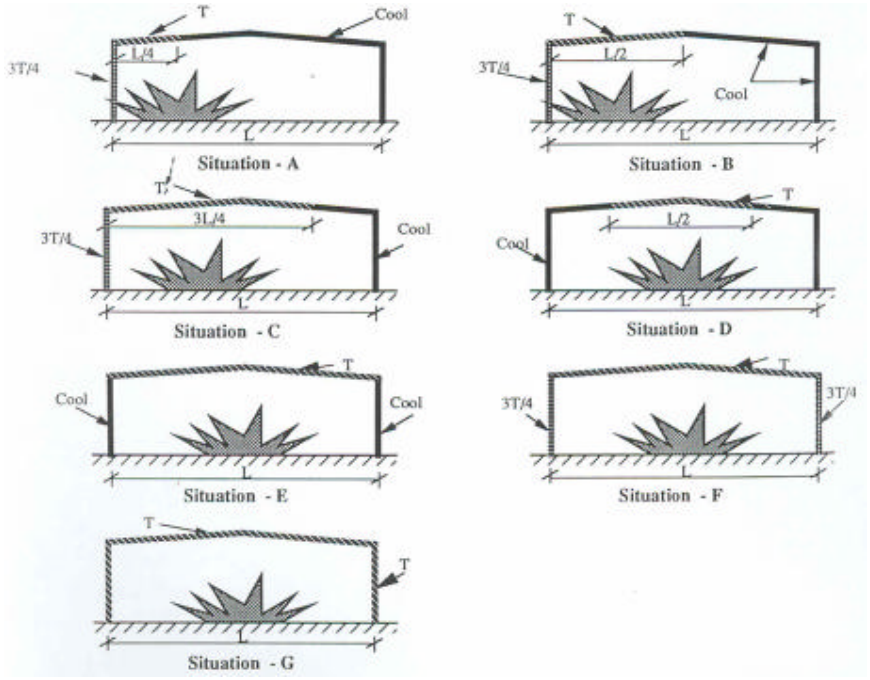

Figure 4-25 Heating Situations considered in the analyses by O'Meagher *et al*. (1992)

Multi-Bay Buildings

O'Meagher *et al*. (1992) describe that for multi-bay buildings where the bays are not separated by fire-resistant walls, the behaviour in fire will be similar to that found for single-bay buildings in which inwards collapse will occur. If the building is separated into a number of compartments, adequate lateral restraint to the top of the wall will be provided by the cooler roof members and effective compartmentation can be achieved.

Overall Building Behaviour

O'Meagher *et al*. (1992) utilised his results of 2D analyses carried out to study the behaviour of the whole building under elevated temperatures. The part of the building affected by the fire is resisted initially by the cooler roof immediately adjacent to the fire acting as a 'stressed skin' and the unheated roof diaphragm. As the forces to be resisted become too large, the cooler purlins and edge tie member will resist these larger forces and act as catenary members between the cooler sections of the roof structure. As the fire spreads outwards from its point of origin it will progressively affect the adjacent steel frames. The collapse of the frames which are located close to the point of fire origin will act as "anchors" to the rest of the building (Figure 4-26) causing it to collapse in an acceptable mode as shown in Figure 4-24.

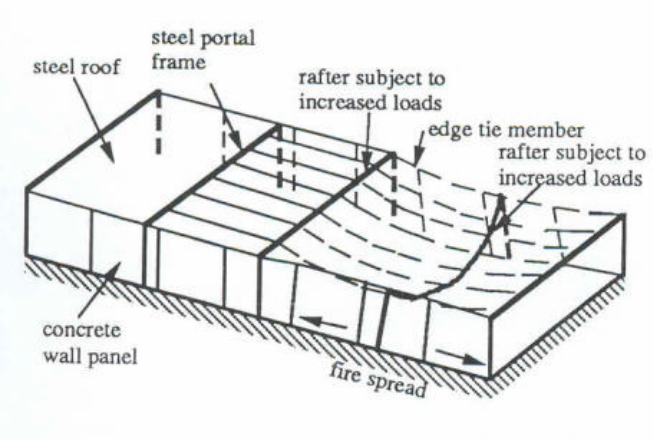

Figure 4-26 Overall building behaviour (O'Meagher *et al*., 1992)

O'Meagher *et al*. (1992) suggest that the roof must be properly braced and the steel frames must be tied adequately together to achieve the inwards collapse mode. They have also suggested the use of eaves tie members acting in combination with the roof purlins. They describe that there is no need to apply fire protection to either the purlins or the eaves tie member as the forces developed in these members during such progressive collapse are very small compared with their ambient capacity and also they will have sufficient capacity even at elevated temperatures. However, the connections between the rafter and the wall must be carefully detailed to avoid sudden roof collapse and to ensure that the desirable collapse mode occurs.

Structural models for buildings with a steel roof and concrete walls (Models 2 and 3)

The analysis of the model with non-cantilevered walls (Model 2 in Figure 4-23) can be easily performed using statics. The detail of the analysis is not presented here as this type of building is not commonly found in New Zealand. It has been found that adequate lateral restraint must be present in order to allow the simply supported rafter to deform downwards at elevated temperatures and pull the walls inwards. This will act as an imperfection and anchor to ensure that the remaining frames will deform in an acceptable manner. However, this assumes that the walls are adequately connected to the rafter and to each other.

The analysis with cantilevered walls involved various frame geometries, in-plane restraint from the roof and tensile capacity of the concrete walls. The heating situations considered are shown in Figure 4-27. The results showed that a frame will collapse in an unacceptable manner unless sufficient restraint is provided by the roof.

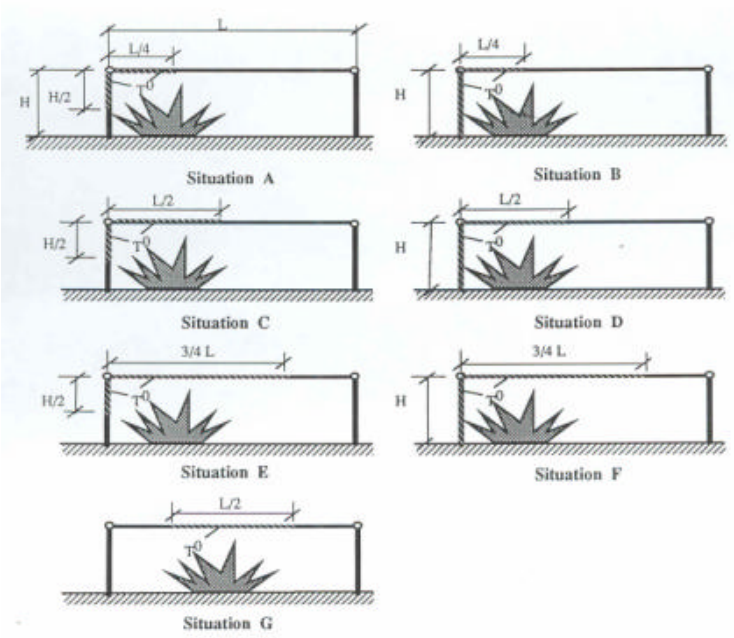

Figure 4-27 Heating situations considered for buildings with cantilevered walls (O'Meagher *et al*., 1992)

This is particularly valid if a fire occurs near one of the walls and the wall is exposed to substantial heating over the height. The steel rafter immediately above the fire will expand as its temperature increases and since the heated and unheated walls are tied together by the rafter, the movement of the heated wall will be resisted by the cooler wall. In some cases, the cooler wall will attract sufficiently high force such that it cracks at the base when the tensile strength is exceeded. The equilibrium of the frame is then dependent only on the stability of the heated wall. The heated wall will continue to deform outwards providing the fire has not decayed and the frame will collapse outwards once the heated wall forms a plastic hinge at the base and the forces generated are too large to be resisted by the cooler parts of the building (refer to Figure 4-28).

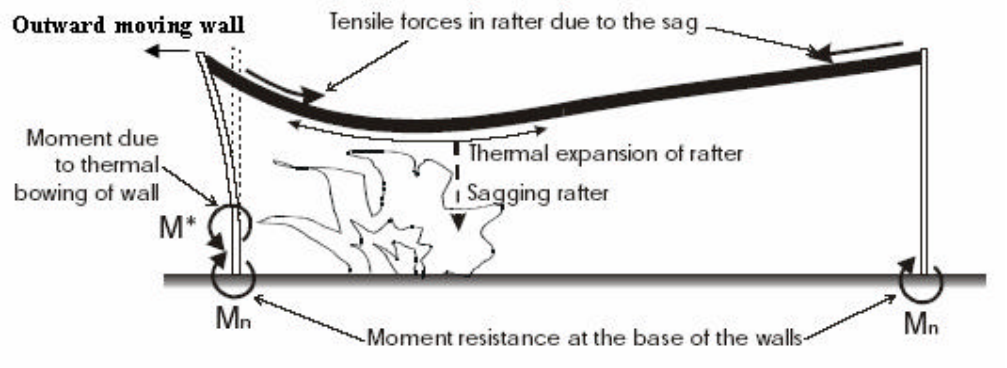

Figure 4-28 Outwards collapse of Cantilevered Wall Building (Lim, 2000)

O'Meagher *et al*. (1992) recommend that for this form of construction, it is important that the rafter deforms downwards as soon as possible under elevated temperatures as this will pull the walls inwards and achieve the desirable deformation mode as illustrated in Figure 4-24.

Multi-Bay Buildings

O'Meagher *et al*. (1992) describes how multi-bay buildings with fire occurring in an end bay, outwards collapse of the external wall is not possible due to the lateral support provided by the cool interior roof. However, this is assuming that the steel roof is properly connected to the external and interior walls. For a fire occurring in an interior bay, the interior walls will be laterally supported by the adjacent cooler roofs and will act as effective compartmentation to the fire.

4.4.3 Structural Fire Behaviour by Lim (2000)

Lim (2000) has used SAFIR to investigate the fire behaviour of industrial buildings with a roof structure supported on internal steel columns and cantilevered wall panels similar to that shown in Figure 4-5. Figure 4-29 shows the structural model used in his analysis and the fire occupies only half of the building. The spring represents the stiffness provided by the roof bracing or roof diaphragm which carries transverse loads back to the end walls.

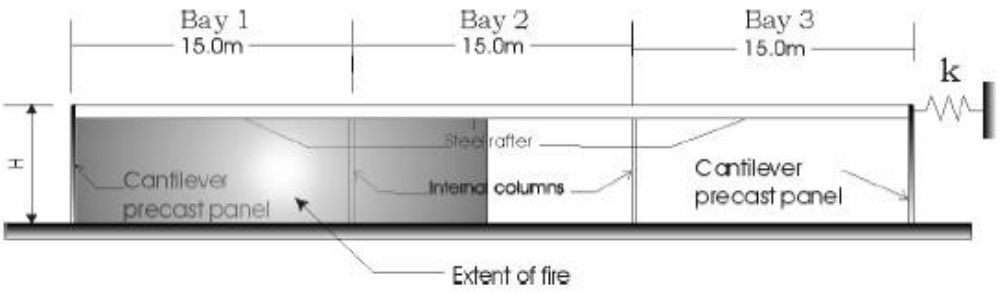

Figure 4-29 Structural model as representation of real building (Lim, 2000)

Unbraced and partially braced frames were analysed. Unbraced frames were analysed by assuming zero stiffness for the spring and by providing pinned connections between the steel beam and columns. Unbraced frames are found to be very unstable and failure is sideways collapse after the flexural resistance at the base of the wall panels is exceeded (Figure 4-30).

Scale factor = 2x

Figure 4-30 Sideway collapse of an unbraced frame with 6m high walls (Lim, 2000)

Partially braced frames were analysed by providing moment-resisting connections between the beams and columns and providing a spring of intermediate stiffness. It was found that the behaviour of a partially braced frame depends on the relative strength and stiffness of the heated wall panel which is trying to pull the building outwards due to thermal bowing, and the strength and stiffness of the beams and columns and roof bracing, all of which are resisting outwards collapse of the heated wall. Lim (2000) has shown that tall buildings with slender walls tend to collapse outwards, whereas less slender walls tend to be pulled inwards by a collapsing rafter during a fire. The outwards collapse of the frame occurs when plastic hinges form in the unheated columns resulting in the loss of sway resistance. For the frames collapsing inwards, the fire causes plastic hinges to form in the steel rafter and when

the rafter collapses, the attached wall panel is pulled inwards. Figure 4-31 shows an inwards collapse of a frame with 6 m high walls.

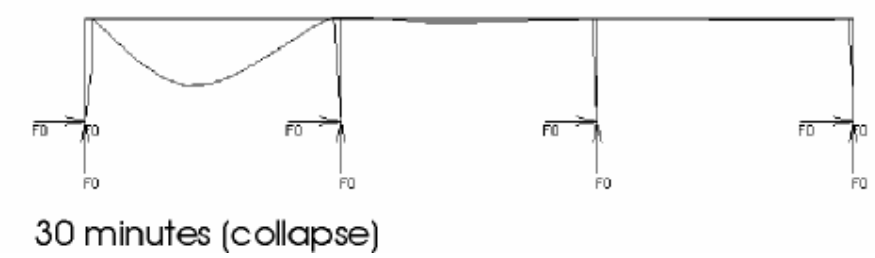

Scale factor = 2x

Figure 4-31 Inwards collapse of a frame with 6m high walls (Lim, 2000)

4.4.4 Structural Fire Behaviour by Wong *et al*. (2000) and Wong (2001)

Failure Temperatures of Steel Portal Frames using Plastic Theory

Wong *et al*. (2000) propose a simplified approach to estimate the failure temperatures of steel portal frames in fire based on plastic theory. The results from the approach were compared against detailed analyses from the finite element programme VULCAN developed at the University of Sheffield and it was shown that the proposed method gives a reasonably good estimation of the failure temperatures, particularly for the worst fire scenario in which the frame is heated overall.

Wong *et al*. (2000) show that the reduction factor, η, for the ambient plastic resistance moment (M_p) of the rafter section to cause the failure mechanism shown in Figure 4-32 is described by equation (4-1). The whole portal frame is assumed to be fully involved in a fire and the columns are pinned at the base.

$$\eta = \frac{wL^2}{M_p(3+\frac{h_1+2h_2}{h_1})} \qquad \textbf{(4-1)}$$

where,

w = Uniformly distributed load on the rafter (kN/m)

L = Half the span of the frame (m)

M_p = Plastic section capacity of the frame (kNm)

h_1 = Vertical distance from ground to knee (m)

h_2 = Vertical distance from knee to apex (m)

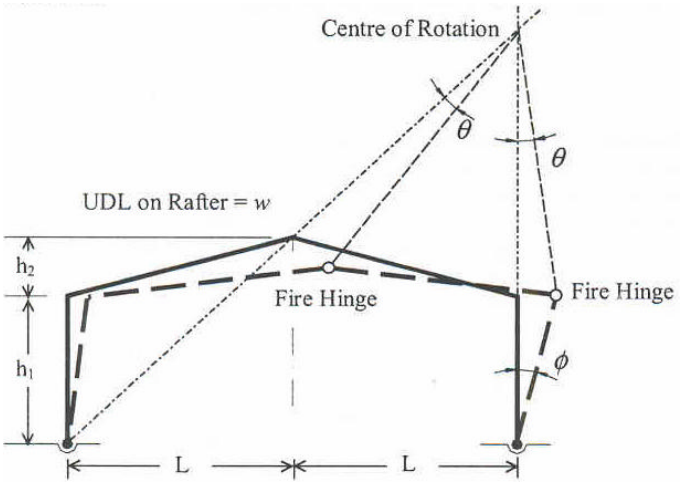

Figure 4-32 Failure mechanism for a pinned base steel portal frame fully exposed to a fire (Wong *et al.*, 2000)

Experimental Tests and Finite Element Modelling using VULCAN

Wong (2001) has conducted fire tests on a scaled steel portal frame structure and finite element modelling using VULCAN. The finite element modelling included two and three dimensional analyses, and a number of parameters were investigated, including the effects of vertical and horizontal loads, frame geometry, heating condition and rotational stiffness. The influence of secondary members was also investigated in the three-dimensional studies using different fire scenarios.

The fire tests were conducted on a scaled-down structure of steel portal frames with 30 m span and 12 m column height using a scale factor of 5 (Figure 4-33). The supports at the column bases were pinned. The fire tests involved steel sheeting, supported on Z-purlins and I-beams (i.e. universal beams) and the liquid heptane was used as the fire source. The roof structure was heated and it was found that the purlins were able to give a substantial level of horizontal restraint to the rafter and the heated rafter experienced a snap-through failure mechanism, in which fire hinges could clearly be identified near the eaves (Figure 4-34). In addition, the collapse of the rafter pulled the eaves inwards.

Figure 4-33 Scaled-down steel portal frame structure (Wong, 2001)

Figure 4-34 Collapse of the roof structure (top) and plastic hinges formed during the test (bottom) (Wong, 2001)

Wong (2001) has demonstrated that the upward movement of the apex is larger for frames with higher span/height ratio from the finite element modelling results. However, all the frames analysed fail at approximately 700°C, even through the span/height ratio varies from 2 to 12. It has been found that the failure temperatures are influenced by the load ratio and not by the frame geometry.

The extra rotational stiffness of nominally pinned bases is shown to be beneficial to the failure temperature of the portal frame compared to the normal assumption of ideally pinned bases. Wong (2001) mentions that heating may cause sideways overturning of the frame for ideally pinned portal frames. However, there is little evidence that this has ever taken place in reality but it demonstrates the importance of considering various fire scenarios as potential worst cases. Wong (2001) states that the overall rotational stiffness, in particular the interaction between the foundation and the soil, and the effects of elevated temperatures on the support connections are not well known. Therefore, it is difficult to quantify the actual benefit of the semi-rigid behaviour of the column base.

4.5 Concrete Walls

When a fire occurs in an industrial building, the concrete wall panels will be subjected to different forces apart from the heat induced stresses. In the initial stages of the fire, the heating of the steel rafter can cause axial thrusts to the top of walls. In the later stages of the fire, the rafter will sag and will impose catenary forces which will pull the walls inwards providing the connections holding the walls to the supporting frame are still strong enough at elevated temperatures. Additional forces may also be transmitted to the walls and the adjacent structures from the collapse of the heated frame. The walls may also be subjected to simultaneous wind forces. Explosions occurring inside the building could also cause impact forces on the walls. This section described the phenomenon of thermal bowing and the previous research carried out on concrete walls.

4.5.1 Thermal bowing

It is well understood that when a structural element is heated on one side, the temperature gradients that exist across the thickness of the element will result in non-uniform thermal expansion and cause the element to bow. This phenomenon is known as thermal bowing. The one side heating of materials such as concrete and brickwork with low thermal conductivity will result in steep thermal gradients at the heated face and the thermally induced curvature of these materials is significant.

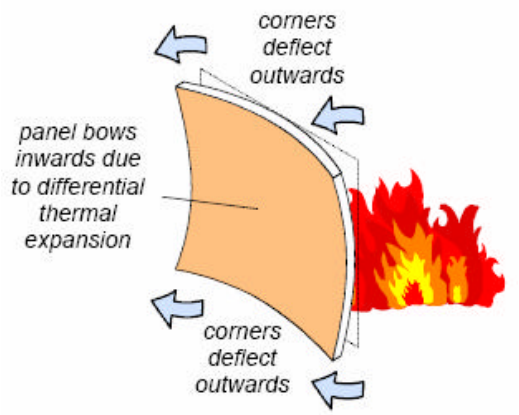

Figure 4-35 Thermal bowing of a concrete wall (Bennetts and Poh, 2000)

4.5.2 Behaviour of Concrete Walls at elevated temperatures

Munukutla (1989), O'Meagher and Bennetts (1991) and O'Meagher (1994) have investigated the behaviour of concrete walls at elevated temperatures using FIREWALLS, a finite element computer programme. A brief description of FIREWALLS is given in Section 4.5.4. Lim (2000) has used SAFIR to study the behaviour of free-standing cantilever walls and propped cantilevers with slenderness ratios ranging from 40 to 80. This section summarises the findings from their analyses.

Munukutla (1989) studied the behaviour of cantilever wall and found that the deflections at the top of the wall increases at any given time when the slenderness ratio increases. The time to failure of a cantilever wall also decreases with increasing slenderness ratio. A propped cantilever wall which simulates a wall attached to a fire protected rafter at the top was also investigated. Munukutla (1989) concludes that increasing axial load on the wall will increase the moment capacity, which in turn causes the horizontal reaction to increase. It has also been found that the horizontal reaction of the wall decreases proportionately to the height and increases with increasing thickness.

O'Meagher and Bennetts (1991) have also used the programme to investigate the behaviour of walls that are pinned at both ends. A parameter study of the effects of various parameters was conducted, which includes different slenderness ratios (H_w/t_w), amount and locations of reinforcement, and axial loads applied at the top of

the walls. It should be noted that their walls have axial loads applied at the top, which is very uncommon for typical industrial buildings found in New Zealand. It has been found that the load capacity of the wall reduces significantly with high slenderness ratios. It has also been found that walls with greater cover to reinforcement perform better. It has also been shown that the introduction of end restraint to the wall reduces the horizontal deflection.

O'Meagher (1994) carried out comprehensive structural analyses on walls with pinned and fixed restraints. The ISO 834 standard fire curve was applied to one side of the walls and two different heating conditions were considered. His results show that when the full height of a wall is heated, the deflections of the wall are much larger than a wall heated along the top two-thirds of its height. Lim (2000) has also found that free-standing cantilever walls exposed to ISO fire at only the top three quarters of the wall height are able to survive the fire longer. He has also found that the results are sensitive to the design fire used in the analysis.

Lim (2000) obtained the stress distribution through a 150 mm thick free-standing cantilever wall exposed to ISO 834 standard fire on one side (see Figure 4-36). The concrete near the heated surface expands as the temperatures increases, causing local thermal expansion which induces compressive stresses near the hot face, balanced by tensile stresses in the central reinforcement and additional compressive stresses near the cool face of the wall. The tensile stresses in the central reinforcement reach the yield stress of the steel, which is well off the scale in the figure. Figure 4-37 shows the internal actions and reactions taking place at the base of the wall due to heating on one side.

Lim (2000) concludes that tall and slender walls are likely to buckle or collapse outwards if they are not well connected to the steel frame or if the building has insufficient resistance to transverse forces. He suggests that if the wall panels cannot be effectively connected to the steel frame, then measures have to be taken to control the thermal bowing deflections including provision of intermediate concrete columns fixed to the wall panels, increasing the thickness of the wall panels, or increasing the reinforcing in the wall panels. In the event of a fire, the strength and stiffness of the eaves tie members and connections between the wall panels and the supporting

structure may be compromised. If these fail and the walls are cantilevered at the base, the walls would behave very similar to free-standing cantilever walls and collapse outwards.

Lim (2000) has shown that propped cantilever walls do not suffer large out-of-plane deflections when subjected to a fire on one side. They bow inwards towards the fire and form a plastic hinge at the base. Slender propped cantilever walls exhibit larger out-of-plane deflection and fail early compared to stockier propped cantilever walls, however, stockier walls impose larger horizontal forces on the supported rafter.

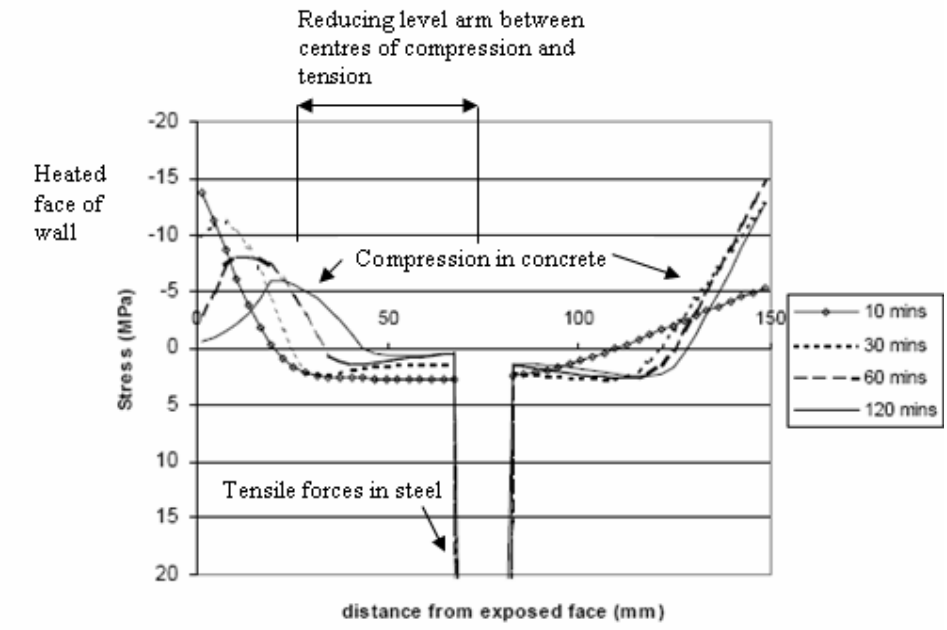

Figure 4-36 Stress distribution in a 150 mm thick cantilever wall exposed to the ISO 834 standard fire (Lim, 2000)

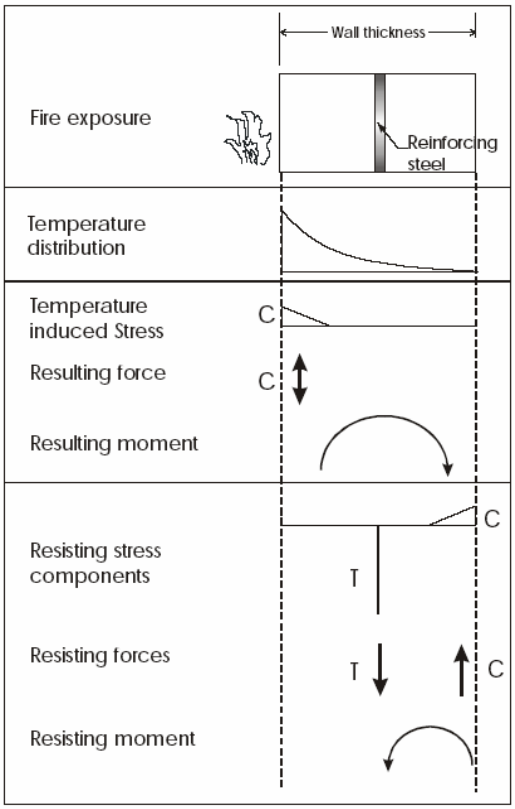

Figure 4-37 Actions and reactions due to heating on one side (Lim, 2000)

4.5.3 External Concrete Wall Design Considerations

The results from O'Meagher *et al*. (1992) suggest that cantilevering the concrete walls will not ensure an acceptable collapse mode unless sufficient restraint is provided by cooler parts. O'Meagher *et al*. (1992) further discussed the design of external walls for typical industrial buildings and suggest that these walls should not be constructed such that they are cantilevered out of the ground and not attached to the rest of the structure. This is because the walls are very unlikely to remain essentially intact and vertical throughout the fire while the steel frame deforms. The use of cantilevered walls will result in outwards collapse of the walls due to thermal bowing effects. As mentioned previously, outwards collapse of a wall may endanger persons outside the building or the adjacent property. The performance of these walls may therefore be such that the objectives of the building code will not be satisfied.

Munukutla (1989) proposed the use of intermediate columns to reduce the effective height of the wall panels and to reduce deformation at the top. O'Meagher *et al*. (1992) have stressed that the fire resistance of a cantilever wall is very much less than that associated with a wall which is pinned at both ends due to larger deflections that will occur in the cantilever wall. They recommended that a cantilever wall will need to be substantially thicker than a pinned wall of the same height if the same fire resistance is to be achieved.

For buildings with the steel roof structure supported on tall cantilever walls and internal steel columns, Lim and Buchanan (2003) suggest that all panels must be well connected to each other at the top using an eaves tie member well bolted to each member. They also suggest that if a full roof diaphragm can be relied on, the wall panels can have a slenderness ratio of up to 100. If only partial roof diaphragm action can be relied on, the wall panels should not exceed 9m and the slenderness ratio should not exceed 65. However, if there is no bracing from the steel roof framing, the concrete wall panels must be designed with a cantilever base with a height of less than 6 m if they are load bearing, or 8 m in height if they are non-load bearing.

4.5.4 FIREWALLS

Introduction

FIREWALLS is a computer programme developed to analyse the structural performance of a concrete wall exposed to fire. This programme was originally developed by O'Meagher and Bennetts (1987) and was restricted to walls with both ends pinned. It was later modified by Munukutla (1989) to include various boundary conditions at the top and bottom of the wall. O'Meagher and Bennetts (1991) analysed the behaviour of walls pinned at both ends based on different slenderness ratios (H_w/t_w), amount and locations of reinforcement, and axial loads applied at the top of the walls. The effect of end restraint on the fire resistance was also discussed. The results of their analyses are summarised in Section 4.5.2. This section gives a brief description of the computer model.

Description of the Theoretical Model

The model allows for geometric as well as material non-linearity, and is based on consideration of strain compatibility and force equilibrium in the wall. The thermal and structural behaviour of the wall is assumed to be uncoupled.

4.5.4.1 Thermal Analysis

The thermal distribution across the thickness of the wall exposed to fire on one side is modelled using a finite element procedure. The temperatures thus generated are used as input data to the structural analysis to permit the influence of the temperature on mechanical properties to be taken into account. The original programme was written to read temperature data generated by the computer programme, TASEF-2, developed by Wickström (1979). Munukutla (1989) developed another computer programme, HEAT, to estimates the temperature distribution through concrete walls and on the unexposed surface during an ISO 834 standard fire test. The flow chart in Figure 4-38 describes the overall analysis procedure.

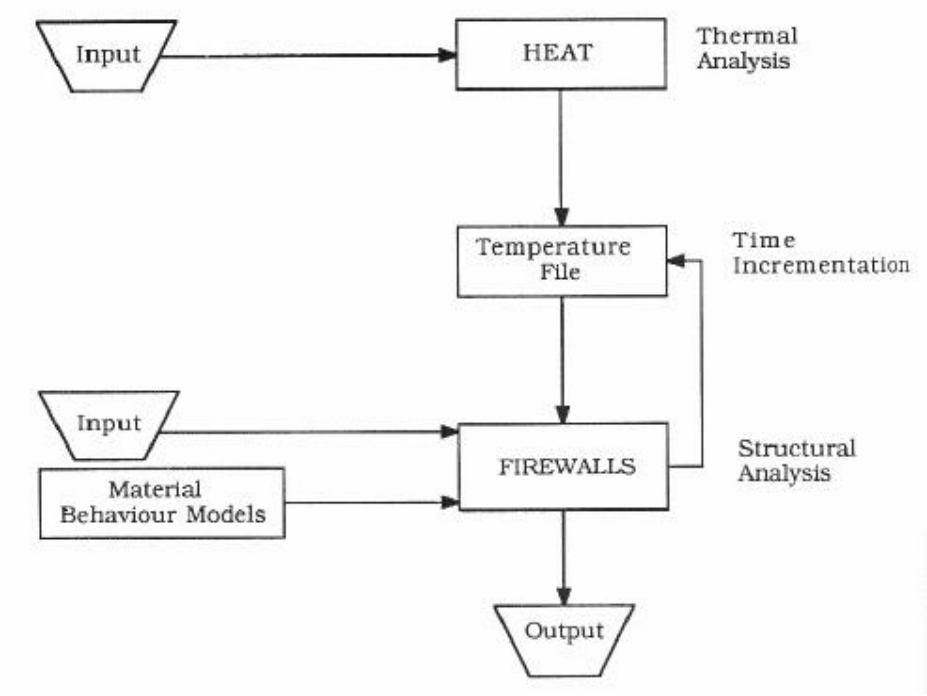

Figure 4-38 Flowchart showing the overall analysis procedure taken by Munukutla (1989)

4.5.4.2 Structural Analysis

The model for predicting the structural behaviour of walls in fire takes account of the geometric or compatibility relationships, the deformation behaviour of concrete and reinforcing steel under elevated temperatures (the constitutive equations) and equilibrium requirements as described in more detail below.

Geometric Assumptions

Discretisation of Wall

The unit length of wall is divided is divided into a number of segments throughout its height. Each segment is then divided into a number of transverse elements across its thickness. This is shown in Figure 4-39.

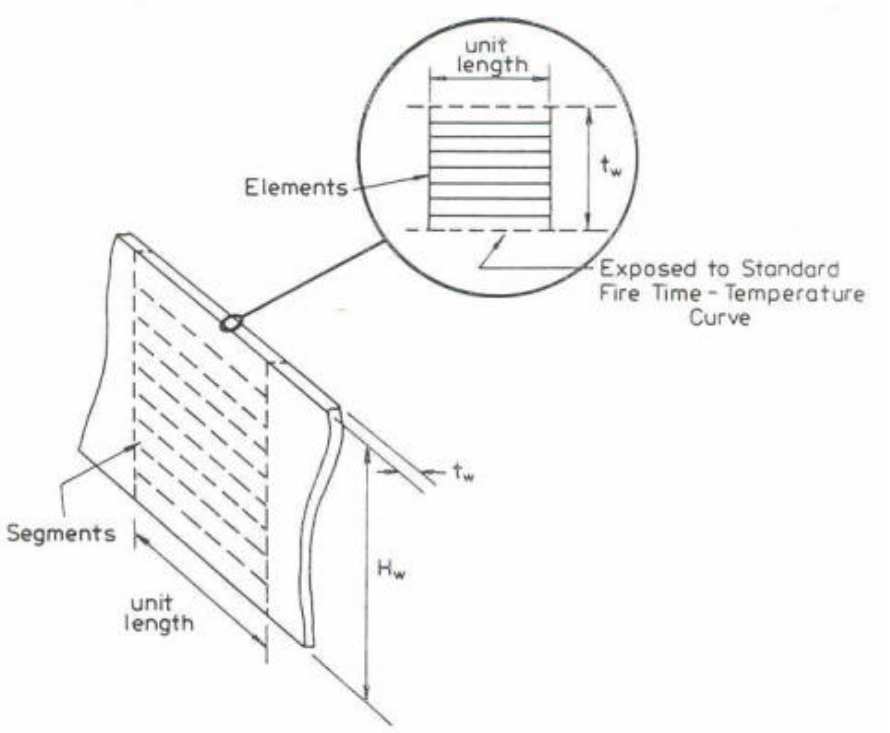

Figure 4-39 Discretisation of the wall (O'Meagher and Bennetts, 1991)

Strain State in a Segment

Within any segment it is assumed that the deformation of the elements is such that plane sections remain plane. In addition, within a segment the curvature is assumed to be constant.

Deformation Behaviour or Constitutive Equations

Constitutive equations are used to describe concrete and steel deformation. For both concrete and steel, strain resulting from thermal expansion, stress related strain and creep strain are considered. For concrete, transient strain is also incorporated into the concrete constitutive equation. A comprehensive description of each strain component in concrete is given by Anderberg (1976). The variation of reinforcing steel strain components is taken from Bennetts (1981) and the creep strain in steel is calculated using the creep model proposed by Harmathy (1967).

Equilibrium requirements

As the strain state within a segment is considered to be constant, the strain state and therefore stress state can be determined by satisfying the following equilibrium equations shown in Figure 4-40.

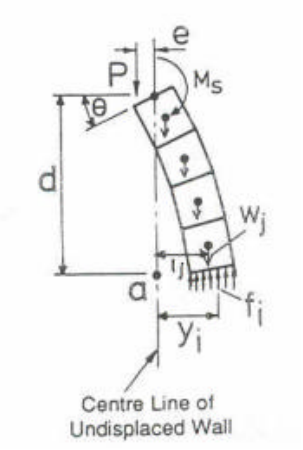

$$\Sigma f_i = P$$

$$\Sigma f_i y_i - \Sigma W_j I_j - M_s(H-d)/H + P.e = 0$$

where,

P = Applied vertical load

M_s = Spring moment = $K\theta$

$f_i y_i$ = Element force x moment arm

H = Wall height

$W_j I_j$ = Self weight of wall x moment arm

e = Eccentricity of applied load

d = Distance from a to location of the spring

Figure 4-40 Equilibrium equations of the wall (O'Meagher and Bennetts, 1991)

P-delta effects

To allow for P-delta effects, it is necessary to calculate the lateral displacement of the wall at each segment boundary. Given the curvatures of the wall at each segment boundary, the deflected shape of the wall can be determined as shown in Figure 4-41.

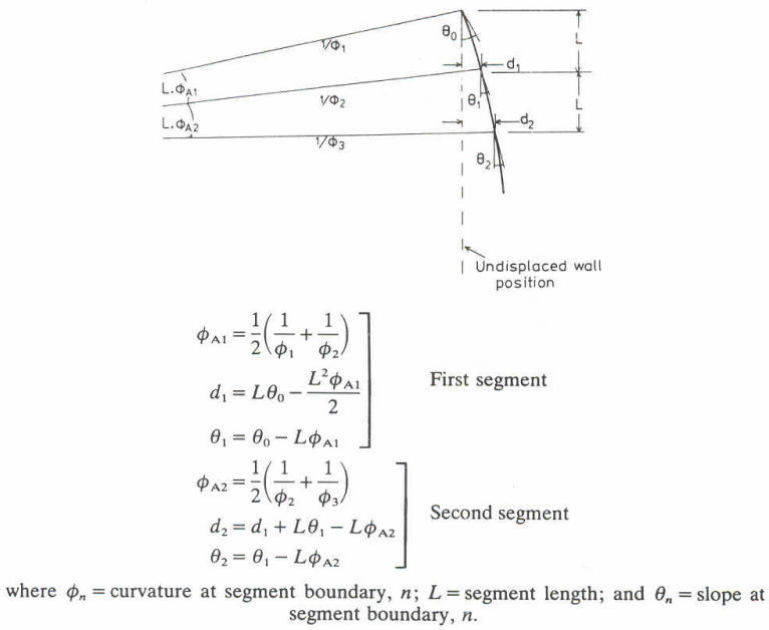

$$\left.\begin{aligned} \phi_{A1} &= \frac{1}{2}\left(\frac{1}{\phi_1}+\frac{1}{\phi_2}\right) \\ d_1 &= L\theta_0 - \frac{L^2\phi_{A1}}{2} \\ \theta_1 &= \theta_0 - L\phi_{A1} \end{aligned}\right\} \text{First segment}$$

$$\left.\begin{aligned} \phi_{A2} &= \frac{1}{2}\left(\frac{1}{\phi_2}+\frac{1}{\phi_3}\right) \\ d_2 &= d_1 + L\theta_1 - L\phi_{A2} \\ \theta_2 &= \theta_1 - L\phi_{A2} \end{aligned}\right\} \text{Second segment}$$

where ϕ_n = curvature at segment boundary, n; L = segment length; and θ_n = slope at segment boundary, n.

Figure 4-41 Procedure for displacement calculation (O'Meagher and Bennetts, 1991)

4.5.4.3 Time Steps

An incremental analysis procedure is adopted to evaluate the structural behaviour due to the material properties vary with temperature and therefore with time. The time steps taken by O'Meagher and Bennetts (1991) and Munukutla (1989) are as follows:

Time range (Hr)	Time Step Increment (Hr)
0 – 1	0.01
1-4	0.1

4.5.4.4 Solution Procedure

For each time step, each segment boundary down the wall is analysed in turn. A set of total compatible strains is proposed for the concrete and the steel elements. The stress-related strains for the concrete and the steel elements are then obtained using the stress-strain laws modified for element temperatures.

Equilibrium at the segment boundary is checked to determine whether the proposed strains state is valid. If equilibrium is achieved then the next segment boundary down the wall can be analysed for the current time step. If there is no equilibrium, a new set of total strains is proposed. When a set of proposed total strains which satisfy equilibrium cannot be found, then the wall is regards as having failed. Once a solution has been obtained satisfying both equilibrium and boundary conditions, the P-delta effects are considered and the calculations above are repeated. When a very small change between successive displaced shapes is obtained it is considered that a solution for the current time step has been found.

4.6 Design of Connections between Concrete Walls and Supporting Structure

The Building Code of Australia (Australian Building Codes Board, 2004) specifies the requirements for the performance of concrete external walls that could collapse as complete panels when exposed to fire on one side (refer to Section 2.2.3). The panels become detached due to poor design and detailing of the connections between the supporting structure and the panels. Bennetts and O'Meagher (1995) provide design details for the connections which may satisfy the requirements of the Building Code of Australia. Bennetts and Poh (2000) have reviewed their design details and stressed that the outwards collapse of wall panels depends on, to a lesser extent, the behaviour of the wall panel and bare steel frame; and to a large extent, the connections between the panel and the frame.

4.6.1 Design Philosophy adopted in Australia

Bennetts and Poh (2000) suggest that the connections must be able to hold the panels if the supporting columns deform outwards. Similarly, if the supporting columns deforms inwards, the connections must be able to pull the panels inwards (see Figure 4-42). The connections should also allow for substantial relative deflection between the panel and the column at the point of attachment. The forces developed in the connections depend on the degree of restraint imposed on the panel. For example, high restraint will develop high forces in the connections and vice versa. This is particularly true if steel columns are protected with concrete encasement. The concrete encasement does not only reduce the temperature rise but also increases the strength and stiffness of the steel columns.

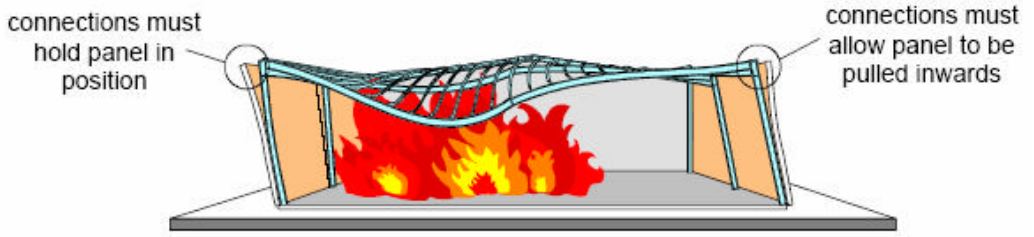

Figure 4-42 Connections attaching the wall panels to the frame (Bennetts and Poh, 2000)

Rigid Connection

Figure 4-43 shows a typical rigid connection used to attach wall panels to the supporting structure. This type of connection can only be used when the potential movement of a wall panel at the points of restraint is relatively small. Bennetts and Poh (2000) describe that this type of connection is only suitable for a panel having a height of less than 2.5 metres, or the panel is supported at the top and bottom only, or the panel is supported by a column which has an ambient capacity of less than 50 kNm (Figure 4-44).

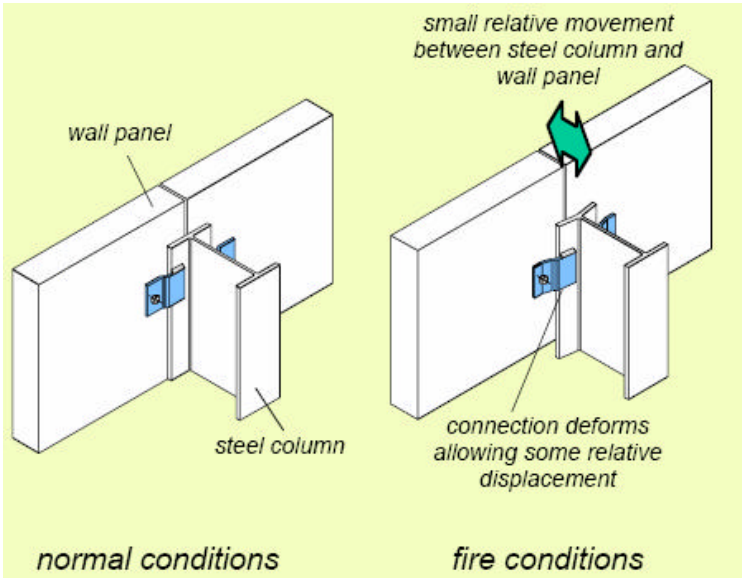

Figure 4-43 Typical rigid connection (Bennetts and Poh, 2000)

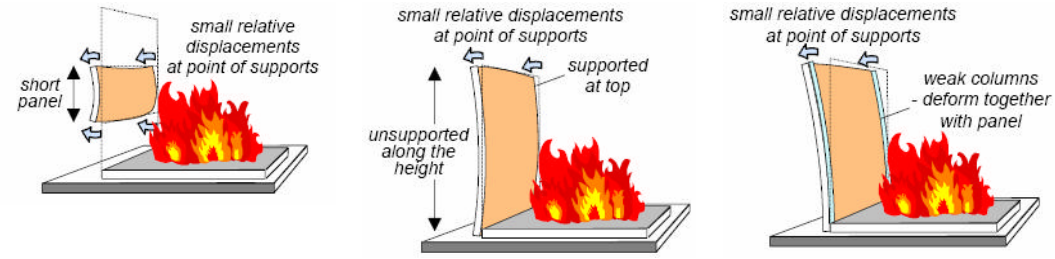

Figure 4-44 Conditions for using rigid connections (Bennetts and Poh, 2000)

Flexible Connection

Figure 4-45 shows a flexible connection which can stretch during fire to minimise the development of high restraining forces. This type of connection must be used when a panel having a height of more than 2.5 metres and is supported by a relatively stiff structure. This includes wall panels attached to a column having an ambient bending capacity of greater than 50 kNm or by another panel at right angles (Figure 4-46).

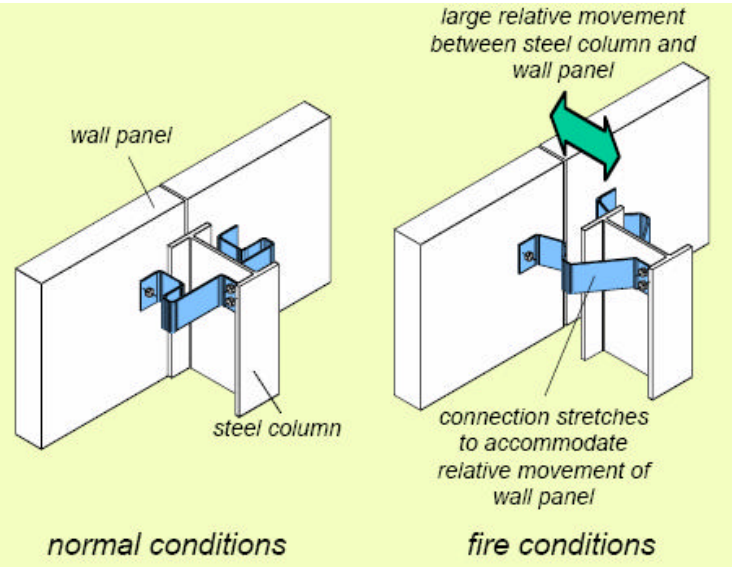

Figure 4-45 Typical flexible connection (Bennetts and Poh, 2000)

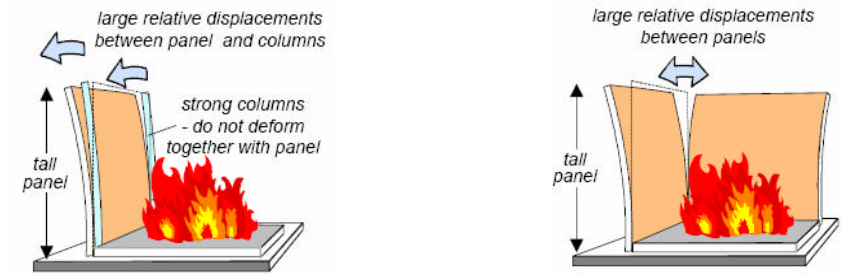

Figure 4-46 Conditions for using flexible connections (Bennetts and Poh, 2000)

Bennetts and O'Meagher (1995) have proposed two flexible connections between the walls and the column given that the bending capacity of the column exceeds 50 kNm (Figure 4-47). The use of the flexible connection shown in Figure 4-47 (a) is for universal columns of 360UB or larger and is subjected to the criteria shown in the figure. The use of flexible connection shown in Figure 4-47 (b) is appropriate for

situations where the panel height is less than 7.5 metres and the supporting columns are spaced at less than 7.5 metres.

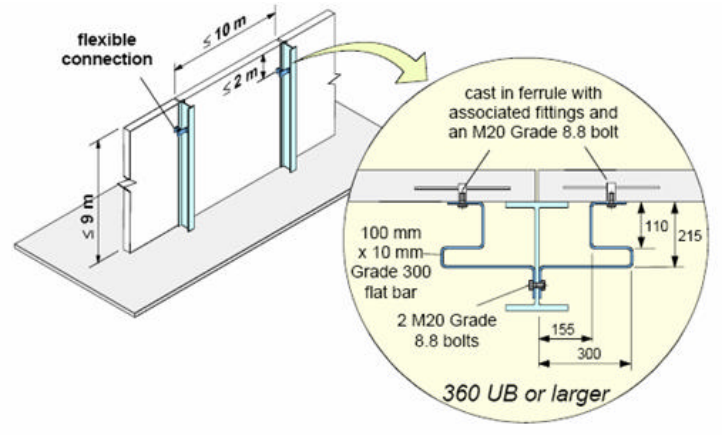

(a)

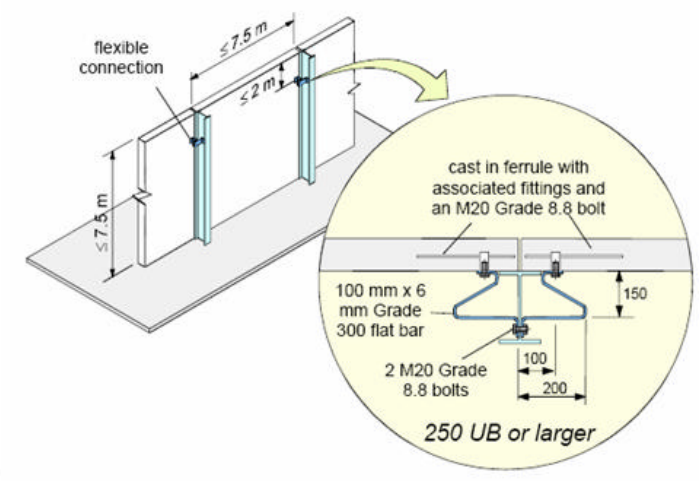

(b)

Figure 4-47 Details of flexible connections (Bennetts and Poh, 2000)

In cases where the side wall panel meets the end wall panel at right angles in a corner and there is no column located at the junction to support the panels, the panels at that junction are required to support each other. Excessive deformation will occur at the point of attachment due to the tendency of both panels to bow outwards at elevated temperatures (refer to Figure 4-48). Bennetts and O'Meagher (1995) suggest that a single flexible connection shown in Figure 4-49 is adequate for connecting the panel together. The connection detail is similar to that shown in Figure 4-47 (a) and for smaller panels, the connection detail shown in Figure 4-47 (b) may be used provided the panel sizes are less than 7.5 metres high by 7.5 metres wide.

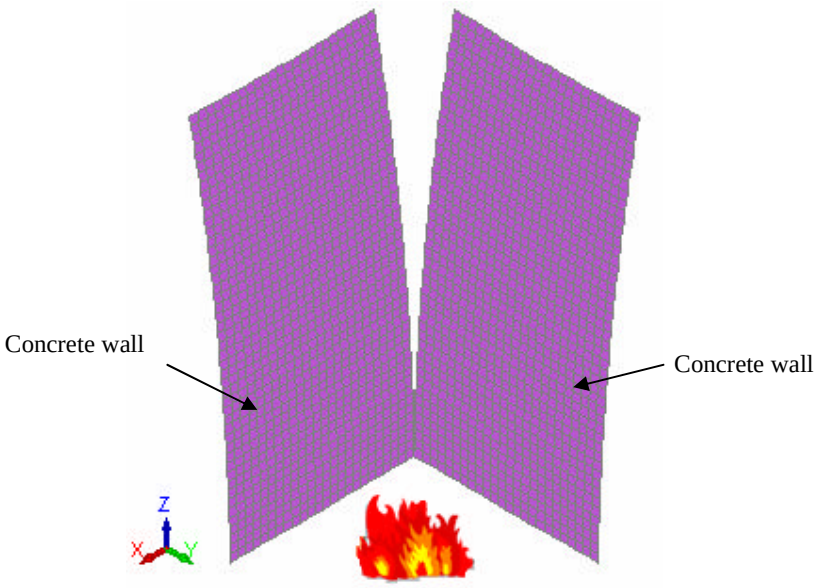

Figure 4-48 Thermal bowing of walls located in a corner

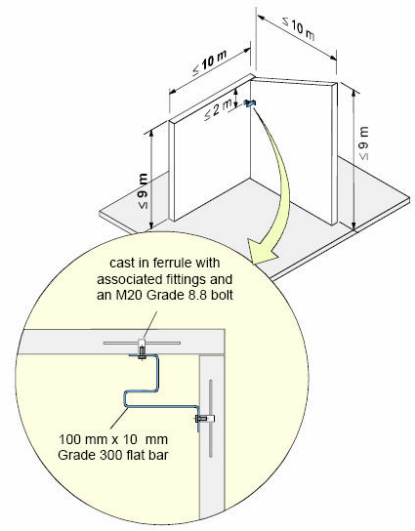

Figure 4-49 Flexible connection to be used in a corner (Bennetts and Poh, 2000)

4.6.2 Design of Connections in New Zealand

Clifton and Forrest (1996) argue that the connection details recommended above in Bennetts and O'Meagher (1995) and similarly in Bennetts and Poh (2000) are not suitable in New Zealand due to seismic requirements. Clifton and Forrest (1996) suggest the use of the eaves channel restraint shown in Figure 4-50. The restraint system consists of a channel which runs between the portal frame knees at eaves level, and is connected to the panels and to the portal frame. The design of the system under both fire and earthquake conditions is given in Clifton and Forrest (1996). In a severe fire, the channel will form a fire hinge just beyond the connection to the panel and allow the required rotation to occur as shown in Figure 4-51. The channel is connected to the steel column through a single bolt and a sliding hole to allow the outwards bowing of the wall panels.

For the connection to support the side wall and the end wall in a corner, a practicable detail for the connection cannot be developed to accommodate the same degree of movement which can occur in fire conditions, while still work in seismic conditions. Clifton and Forrest (1996) have reached a compromise solution involving a bent plate and slotted holes shown in Figure 4-52.

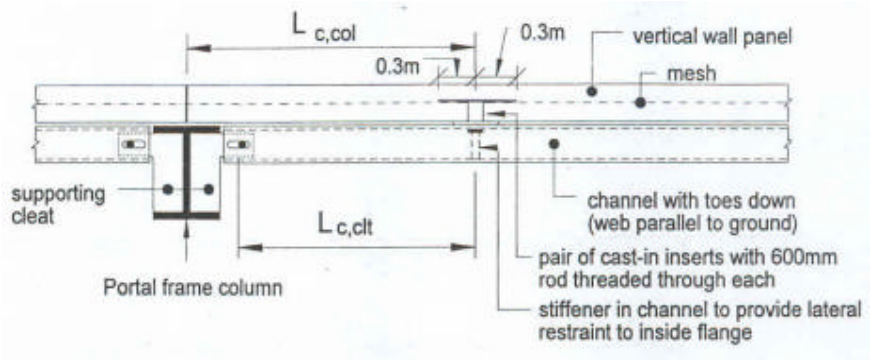

Figure 4-50 Detail of eaves channel restraint (Clifton and Forrest, 1996)

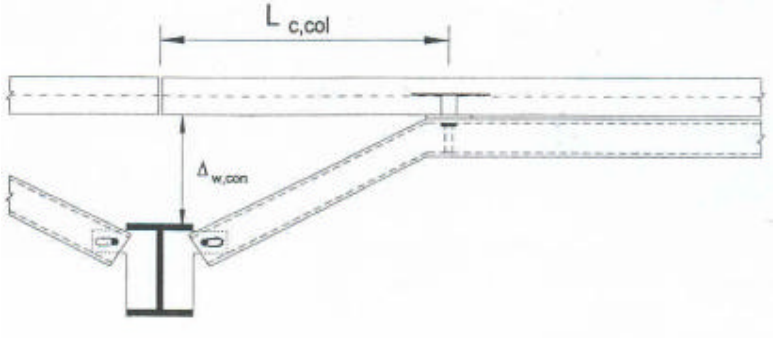

Figure 4-51 Eaves channel restraint under elevated temperatures (Clifton and Forrest, 1996)

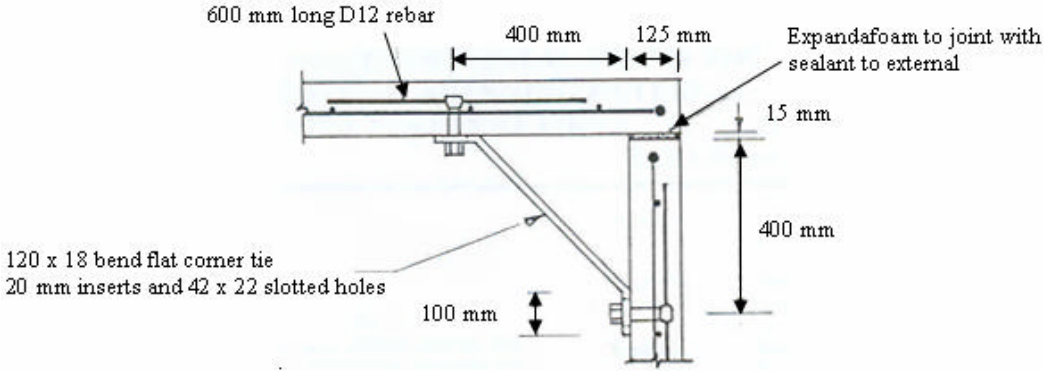

Figure 4-52 Connection detail between side wall and end wall (Clifton and Forrest, 1996)

4.7 Connection Details at Column Base

The details of fully fixed and pinned connections at the column base are shown in Figure 4-53. It is common to design a steel portal frame by assuming partially fixed support conditions at the column base. The connections must provide adequate column moment restraint to prevent outward collapse of the column and the attached walls during a fire. Clifton and Forrest (1996) have suggested that a nominally pinned four bolt extended endplate should be provided for overall stability and this connection requires the use of the following:

- a 20 to 25 mm thick endplate
- four M20/4.6 bolts or larger
- a 6 mm fillet weld all round between the baseplate and the columns

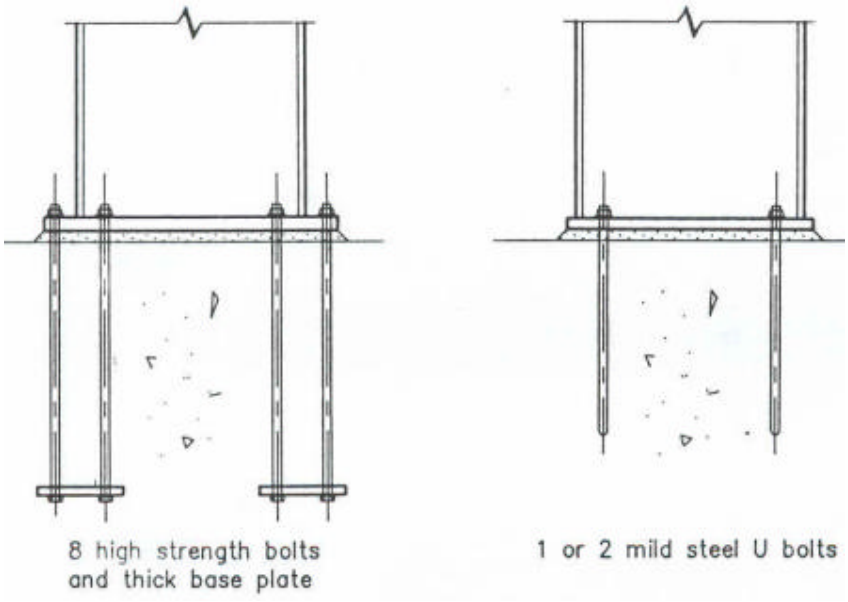

Fixed *Pinned*

Figure 4-53 Typical connection details for fixed and pinned conditions at column base (Woolcock *et al.* ,1993)

4.8 Reports of Fire Incidents in Warehouse and Industrial Buildings.

Cosgrove (1996) conducted a survey on warehouse and industrial fire incidents in New Zealand and found that a total of 626 fire incidents have occurred from 1988 to 1994. This includes 121 incidents related to warehouse facilities, and 505 to manufacturing complexes. Although warehouse and industrial building fires account for only about 15% of all fires, they represent up to 50% of financial loses. The highest number of fire incidents occurred at wood and paper products facilities (42%), followed by wood product facilities (11%) in the manufacturing industry. In warehouse occupancies, fire incidents in general storage faculties dominate (27%), followed by wood and paper products (21%).

Cosgrove (1996) also investigated the extent of damage for all incidents, and found that either the fire was contained within the area of fire origin, or it grew and involved the whole building since most industrial buildings consisted of large unpartitioned spaces. If a fire becomes out of control, then the whole structure would be likely to be damaged in some form.

4.8.1 Real Fire Incidents

In the event of a major fire within such an industrial building, it is possible that the external wall, or part of it, may collapse outwards. This possibility has been realised in a number of fires and fire fighters are concerned about the detachment of concrete panels in fire. The collapse of external wall panels does not give adequate warning as opposed to the progressive collapse of unreinforced masonry walls.

This section describes the observed structural fire behaviour of typical steel portal frame buildings from two severe fire events (Fire Hazard Category 4) in Christchurch. The construction form of the buildings is similar to that shown in Figure 4-1. Concrete tilt-up wall panels were attached to the columns or to each other at the corners using bolted connections similar to Figure 4-12 (b) and Figure 4-15 (d) shown previously.

Christchurch, 2003

A fire occurred in a storage warehouse for expanded polystyrene products in Christchurch in 2003. The building was located close to boundary on three sides (Figure 4-54). Some portal legs were encased in concrete to about two-thirds of the full height and the lower portions of the end walls were attached to cast *in-situ* concrete columns. The bolted connections holding the side wall and end wall at the corner were protected with intumescent materials. A fire rated store room was also constructed in the north-west corner of the building using tilt-up concrete walls. The building was fully involved in the fire and the flame height was observed to fluctuate between 2 to 3 metres above the building. The fire service personnel had decided to let the fire extinguish itself as the fire was outside their control at the time they arrived. Surprisingly, the fire rated store room including the roof structure was only affected by the fire to a small extent.

During the fire, large horizontal deflections had been observed for the walls at the corners of the building. After the fire, the end walls suffered permanent deformations, although the degree of deflection was very much less than that observed during the fire (Figure 4-55). The plastic skylights had melted and the roof collapsed onto the ground. The purlins and steel rafters were observed to deform excessively in torsion (Figure 4-56). The purlins in one of the bays closest to the end walls failed at one end and the other end was attached to the end walls (Figure 4-57). Extensive spalling of concrete had also occurred during the fire. Spalling of concrete is discussed further in Section 4.8.2. Although the roof had collapsed during the fire, the elements engulfed in the flame may still be exposed to very high temperatures.

Although the walls did not collapse during the fire in this incident, the wall panels attached to the unprotected columns were very unstable after the fire and were pushed onto the ground for safety purposes. The walls attached to the protected columns were still standing upright after the fire (Figure 4-58). Interestingly, the corner of a western wall panel had been observed to break off during the fire (Figure 4-59). This western wall was attached to a protected column on one side and an unprotected column on the other side. The break off of the corner was possibly due to inwards pulling at the top of the unprotected column induced by the collapsing rafter.

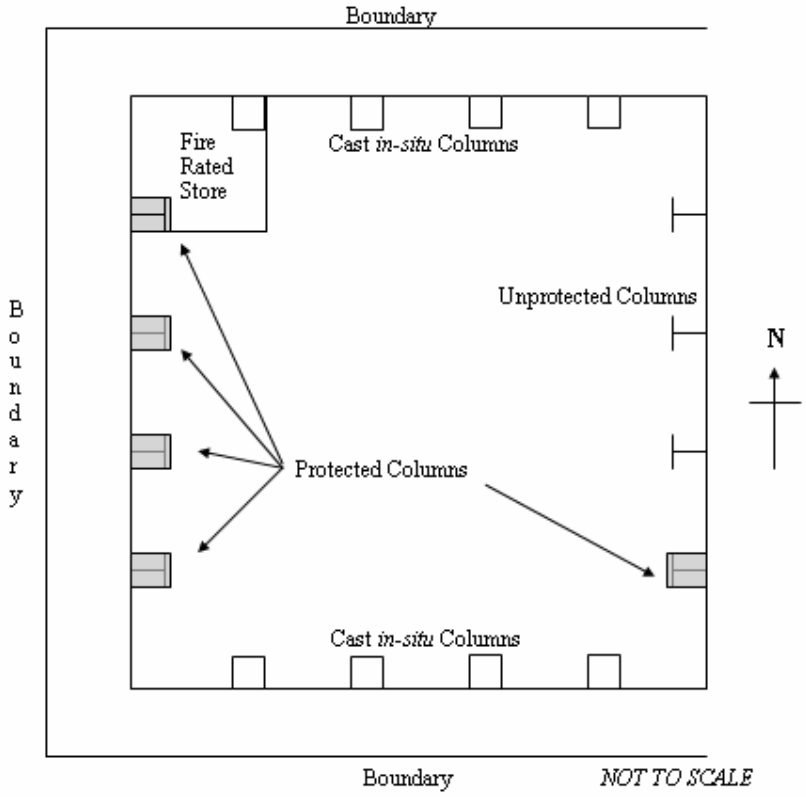

Figure 4-54 Layout of the warehouse

Figure 4-55 Slight deformations of end walls after the fire (Courtesy of Structex Limited)

Figure 4-56 Deformation of steel rafter and purlins in torsion (Courtesy of Alan Reay Consultants Limited)

Figure 4-57 Concrete spalling on the surface exposed to high temperatures (Courtesy of Alan Reay Consultants Limited)

Figure 4-58 Concrete walls attached to partly protected columns after the fire (Courtesy of Alan Reay Consultants Limited)

Figure 4-59 Corner of concrete wall broke off during fire (Courtesy of Alan Reay Consultants Limited)

Christchurch, 2005

A fire occurred recently in a recycling plant with compacted recyclable papers in Christchurch. Large amount of paper was stored inside the building and was either loose on the floor to a height of 2 metres or was in compacted bale form stacked to near the ceiling at the time of fire. The building was located close to boundary sites on the west and south sides (Figure 4-60). The northern walls were attached to the inner flange of the unprotected steel columns as a smooth finish was required for the interior. The portal legs close to the south boundary were encased in concrete to about two-thirds of the full height. The west end walls were pin based at the ground but attached to cast *in-situ* cantilever concrete columns. In this case, the bolted connections holding the side wall and the end wall at the corner were protected by concrete material (Figure 4-61). Although large fires had been extinguished by the fire service, smouldering fires still existed for a few days.

During the fire, the side walls have been observed to bow towards the fire (Merry, A. from New Zealand Fire Service, *personal communication*). Large horizontal deflections had also been observed at the top of the walls at the corners and evidence after the fire suggests that pull-out failure occurred at the top rigid connection and was due to the large forces generated from the outwards thermal bowing of the walls (Figure 4-62). The side walls near the north-west corner were demolished during the fire in order to create a safe route for the fire-fighters to extinguish the fire inside the building. When the walls were being pushed over, the corner south side wall on the other side of the building became detached from the supporting elements and fell outwards (Figure 4-63).

After the fire, the side walls attached to the protected columns suffered permanent deformation. Similarly, the wall panels attached to unprotected columns were very unstable after the fire and were demolished onto the ground. The plastic skylights were melted by the fire and the roof collapsed into the building (Figure 4-64). One of the steel rafters was observed to deform excessively in torsion (Figure 4-65 and Figure 4-66). In this case, only a small area of concrete spalling from the walls was observed. However, some of the concrete encasement protecting the steel columns had fallen off during the fire (Figure 4-67).

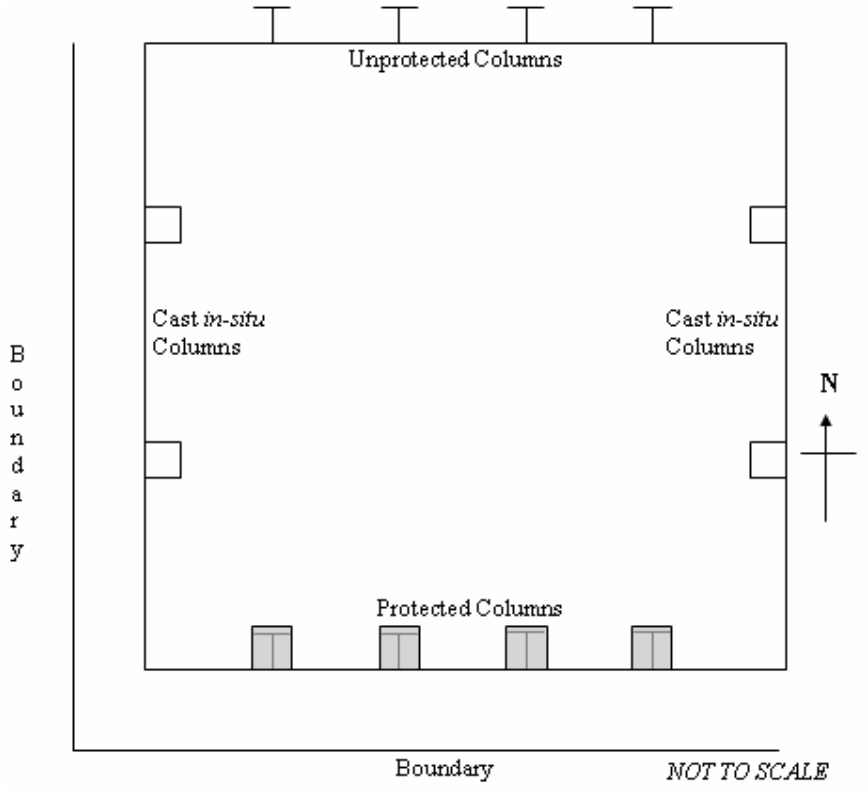

Figure 4-60 Layout of the recycling plant

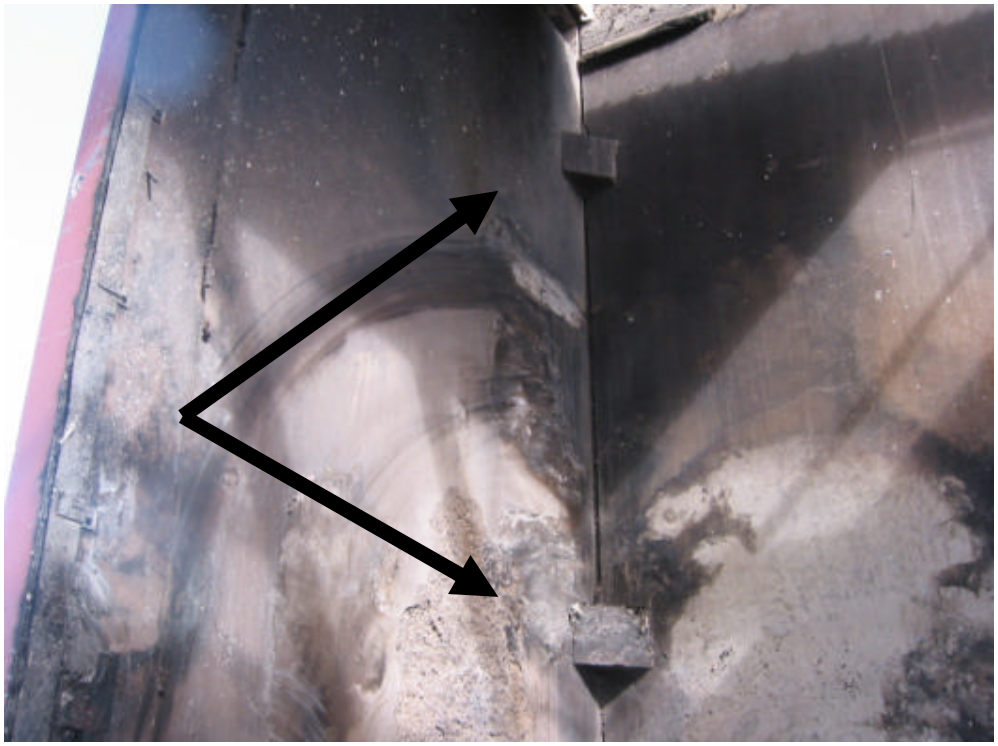

Figure 4-61 Concrete protection to connections between end wall and side wall

Figure 4-62 Pull-out failure of bolted connection

Figure 4-63 Outwards collapse and slight permanent deformations of walls after the fire

Figure 4-64 Collapse of some parts of roof structure

Figure 4-65 Collapse of steel rafter

Figure 4-66 Collapse of steel rafter

Figure 4-67 Concrete encasement fell off during fire

4.8.2 Spalling

Spalling is the separation of concrete from the surface of concrete structures when they are exposed to high and rapidly rising temperatures experienced in fires. It may be insignificant in amount or it can seriously affect the stability and fire resistance of the structure. The Institution of Structural Engineers (1975) and Malhotra (1984) have described the types, factors influencing, and the prevention of it.

Types of Spalling

To facilitate understanding of the phenomenon of spalling, it has been categorised into three different types on the basis of extent, severity and the nature of occurrence as follows:

1. Explosive spalling

   This type of spalling occurs during the early stages of heating and is characterised by the separation of pieces of concrete, accompanied by a loud noise. It is capable of causing physical damage on impact. In many cases, this type of spalling is restricted to the unreinforced part of the section and usually does not proceed beyond a reinforcing layer.

2. Local spalling.

   This type of spalling consists of aggregate splitting, corner break-off and surface pitting.

3. Sloughing off.

   This is a gradual form of breakdown of concrete elements after prolonged heating. Surface layers of concrete are separated from the main structural member by long irregular cracks and cavities.

Factors influencing the occurrence of spalling

The following factors influence the occurrence of spalling:

1. The principle cause of spalling is the moisture content of the concrete.
2. The other contributory factors are the number of faces exposed to heating, the presence or absence of reinforcement and the thickness of the member.
3. The level of stress in the concrete. High compressive and thermal stresses increase the probability of spalling and promote explosive spalling.

4. Cracking due to aggregate expansion, reinforcement expansion or tensile stress.
5. The rate of heating of the structure. Rapid heating is more likely to cause spalling than a slow rate of heating.
6. The quantity of reinforcement, the magnitude of compressive stress, and the quality of concrete are less important than other factors.

It is generally agreed that spalling most often occurs when water vapour is driven off from the cement past during heating, with high pore water pressures creating effective tensile stresses in excess of the tensile strength of the concrete.

Prevention of Spalling

The research studies and other investigation carried out suggest the following preventive measures to eliminate spalling or to reduce the damage it is likely to cause:

1. Reduce the moisture content
2. Reduce the compressive stresses
3. Use lightweight concrete
4. Provide additional reinforcement
5. Provide additional protection by means of a coating or by incorporating polypropylene fibres.

High strength concrete tends to be more susceptible to spalling because it has smaller free pore volume (higher paste density), so that the pores are filled with high-water water vapour more quickly and the low porosity results in slower diffusion of the water vapour through the concrete. The most economical method of preventing spalling is the addition of fine polypropylene fibres to the concrete mix (0.15 to 0.33 %). These fibres melt during fire exposure, increasing the porosity by leaving cavities through which the water vapour can escape (Kodur, 1997).

Jansson and Bostrom (2004) have carried out experimental tests to study the probability of spalling and the amount of spalling of different quality concretes. Self-compacting concrete as well as different tunnel lining concretes have also been investigated. All tested concretes, except the concretes where polypropylene fibres had been added, spalled severely. It is concluded that even if the spalling cannot be

completely avoided by using polypropylene fibres, a manageable level of spalling could be achieved.

Figure 4-68 shows the fire test results with extensive spalling in the segment which does not contain polypropylene fibres. Kitchen (2004) states that the mechanism by which fibres prevent the spalling is related to the amount of fibre in the concrete. Polypropylene fibres start to melt at 160^{o}C, leading to a reduction in volume of the individual fibres. The voids create routes that let the water vapour escape and the internal stresses hardly reach the critical point and no concrete is explosively expelled from the structure.

Figure 4-68 Fire test results showing spalling of concrete without *(left)* and with *(right)* polypropylene fibres (Kitchen, 2004)

5 ANALYSIS METHOD

5.1 Introduction

This chapter describes SAFIR, the finite element programme used for the analysis of this project. Using simple formulae to analyse the structural behaviour of a complex structure under fire conditions is not possible. It is necessary to use a computer programme such as SAFIR to investigate the behaviour of structures under elevated temperatures.

5.2 SAFIR

5.2.1 Introduction

The SAFIR finite element programme was developed at the University of Liège, Belgium, by Jean-Marc Franssen and is based on an earlier programme called CEFICOSS (Computer Engineering of the Fire design of Composite and Steel Structures). This chapter summarises the contents in the *User's Manual for SAFIR 2004* (Franssen *et al*., 2004).

SAFIR incorporates various elements for different idealisations, calculation procedures and various material models for incorporating stress-strain behaviour. The elements include 2D solid elements, 3D solid elements, beam elements, shell elements and truss elements. The stress-strain material laws are generally linear-elliptic for steel and non-linear for concrete. Within this report only 2D solid elements are used for the thermal analysis and this is based on an assumption of the same temperatures at each point along the member. For the structural analysis, both 2D and 3D beam elements are used in this project.

SAFIR uses a step-by-step iteration to evaluate the behaviour of structures with respect to time. Although it was developed specifically for the analysis under fire conditions, it can also be used to determine the ultimate load bearing capacity of structures which are not subjected to elevated temperatures.

5.2.2 Analysis Procedure

The analysis of a structure exposed to fire consists of three main steps in SAFIR. The first step is to perform thermal analysis on the structural members. The second step is the torsional analysis of 3D beam elements whereby a section is subjected to warping and where the warping function and torsional stiffness of the cross section are required to predict the behaviour at elevated temperatures. The last part of the analysis, termed the 'structural analysis', is carried out for determining the response of the structure due to applied loads and thermal distribution evaluated from the thermal analysis.

Thermal Analysis

This analysis is performed while the structure is exposed to fire and both plane sections and three dimensional structures can be analysed. Heat transfer between the fire and the surface of the structure is by convection and radiation. A heat flux can also be imposed on the surface of the sections. Heat transfer in the plane sections is by conduction and the temperature is non-uniform. Radiation in internal voids of the section can also be considered in the thermal analysis. It is also possible to take into account the fact that some layer of concrete or part of the protective material has fallen off the structure. In this case, a new thermal analysis has to be performed on a new structure that is only one part of the previous structure.

For a complex structure, the sub-structuring technique is used, where the total structure is divided into several substructures and a temperature calculation is performed successively for each of the substructures. In this project, the steel components of the building are steel portal frames, secondary purlins and brace channels, and separate temperature analysis is required for each of the section types. From these analyses, the temperatures across the cross section are obtained and are stored for subsequent structural analysis where these sections are present.

To perform the thermal analysis, the cross-section of the element is first defined. Plane sections are then discretised by triangular or quadrilateral (non-rectangular and rectangular) solid elements (Figure 5-1). For universal beam (UB) sections, this can be easily done with a pre-processor, *WizardXP*, written by Jean-Marc Franssen. The pre-processor also allows a concrete slab or a wall and a uniform thickness of

protective material to be added to the UB section (Figure 5-2). In three-dimensional thermal analysis, the sections are discretised by solid elements (prismatic or non-prismatic) with six or eight nodes (Figure 5-1). Each solid element in the section can have its own material and materials such as steel, concrete, insulation and aluminium can be utilised to define the section.

The cross section of the element is then subjected to a time-temperature fire curve and analysed with the main programme *SAFIR2004* to determine the thermal distribution across the section. The fire curves are either built into the programme code (ISO 834, ASTME119 or hydrocarbon fire) or user-defined fire curves with or without decay phases can be utilised. The results can be viewed with a post-processor, *Diamond 2004*, written by M. Dan PNTEA (Figure 5-3).

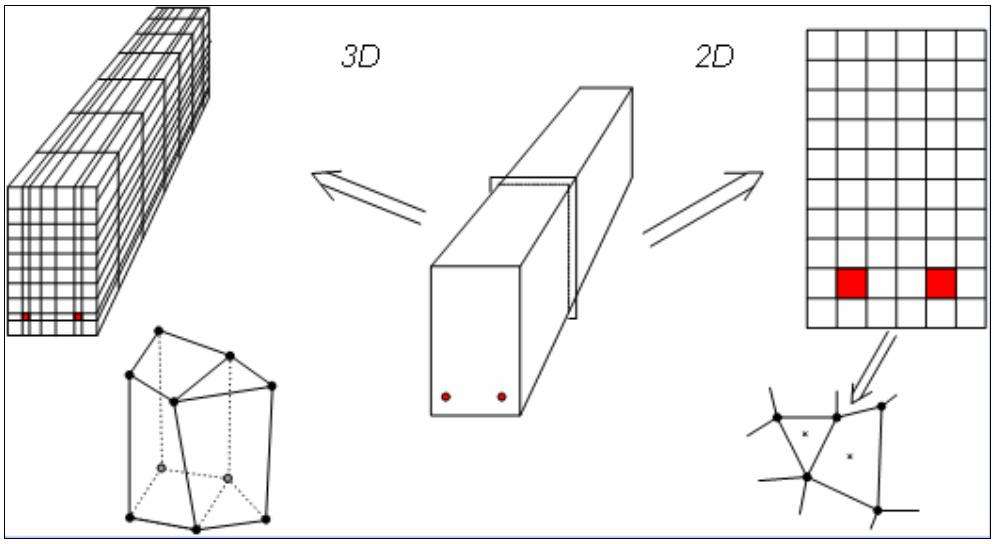

Figure 5-1 2D and 3D discretisation of structure in thermal analysis

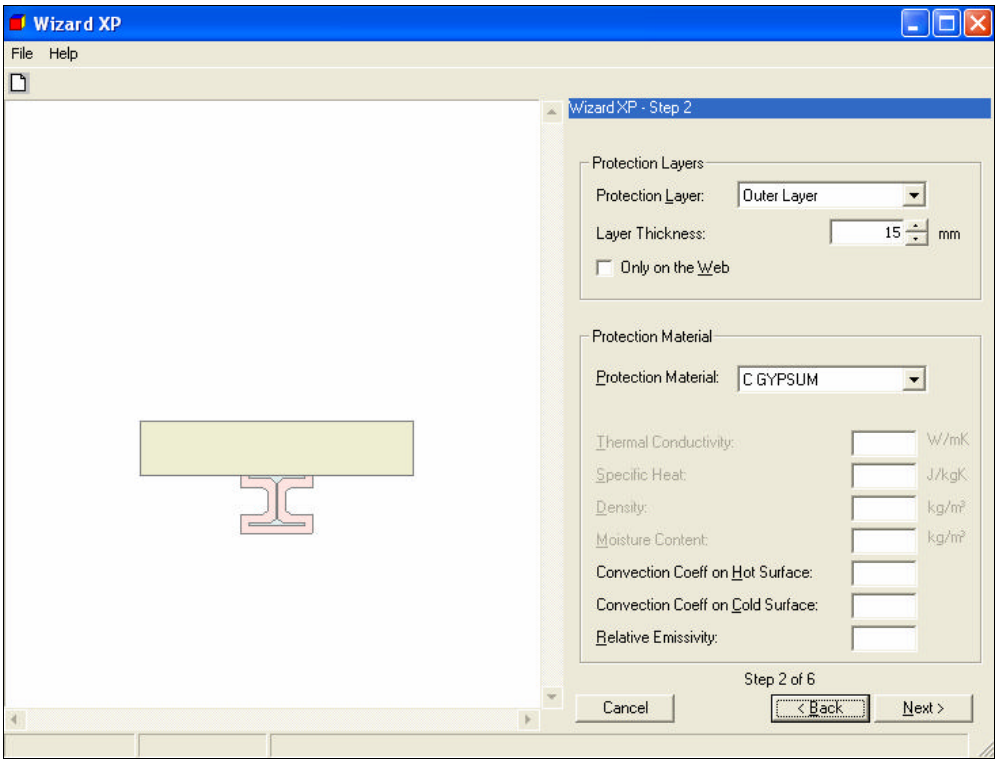

Figure 5-2 WizardXP pre-processor interface

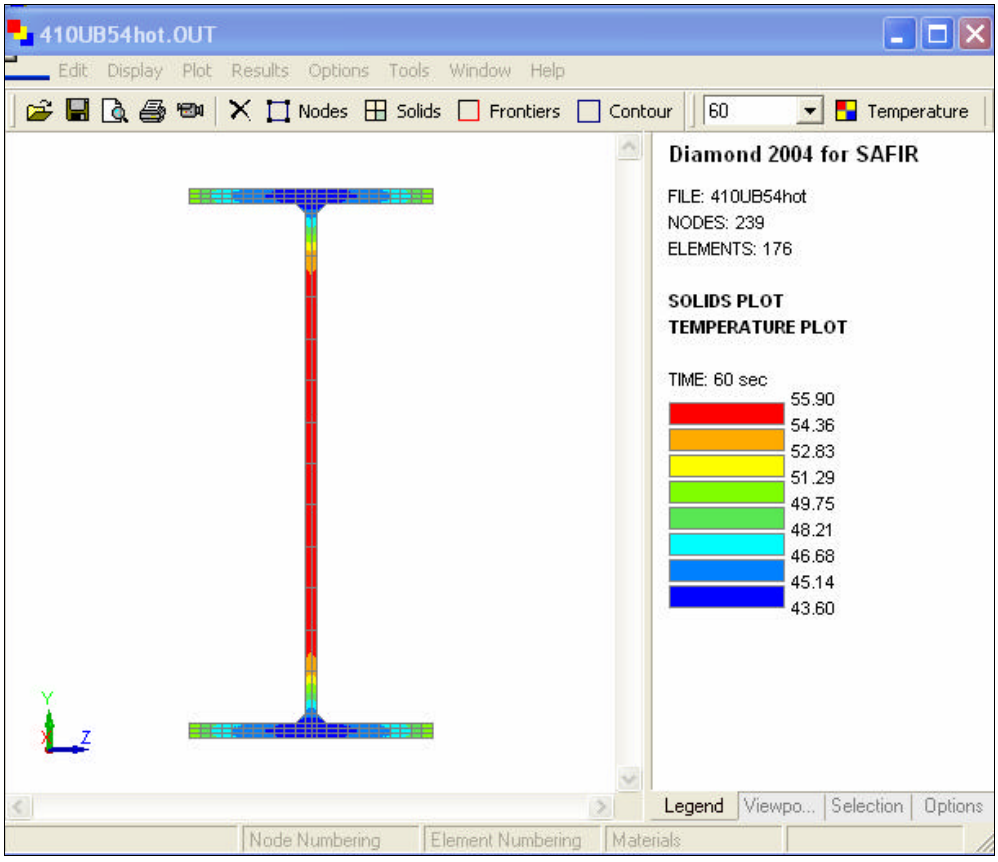

Figure 5-3 Diamond 2004 post-processor interface

Torsional Analysis of 3D Beam Elements

The torsional analysis is performed when analysing structures with 3D beam elements, either because the beam cross-section was subject to warping or because the torsional stiffness is not available from tables or formulae. The 2D solid elements of the discretised section are used to calculate the warping function and the torsional stiffness of the cross section. The torsional properties and warping function obtained from this calculation are added to the results obtained from the temperature analysis of the same cross section for subsequent structural analysis

The materials are considered to be in the elastic range at the ambient temperature. The torsional stiffness remains constant during the simulation of structural analysis and a function describing the decreasing stiffness with time due to elevated temperatures is not possible at this stage. However, the torsional stiffness obtained at ambient temperature can be reduced to another constant value in order to take into account the reduced stiffness at elevated temperatures.

Structural Analysis at Elevated Temperatures

SAFIR utilises a step-by-step iterative procedure to obtain the mechanical behaviour of the structure at elevated temperatures. Both plane and three dimensional structures can be analysed. The temperature history of each structural member is first read from the output files created during the thermal analysis to analyse the structure. The structures can be discretised by three different types of elements:

1. Truss elements, made of one single material with one uniform temperature per element,
2. Beam elements, either pure steel, reinforced concrete or composite-steel sections,
3. Shell elements.

For each calculation, convergence must be obtained such that equilibrium exists between the external load and the internal stress. For the type of convergence procedure during the structural analysis, the programme can use a pure Newton-Raphson procedure or a modified Newton-Raphson procedure. The pure Newton-

Raphson procedure is recommended for structures made of beam elements, and the modified Newton-Raphson procedure is recommended for structures made of shell elements.

The procedure repeats itself in every time step and stops when the specified final time is reached or numerical failure occurs, whichever occurs first. Local failure or instability of a structural member does not lead to overall structural failure and can be dealt with by the dynamic algorithm (refer to Section 5.3). Automatic adaptation of time step is possible with the dynamic algorithm. The following data can be obtained at each time step:

- Displacement at each node of the structure
- Axial and shear forces and bending moments at integration points in each finite element
- Strains, stresses and tangent modulus in each mesh at the integration points of each finite element.

In structural analyses, large displacements, the effects of thermal strains (thermal restraint) and the non-linear temperature dependent material properties can be taken into account. Residual initial stresses or strains and imposed displacements can also be introduced. The unloading of the material is parallel to the elastic-loading branch. Structures with external supports inclined at an angle to the global axes can also be analysed. Nodal coordinates can be introduced in either Cartesian or cylindrical coordinate systems.

5.2.3 Beam Element

This section describes the beam element in SAFIR and other elements available will not be described. The beam element has been used in this project for the steel components of a steel portal frame structure (refer to Chapter 7). The contents in this section are extracted from the *Elements of Theory for SAFIR 2002* (Franssen *et al*., 2002)

The beam element is straight in its undeformed geometry and its position in space is defined by three nodes: the two end nodes (N1 and N2), and a third node (N4) defining the position of the local y axis of the beam (Figure 5-4). The node (N3) is used to support an additional degree of freedom. The first three degrees of freedom represent the displacements in x, y and z respectively; the next three degrees of freedom represent the rotations in the x, y and z directions. The last degree of freedom, or the 7th degree of freedom is for warping.

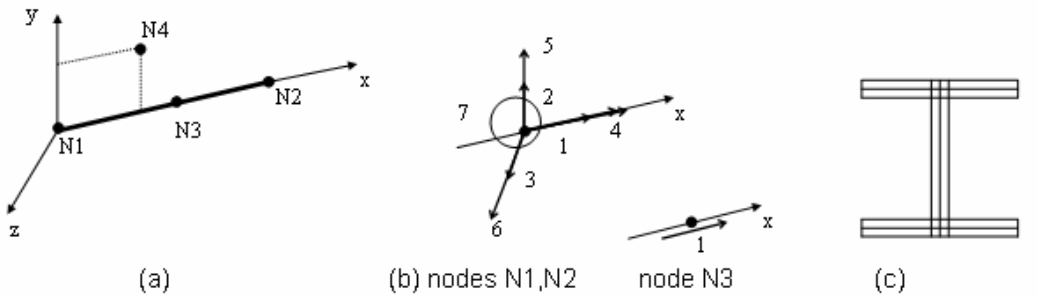

Figure 5-4 Beam element: (a) Local axes (b) Degress of freedom at nodes (c) Cross section (Franssen *et al.*, 2002)

As mentioned in the thermal analysis, the solid elements are used to describe the geometry of the cross section. The cross section of the beam is subdivided into small solids (triangular, quadrilateral or both). In this project, both triangular and quadrilateral solids were used to discretise the 410UB54 steel frame. The root fillets of the universal beam were modelled using triangular solid elements. The material behaviour of each fibre is calculated at the centre of the solid element and it is constant for the whole element.

The following assumptions are made in the structural analysis using beam element:

- The Bernoulli Hypothesis is considered such that the cross section remains plane under bending moment.
- Plastifications are only considered in the longitudinal direction of the member (i.e. uniaxial constitutive models)
- Non-uniform torsion is considered in the beam element.

The programme has been validated and used in several case studies carried out in the past (Nwosu and Kodur, 1998). Lim *et al*. (2004) have recently carried out numerical

modelling and experimental tests on several two-way reinforced concrete and composite steel-concrete slabs exposed to the ISO 834 standard fire. The slabs were modelled using shell elements in SAFIR and the results showed agreement with fire tests.

5.2.4 Sign Conventions

Global and local axes

The Cartesian system of coordinate is used for the global axes when defining a structure that is to be analysed in SAFIR. For two-dimensional (plane) problems, the axes are named G1and G2, while the local axes are named L1 and L2. The applied force and displacements are positive in the direction of G1 and G2. The applied moment and rotations are positive in a counter-clockwise direction. For the three-dimensional problem, the global axes are named G1, G2 and G3 and the local axes are named L1, L2 and L3. The movement G1-G2-G3 is dextrorsum; the applied force, moments, displacements and rotations are all positive in the G1, G2 and G3 directions.

Stresses

The stresses are positive in tension. The axial forces are obtained as a summation of all the stresses, are also positive in tension. The bending moments in the beam elements are obtained as a summation of yi σi, with yi measured on the local axis L1, are positive when the fibres having a positive local coordinate are in tension (i.e. moments at supports for a fully fixed beam).

The terminology used in New Zealand is that ‘positive bending moment’ is defined when fibres having a negative local coordinate are in tension (i.e. bending in a simply supported beam). The term ‘negative bending moment’ is used to describe the moments where fibres that have a positive local coordinate are in tension (i.e. end moments of a fully fixed beam). It should be noted that SAFIR plots positive moments on a negative scale and therefore the bending moment diagrams shown in this report have positive moments plotted on a negative scale. This means that the bending moment diagrams in SAFIR are consistent with the sign convections used in New Zealand, although the values given have the opposite sign (refer to Figure 5-5).

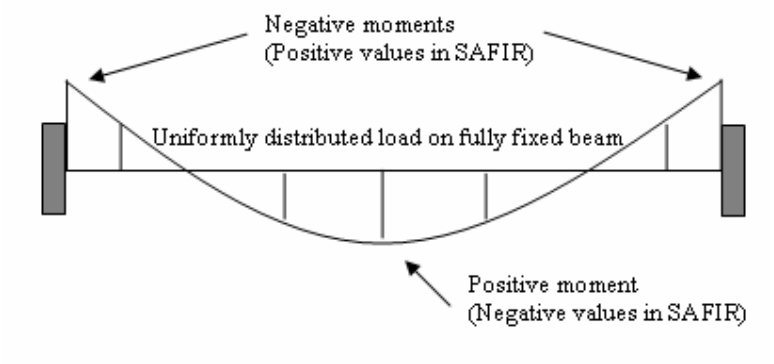

Figure 5-5 Bending moment diagram for a fully fixed beam and sign convention in SAFIR

5.2.5 Material Properties

The material models in the SAFIR programme code are available for analysis at ambient and elevated temperatures. Valid material properties for the analyses at ambient temperature are elastic, bilinear and Ramberg-Osgood material properties. At elevated temperatures, steel materials such as structural steel, reinforcing steel and prestressing steel according to the Eurocode are available. For concrete materials, the properties are taken according to the Eurocode and Schneider's model for calcareous and siliceous aggregate concrete.

Stress-strain relations of Concrete and Steel

The relations in these materials are non-linear and are temperature dependent. In structures exposed to fire, the materials are subjected to initial strains (ε_i), thermal effects (ε_{th}) and stress related effects (ε_σ). The stresses are computed by the difference between the total strain (ε_{total}) obtained from the nodal displacements, and the initial and thermal strains.

5.2.6 Common Features in all Analyses

The following are common features in all the simulations:

- Thermal and mechanical properties of steel and concrete according to the Eurocodes 2, 3 and 4 are embedded in the code and can be used directly in the models.
- The same temperature or the same displacement can be imposed at two different nodes by the use of a master-slave relationship.

- The matrix can be optimised in order to reduce computational effort and storage by using an internal renumbering of the of the system equations.
- The programme comes with its own pre-processing and post-processing capabilities. These are the *WizardXP* and *DIAMOND 2004* codes respectively. The results can also be extracted to spreadsheets (i.e. Microsoft Excel) from the output files.

5.3 The New Version of SAFIR (SAFIR 2004)

In the previous versions of SAFIR, analysis of structures submitted to fire is performed by a succession of subsequent static analyses of the structure taking into account the variations of the displacement and the temperature profile in the structure from one time step to the next. The new version of SAFIR (*SAFIR 2004*) has the dynamic algorithm implemented to cope with the partial or local failure (Franssen and Gens, 2004). Because acceleration and damping terms are now considered, the programme is now able to counterbalance the negative stiffness during the unstable states of the structure.

In the traditional algorithm (i.e. static analysis), if the loads at all degrees of freedom of the structure are noted {F} and if the corresponding displacements that have to be determined are noted {u}, then equation (5-1) is used to determined the incremental displacements. In the dynamic algorithm, equation (5-2) is the basic equation for a dynamic analysis, with a damping matrix in relation to the velocity term and mass matrix in relation to the acceleration term added.

$$\{\Delta F\} = [K]\{\Delta u\} \qquad \textbf{(5-1)}$$

where,

$\{\Delta F\}$	is either the incremental of external applied forces or the out of balance forces.
$[K]$	is the stiffness matrix of the structure.
$\{\Delta u\}$	is the displacement at the nodes.

$$\{\Delta F\} = [K]\{u\} + [C]\{\dot{u}\} + [M]\{\ddot{u}\} \qquad \textbf{(5-2)}$$

where,

$\{\Delta F\}$	is either the incremental of external applied forces or the out of balance forces.
[K}	is the stiffness matrix of the structure.
[C]	is the damping matrix.
[M]	is the mass matrix.
$\{u\},\{\dot{u}\},\{\ddot{u}\}$	are the displacement, velocity and acceleration at the nodes.

Franssen and Gens (2004) have mentioned that numerical failure is observed when the simulation cannot be performed any further as the stiffness matrix becomes negative and may happen when only part of the structure is in an unstable position. They have shown that the simulation time can now be extended beyond the moments of partial and temporary collapse. Moreover, even when the "true" fire resistance time is reached, the simulation can be performed for substantially larger displacements, which gives a much better insight into the failure mode and allows, in certain cases, to judge the possibility of progressive collapse.

Vassart *et al.* (2004) have carried out 3D simulations of industrial buildings in case of fire using ABAQUS, ANSYS and SAFIR. Figure 5-6 shows the structure analysed in their analyses. The rafters span 20 metres between the columns and the frames are spaced at 7.5 metres. For the calculation of the temperature in steel, an ISO fire curve was used.

Figure 5-7 shows a 3D model analysed where only the left side of the centre frame was heated. Figure 5-8 and Figure 5-9 show the vertical displacement at the apex of the heated frame (node b) and the deformed structure with the deformations scaled up to 10 times the original deformations, respectively. It should be noted that the deflected shape of the structure is not visible without scaling the deformations. It was found that the load applied to the heated frame is progressively transferred to the neighbouring unaffected frames, and finally the two neighbouring frames prevent the heated frame from collapsing onto the ground (Figure 5-9).

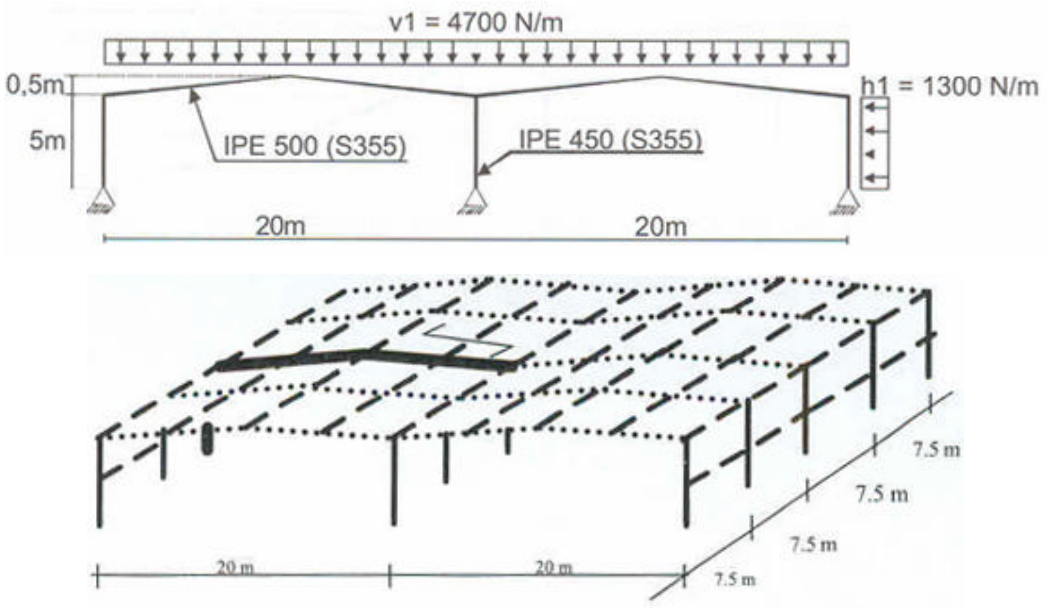

Figure 5-6 Structure used for the analyses in ABAQUS, ANSYS and SAFIR by Vassart *et al.* (2004)

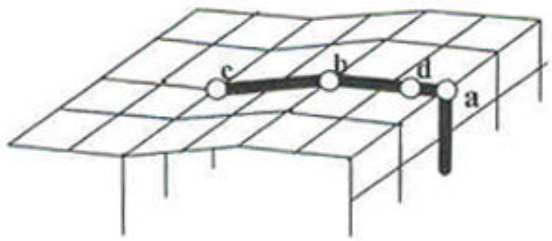

Figure 5-7 3D model with the central left frame heated (Vassart *et al.*, 2004)

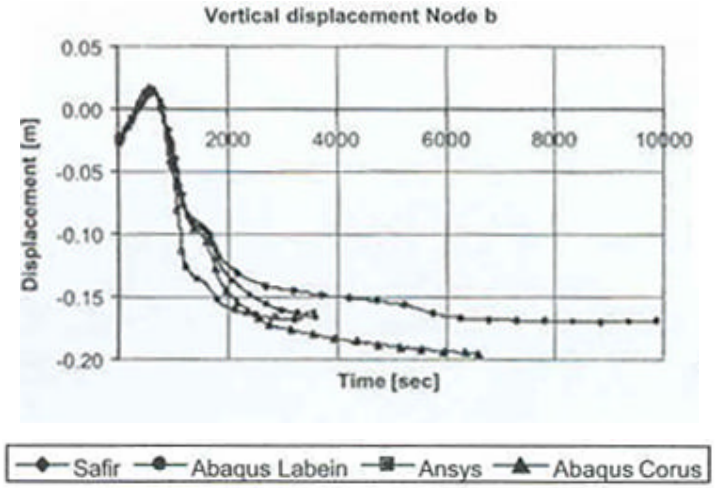

Figure 5-8 Variation of vertical displacement at the apex (Vassart *et al.*, 2004)

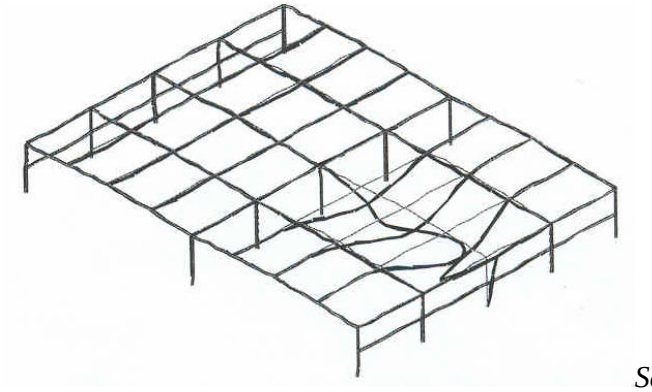

Scale factor = 10x

Figure 5-9 Deflected shape at the end of the simulation (Vassart *et al*., 2004)

Figure 5-10 shows another 3D model analysed where the purlins connected to the heated frame were also affected by the fire. Statical analyses were first carried out using the three different software packages. However, lateral buckling of a purlin occurred and caused the analysis to stop in the early stages of fire. The dynamic analysis allowed this buckling and the post-local failure stage was analysed. Figure 5-11 and Figure 5-12 show the vertical displacement at the apex of the heated frame (node b) and the deflected shape at the end of the simulations respectively. The deflected shape shows that it is now possible to simulate the behaviour of the global structure until the complete failure or very large displacements.

Vassart *et al*. (2004) concluded from the results of their analyses that the three software packages give close results for the three dimensional analysis. It was also found that the statical finite element calculation stopped due to local failure (such as lateral buckling of purlin). To solve this problem, dynamic analysis must be used to analyse the structural behaviour after the buckling of the purlins so that post-local failure stage can be analysed. Therefore, it is now possible to simulate the complete failure mechanism, to predict the influence of a local failure on the global behaviour of the structure and to follow eventually the progressive collapse. The fire resistance time can now be determined where in the past many numerical failures corresponding to local failure were interpreted as fire resistance time for the whole structure.

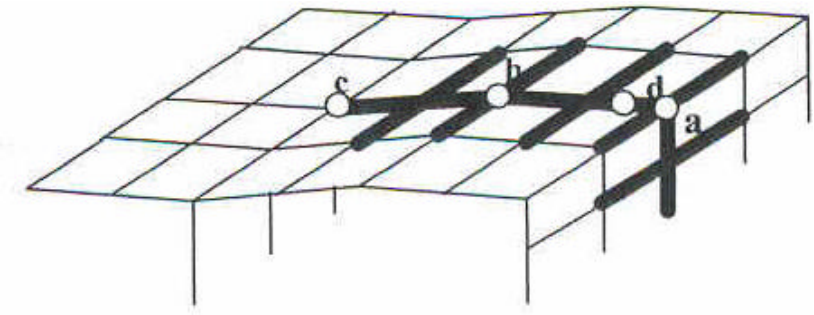

Figure 5-10 3D model with the central left frame and the adjacent purlins heated (Vassart *et al.*, 2004)

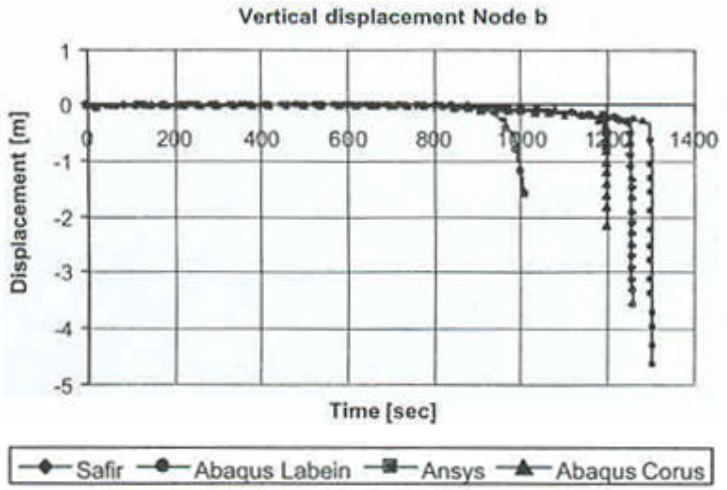

Figure 5-11 Variation of vertical displacement at the apex (Vassart *et al.*, 2004)

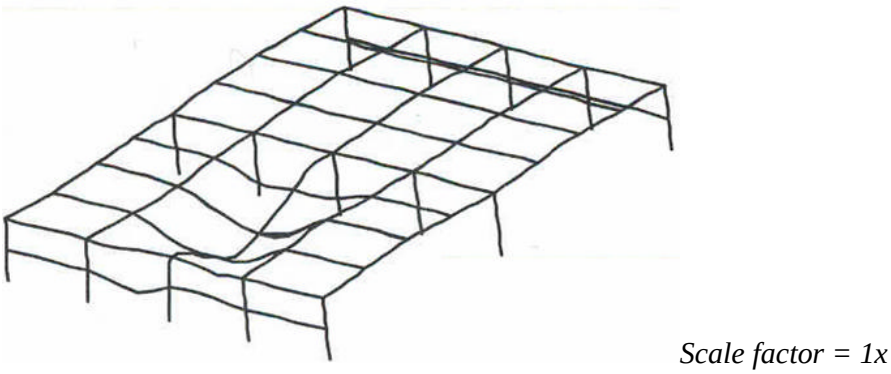

Figure 5-12 Deflected shape at the end of the simulation (Vassart *et al.*, 2004)

6 DESIGN OF BUILDING ACCORDING TO NZS 4203:1992 AND NZS 3404:1997

6.1 Introduction

This chapter describes the design of a typical steel portal frame building in Christchurch. In order to analyse the building under elevated temperatures, the types of elements of the structure must first be determined. The New Zealand Loading Code NZS 4203:1992 is used to estimate the loads on the structure. The Dimond Hi-Span (DHS) purlins and brace channels are chosen from the Hi-Span design manual (Dimond Industries, 1995) and the steel portal frame is designed according to the New Zealand Steel Structures Standard NZS 3404:1997. This building will be used in SAFIR for the analyses in this research project and the modelling of parts the structural elements is described in Chapter 7.

6.2 Building Description

A typical industrial building with the dimensions shown in Figure 6-1 is designed according to the New Zealand standards. The building is 40 metres long by 30 metres wide and the roof is inclined at 7.9^{o}. The columns are 6 metres high and the distance from ground level to the apex of the frame is approximately 8.06 metres. The steel frame is composed of a 410UB54 universal beam and the roof structure consists of 410UB54 rafters, DHS250/15 purlins and DB89/10 brace channels. The steel purlins and brace channels are from the Dimond Industries. The steel frames have a span of 30 metres and are spaced at 7.2 metres. This is except in the end bays where the purlins are shorter in length due to wind loads from the end walls. The purlins are spaced equally at about 1.5 metres and span between the steel frames. The concrete panels are not shown in the figure and are represented by appropriate boundary conditions or restraints to the steel members in SAFIR (refer to Chapter 8).

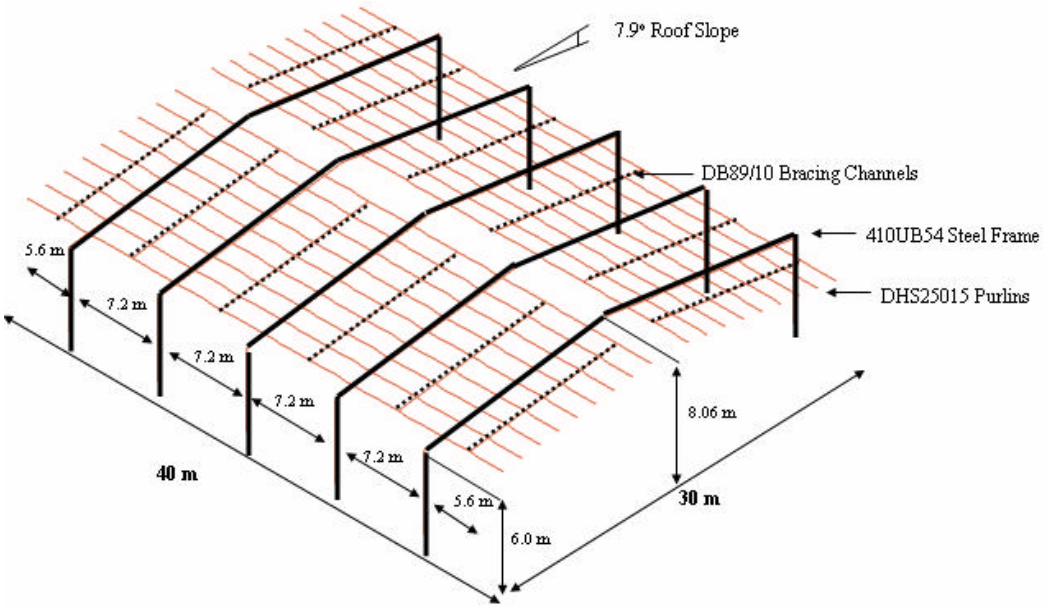

Figure 6-1 Dimensions and structural elements of the building

6.3 Load Cases according to NZS 4203:1992

This section of the report describes the load cases identified and analysed for a typical industrial building in Christchurch. The New Zealand Loading Code NZS 4203:1992 requires buildings to satisfy the ultimate and serviceability limit states with different combinations of dead, live, wind, snow and earthquake loads. The combinations of loads are reproduced here for clarity and are shown in Table 6-1 and Table 6-2. It should be noted that the load combinations involving earthquake load are not shown in the tables. For typical industrial buildings, the governing design load cases are usually due to gravity loads or wind loads (Banks, G. *personal communication*).

Table 6-1 Combinations of loads for the serviceability limit state (NZS 4203:1992)

Load Case	Combinations of loads
1)	$G \& Q_s$
2)	$G \& Q_s \& W_s$
3)	$G \& S_s$

Table 6-2 Combinations of factored loads for the ultimate limit state (NZS 4203:1992)

Load Case	Combinations of loads
1)	1.4G
2)	1.2G & 1.6Q
3)	1.2G & Q_u & W_u
4)	0.9G & W_u
5)	1.2G & Q_u & 1.2 S_u

Live Loads and Snow Loads

The live load (Q) for the roofs of industrial building is 2.5 kPa (Roofs with no access for pedestrian traffic, Table 3.4.1 of NZS 4201:1992). The serviceability live load (Q_s) can be conservatively taken as 2.5 kPa. There is no ultimate live load (Q_u) on the roofs (Table 2.4.2 of NZS 4203:1992). For buildings in Christchurch in low altitude zones (snow zone 4), the ultimate snow load (S_u) is found to be 0.3 kPa from the loading standard. Buchanan (1999) also gives a design snow load (S_u) of 0.3 kPa and the serviceability snow load (S_s) is taken as 50% of the ultimate snow load (i.e. S_s = 0.15kPa). The live loads and snow loads are summarised as follows:

Q = 0.25 kPa

Q_s = 0.25 kPa

Q_u = 0 kPa

S_s = 0.15 kPa (50% of S_u)

S_u = 0.30 kPa

Wind Loads

Part 5 of NZS 4203:1992 gives the design wind loads on buildings considering locality, orientation, altitude, terrain category, size of the building, shielding effects, hill effects, channelling effects and structural rise. A building in Christchurch is most likely to be located on a flat terrain with numerous closely spaced obstructions. The loading code requires forces, F, on enclosed building elements such as a wall or a roof to be calculated from equation (6-1), where p_e and p_i are external and internal wind pressures, respectively, and A is tributary area of the building element.

$$F = \sum (p_e - p_i)A \qquad \textbf{(6-1)}$$

From the internal and external wind pressures calculated and the directions of the wind (i.e. longitudinal wind or cross wind), a total of six wind load cases on the building has been identified. This is summarised in Table 6-3 with notations in reference to Figure 6-2. The serviceability wind loads can be found by taking 65% of the ultimate wind loads shown in the table (i.e. $W_s = 0.65\ W_u$)

.

Table 6-3 Load cases for wind loads

Load Case	Ultimate Wind Pressure (kPa)			
	L1	L2	R2	R1
W_u1	0.890	-0.092	0.643	-0.153
W_u2	-0.031	-1.010	-0.275	0.765
W_u3	0.059	-0.092	-0.092	-0.059
W_u4	0.059	0.184	0.184	-0.059
W_u5	-0.859	-1.010	-1.010	0.859
W_u6	-0.859	-0.275	-0.275	0.859

Note:

L1 *Wind pressure on sidewall L1*

L2 *Wind pressure on roof L2*

R2 *Wind pressure on roof R2*

R1 *Wind pressure on sidewall R1*

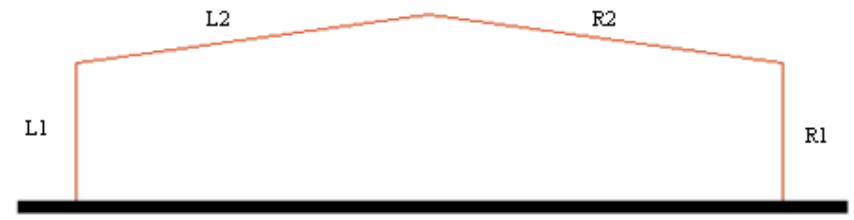

Sign Convention:

+ve pressure denotes pressure towards a surface

-ve pressure denotes pressure away from a surface

Figure 6-2 Wind loads on the building according to NZS 4201:1992

6.4 Design of Purlin and Brace Channel

Purlins act principally as beams to support the roof sheeting but also perform as struts and compression ties in restraining rafters laterally against buckling. DHS250-15 purlins restrained by one DB89/10 brace channel at midspan are chosen and checked against the load cases identified using the design capacity tables given in the Hi-Span design manual (Dimond Industries, 1995). The design capacity of the DHS purlin is limited by buckling of the compression flange and is dependent on the number of restraints given (i.e. number of brace channels along the length of the purlins). The worst tributary width of the purlin is shown in Figure 6-3 and the dead loads and ultimate wind loads (from Table 6-3) for checking the members are as follows:

G (Roof sheeting)	= 0.07 kPa	(Includes insulation foil, plastic and steel sheeting)
G (DHS250–15 purlins)	= 0.056 kN/m	
W_u	= -1.01 kPa	(Uplift)
W_u	= 0.64 kPa	

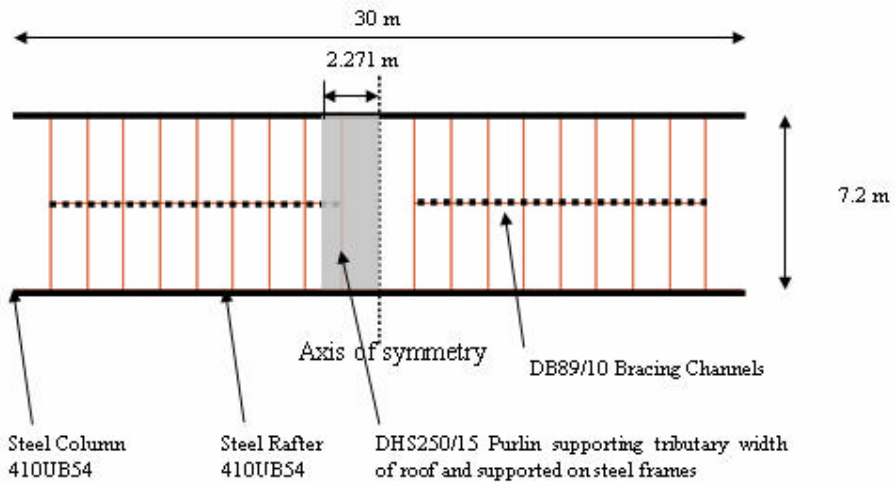

Figure 6-3 Plan view of industrial building showing the tributary area of the purlin

When the applied load is downwards, it is assumed that the purlin is fully braced such that the top flange is fully restrained by screw fastened roof sheeting. When the applied load is due to wind uplift, the capacity of the purlin is determined from the tables with one brace channel provided. A worst case is also checked such that the top flange of the purlin is not fully restrained and is braced with only one brace channel at

midspan under gravity loads The serviceability uniformly distributed load is the load at which midspan deflection equates to span/150 (i.e. 7200/150 = 48 mm). The DHS 250/15 purlin and DB89/10 bracing channel satisfy both the ultimate and serviceability limit states.

6.5 Design of Steel Portal Frame

A 410UB54 universal beam is selected for the columns and the rafters which form the portal frame of the building. The dead loads on the frame include the self weight of the universal beam in addition to the loads from roof sheeting, purlins, and brace channels as stated in Section 6.4. The design of the steel frame is only carried out for the ultimate limit state and is based on elastic analysis. The serviceability limit state is not considered here as requirements for excessive deflection and excessive vibration are not specifically given in the standard.

Each frame is required to resist wind forces in the plane of the frame by flexural action. The tributary width of the frame is shown in Figure 6-4 and the load cases shown in Table 6-2 are analysed by assuming pinned support conditions at the column bases. Table 6-4 summarises the load cases for the frame analysis. The bending moment and axial force diagrams are obtained from SAFIR and are shown in Appendix A and Appendix B, respectively. The critical load cases are 1.2G & 1.6Q due to gravity loads and 0.9G & W_u5 (see Table 6-4) due to wind uplift. Figure 6-5 to Figure 6-8 show the bending moment diagrams and shear force diagrams of the critical load cases. The critical values of bending moments and the coincident axial loads for the design of column and rafter are summarised in Table 6-5. In the design of the columns and rafters in the portal frames, the combined actions from bending moment and axial force are checked against the section capacities in accordance with NZS 3404:1997.

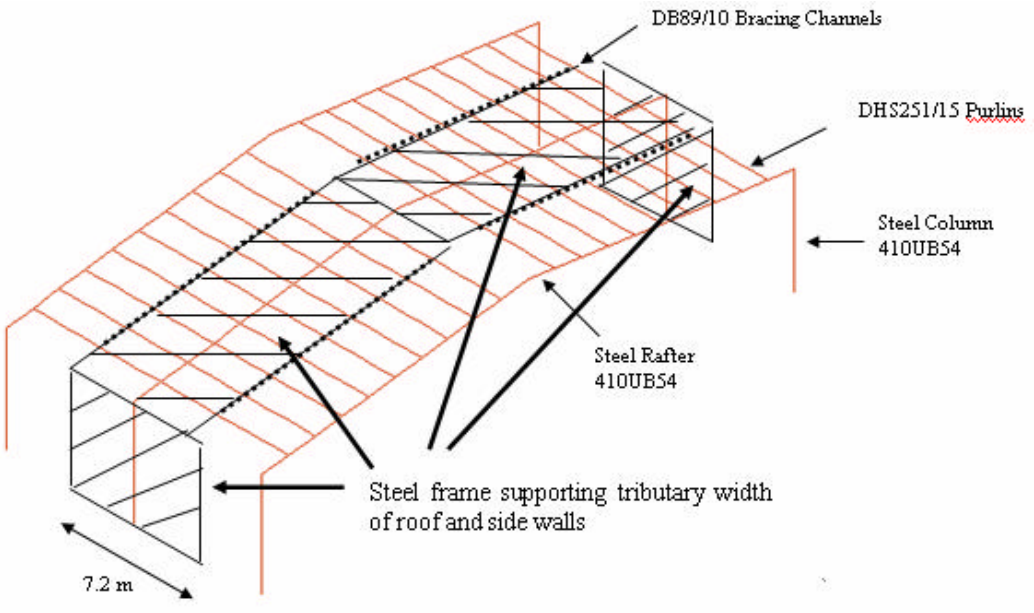

Figure 6-4 Sketch of industrial building showing the tributary area of the steel frame

Table 6-4 Load cases for the frame analysis

Load Case	Combinations of loads
1)	1.4G
2)	1.2G & 1.6Q *
3)	1.2G & Q_u & W_u1 1.2G & Q_u & W_u1 1.2G & Q_u & W_u1 1.2G & Q_u & W_u1 1.2G & Q_u & W_u1 1.2G & Q_u & W_u1
4)	0.9G & W_u1 0.9G & W_u2 0.9G & W_u3 0.9G & W_u4 0.9G & W_u5 ** 0.9G & W_u6
5)	1.2G & Q_u & 1.2 S_u

Note:

** denotes critical load case due to gravity loads*

*** denotes critical load case due to wind uplift*

Table 6-5 Design cases for the column and rafter in portal frames

Column Design			
Design Case	**Description**	**M* (kNm)**	**N* (kN)**
(i) 1.2G & 1.6Q	Inside flange in compression	264	66 (Compression)
(ii) 0.9G & W_u5	Inside flange in tension	289	79 (Tension)
Rafter Design			
Design Case	**Description**	**M* (kNm)**	**N* (kN)**
(i) 1.2G & 1.6Q	Inside flange in compression	264	52 (Compression)
(ii) 1.2G & 1.6Q	Inside flange in tension	149	45 (Compression)
(iii) 0.9G & W_u5	Inside flange in tension	289	77 (Tension)
(iv) 0.9G & W_u5	Inside flange in compression	149	67 (Tension)

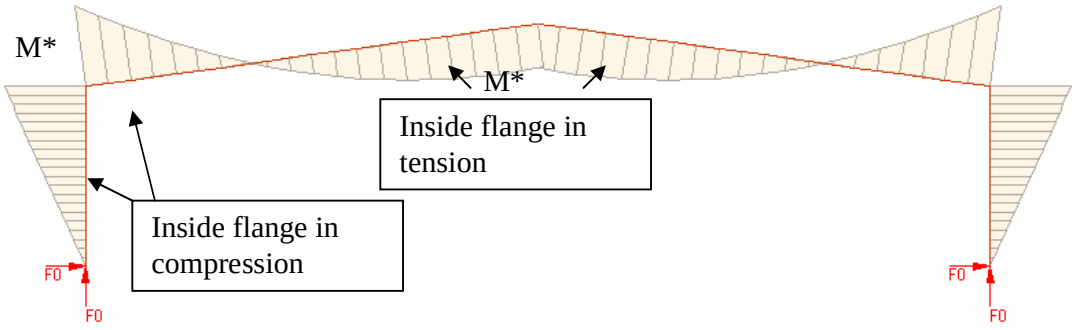

Figure 6-5 Bending moment diagram for load case No.2 (1.2G & 1.6Q)

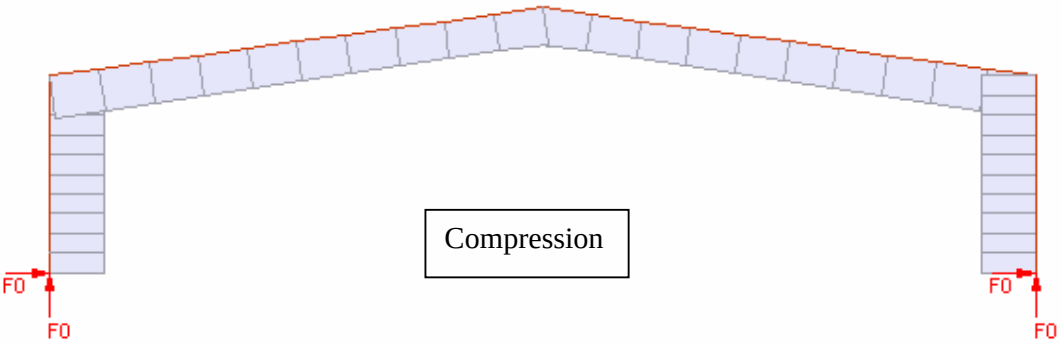

Figure 6-6 Axial force diagram for load case No.2 (1.2G & 1.6Q)

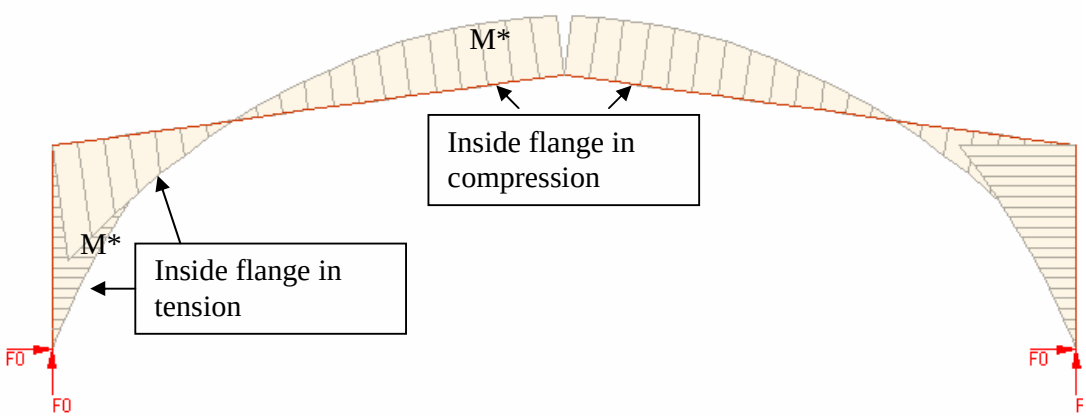

Figure 6-7 Bending moment diagram for load case No.4 (0.9G & W_u5)

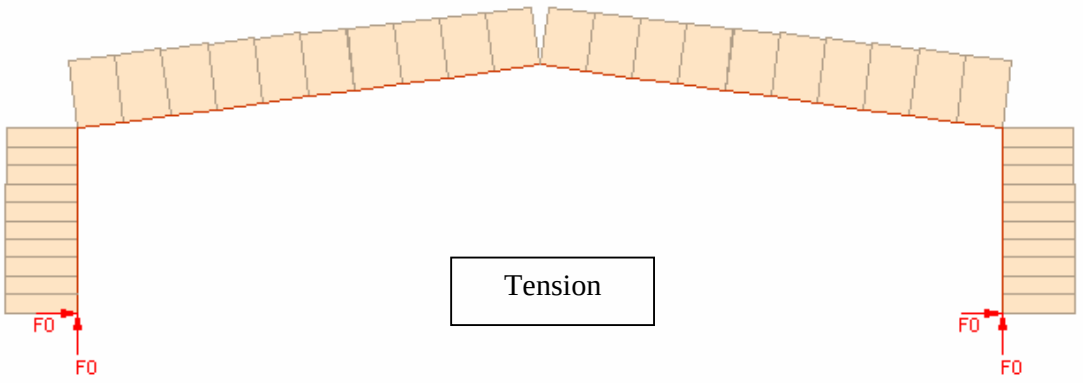

Figure 6-8 Axial force diagram for load case No.4 (0.9G & W_u5)

The nominal axial and bending capacities are obtained through a consideration of flexural and flexural-torsional buckling respectively. In the checking of the critical bending moment at the knee and the coincident axial compressive force for the column under load case No.2 (1.2G & 1.6Q) due to gravity loads, apart from the restraint at the top of the column, an additional restraint must be provided at the mid-height of the column to prevent buckling about the weak axis. It is assumed that this is effectively achieved by connecting the column to the wall at mid-height and column buckling is restricted by the concrete panels.

In the checking of the combined actions from the critical bending moments and the coincident axial forces for the rafter under the critical load cases, the whole rafter span is used as the effective length since no fly braces to laterally restrain the bottom flange of the rafter is to be provided.

7 MODELLING OF PARTS OF THE STEEL PORTAL FRAME BUILDING

7.1 Introduction

This chapter of the report describes the finite element modelling of the building in SAFIR. It includes the cross section and discretisation of the steel elements, the fire growth models and the gravity loading used in the SAFIR programme under fire conditions. This chapter explains how the building described in Chapter 6 has been built-up progressively, with separate structural analysis performed on two and three dimensional single portal frames, one single purlin, part of a roof structure and a two bay portal frame structure. Analyses with static and dynamic algorithms in SAFIR have been carried out and the discrepancy between the two algorithms is described in this chapter. None of the analyses in this chapter represent the completed building and the fire analysis of the whole building is described in Chapter 8.

7.2 Cross Sections of the Steel Elements

The frame studied in this report is a 410UB54 steel universal beam and the roof structure consists of 410UB54 rafters, DHS250/15 purlins and DB89/10 brace channels. The cross sections of the steel structural members are shown in Figure 7-1 and the dimensions are tabulated in Table 7-1.

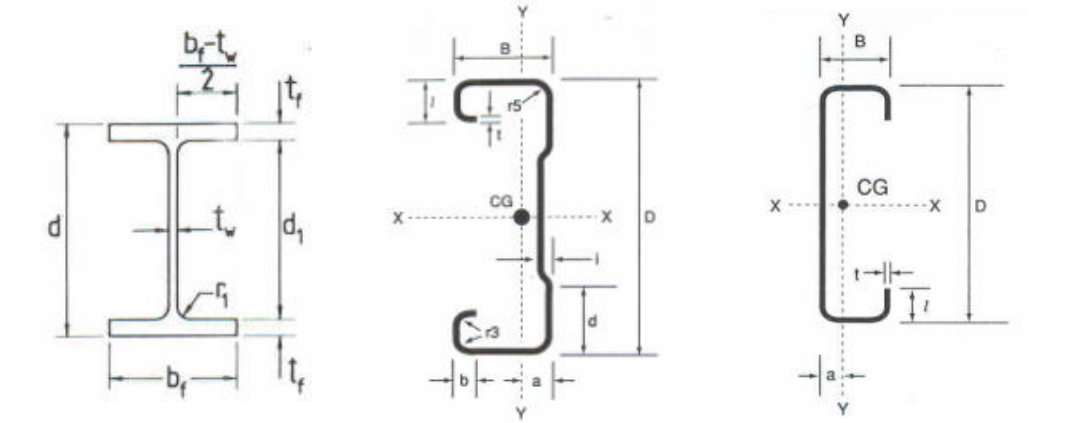

Figure 7-1 Cross sections of the steel members (AISC, 1994 and Dimond Industries, 1995)

Table 7-1 Dimensions of the steel elements (AISC, 1994 and Dimond Industries, 1995)

Dimensions	Notations	(mm)
410UB54 universal beam for the portal frame		
Depth of section	d	403
Flange width	b_f	178
Flange thickness	t_f	10.9
Web thickness	t_w	7.6
Roof radius	r_1	11.4
Depth between flanges	d_1	381
DHS250/15 for the purlins		
Depth of section	D	250
Width of section	B	85
Section thickness	t	1.45
Refer to Figure 7-1	d	67
Refer to Figure 7-1	i	6
Refer to Figure 7-1	b	12
Refer to Figure 7-1	*l*	33
Refer to Figure 7-1	a	28.5
DB89/10 for the brace channel		
Depth of section	D	89
Width of section	B	34
Section thickness	t	0.95
Refer to Figure 7-1	*l*	6
Refer to Figure 7-1	a	8.99

7.2.1 Discretisation of the Sections

The cross-sections of the steel members are discretised in SAFIR and are shown in Figure 7-2. The purlin and brace channels have been modified for the SAFIR discretisation and the root fillets of the 410UB54 section were modelled as triangular elements rather than their actual circular profile. The grids of finite elements are then used to calculate the temperature distribution across each cross section considered.

The fire growth models and the surface exposed to the fire are described in the next section. Welsh (2001) carried out sensitivity analysis on mesh discretisation of a composite section and found that using very fine discretised section has little effect on the thermal and structural output. Using a very fine discretised section increases the computational time and the discretisation used in this research was deemed to be adequate.

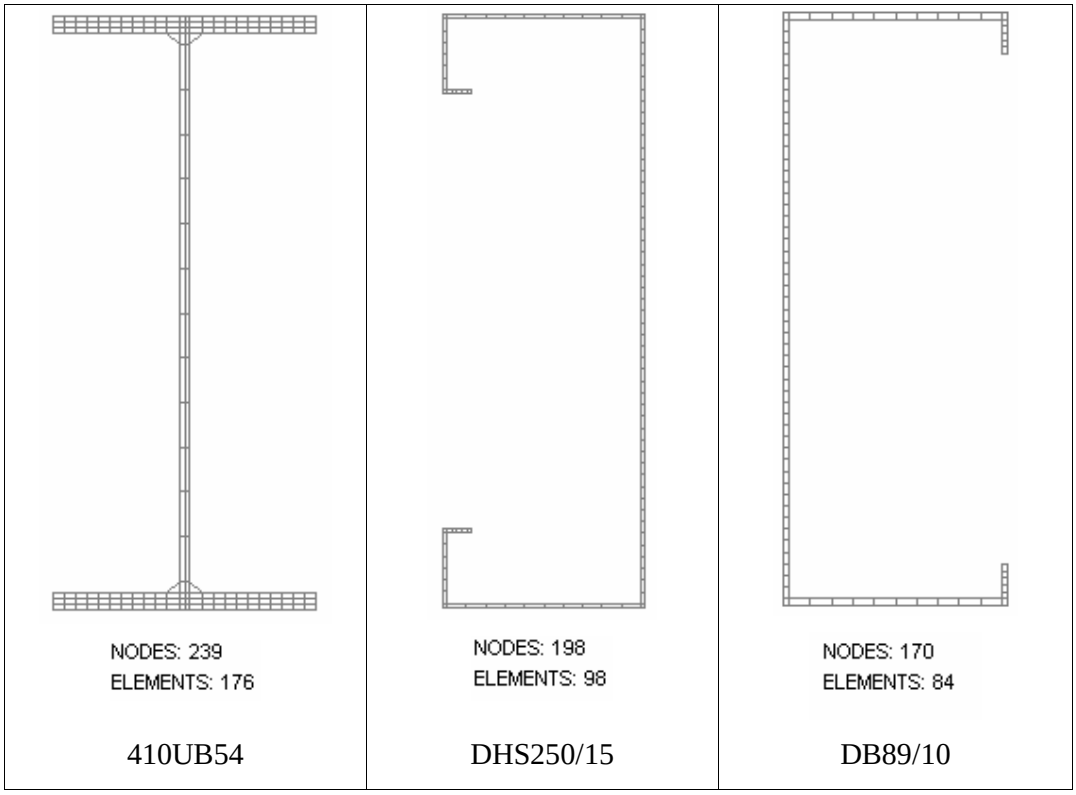

Figure 7-2 Discretised cross-sections of the steel elements

7.2.2 Thermal Analysis

SAFIR first calculates the temperature profile through a given cross-section. As the analysis used is only two-dimensional, a representative temperature profile with time is calculated for the cross-section. Heat can only transfer through the cross-section and not along the length of the beam.

Two fire models are used in this report to simulate thermal effects on the steel members. The first model uses the ISO 834 standard fire curve and the second model is the Eurocode External fire curve. The ambient temperature for both models is taken

as 20^{o}C. The time-temperature curves are entered into the SAFIR thermal analysis and the fire curves relate to the gas temperature of the fire that surrounds the steel members. The ISO fire curve may not represent the gas temperature surrounding the steel members well for a large compartment but is chosen for the purposes of the analysis. The Eurocode External fire curve assumes that the roof collapses and results in structural members exposed to lower temperatures (refer to Section 4.3.3). It should be noted that most of the analyses carried out in this project use the ISO 834 standard fire.

ISO 834 Standard Fire Curve

The ISO 834 standard fire curve is taken as a standard case for simulations in this report (Figure 7-3). The ISO fire is a non-linear rapid growth fire where in the early stages of fire growth is comparable with a temperature increment of approximately 212^{o}C per minute for the first two minutes. In the ISO 834 standard fire curve the temperature (T) is defined (Buchanan, 2001) as:

$$T = 345\log_{10}(8t+1) + T_0 \quad \textbf{(7-1)}$$

where,

t is the time (minutes)

T_0 is the ambient temperature (^{o}C)

Eurocode External Fire Curve

The Eurocode External fire curve can be used to model temperatures of a well-ventilated fire. The Eurocode External fire curve follows the ISO 834 standard fire curve closely until it reaches its maximum temperature (Figure 7-3). In this case, the maximum temperature is taken as 660^{o}C.

A cooling phase is also introduced to the External fire. In Figure 7-3 the External fire with a duration of 30 minutes is followed by a linear cooling phase. The linear decay rate used in the formation of this time temperature curve is from the Eurocode 1 (EC1, 1994). The Eurocode suggests a decay rate of 625^{o}C per hour for fires with a burning period of less than half an hour. At 30 minutes the External fire temperature has reached the maximum temperature of 660^{o}C leaving a cooling duration of 60 minutes

to reach 20°C. The temperature (T) of the External fire curve is defined (Buchanan, 2001) as:

$$T = 660(1 - 0.687e^{-0.32t} - 0.313e^{-3.8t}) + T_0 \quad \textbf{(7-2)}$$

where,

t is the time (minutes)

T_0 is the ambient temperature (°C)

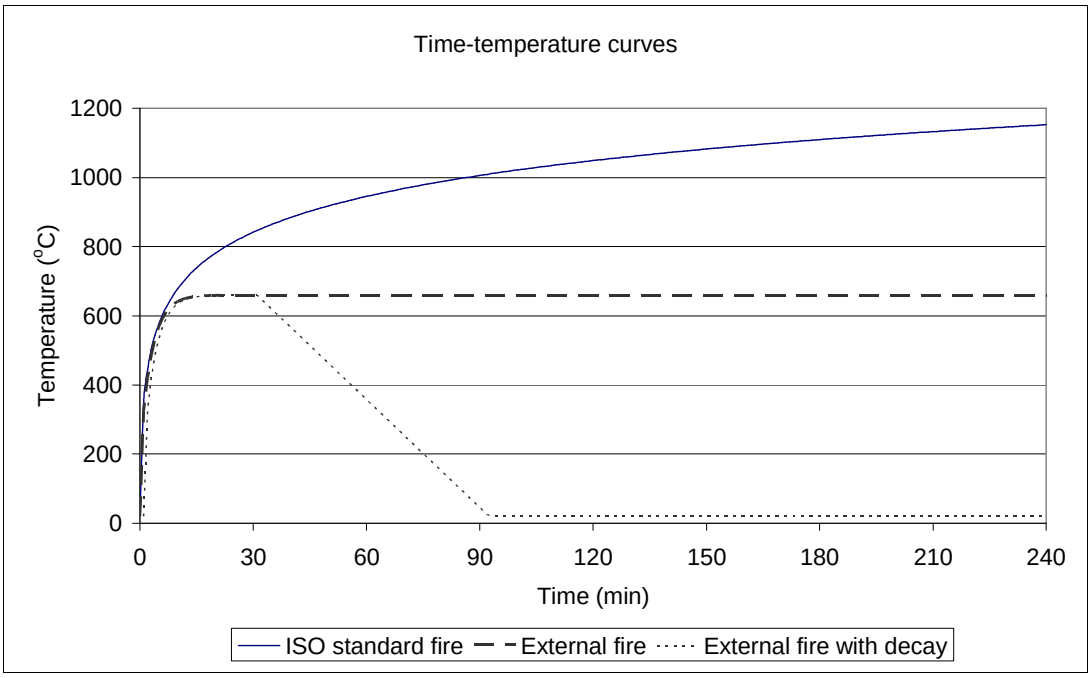

Figure 7-3 Time-temperature curves used in the analysis

Thermal Boundary

The steel elements are thermally exposed on all faces, as shown in Figure 7-4. The convection coefficient on hot steel surfaces and the relative emissivity are taken as 25 W/m^{2}K and 0.5, respectively (Franssen *et al.*, 2004). In reality, the external flange of the steel columns will be protected by the attached concrete panels. An assumption is made such that the concrete panel fails to act as an insulating material to the external flange. During the initial stages of fire, the top flange of the purlins may not be exposed directly to high temperatures due to the attachment of the roof sheeting. However, this is not taken into account and it is assumed that all faces of the purlins are exposed to elevated temperatures. This is particularly true when the roof sheeting

collapses. However, it is not easy to predict the failure temperature of the sheeting and therefore it is not considered in this project.

The temperature profiles of the steel elements exposed to the various fire curves are shown in Figure 7-5 to Figure 7-7. Due to the thin thicknesses of the purlin and the brace channel, the temperatures are fairly uniform throughout the whole cross-sections and the difference between the maximum and minimum temperatures is small. The temperature profiles of the purlin and brace channel follow closely the applied fire curves after 10 minutes. For the Eurocode External fire with a decay phase, Figure 7-7 shows that the 410UB54 section suffers a minimal phase lag such that the temperature of the steel section is slightly higher than the fire temperature during the decay phase.

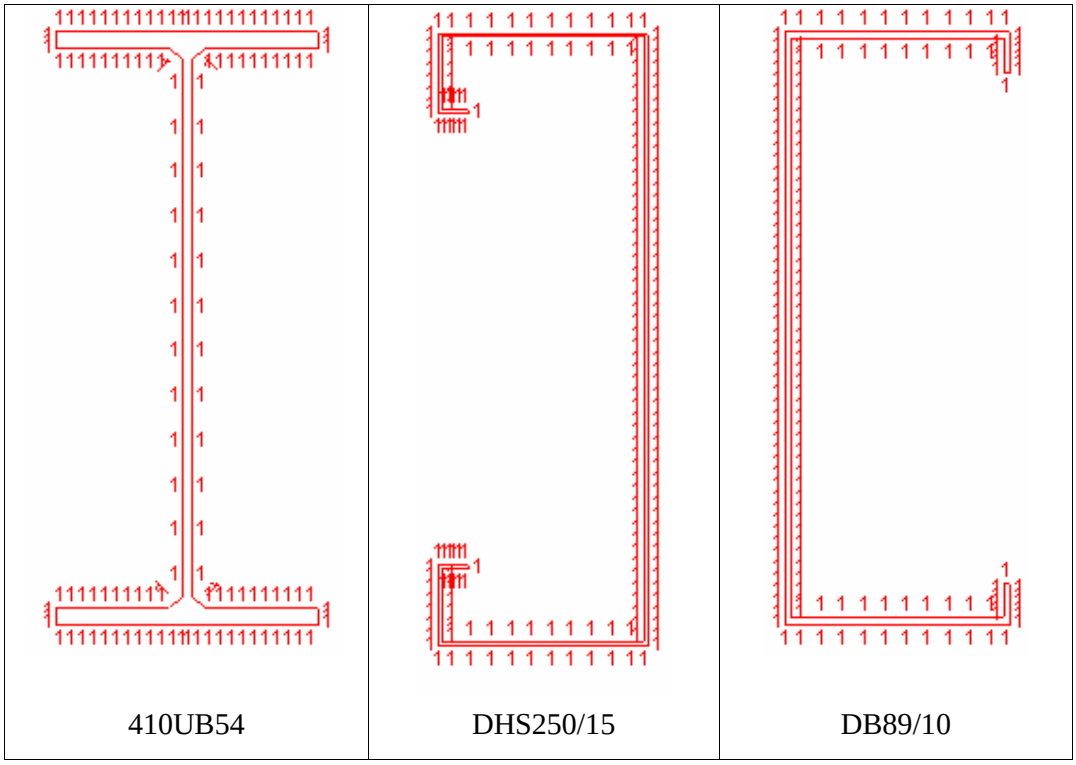

Figure 7-4 Thermal boundaries of the steel members

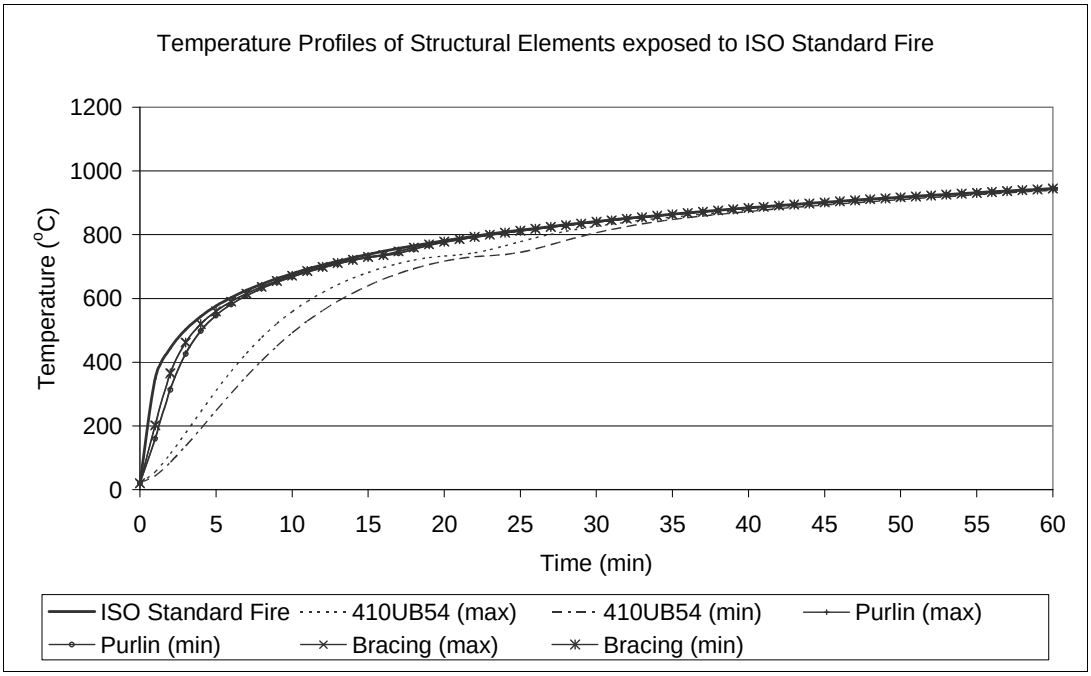

Figure 7-5 Temperatures profiles of the structural elements exposed to ISO 834 standard fire.

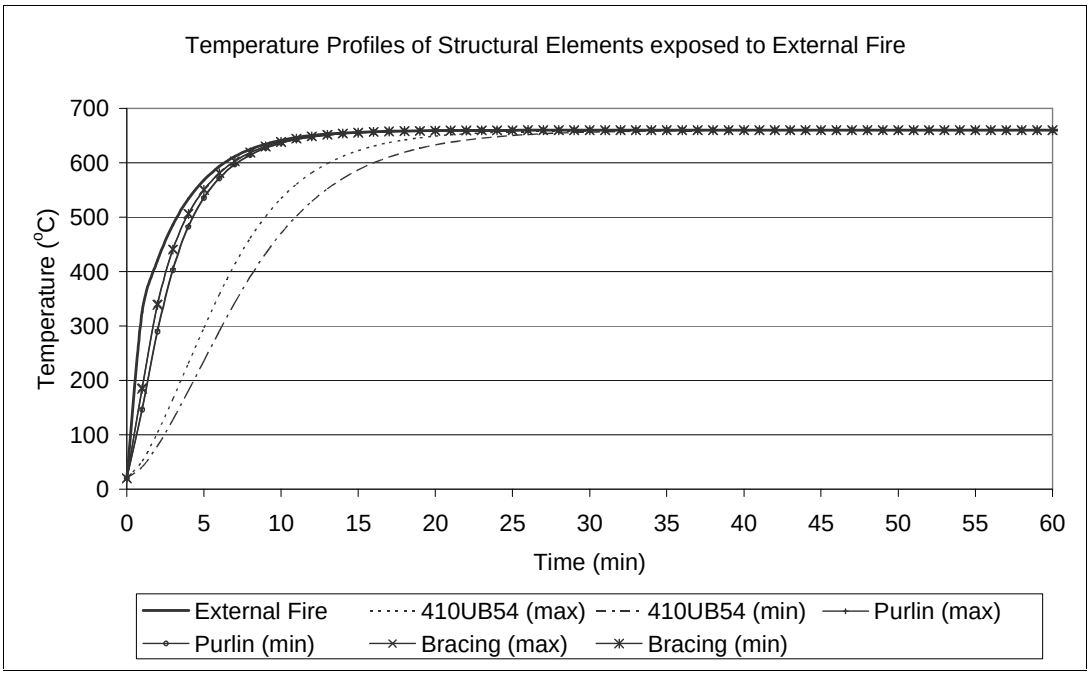

Figure 7-6 Temperatures profiles of the structural elements exposed to Eurocode External fire.

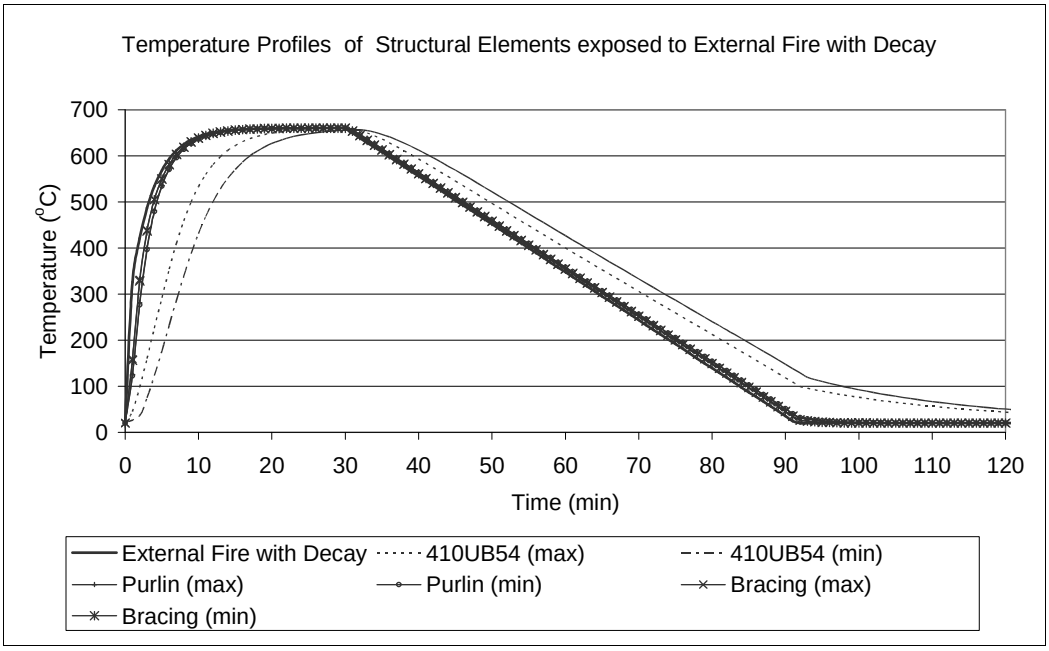

Figure 7-7 Temperatures profiles of the structural elements exposed to Eurocode External fire with a decay phase.

7.3 Gravity Load

The New Zealand loading code NZS 4203:1992 requires only the gravity load to be considered for the affected members during a fire (refer to Section 2.2.6). The gravity load consists of the dead load (G) of the steel structure and the ultimate live load (Q_u) on the roofs. The ultimate live load (Q_u) on the roofs can be ignored according to NZS 4203:1992. Therefore, the gravity load used in the analyses of this research project is the dead load (G) of the steel structure, and is applied as a uniformly distributed load (UDL) along the whole length of the steel members (i.e. 410UB54, DHS250/25 and DB89/10) and the UDL on the DHS250/25 purlins includes the dead load of the roof sheeting in addition to their self-weight. The dead loads of the components of the steel structure are tabulated in Table 7-2 and it is assumed that the loads are applied though the centroid of the cross-sections.

In reality, due to melting of plastic skylights and collapse of steel sheeting, only a portion of the roof sheeting will be present during the fire. The percentage of dead weight of roof sheeting likely to remain at the time of rafter collapse is given in

Newman (1990). For simplicity, it is assumed that the self-weight of the roof sheeting stays constant throughout the duration of the fire in this project.

Table 7-2 Loadings used in the analyses of this project

Component of dead load (G)		**Value**	**Unit**
Steel frame	G (410UB54)	527	N/m
Purlin &	G (DHS250/15)	56	N/m
roof sheeting	G (Roof sheeting)	0.07	kPa
Brace channel	G (DB89/10)	12	N/m

Wind loading

It is generally assumed that during a fire it is reasonable to expect a wind load lower than the normal design value. This is because the life of a fire is measured in hours and the design life of a building in tens of years. The effects of reduced wind loads on portal frames with collapsed rafters have been assessed by Newman (1990) and it is concluded that for frames up to 8 m high to eaves, the effect of wind is minimal and can be neglected. For frames greater than 8 m in height wind loading should be included but a lower level than normal design values, and the design wind speed should be reduced by multiplying the design value by an additional factor of 0.58. In this project, wind load is not taken into account for the analyses under fire conditions.

7.4 Structural Analysis

Structural analysis is first carried out on a single steel portal frame with both two (2D) and three (3D) dimensional finite element models. Three dimensional structural analysis is then performed on a single purlin orientated at 7.9^{o} from the vertical axis due to the roof slope. 3D structural analysis takes into account the torsional stiffness and the warping of the cross section and is described in more detail below. Several purlins with a brace channel provided at midspan are then placed on two steel universal beams which are fully fixed at the ends to simulate part of the roof structure. The analytical modelling is then extended to a two bay portal frame structure. The diaphragm action of the roof sheeting is ignored in all structural models. The sequence of the structural models is shown in Figure 7-8. The ambient, thermal and mechanical properties of structural steel are described in Chapter 3.

Analyses with the static and dynamic versions of SAFIR have been carried for the different models and the discrepancy between the two versions is described below. For "dynamic" analyses, the damping coefficient of the structure is taken as zero since SAFIR already contains numerical damping (Franssen *et al.*, 2004). The programme also requires the rotational inertia of the beam cross section which can be calculated using equation (7-3). The value of the rotational inertia can be estimated from using a more simplified equation shown below (equation (7-4) given by Franssen, J.M., *personal communication*). Using equation (7-4), the rotational inertias for a 410UB54 steel section, DHS250/15 purlin and DB89/10 brace channel are found to be 1.6 kg.m, 0.06 kg.m and 0.002 kg.m, respectively. The ISO 834 standard fire curve has been used throughout this section.

$$\text{Rotational inertia} = \sum \rho_i (I_{xx,i} + I_{yy,i} + y_{CG,i}^2 A_i + Z_{CG,i}^2 A_i) \quad \textbf{(7-3)}$$

$$\text{Rotational inertia} \approx \sum \rho_i (I_{xx,i} + I_{yy,i}) \quad \textbf{(7-4)}$$

where,

ρ_i = Density of the material *i* (kg/m^3)

I = Second moment of area of material *i* about the major or minor axis (m^4)

Torsional Analysis

SAFIR requires torsional analysis to be performed on cross-sections of all 3D beam elements in the finite element models before structural analysis is carried out. The torsional analysis calculates the elastic torsional stiffness and the warping function of the cross section at ambient temperature. In reality, the calculated value of elastic torsional stiffness will decease during the fire due to the increased temperature and the subsequent decrease in material stiffness. It is not possible to calculate the change in the torsional stiffness as a function of time in SAIFR and only a constant value can be entered. The calculated torsional stiffness can be divided by a factor of two to represent the decreased stiffness at elevated temperatures (Franssen, J.M., *personal communication*).

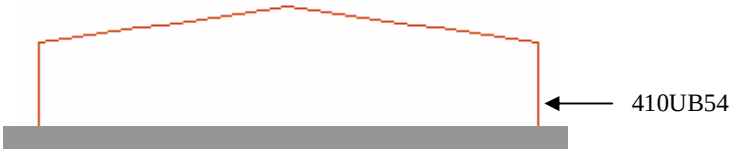

(a) Frame for 2D and 3D analyses

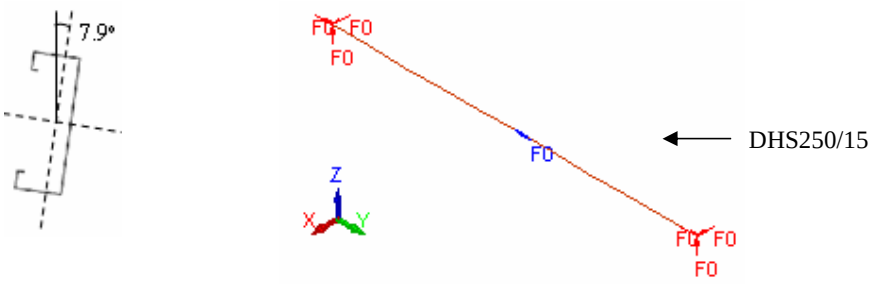

(b) Purlin oriented at 7.9° from the vertical axis for 3D analysis

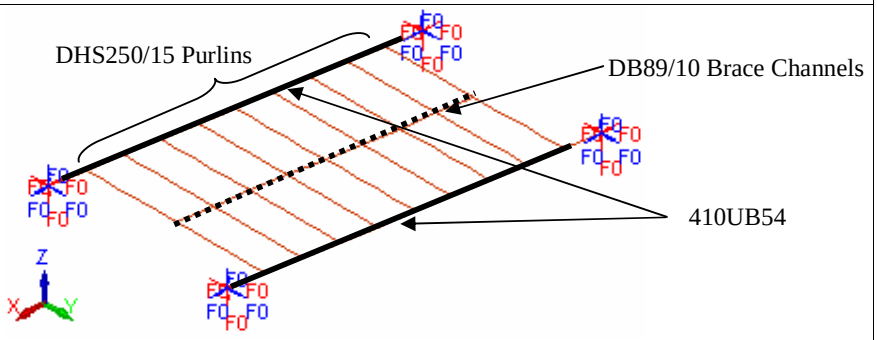

(c) 3D model of purlins with brace channel supported on fully fixed 410UB54 beams

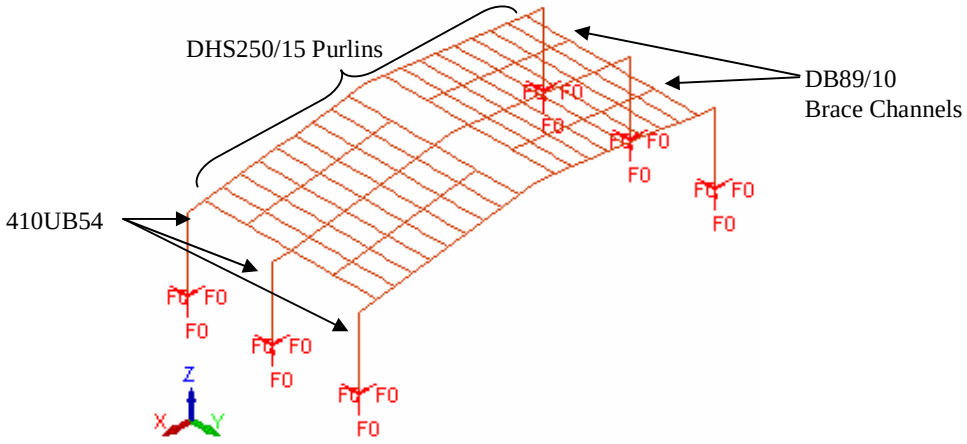

(d) 3D model of a two bay portal frame structure

Figure 7-8 Structural models for the analyses carried out with both static and dynamic algorithms in SAFIR

7.4.1 2D Analysis of the Frame (2D Frame)

The fully pinned bases of the frame are never achieved in reality and some degree of fixity will always be provided at the bolted connections. Both fully pinned and fully fixed support conditions at the column bases have been modelled in SAFIR for the 2D frame shown in Figure 7-8 (a). These are the two extreme cases for the behaviour of the frame and the partially fixed supports will lie somewhere between these two cases. The main difference between two and three dimensional analyses is that the out-of-plane deformation of the frame is not considered in a 2D analysis (i.e. out-of-plane buckling and collapse are not possible).

The frame is discretised into 40 beam elements as shown in Figure 7-9. The elements are joined together by nodes with 3 degrees of freedom, 2 translations and 1 rotation.

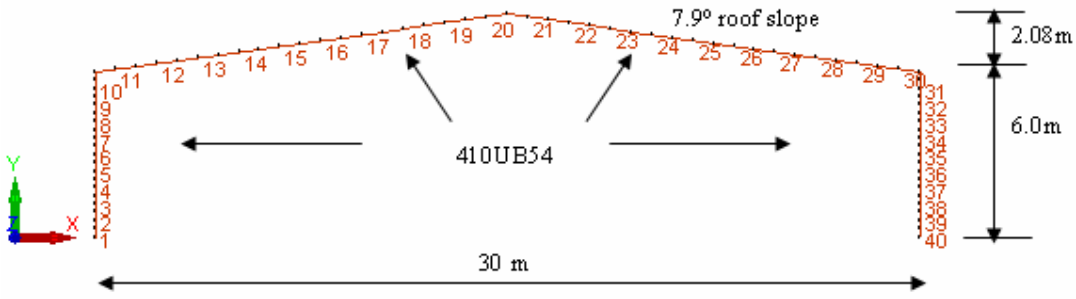

Figure 7-9 Structural model of 2D frame in SAFIR showing the element numbers

7.4.1.1 "Static" Cold Analysis

The 2D frame is first analysed under cold conditions and the ultimate load bearing capacity of the frame is determined using the static algorithm in SAFIR. An increasing uniformly distributed load is applied on the rafter and this gives the load-displacement curve at the apex of the frame (Figure 7-11). It is important that the universal beam (410UB54) is orientated correctly in the structural model and therefore the apex vertical deflection from the finite element model is checked against the design formula given in Buchanan (1999).

The apex vertical deflection for a pinned portal frame with straight members can be calculated using equation (7-5) with the coefficients given in Figure 7-10. Substituting the values of frame dimensions and section properties into the equation, a linear load-

displacement is obtained. Figure 7-11 compares the load-displacement curves obtained from SAFIR and the design formula. It is clear that both results show close agreement with each other and SAFIR shows the non-linear behaviour of the frame. The ultimate uniformly distributed load of the pinned support frame obtained from SAFIR is 6190 N/m.

The supports of the 2D frame are then changed to fully fixed and the load-displacement curve is obtained from SAFIR. The ultimate uniformly distributed load of the fixed support frame is 7100 N/m, which is approximately 15% higher than that of the pinned support frame. Figure 7-12 shows the load-displacement curves for the two different support conditions.

$$\Delta_{Apex} = \frac{wL^3 s(5B - 3C)}{192NEI_2} \qquad \textbf{(7-5)}$$

where,

W = Uniformly distributed load on the rafter (N/m)

L = Span of the rafter (m)

E = Elastic modulus of the steel section (MPa)

I = Second moment area of the steel section (m^4)

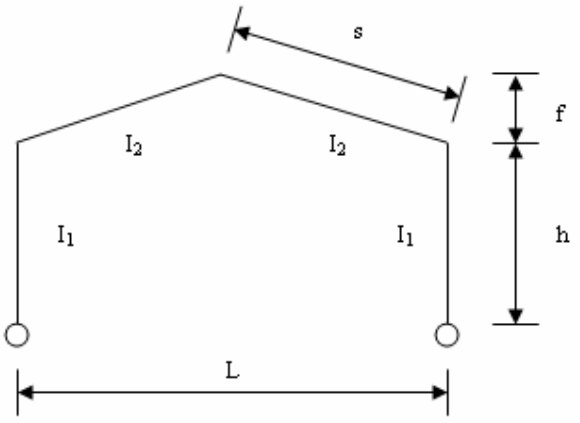

$$k = \frac{I_2}{I_1}\frac{h}{s}$$

$$\phi = \frac{f}{h}$$

$$m = 1 + \phi$$

$$B = 2(k+1) + m$$

$$C = 1 + 2m$$

$$N = B + mC$$

Figure 7-10 Coefficients for calculating the apex vertical deflection of a pinned portal frame (Buchanan, 1999)

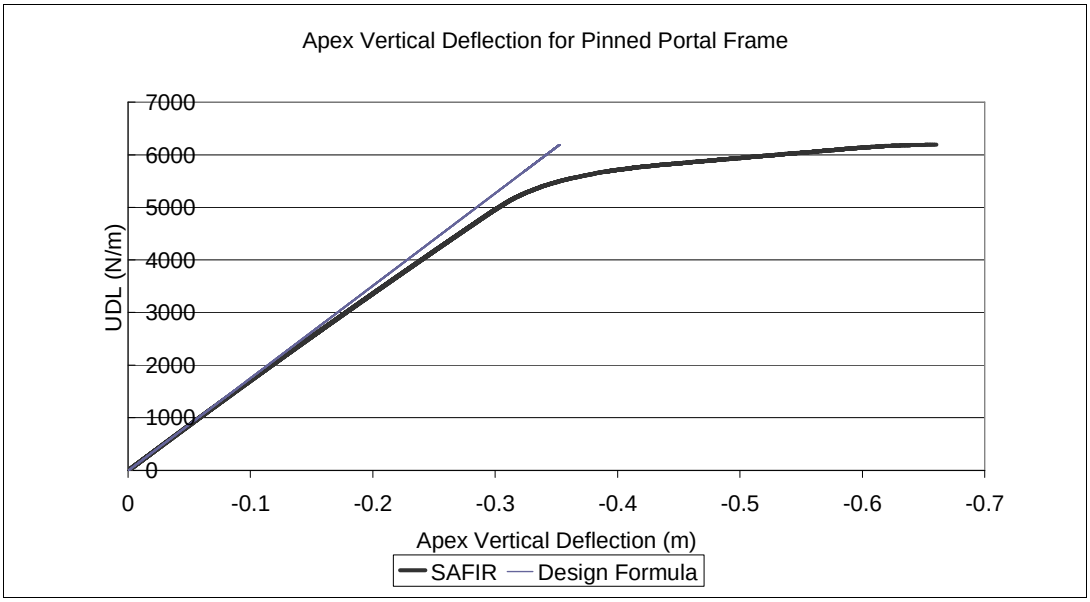

Figure 7-11 Load-displacement curves for pinned portal frames under "static" cold conditions

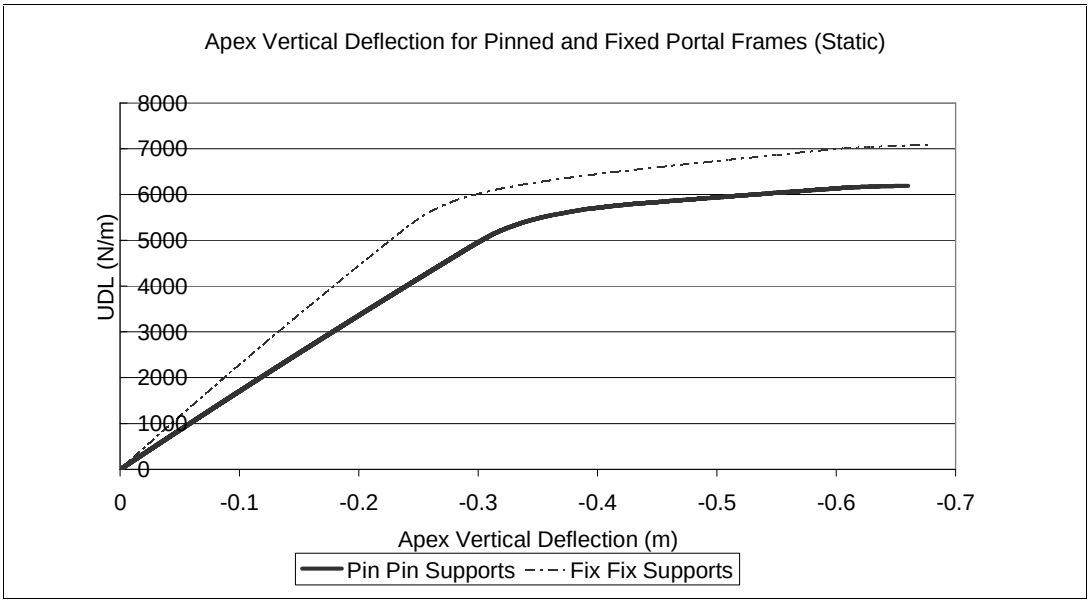

Figure 7-12 Load-displacement curves for pinned and fixed portal frames under "static" cold conditions

7.4.1.2 "Dynamic" Cold Analysis

Both pinned and fixed support conditions of the 2D frame are now analysed using the dynamic algorithm in SAFIR. The apex load-displacement curves are also obtained and are shown in Figure 7-13. The figure shows that the results from the "dynamic" analysis match the "static" analysis and is capable of showing further deflections. In addition, the "dynamic" analysis shows more clearly the run-away displacement trend

of the frames. Although total collapse of the frames cannot be seen at the end of the simulations, the results show a different collapse mechanism for the pinned support frame (Figure 7-14). The pinned support frame collapses outward with a sway mode of failure whereas the collapse of the fixed support frame is inwards.

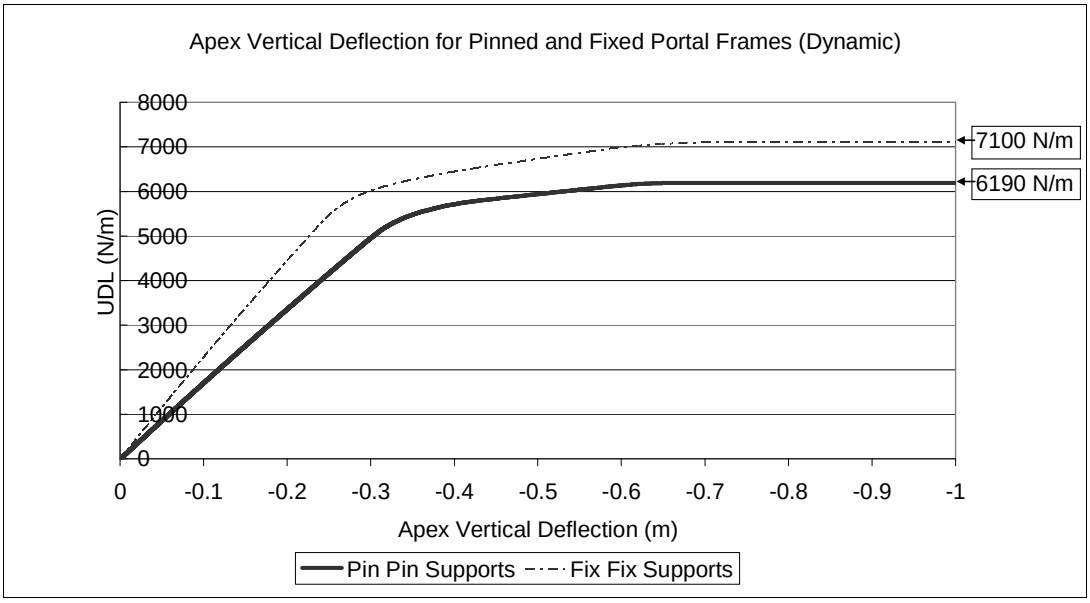

Figure 7-13 Load-displacement curves for pinned and fixed portal frames under "dynamic" cold conditions

"Static" Cold Analysis	"Dynamic" Cold Analysis
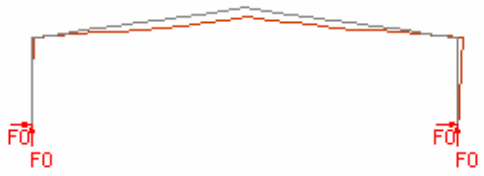	
Pinned supports	*Pinned supports*
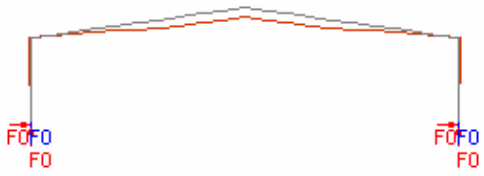	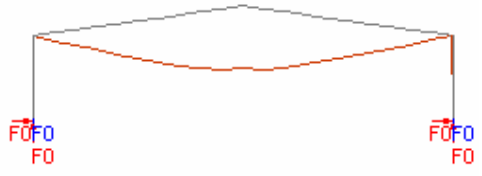
Fixed supports	*Fixed supports*

Figure 7-14 Deflected shapes at the last time step from SAFIR (Scale = 1x)

7.4.1.3 Load ratio of the Steel Portal Frame

The load ratio is the ratio of the expected loads on the structure during a fire to the loads that would cause collapse at normal temperatures and low load ratio signifies good fire resistance (Buchanan, 2001). There are two methods of determining the load ratio of the frame. The first method is based on the number of plastic hinges required to form a collapse mechanism of the frame and can be found using hand calculations. The second method is based on the results obtained from SAFIR. Both methods give a lower load ratio for the fixed base frame (i.e. higher fire resistance).

Hand Calculations

The expected uniformly distributed load along the length of the rafter during a fire emergency is found to be 1269 N/m from Table 7-2 and the tributary area shown in Figure 6-4. The bending moment diagrams for both fixed and pinned frames are shown in Figure 7-15.

Pinned base frame

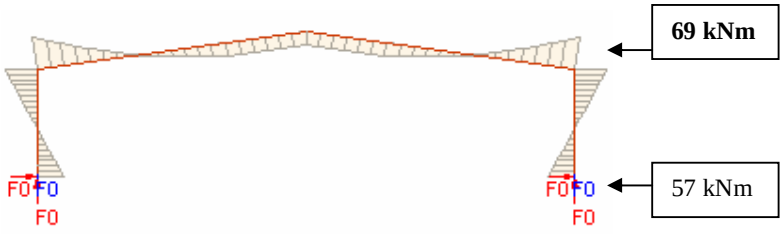

Fixed base frame

Figure 7-15 Bending moment diagrams under uniformly distributed load of 1269 N/m on the rafter

For a typical portal frame, four plastic hinges are required to form a collapse mechanism under cold conditions. Under fire conditions, only two plastic hinges are required to form at the knees of the frame to have a collapse mechanism. The formation of these plastic hinges will cause the steel rafter to deform downwards in a runaway displacement trend. Therefore, the eaves moments govern the load ratio of

the steel portal frame and failure only occurs when the plastic section capacity is exceeded at the knees. The plastic section capacity of a 410UB54 universal beam is 339 kNm (i.e. Mp = S x f_y) and this gives the following load ratios:

Pinned base frame, load ratio = **75**/339 = 0.221 ≈ 0.22
Fixed base frame, load ratio = **69**/339 = 0.204 ≈ 0.20

SAFIR

The load ratio can also be obtained from SAFIR using the load-displacement curves shown in Figure 7-13. As mentioned above, the expected uniformly distributed load on the steel rafter under fire conditions is 1269 N/m. Figure 7-13 gives ultimate uniformly distributed loads of 6190 N/m and 7100 N/m for pinned and fixed base frames, respectively. Therefore, the following load ratios are obtained:

Pinned base frame, load ratio = 1269 /6190 = 0.205 ≈ 0.21
Fixed base frame, load ratio = 1269/7100 = 0.179 ≈ 0.18

7.4.1.4 "Static" and "Dynamic" Hot Analyses

The 2D frame is now analysed under fire conditions and the whole frame is fully exposed to the ISO fire curve. Similarly, the uniformly distributed load applied on the rafter is 1269 N/m and includes the dead load from the purlins and the roof sheeting. A horizontal force of 12.7 N (i.e. 1% of the UDL applied on the rafter) has been applied at the top of the left column to simulate initial geometrical imperfection (Figure 7-16). Both static and dynamic versions of SAFIR have been used and the results are shown in Figure 7-17 to Figure 7-19.

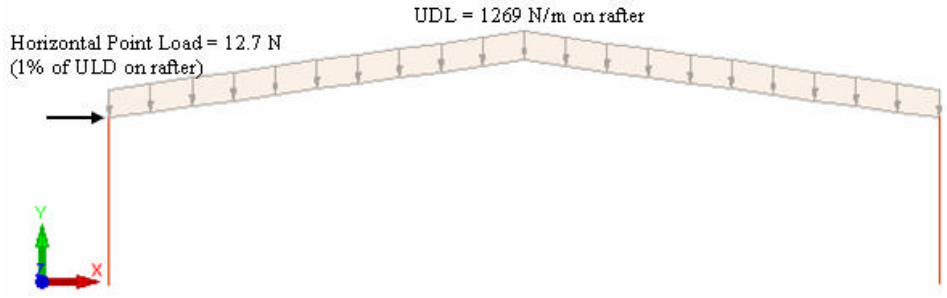

Figure 7-16 Loadings used in the "static" and "dynamic" hot analyses of 2D frame

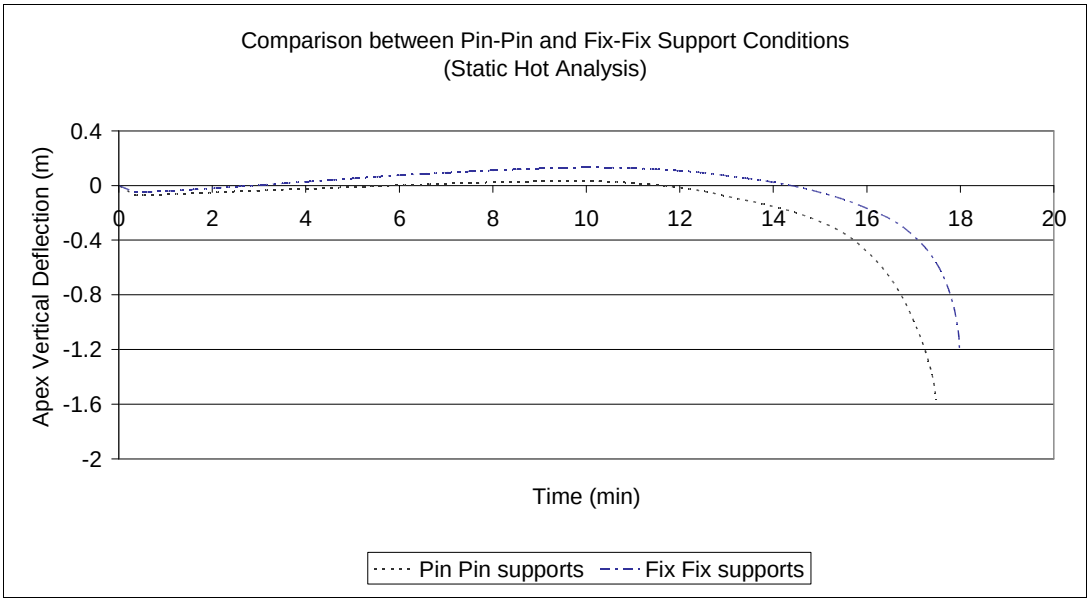

Figure 7-17 Apex vertical deflection for pinned and fixed portal frames under "static" hot conditions

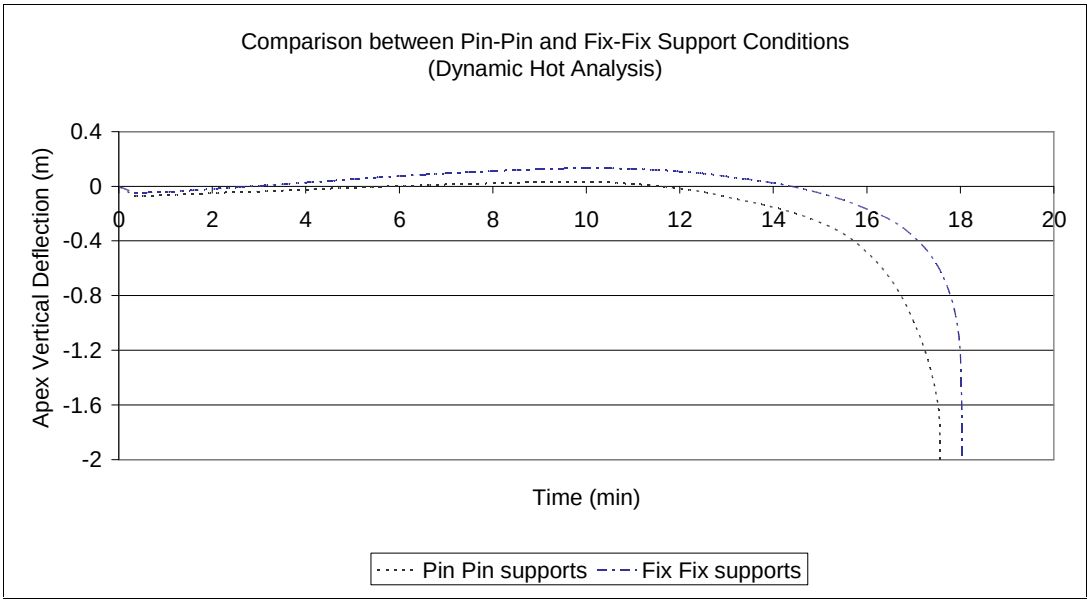

Figure 7-18 Apex vertical deflection for pinned and fixed portal frames under "dynamic" hot conditions

“Static” Hot Analysis	“Dynamic” Hot Analysis
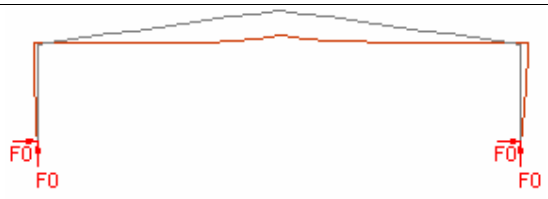 *Pinned supports*	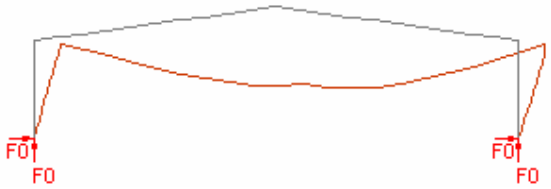 *Pinned supports*
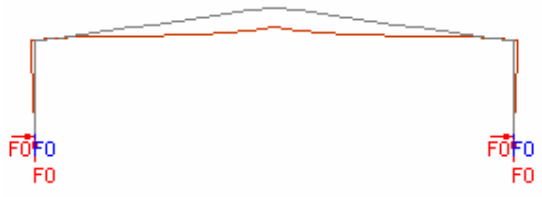 *Fixed supports*	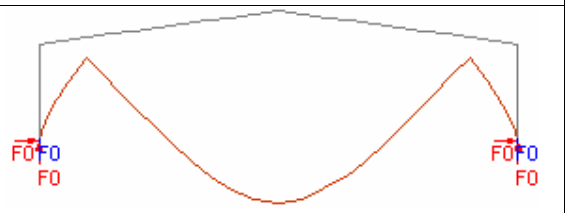 *Fixed supports*

Figure 7-19 Deflected shapes at the last time step from SAFIR (Scale = 1x)

The results from both static and dynamic algorithms match each other precisely for the first time steps. However, the “static” analyses have stopped due to premature numerical failure before the frames can be seen to collapse inwards or outwards. The “dynamic” analyses were capable of iterating into very small time step near the end to show the complete failure modes of the frame. Figure 7-19 shows that fixed support frames collapse inwards whereas pinned support frames fail in a sideway mode which is unacceptable. If the frames were only analysed using the static algorithm in SAFIR, this would give misleading collapse modes.

7.4.2 3D Analysis of the Frame with no Purlins (3D Frame)

3D analysis is conducted on the same frame under both cold and hot conditions. Static and dynamic versions of SAFIR have also been used for the analysis of the 3D frame. For the analyses under cold conditions, an increasing uniformly distributed load is applied to the rafter as in the 2D frame analyses. For the hot conditions, the uniformly distributed load of 1269 N/m is applied to the rafter and the frame is heated throughout with an ISO 834 standard fire. The 3D frame analyses take into account the warping and torsion of the cross section. The frame is discretised into 40 beam elements as shown in Figure 7-20. The elements are joined by nodes with 7 degrees of freedom, 3 translations, 3 rotations and 1 warping.

Two nodes have been created at the apex of the frame (i.e. the nodes have the same coordinates in space), one representing the degrees of freedom from the left rafter (beam element no. 21) and the other (beam element no. 20) from the right rafter. It is assumed that full compatibility can be achieved at the apex and warping is effectively transmitted between the two nodes. This is equivalent to one node at the apex connecting the adjacent beam elements of the rafters and the two nodes are created here to give the flexibility of changing the connection types if required.

Similarly, two nodes have also been created at the knees to represent the degrees of freedom from the column and the rafter. In this case, the warping between the two nodes is not transmitted and the nodes share the same translations and rotations.

At the column bases of the frame, the warping of the cross section will be restrained by the endplate which is bolted through to the concrete foundation (refer to Figure 4-53). This is achieved in the finite element models by restraining the 7^{th} degree of freedom (i.e. warping). In addition, for the fixed support frame, all the degrees of freedom are restrained at the column bases (i.e. full restraint against translations, rotations and warping). However, for the pinned support frame, only the translations and warping are restrained giving the column bases to rotate freely in any direction.

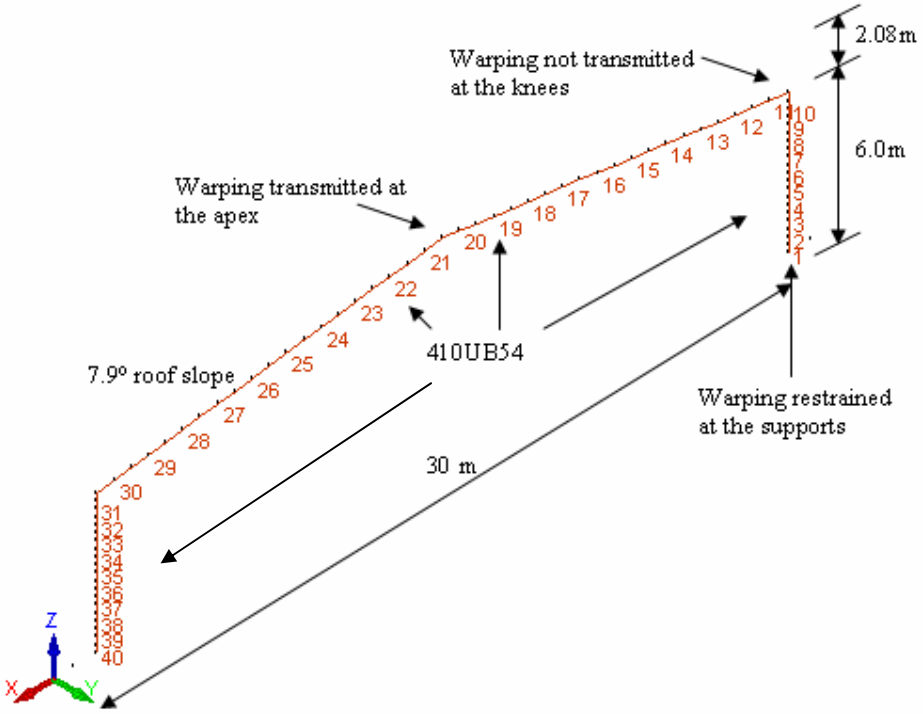

Figure 7-20 Structural model of 3D frame in SAFIR showing the element numbers

The portal frame with no purlins is very unstable in a three dimensional analysis. Numerical failures occurred during the first few time steps in all the "static" analyses. The results from the "static" analyses are not discussed further here. In contrast, the "dynamic" analyses were capable of iterating to very small time steps and showed the collapse of the frames. Figure 7-21 and Figure 7-22 show the out-of-plane collapse of the frames for both cold and hot conditions. For the cold conditions, the frame with pinned support conditions is very unstable and collapses at a very low load when compared to the fixed support frame. When the frame is exposed to elevated temperatures, it becomes very unstable and fails in the early stages of fire regardless of the different support conditions. It should be noted that in reality, purlins and concrete wall panels will provide out-of-plane restraints to the frame and out-of-plane collapse is very unlikely to happen. The results from the analyses of 3D frame with no purlins again show that SAFIR is capable of handling very large deflections with the dynamic algorithm.

Pinned Support Frame	Fixed Support Frame
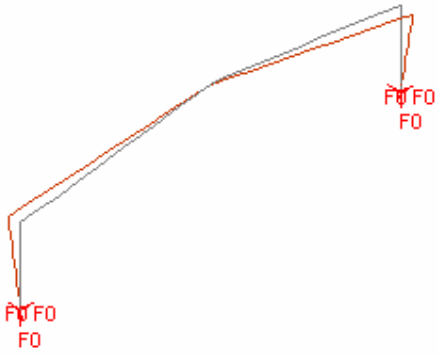	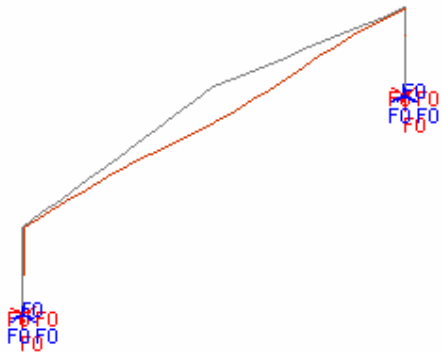
UDL = 110 N/m	UDL = 1000N/m
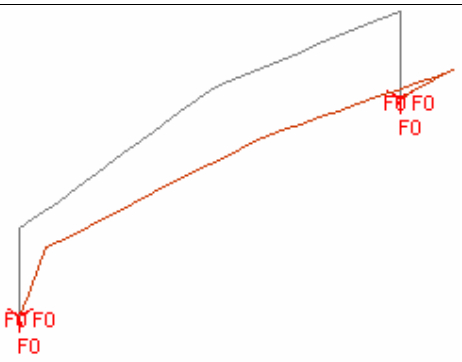	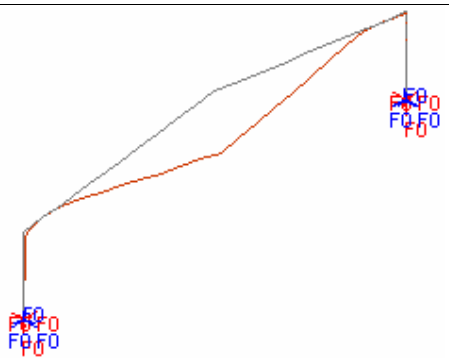
UDL = 125 N/m	UDL = 1555 N/m
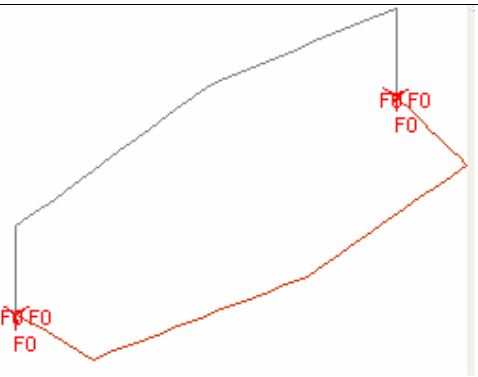	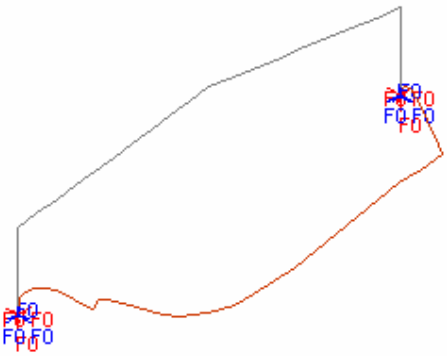
UDL = 127 N/m	UDL = 1558 N/m

Figure 7-21 Variation of deflected shapes showing the out-of-plane collapse of frames under "dynamic" cold conditions

Pinned Support Frame	Fixed Support Frame
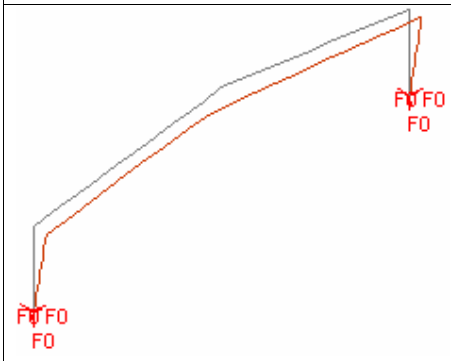 *Time = 16 seconds*	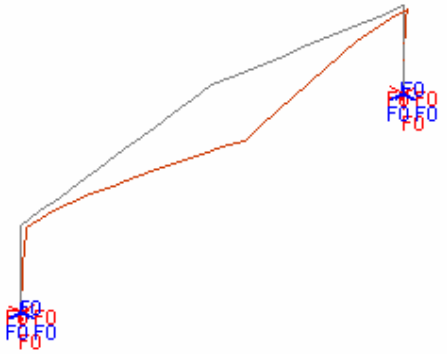 *Time = 19 seconds*
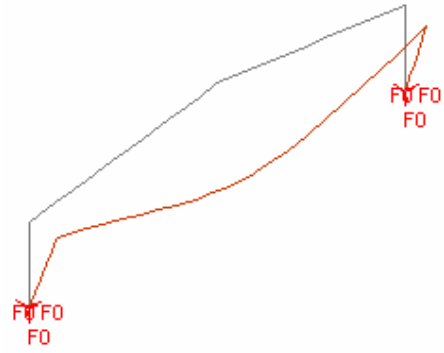 *Time = 17 seconds*	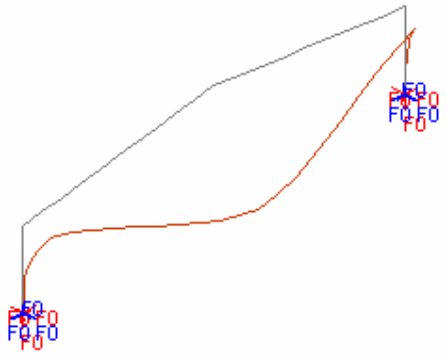 *Time =20 seconds*
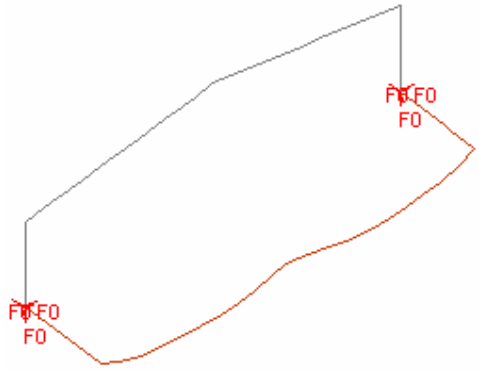 *Time = 18 seconds*	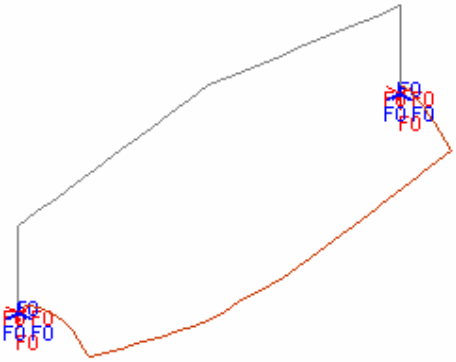 *Time = 21 seconds*

Figure 7-22 Variation of deflected shapes showing the out-of-plane collapse of frames under "dynamic" hot conditions (Note: Load applied = 1269 N/m on the rafter)

7.4.3 3D Analysis of the Purlin with no Lateral Restraint

A single DHS250/15 purlin is analysed in three dimensions in this section. The DHS purlins have the tendency to buckle and therefore two dimensional analysis is not performed. The purlin spans 7.2 m between the supports (i.e. supports on rafter) and is orientated at 7.9^{o} from the vertical axis due to the roof slope of the building. Figure 7-23 shows the cross section of the purlin and the shear centre (SC) is offset at a distance from the centre of gravity (CG). The purlin is discretised into 10 beam elements as shown in the figure.

SAFIR requires the location of the shear centre in the structural analysis input file. For the sections with two axes of symmetry, the position of the shear centre is at the centroid (i.e. 410UB54). For the DHS250/15 purlin, the section has only one axis of symmetry and the shear centre lies along the axis of symmetry. The location of the shear centre on this axis can be obtained from equation (7-6) (Gorenc *et al.*, 1996). Using equation (7-6), the shear centre of the DHS250/15 purlin is found to be 67 mm offset from the centre of gravity.

$$X_{sc} = \frac{I_{x1}X_1 + I_{x2}X_2 + I_{x3}X_3 + ...}{I_{x1} + I_{x2} + I_{x3} + ...} \qquad \textbf{(7-6)}$$

where,

X_{sc} = The distance from an arbitrary point on the symmetric axis to the shear centre

X_1, X_2, X_3 = The distances of the centroids of areas A_1, A_2, A_3 of the section from the same arbitrary point

I_{x1}, I_{x2}, I_{x3} = The *I*-values of areas A_1, A_2, A_3 about the symmetric axis.

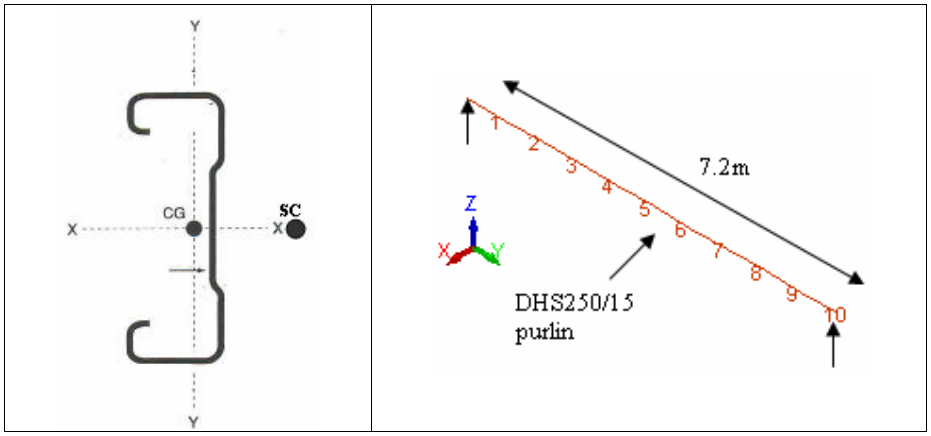

Figure 7-23 Centre of gravity, shear centre and beam elements of the DHS250/15 purlin

As mentioned in Section 7.3 above, the load from the roof sheeting is assumed to be applied through the centre of gravity (centroid) and this will create a twisting moment about the longitudinal axis. In this section, the purlin is analysed under various boundary conditions as shown in Figure 7-24. Both static and dynamic algorithms in SAFIR are carried out for both cold and hot conditions. The cold analysis involves an increasing uniformly distributed load added along the length of the purlin whereas the hot analysis involves a uniformly distributed load of 162 N/m (G (purlin + roofing)) on the purlin.

In reality, the top flange is in compression under gravity load and buckling of the purlin will be restricted by the fixings to the roof sheeting. During the initial stages of a fire, the affected part of the building will be helped to resist the effects of the fire by the cooler roof immediately adjacent (i.e. by stressed skin action) and the unheated roof diaphragm (O'Meagher *et al.*, 1992). The modelling of roof sheeting is complicated and may not be realistically represented by beam elements. It should also be noted that the lateral restraint provided by the roof sheeting will be compromised when the fire grows to a certain extent. Therefore, lateral restraint provided by the roof sheeting is ignored in the finite element models. However, it is possible to model the roofing by using a layer of thin shells in SAFIR. This lies outside the scope of the research and is not considered in this project.

Finite element model	Description of the model
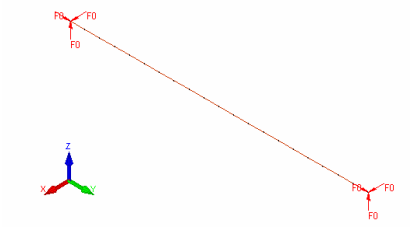 Pin Pin	At both ends of the supports, the purlin is restrained translationally in all directions and is not free to move. There is no bending moment induced at both supports and the purlin is free to twist about the longitudinal axis.
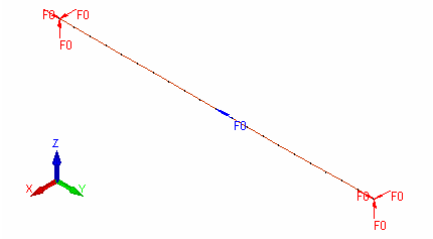 Pin Pin Braced	A rotational restraint is introduced at the midspan to simulate the effects from a brace channel. This restraint only prevents the purlin from twisting about the longitudinal axis at midspan and translations are not fixed at that point. Similarly, the purlin is free to twist at the ends.
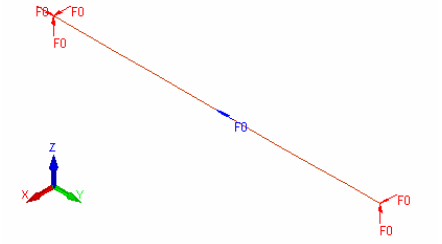 Pin Roller Braced	The axial restraint is released at one support to simulate a pin roller purlin. At the roller support, it is free to move axially.
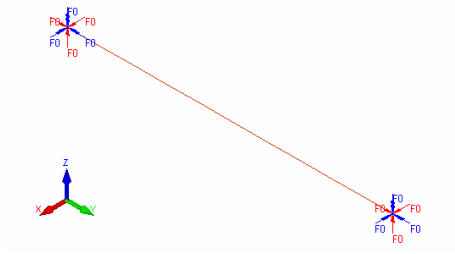 Fully Fixed end supports	The purlin is now fully restrained translationally and rotationally at both supports without any rotational restraint imposed at the midspan. Bending moment will be induced at the supports.

Figure 7-24 Various boundary conditions for the analyses of a single DHS250/15 purlin

7.4.3.1 "Static" and "Dynamic" Cold Analyses

For the analyses under cold conditions, the midspan in-plane and out-of-plane load displacement curves are shown in Appendix C. The load and the associated in-plane displacement for each boundary condition analysed are tabulated in Table 7-3. The

load was obtained when SAFIR failed to iterate to the next time step (i.e. numerical failure) or when the simulation stopped at which the specified applicable uniformly distributed load of 14.4 kN/m in SAFIR (i.e. arbitrarily chosen as the maximum load limit in SAIFR) was reached.

Most of the simulations were able to iterate until the specified load was reached (i.e. UDL = 14.4 kN/m). However, numerical failure occurred at the first time step for the pin-ended purlin without any restraint at midspan. This is because the purlin rotated indefinitely about the longitudinal axis (i.e. global y-axis in the figure) due to the offset between the shear centre (SC) and the centre of gravity (CG) and the moment created by the applied load.

The load-displacement curves show that both "static" and "dynamic" analyses match precisely to each other. Interestingly, numerical failure occurred when the load reached 1.2 kN/m for the purlin with pin roller supports in the "static" analysis. The analysis with the dynamic algorithm had overcome the numerical failure and was able to show the behaviour of the purlin until the simulation ended. Comparing the load-displacement curves from both algorithms in SAFIR (refer to Appendix C), it is found that the numerical failure occurred is due to the onset of a sudden change in the in-plane deflection of the purlin.

Table 7-3 Load and the coincident in-plane deflections for the purlin under cold conditions

Finite element model	**Load (kN/m)**		**In-plane deflection (m)**	
	"Static"	"Dynamic"	"Static"	"Dynamic"
Pin Pin	-	-	-	-
Pin Pin Braced	14.4*	14.4*	-0.30	-0.30
Pin Roller Braced	1.2	14.4*	-0.19	-2.66
Fully Fixed end supports	14.4*	14.4*	-0.27	-0.27

Note: - denotes numerical failure in SAFIR at the first time step

** denotes the specified applicable load of 14.4 kN/m in SAFIR was reached*

7.4.3.2 "Static" and "Dynamic" Hot Analyses

For the analyses under elevated temperatures, the whole length of the purlin is heated according to the ISO fire. The curves for midspan in-plane (i.e. about major axis) and out-of-plane (i.e. about minor axis) displacements plotted against time are shown in Appendix D. The time and the associated in-plane displacement for each boundary condition analysed are tabulated in Table 7-4. The maximum time was obtained when numerical failure occurred in SAFIR or when the simulation stopped at the specified maximum time limit of 14400 seconds or 4 hours.

Similarly, numerical failure occurred at the first time step for the pin-ended purlin without rotational restraint at midspan. However, numerical failure also occurred for the same purlin with rotational restraint provided at the midspan and the cause of this is not known at the stage of writing this report. The results show that both static and dynamic algorithms match reasonably accurately to each other during the first time steps and the dynamic algorithm is able to overcome the premature numerical failures that commonly occur with the static algorithm. This is very important in the 3D modelling of the whole building and dynamic algorithm must be used to obtain the complete failure mechanism of the structure.

Table 7-4 Time and the coincident in-plane deflections for the purlin under hot conditions

Finite element model	**Time (s)**		**In-plane defection (m)**	
	"Static"	"Dynamic"	"Static"	"Dynamic"
Pin Pin	-	-	-	-
Pin Pin Braced	-	-	-	-
Pin Roller Braced	819	2185	-0.23	-2.45
Fully Fixed end supports	8991	14400*	-0.28	-0.58

Note: - denotes numerical failure in SAFIR at the first time step

** denotes the specified applicable load of 14400 s in SAFIR was reached*

7.4.4 Purlins supported on Fully Fixed Beams

A 3D finite element model is set up in SAFIR consisting of nine DHS250/15 purlins which are braced at midspan with a DB89/10 brace channel and are supported on two steel beams (410UB54) fully fixed at the ends to simulate part of the roof structure

(refer to Figure 7-25). The ends of the purlins are joined to the nodes of the rafter (i.e. master-slave relationships between these nodes with the same coordinates in the structural analysis input file) in a way that they behave similarly to the fully fixed end supports shown in Figure 7-24 but with rotation about the vertical axis freed. In practice, the purlins will be bolted to steel cleats which are welded to the top flange of the steel rafter (Figure 7-26). Some degree of fixity will be provided by the bolts to resist twisting about the longitudinal axis and in-plane deflection of the purlin. An assumption is made in the model that the bolts are able to provide full restraint against twisting about the longitudinal axis and in-plane rotation of the purlin. In terms of the warping of the purlins, it is clear that warping is neither transmitted to the rafter nor to the adjacent purlin. A small gap usually exists between the purlins at the support due to geometrical tolerances.

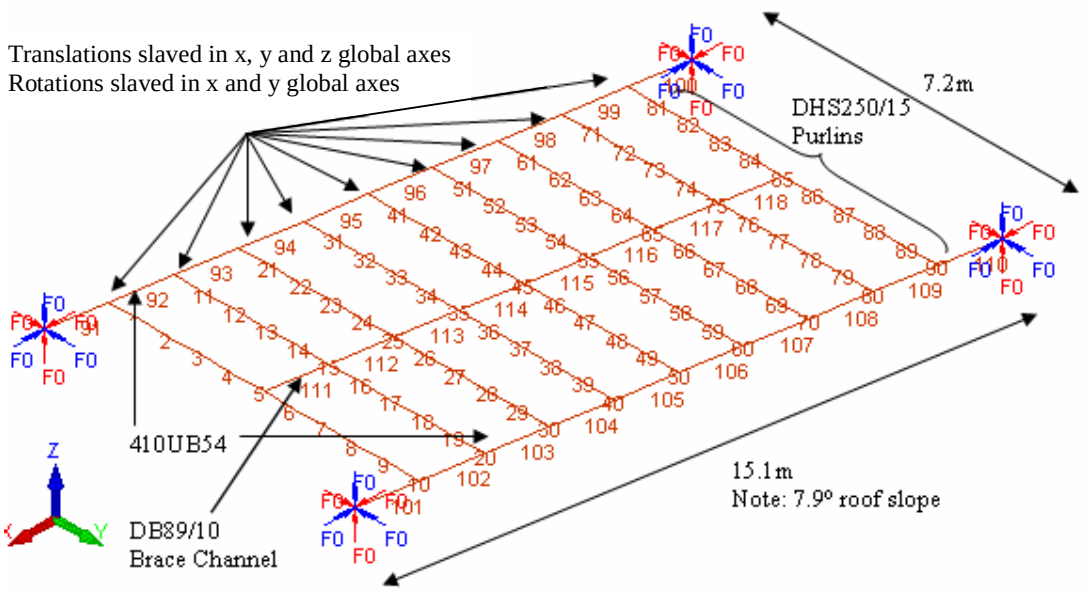

Figure 7-25 3D structural model of purlins and beams in SAFIR showing the element numbers

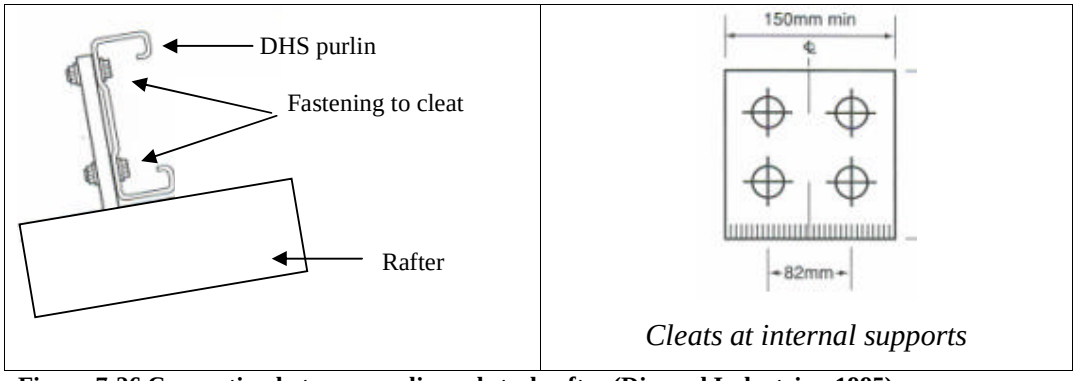

Figure 7-26 Connection between purlin and steel rafter (Dimond Industries, 1995)

It should be noted that for simplicity, it has been assumed that the centreline (centrenode) of the purlin coincides with the centreline (centrenode) of the rafter.

The connection detail between the brace channel and the purlin according to Dimond Industries (1995) is shown in Figure 7-27. The brace channel is bolted on to proprietary steel plates, which are in turn bolted onto the web of the purlin. Similarly, the nodes (i.e. with same coordinates) between the brace channel and the purlin share the same translations in the model (i.e. translation compatibility) and it is assumed that the connection is able to provide restraints against twisting about the longitudinal axis and in-plane rotation of the brace channel.

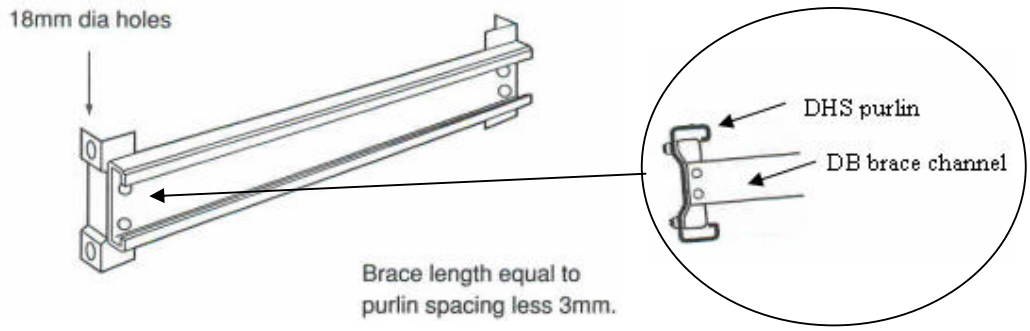

Figure 7-27 Connection between brace channel and purlin (Dimond Industries, 1995)

Analyses have been carried out for cold and hot conditions using both static and dynamic versions of SAFIR. For the hot analysis, all the members are exposed to the ISO 834 standard fire. The cold analysis has an increasing uniformly distributed load applied along the length of the beam elements and the hot analysis includes the self weight of the members and the dead load of the roof sheeting (refer to Table 7-2).

The deflected shapes at the last time step are shown in Figure 7-28 (note: the load limit or the time limit was set to 14.4 kN/m or 14400 seconds, respectively, in SAFIR). The analyses have shown that the dynamic algorithm has successfully overcome numerical failures observed in the “static” analyses and predicted the behaviour of the structure until the load limit was reached under cold conditions, and up to the point where a snap through failure mechanism had occurred under hot conditions.

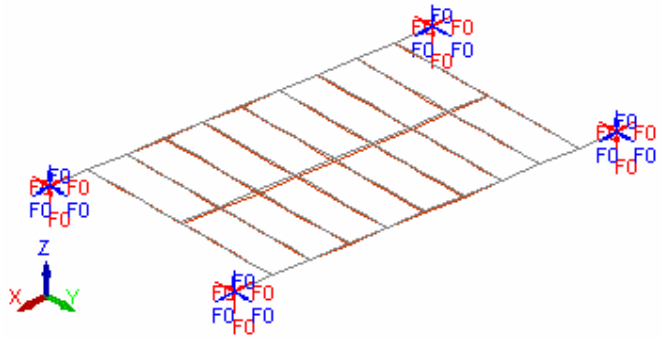

"Static" cold analysis at load = 3.0 kN/m
(Numerical failure)

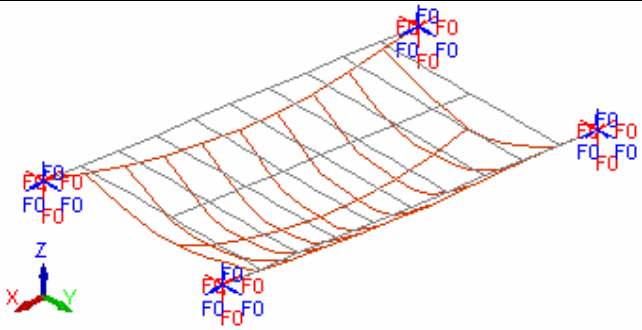

"Dynamic" cold analysis at load = 14.4 kN/m
(Load limit of 14.4 kN/m reached)

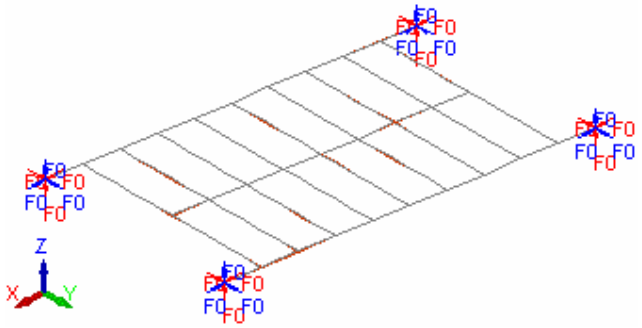

"Static" hot analysis at time = 40 s
(Numerical failure)

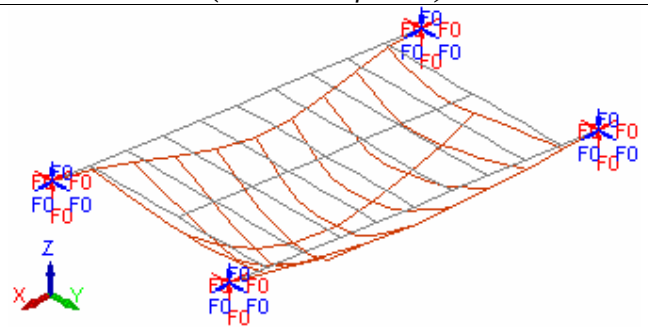

"Dynamic" hot analysis at time = 3402 s
(Snap-through failure)

Figure 7-28 Deflected shapes at the last time step from SAFIR (Scale = 1x)

7.4.5 Two Bay Portal Frame Structure

The modelling is extended to a two bay steel portal frame structure in this section (Figure 7-29). All the steel members are exposed to the ISO 834 standard fire curve and the loads applied are the self-weight of the members and the roof sheeting (refer to Table 7-2). Numerical failure occurred within the first few time steps in the "static" case and the results are not discussed further here.

The deformations for both pinned and fixed support frames using the dynamic algorithm are shown in Figure 7-30 and Figure 7-31. The analyses show that the pinned support structure is very unstable in the weak direction of the 410UB54 frame and collapses in the very early stages. In contrast, the fixed support structure is able to withstand the fire for 10 minutes and collapses when the rafter sags down in a relatively fast manner. All three frames deform excessively in the weak direction. In reality, the out-of-plane collapse is very unlikely to occur due to restraints provided by the surrounding cold structures such as the walls, the purlins, the frames and the roof diaphragm. In addition, this collapse time does not imply that the fire resistance rating (i.e. stability criterion) of this particular structure is 10 minutes although the ISO fire was used in the analysis. The effects of the restraints provided by cold purlins and frames and also the end walls are investigated in Chapter 8.

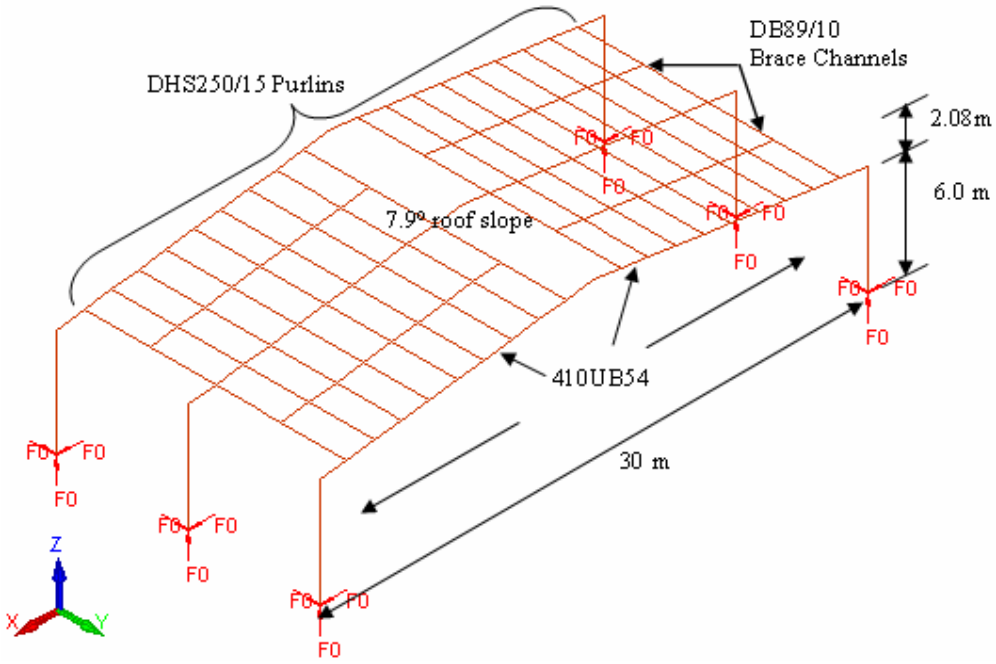

Figure 7-29 3D structural model of two bay steel portal frame structure in SAFIR

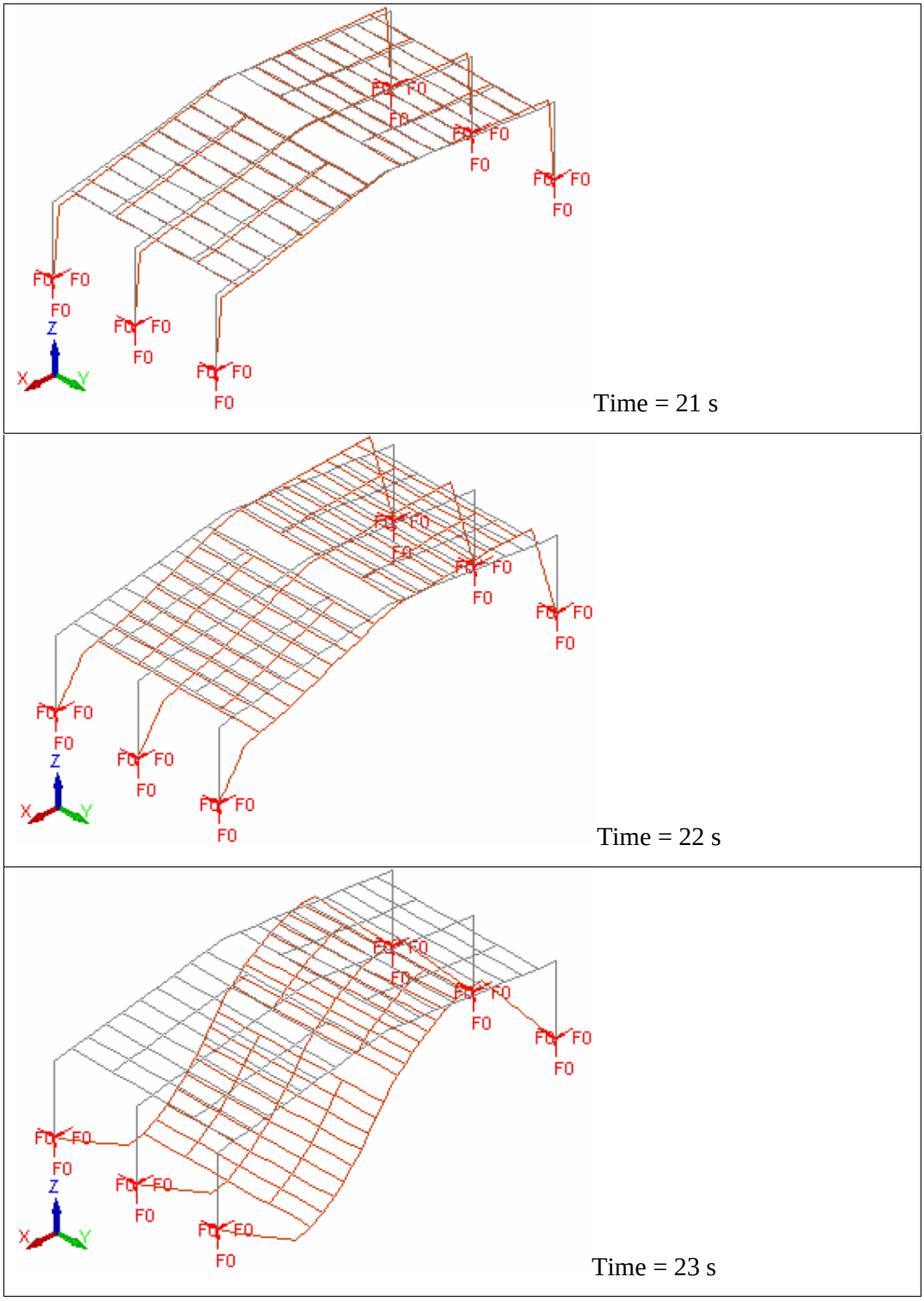

Figure 7-30 Deformations of pinned support structure fully exposed to ISO 834 standard fire (Scale = 1x)

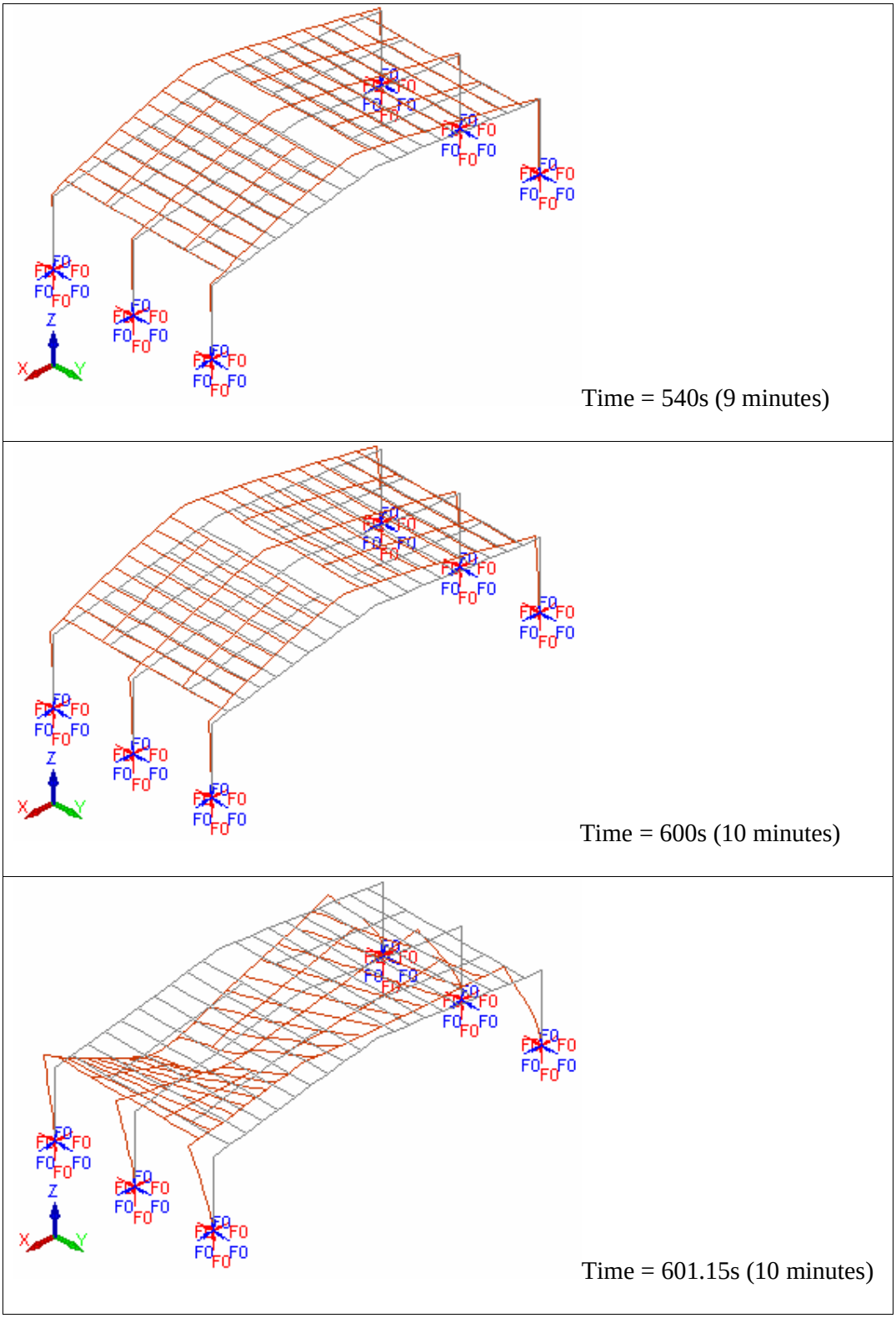

Figure 7-31 Deformations of fixed support structure fully exposed to ISO 834 standard fire (Scale = 1x)

Middle Frame only exposed to fire

It is interesting to expose only one frame to elevated temperature although this is unrealistic in a real fire. In this case, only the middle frame is exposed to the ISO 834 standard fire and the rest of the structure remains at ambient temperature. The structure did not collapse after 4 hours when the maximum time limit was reached. Figure 7-32 shows the deflected shape at the end of the simulation. The heated steel columns can be seen to deform excessively about the weak axis. In the case of the actual structure, out-of-plane restraints will be provided by the connections to the side wall panels at the top and mid-height of the columns (Section 6.5) and these restraints are included in the fire analysis of the complete building in the next chapter.

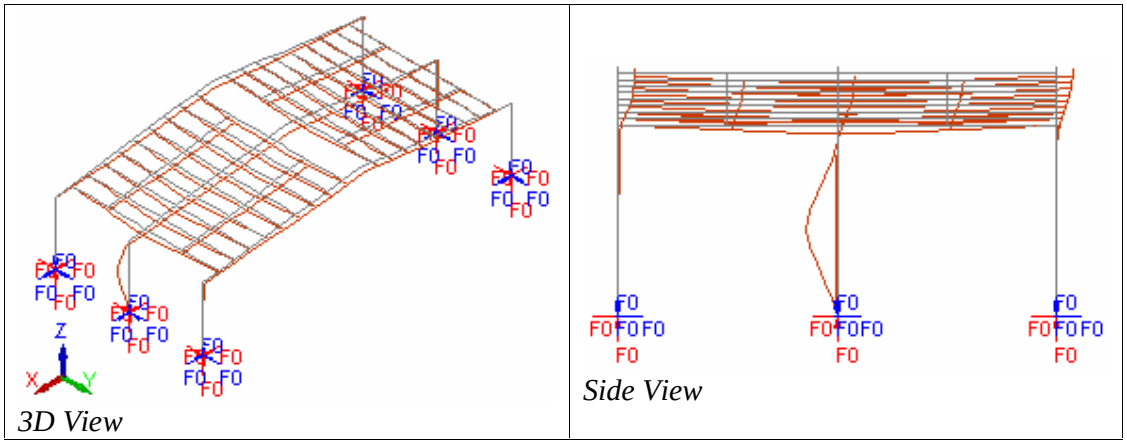

Figure 7-32 Deflected shape at the last time step for the structure with only the middle frame heated.

7.4.6 Conclusions

It is concluded that both static and dynamic algorithms in SAFIR will give identical results in most cases before numerical failure occurs in the "static" case. Numerical failure usually occurs in the static algorithm when the structure itself is very unstable or when the structure undergoes a sudden deformation at elevated temperatures. The latter can give misleading collapse modes for portal frames if numerical failure occurs at a point before full collapse is obtained. Therefore, the dynamic algorithm must be used if meaningful results are to be obtained. It has also been shown that SAFIR is capable of analysing three dimensional steel portal frame structures exposed to elevated temperatures using the dynamic algorithm.

8 FIRE ANALYSIS OF THE WHOLE BUILDING

8.1 Introduction

This chapter investigates the fire behaviour of the whole building as described in Chapter 6. In order to achieve accurate failure modes, the analytical models cover the 3D structural behaviour and include members and restrained effects so that the post-local failure stage can be obtained precisely. Different locations and severities of the fires, different support conditions at the column base, the effect of concrete encasement as passive fire protection to column legs and various boundary conditions or restraints are investigated in this chapter. The main purpose of the analyses is to investigate the different failure modes anticipated for a typical portal frame structure under fire conditions. As described in Section 4.4.2, the inwards failure of the frames is considered as acceptable whereas outwards collapse or sideways failure of the frames is unacceptable. The ISO 834 standard fire curve has been used in most of the analyses; an Eurocode External fire which simulates well-ventilated fires has also been used. The fire analysis of the completed building has been carried out using the dynamic algorithm in SAFIR. The following table summarises the analyses carried out in this chapter and the corresponding sections where they are described. Section 8.2 describes the analytical models used in this chapter.

Table 8-1 Fire analyses carried out in Chapter 8

Section	Heading	Support Conditions	Purlin Axial Restraints	Column Passive Fire Protection	Fire
8.3	Location & Severity of Fire	Fix-Fix & Pin-Pin	Yes & No	No	ISO
8.4	Eurocode External Fire	Fix-Fix & Pin-Pin	Yes & No	No	External
8.5	Out-of-plane Restraints to Columns	Fix-Fix & Pin-Pin	Yes & No	No	ISO
8.6	Passive Fire Protection to Columns	Fix-Fix & Pin-Pin	Yes & No	Yes	ISO
8.7	Partially Fixed Frames	Partially fixed	Yes & No	Yes & No	ISO

8.2 Description of the Analytical Models

The modelling is expanded to full three dimensional finite element models to represent the whole building as described in Section 6.2 (Figure 8-1, reproduced here for clarity). The loads applied to all the analytical models in Chapter 8 are described in Section 7.3 and are shown in Figure 8-2. The diaphragm action of the roof sheeting is ignored in the analytical models and it has been assumed that there is no geometrical imperfection. The boundary conditions or restraints commonly imposed in the analytical models are described below in this section.

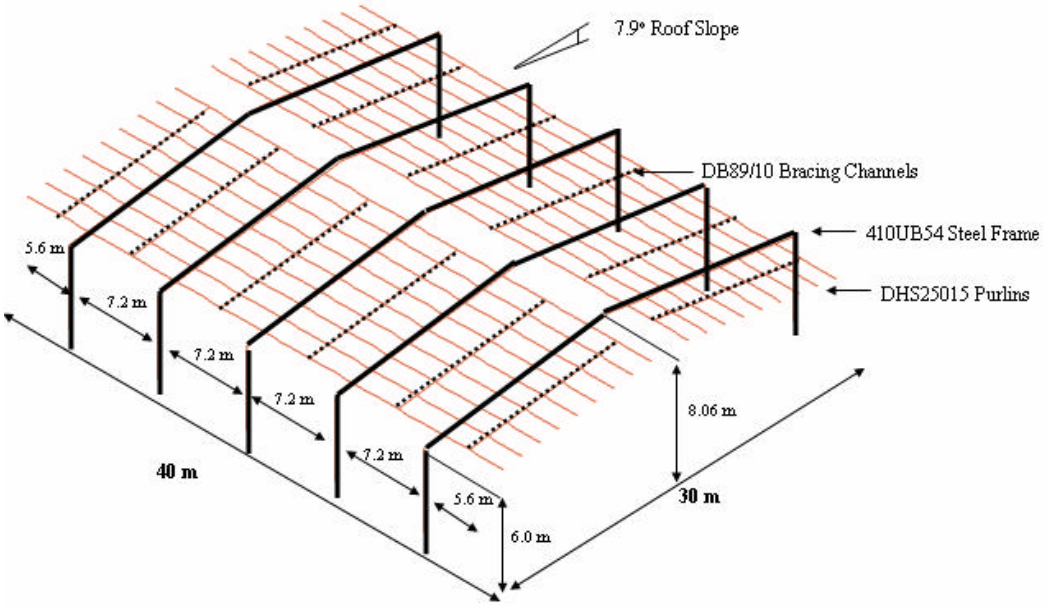

Figure 8-1 Dimensions and structural elements of the building

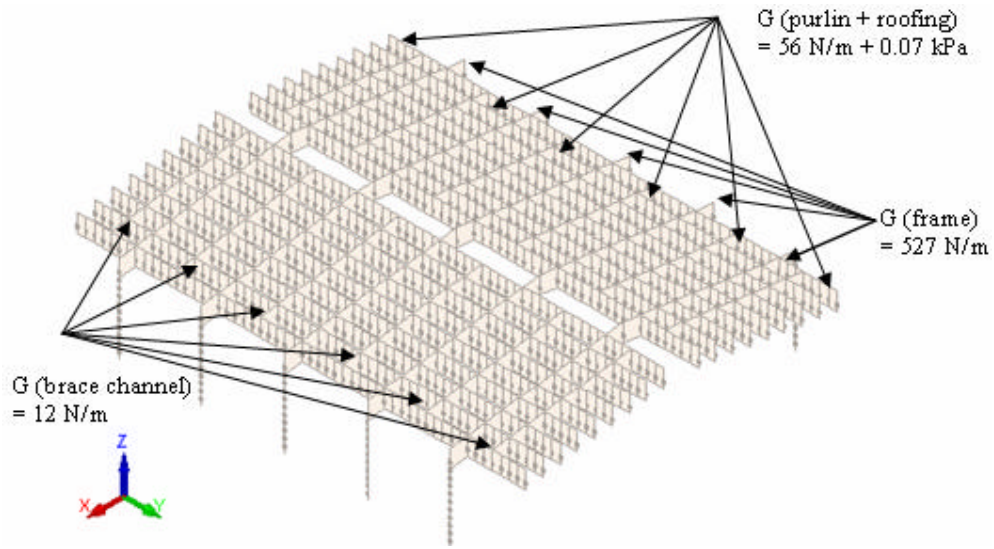

Figure 8-2 Loadings on the analytical models of the complete building

Support Conditions at the Column Base

Figure 8-3 and Figure 8-4 show the boundary conditions or restraints imposed for the structure with fixed and pinned support conditions, respectively, at the column bases. The fix-fix and pin-pin supported frames represent the upper and lower bound of the performance of the structure (i.e. extreme cases, a pin connected joint may only have rotation in the plane of the frame). In Section 7.4.1.3, the load ratios calculated using SAFIR for ideally pinned and fixed support conditions are 0.21 and 0.18, respectively (i.e. lower load ratio signifies better fire resistance). However, the fully pinned bases of the frames are never achieved in reality and some degree of fixity will always be provided from the bolted connections at the supports. A portal frame structure with partial base fixity at the supports is also analysed and is described in Section 8.7.

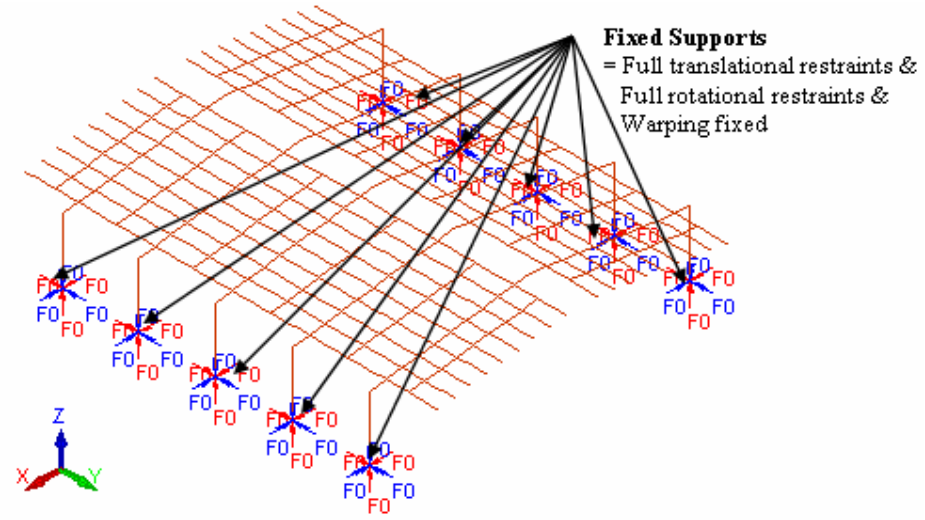

Figure 8-3 Boundary conditions or restraints provided for fixed support conditions at the column bases

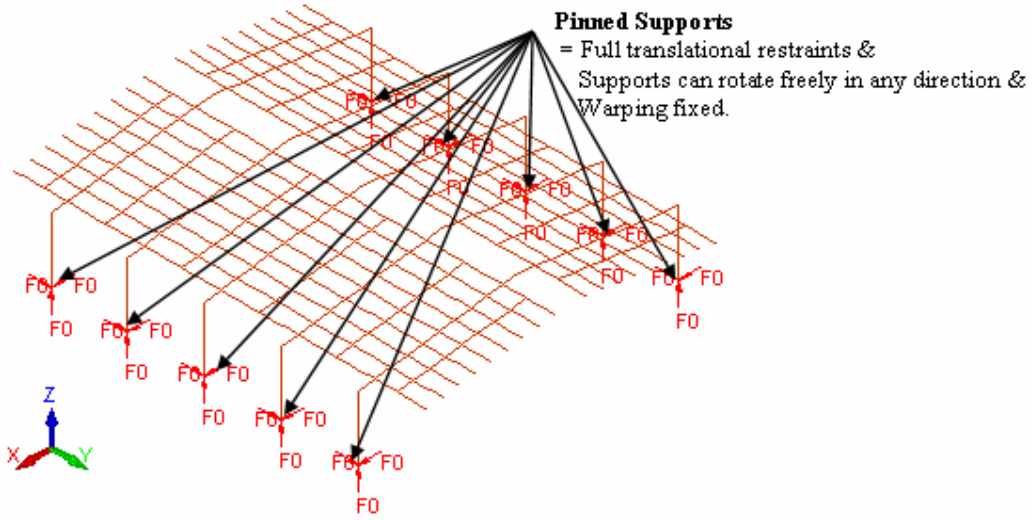

Figure 8-4 Boundary conditions or restraints provided for pinned support conditions at the column bases

Out-of-plane Restraints provided at the Columns

The steel components of the building are modelled using beam elements in the analytical models and the models do not include the concrete boundary walls. The concrete walls and their connections to the supporting structures cannot be modelled realistically using 3D beam elements. Therefore, undeformable restraints are used to represent the connections between the walls and the supporting structures and also the effects of the concrete walls on the overall behaviour of the structure.

Figure 8-5 shows the out-of-plane restraints imposed at the top and mid-height of the columns in the analytical models. These unmovable restraints from the side walls prevent the out-of-plane displacement at the top and mid-height of the columns and are required under ambient conditions to reduce the effective lengths of the columns and to prevent buckling about the weak axis (refer to Section 6.5).

Under fire conditions, the connections to the side walls may fail at high temperatures and the columns may deform excessively in the weak direction. In contrast, providing out-of-plane restraints along the length of the columns to prevent out-of-plane deformations of the columns may change the fire performance of the steel portal frame structure. These two scenarios serve as the extreme cases in terms of connections to the side walls and are investigated in Section 8.5.

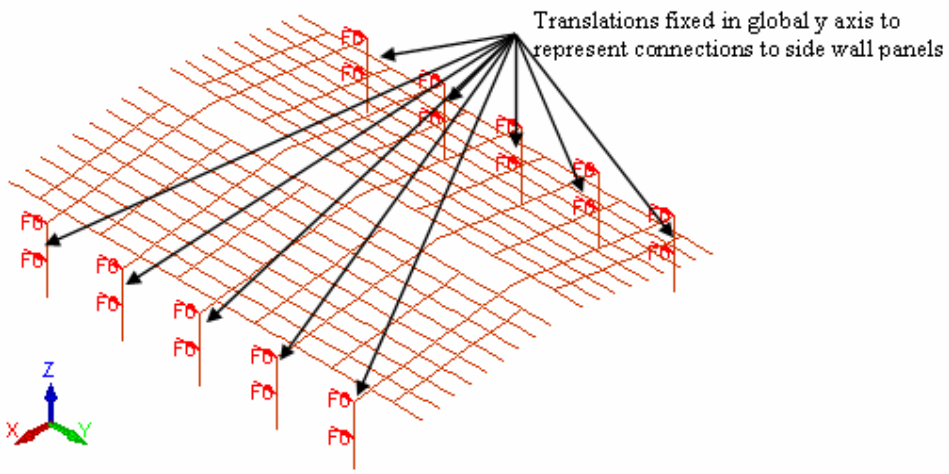

Figure 8-5 Out-of-plane restraints imposed at the top and mid-height of columns to simulate the effects from the side wall panels

Purlin Axial Restraints provided by the End Walls

The end concrete walls are connected to the purlins in the end bays near the top (refer to Figure 8-6) with the connection details similar to those shown in Figure 4-16 and Figure 7-26. The level of axial restraint provided by the end walls to the purlins is not well known and depends on many variables, such as the type of connection at the base, the amount of reinforcement and the thickness of the end concrete walls. In addition, it also depends on the supporting structures to which the walls are attached, the number of tilt-up wall panels between the supporting structures and the types of connections used to join these structural elements together.

Two extreme cases are investigated in this chapter for the purlin support conditions to the end walls, and they are referred to here as either *with* or *without* purlin axial restraint. The most important difference between these two support conditions is the translational fixity in the longitudinal direction of the purlins (i.e. purlin axial restraint) at the locations of the end walls. The axial restraints in the steel purlins can be achieved provided the bolted end connections have sufficient axial load capacity. In a real building, the actual level of purlin axial restraint which will be provided from the end concrete walls will certainly lie somewhere between the two extremes of zero and fully restrained which are modelled in this chapter.

The boundary conditions *with* purlin axial restraints imposed by the end walls are shown in Figure 8-7 and they provide restraints against translations in all three directions, twisting about the longitudinal axis and in-plane rotation of the purlins.

Figure 8-8 shows the boundary conditions *without* purlin axial restraint imposed by the end walls and they may also demonstrate the effects of purlin connection failures at elevated temperatures because steel purlins have been observed to fall to the ground in a very hot fire (refer to Figure 4-57). In this case, the boundary conditions from the end walls only provide restraints against translations in the x and z global axes to simulate a simply supported end of the purlins and also to prevent lateral movement due to the in-plane stiffness of the end walls. In both extreme cases, the warping is not restrained by the end walls due to geometrical tolerances.

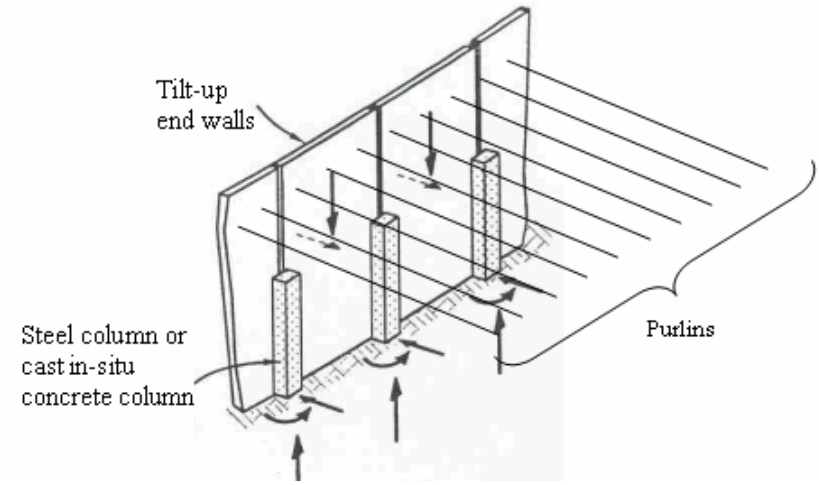

Figure 8-6 Purlins in the end bays attached to tilt-up end walls

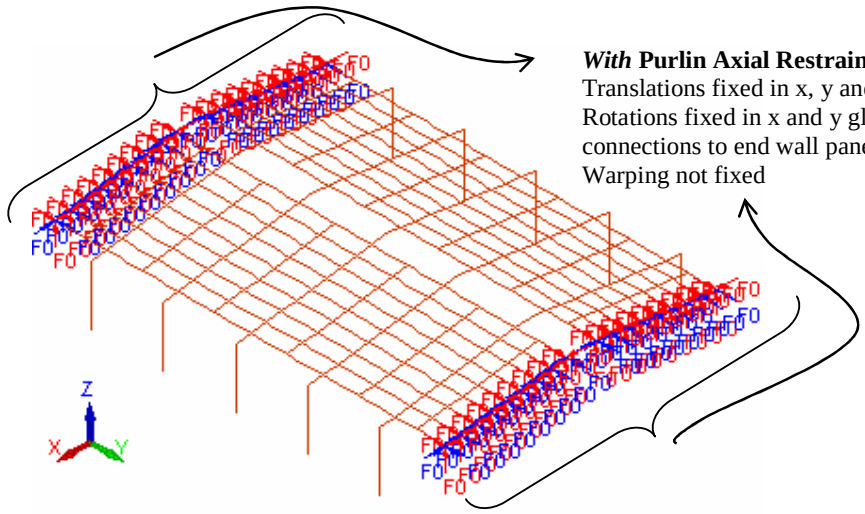

***With* Purlin Axial Restraint**
Translations fixed in x, y and z global axes &
Rotations fixed in x and y global axes to represent connections to end wall panels.
Warping not fixed

Figure 8-7 Boundary conditions *with* axial restraints imposed in the purlins by the end walls

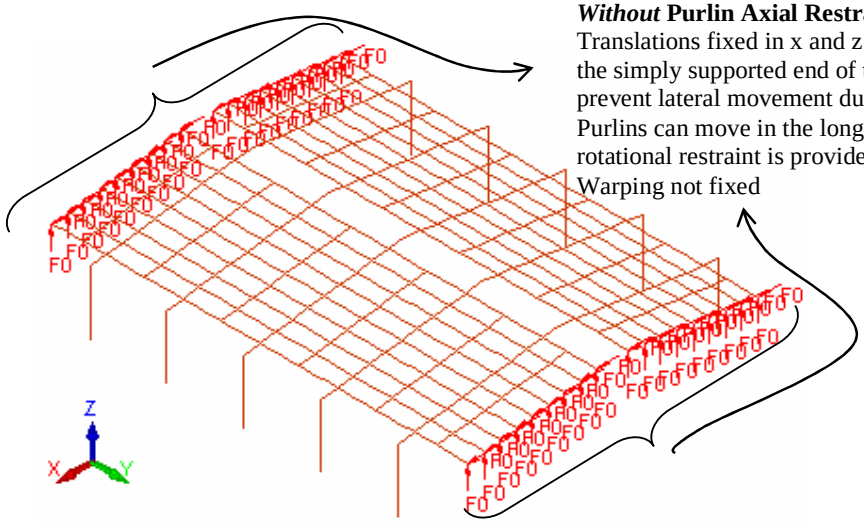

***Without* Purlin Axial Restraint**
Translations fixed in x and z global axes to represent the simply supported end of the purlins and to prevent lateral movement due to the end walls.
Purlins can move in the longitudinal axis and no rotational restraint is provided.
Warping not fixed

Figure 8-8 Boundary conditions *without* axial restraint imposed in the purlins by the end walls

Notation for the Structure

For the discussion of results in this chapter, the following notations are assigned to the structure (i.e. frame number, bay number and etc) and are used thoroughly.

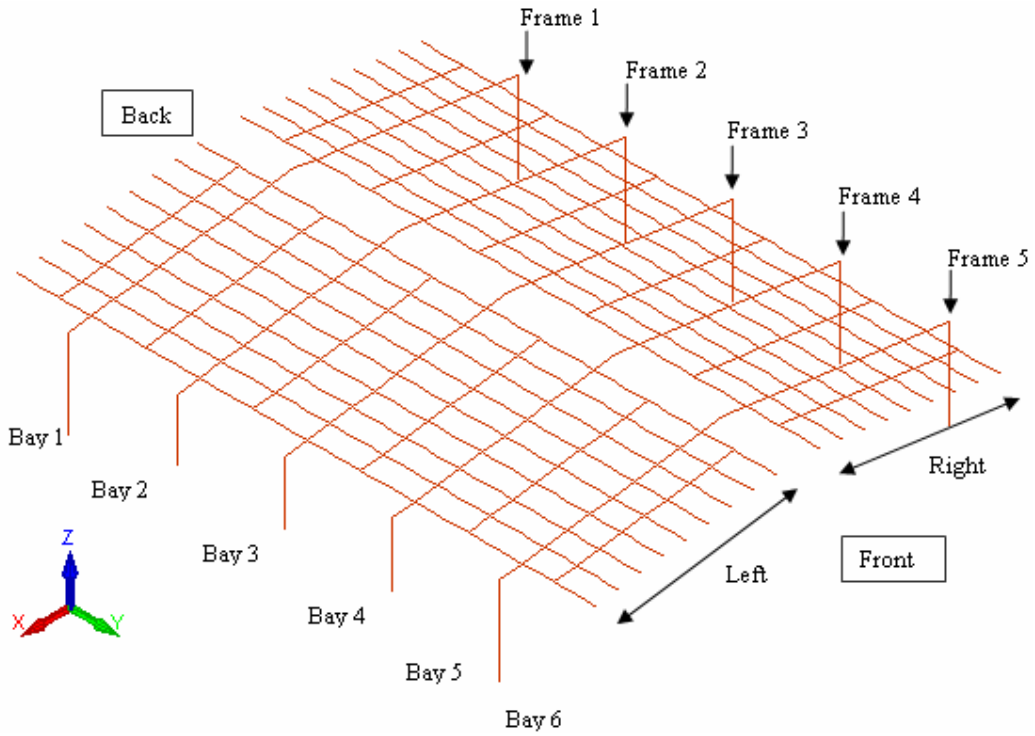

Figure 8-9 Notations used in the discussions of results in Chapter 8

8.3 Location and Severity of Fire

Both localised and fully developed fires are investigated for pinned and fixed support conditions at the column bases and for the structure with and without purlin axial restraints imposed by the end walls. For a fully developed fire, all the steel structural elements are exposed to the fire at the first time step (Figure 8-10); for a localised fire, the fire is assumed to be confined in a small area and occurs either near the centre (Figure 8-11) or near the end (Figure 8-12) of the building. In reality, the fire will not suddenly affect all the structural elements at one moment and will grow and spread outwards to other areas of the building over a certain time period. This is not taken into account in the analysis. Furthermore, full involvement is possible, for instance, as in the fires that recently occurred in Christchurch (refer to Section 4.8.1). For the purpose of gaining an understanding of the behaviour of such buildings in fire, the heated structural elements are exposed to a fire with temperatures equivalent to the ISO fire (refer to Figure 7-3). This fire is conservative compared to an External fire but is not unlikely given that industrial buildings may contain very high fuel loads.

The analyses in this section are summarised and tabulated in Table 8-2. Analyses (1) to (6) were carried out with axial restraints imposed in the purlins by the end walls whereas analyses (7) to (12) were carried out without the purlin axial restraint. It should be noted that localised fires are only investigated here. For the rest of the sections (Section 8.4 to Section 8.7), it is assumed that the fire is well-developed such that all the structural elements are heated according to the fire curves.

Table 8-2 Fire analyses in Section 8.3 - Location and Severity of Fire

Analysis number	Description of location and severity of fire	Support conditions	Purlin Axial Restraints
(1) & (7)	Fully developed fire	Fixed	Yes & No
(2) & (8)		Pinned	Yes & No
(3) & (9)	Localised fire near centre of building	Fixed	Yes & No
(4) & (10)		Pinned	Yes & No
(5) & (11)	Localised fire near end of building	Fixed	Yes & No
(6) & (12)		Pinned	Yes & No

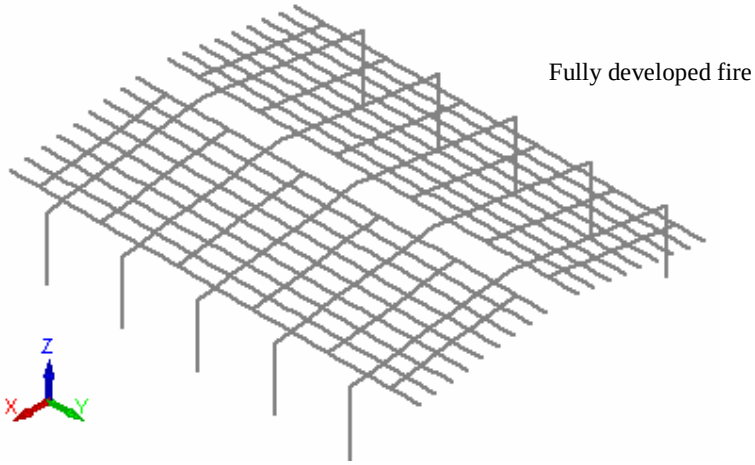

Figure 8-10 Fully developed fire affecting all the structural elements

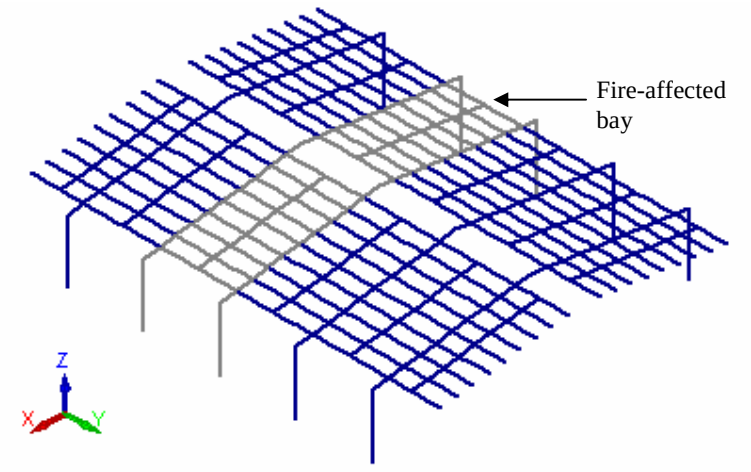

Figure 8-11 Localised fire near the centre of the building

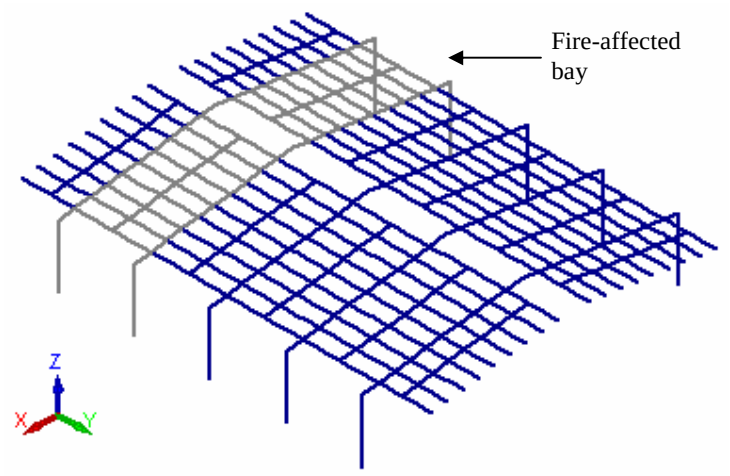

Figure 8-12 Localised fire near the end of the building

8.3.1 Results of Analyses

The results of the analyses are summarised in the following table. It should be emphasised that the simulation end times in the table were obtained either when SAFIR was unable to converge to a solution although measures were taken to try and obtain a converged solution such that total collapse of the structure can be clearly identified, or when the maximum time limit of 60 minutes (arbitrarily chosen) was reached. This means that these times do not necessary correspond to the collapse times of the structure and are valid for analytical models with purlin axial restraints imposed by the end walls. This is further explained in the following discussion.

Table 8-3 Results of analyses in Section 8.3 - Location and Severity of Fire

Analysis number	Description of location and severity of fire	Support conditions	Purlin Axial Restraints	Mode of Failure	Simulation End Time* (minutes)
(1)	Fully developed fire	Fixed	Yes	Catenary	18.5
(2)		Pinned	Yes	Sway	19.6
(3)	Localised fire near centre of building	Fixed	Yes	Catenary	60.0
(4)		Pinned	Yes	Sway	60.0
(5)	Localised fire near end of building	Fixed	Yes	Catenary	60.0
(6)		Pinned	Yes	Sway	60.0
(7)	Fully developed fire	Fixed	No	Inwards	14.9
(8)		Pinned	No	Sway	14.1
(9)	Localised fire near centre of building	Fixed	No	Catenary	60.0
(10)		Pinned	No	Sway	60.0
(11)	Localised fire near end of building	Fixed	No	Inwards	20.5
(12)		Pinned	No	Sway	18.5

**Note: The simulation end times were obtained when SAFIR was unable to converge to a solution or when the maximum time limit of 60 minutes was reached.*

With Purlin Axial Restraints

The analyses have shown that for the steel portal frame structure with purlin axial restraints imposed by the end walls (analyses (1) to (6)), total collapse of the frames exposed to the fire could not be obtained from SAFIR. For the steel portal frame

structure with fixed support conditions (analyses (1), (3) and (5)), the results show that the deformation is almost vertical and the roof structure (steel rafters, purlins and brace channels) deforms into a catenary shape (i.e. **catenary** mode of failure). This is in contrast to the steel portal frame structure with pinned bases (analyses (2), (4) and (6)). The results show that significant sidesway of heated frames occurs when the roof structure (steel rafters, purlins and brace channels) losses its stiffness due to thermal effects and sags down in a relatively fast manner (i.e. **sway** mode of failure). For the failure modes (i.e. **catenary** and **sway**) with purlin axial restraints from the end walls, the vertical deflections at the apex are restricted to less than 3 metres. The results from analyses (1) and (2) will be described briefly to give an understanding of the fire behaviour of this type of structure in three dimensions. For the analyses with localised fires (analyses (3) to (6)), SAFIR successfully obtained the behaviour until the maximum time limit was reached. However, only the results from analyses (3) and (4) will be described as analyses (5) and (6) show similar behaviour.

Without Purlin Axial Restraint

The structural fire behaviour of the whole building is very sensitive to the presence of purlin axial restraints imposed by the end wall panels. SAFIR was able to obtain the complete collapse of the structure when the whole building was heated according to the ISO fire (analyses (7) and (8)), and the collapse of the heated frame supporting the purlins in the end bay when the fire-affected bay was close to the end walls (analyses (11) and (12)). The results from these analyses show that for the structure with fixed support conditions, the heated frames fail in a snap-through mechanism and collapse into the building (i.e. **inward** mode of failure). However, for the structure with pinned support conditions, significant sway of the heated frames always occurs before the heated rafters collapse into the building and to the ground pulling the columns inwards. The sway of the frames results in very large horizontal deflections at the top of the columns. This is deemed to be unacceptable and is identified as the **sway** mode failure in Table 8-3. Interestingly, when the localised fire occurred near the centre of the building (analyses (9) and (10)), collapse of the heated bay did not occur after one hour of ISO fire and the fire behaviour is similar to that obtained from the analyses with purlin axial restraints provided by the end walls (analyses (3) and (4)). For the purposes of understanding the fire behaviour without purlin axial restraint imposed by the end panels, the results of analyses (7) and (8) are described below.

Results from Analysis (1):

Fixed support frames with purlin axial restraints imposed by the end walls, fully involved in fire

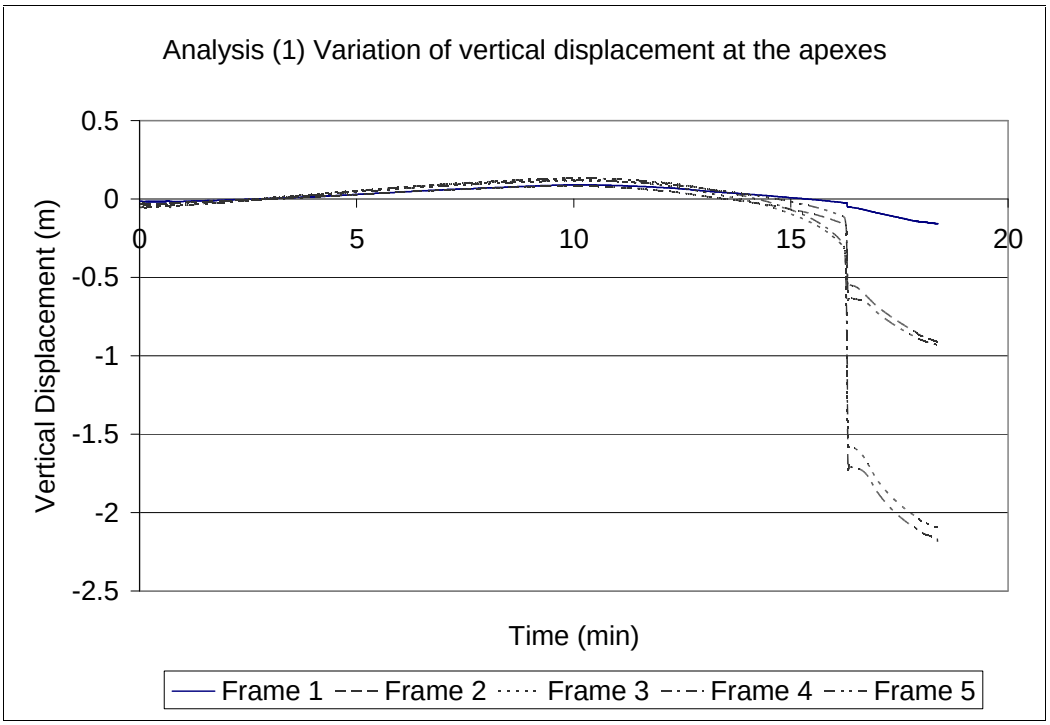

Figure 8-13 Variation of vertical displacement at the apexes in analysis (1)

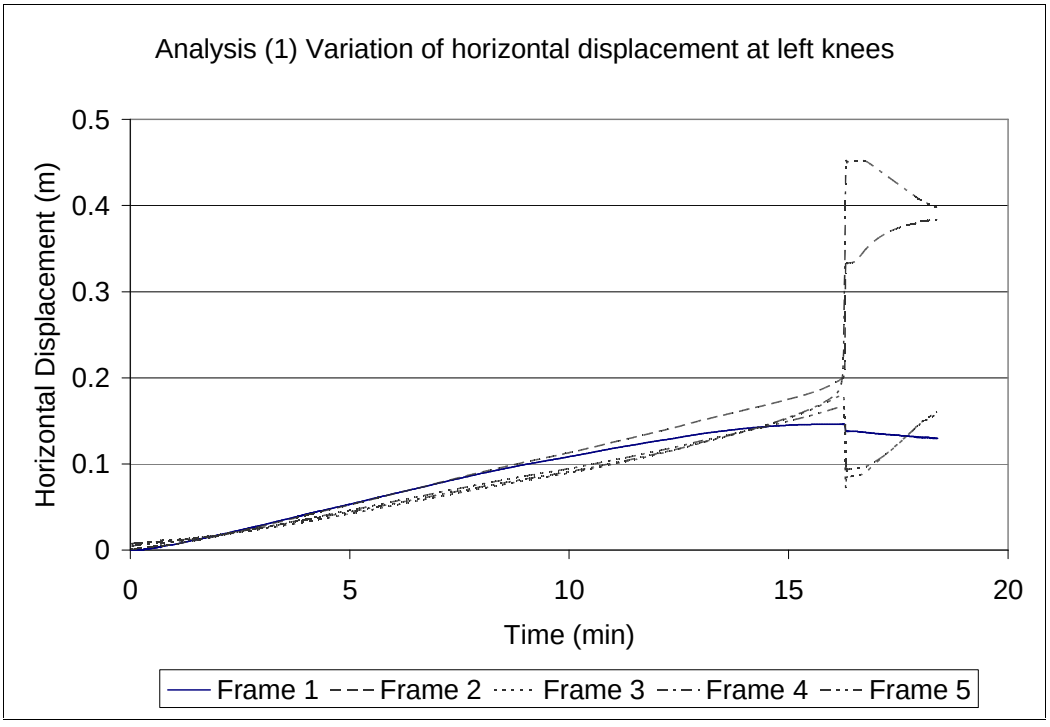

Figure 8-14 Variation of horizontal displacement at left knees in analysis (1)

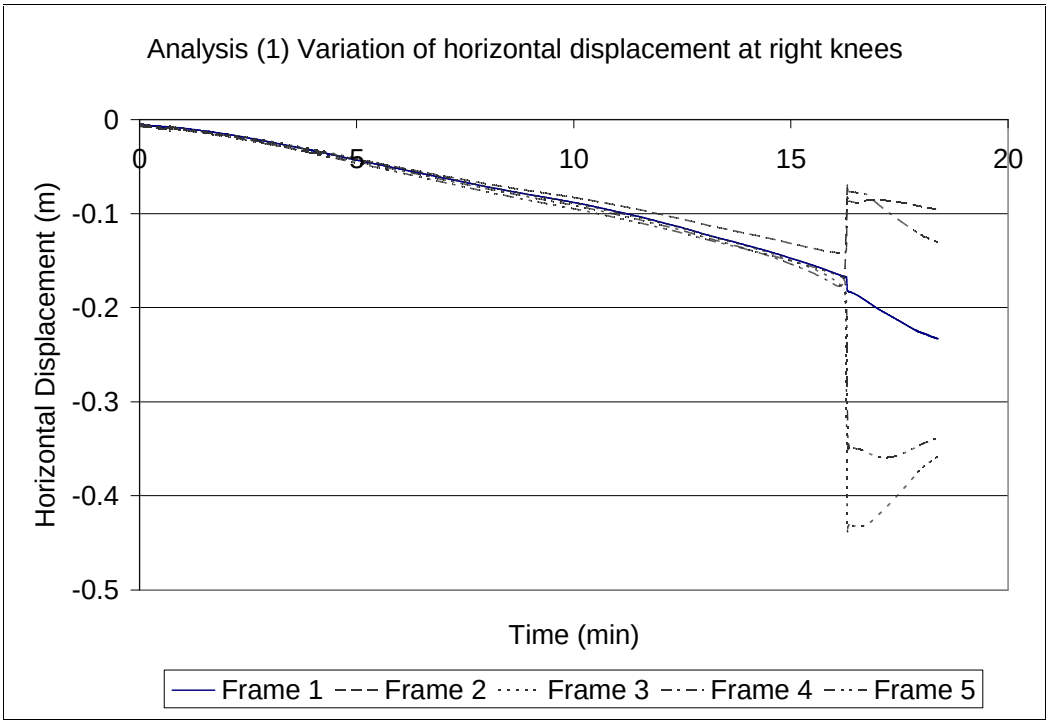

Figure 8-15 Variation of horizontal displacement at right knees in analysis (1)

Overall Structural Behaviour

During the initial stages of the fire, thermal expansion of the columns and rafters causes the apexes of the frames to deflect upwards (Figure 8-13). In addition, the purlins have been observed to buckle out-of-plane locally in bays 3, 4 and 5 (Figure 8-16 (a)). This is due to the thermal elongation of the purlins and the purlin axial restraints imposed by the end wall boundary conditions. At approximately 45 seconds, the structure stabilises itself by concentrating the out-of-plane buckling in the purlins in bay 3 (Figure 8-16 (b)). This deformed shape of the structure is observed until about 16 minutes (Figure 8-17 (a)), when the columns lose their stiffness due to thermal effects and the roof structure (steel rafters, purlins and brace channels) sags down relatively quickly (Figure 8-13 and Figure 8-17 (b)). The rafters and purlins deform into a catenary, resisting the applied loads from the restraints or the boundary conditions imposed by the end walls (i.e. catenary mode of failure). The steel purlins are now in the form of tensile catenary shape, holding the roofing in place between the purlin axial end restraints until SAFIR detected numerical instability in the stiffness matrix at approximately 18 minutes and stopped iterating to the next time

step. The final deflected shape obtained from SAFIR is shown in Figure 8-18. The fire behaviour of the structure is discussed in more detail below.

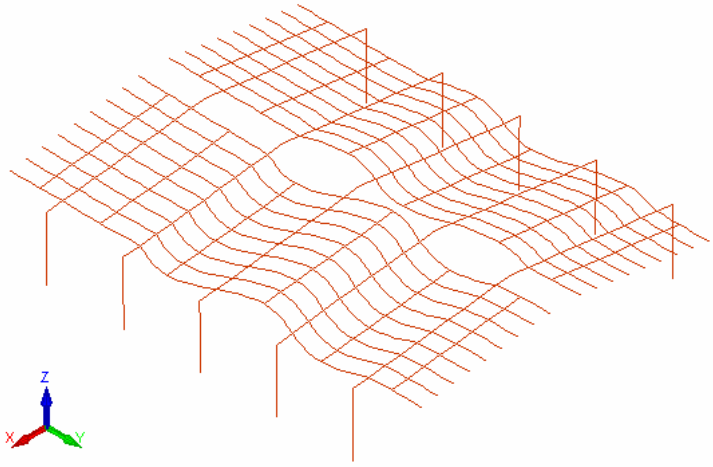

(a) Time = 40 seconds

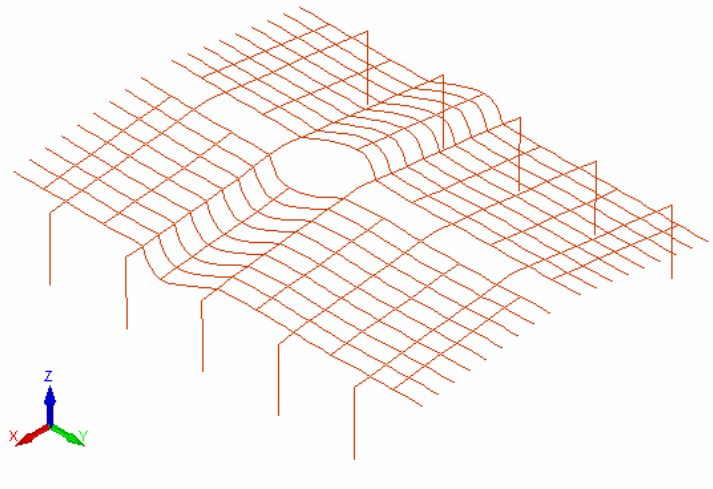

(b) Time = 45 seconds

Scale factor = 5x

Figure 8-16 Initial deformations in analysis (1)

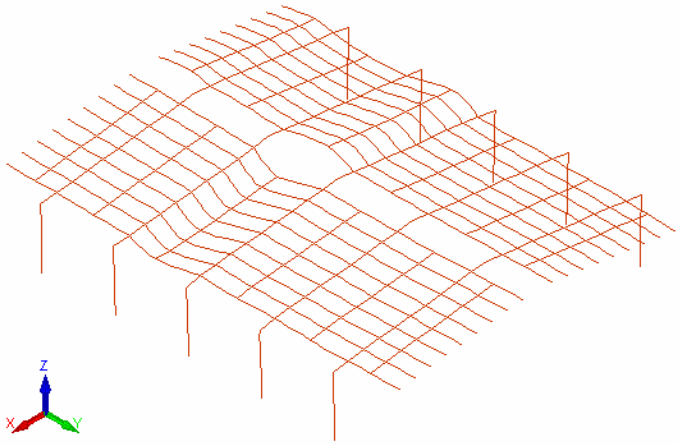

(a) Time = 16.2 minute

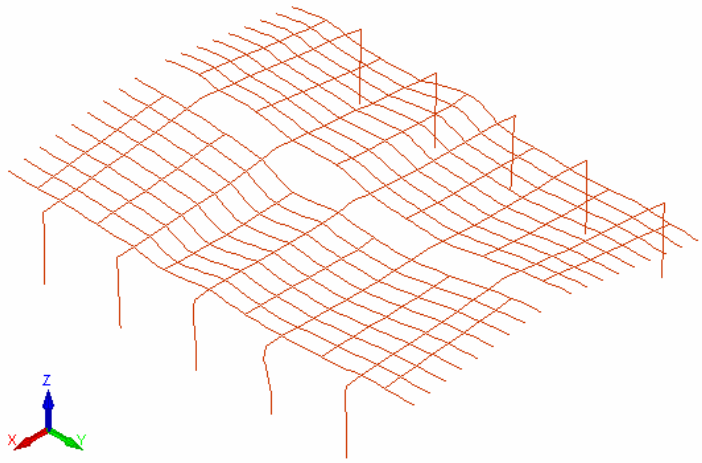

(b) Time = 16.3 minutes

Scale factor = 1x

Figure 8-17 Deflected shapes immediately before and after the rapid sagging of roof (analysis (1))

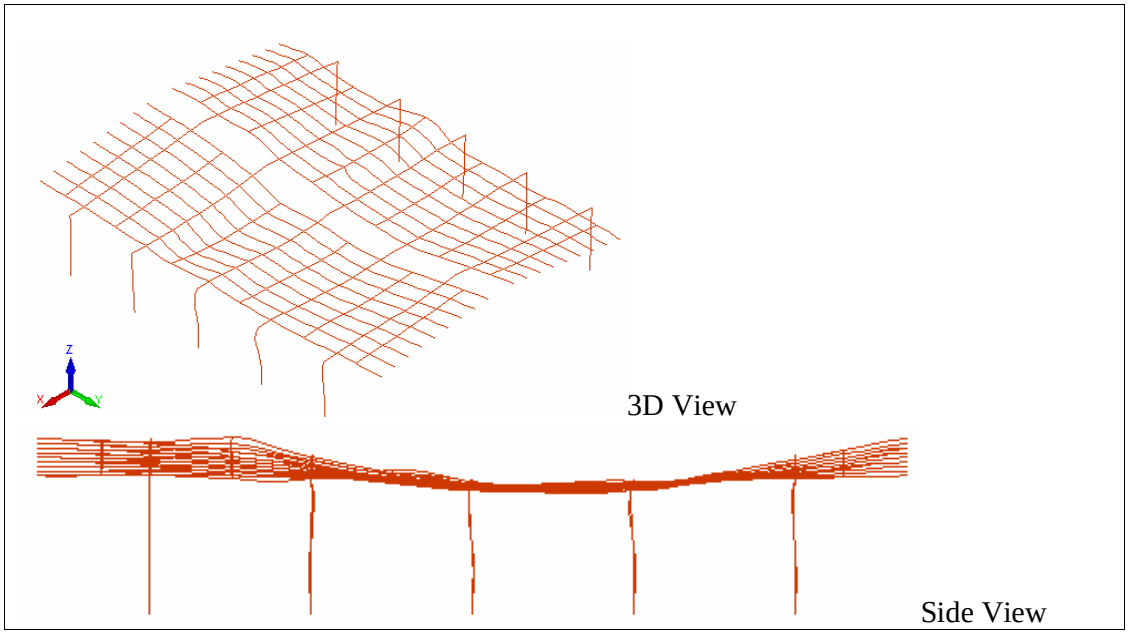

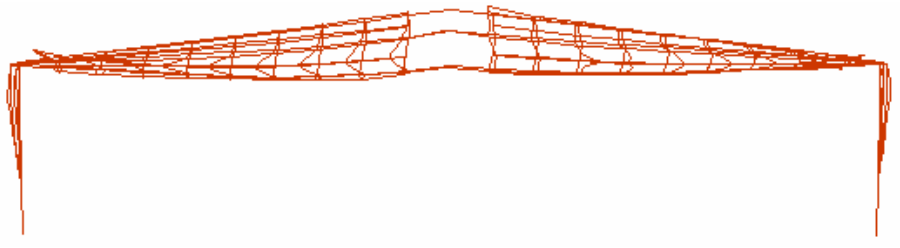

Front View

Scale factor = 1x

Figure 8-18 Final deflected shape from SAFIR (analysis (1))

Figure 8-19 and Figure 8-20 show the out-of-plane deflections of all five frames at the apex (i.e. in the global y direction). During the first 40 seconds, thermal expansion of purlins in bays 1 and 2 pushes frame 2 in the positive global y direction; similarly, the expansion of purlins in bay 6 pushes frame 5 in the negative (opposite) global y direction (see Figure 8-19). This introduces high axial restraint forces to the purlins in bays 3, 4 and 5 and results in local out-of-plane buckling of the purlins as observed in the very early stages of the fire (Figure 8-16 (a)).

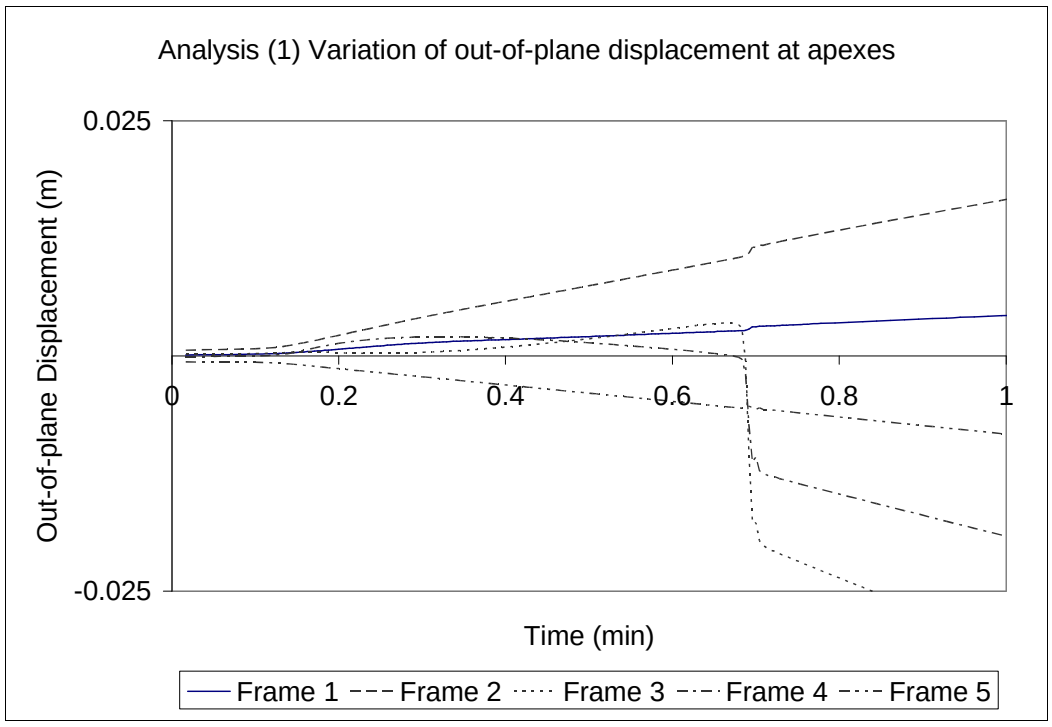

Figure 8-19 Initial out-of-plane displacement at the apexes (analysis (1))

After the whole building stabilises itself at 45 seconds, thermal expansion of the purlins continues and causes the frames to deflect further from the end walls (Figure

8-20). Figure 8.20 also shows that frames 1 and 2 deform in the positive global y direction whereas frames 3, 4 and 5 deform in the negative global y direction (i.e. opposite direction) before the roof structure (steel rafters, purlins and brace channels) deforms into a catenary shape. This implies that axial restraint forces are being concentrated in the purlins in bay 3 and explains why the purlins in that bay buckle excessively until the sagging of the roof structure occurs (Figure 8-16 (b)).

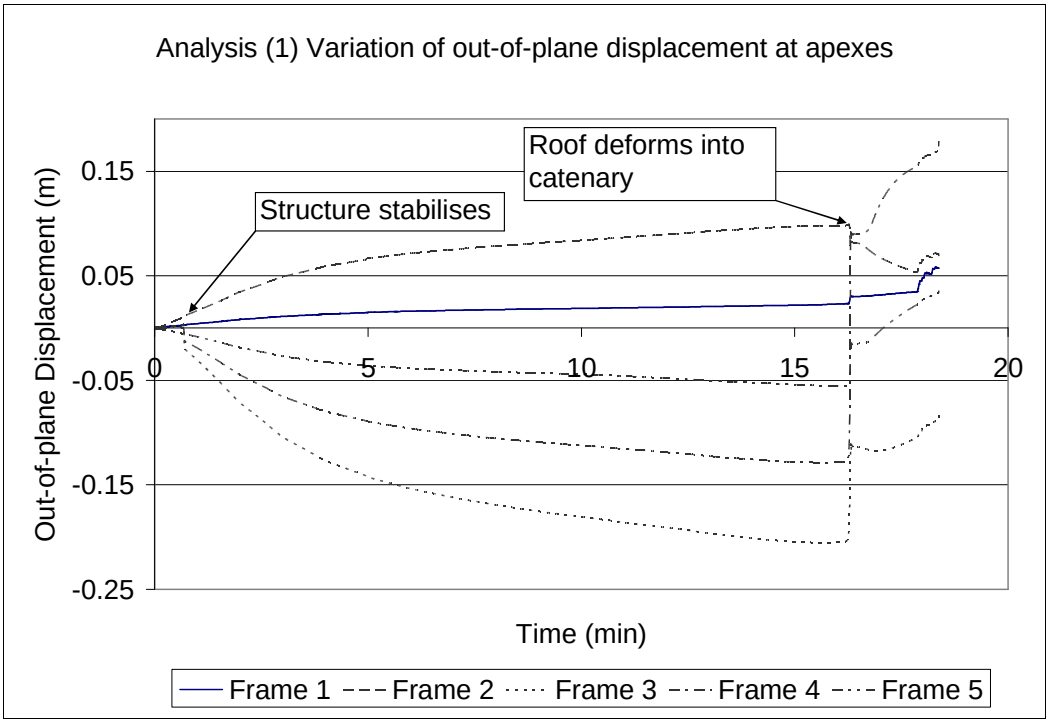

Figure 8-20 Variation of out-of-plane displacement at the apexes (analysis (1))

Figure 8-13 shows that during the initial stages of the heating when all structural members are exposed to low temperatures, the apexes deflect downwards due to the self weight of the purlins and the rafters. As heating continues, the columns and the rafters elongate due to thermal effects, resulting in an upwards deflection trends as shown in the figure. At approximately 10 minutes when the steel members are exposed to fire temperature of approximately 680^{o}C, the reduced strength and stiffness of the structure has caused the roof structure to deflect downwards again. At approximately 16 minutes, the rapid sagging of the roof structure is due to twisting of the columns about their vertical axes (i.e. global z axis, refer to Figure 8-21) and has resulted in a downwards deflection of nearly 1.7 m at the apex of frame 4. As heating continues, the downwards deflection rates are greater until the simulation stopped at

approximately 18 minutes. Frames 3 and 4 both show a downward deflection of 2.15 m at the end of the simulation. The whole building is now being held up by the restraints imposed from the end concrete walls.

Figure 8-14 and Figure 8-15 show the horizontal deflection plots at the knees of the frames. Thermal expansion of the rafters has caused the columns to deflect outwards as much as 0.2 m before the rapid sagging of the roof structure. The sagging of the roof structure introduces a horizontal thrust to the columns, resulting in nearly 0.43 m of horizontal deflection at the top of the column. The columns of frames 3 and 4 suffer the worst outwards thrusts at the top when compared to other frames, and are being pulled inwards when the roof structure continues to sag as time increases until the simulation stopped.

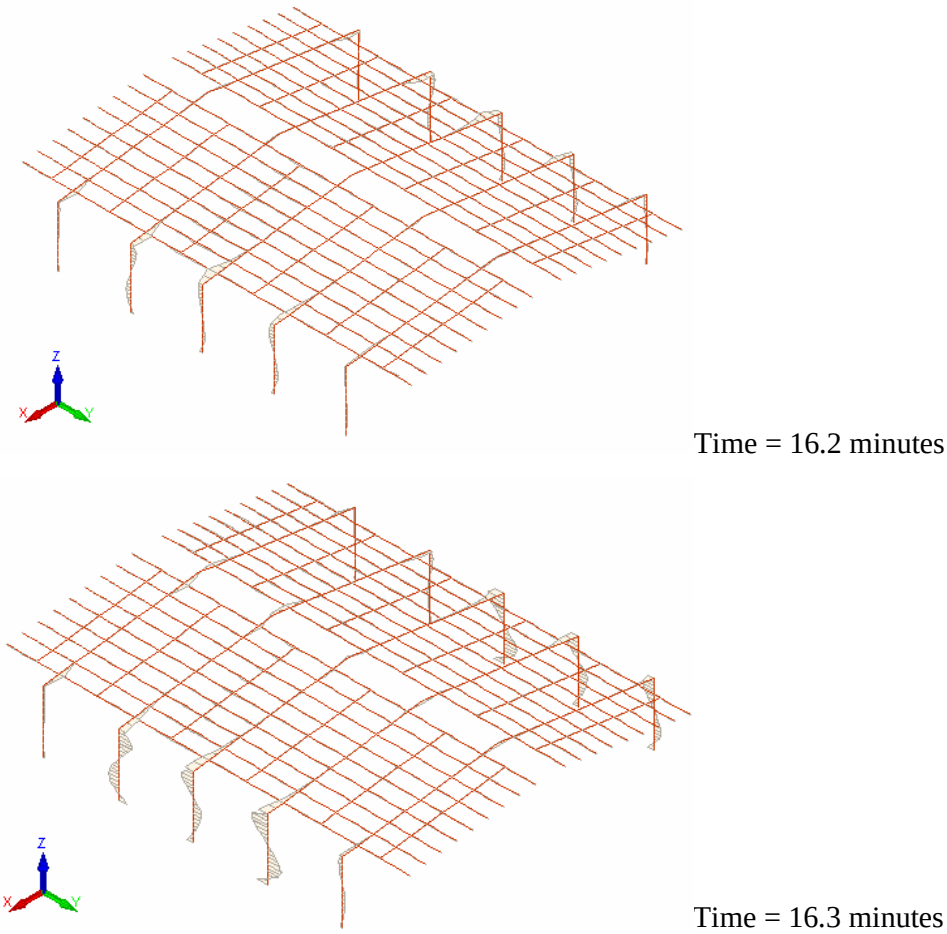

Figure 8-21 Bending moments about the global z-axis immediately before and after the rapid sag of the roof structure (analysis (1))

Results from Analysis (2):

Pinned support frames with purlin axial restraints imposed by the end walls, fully involved in fire

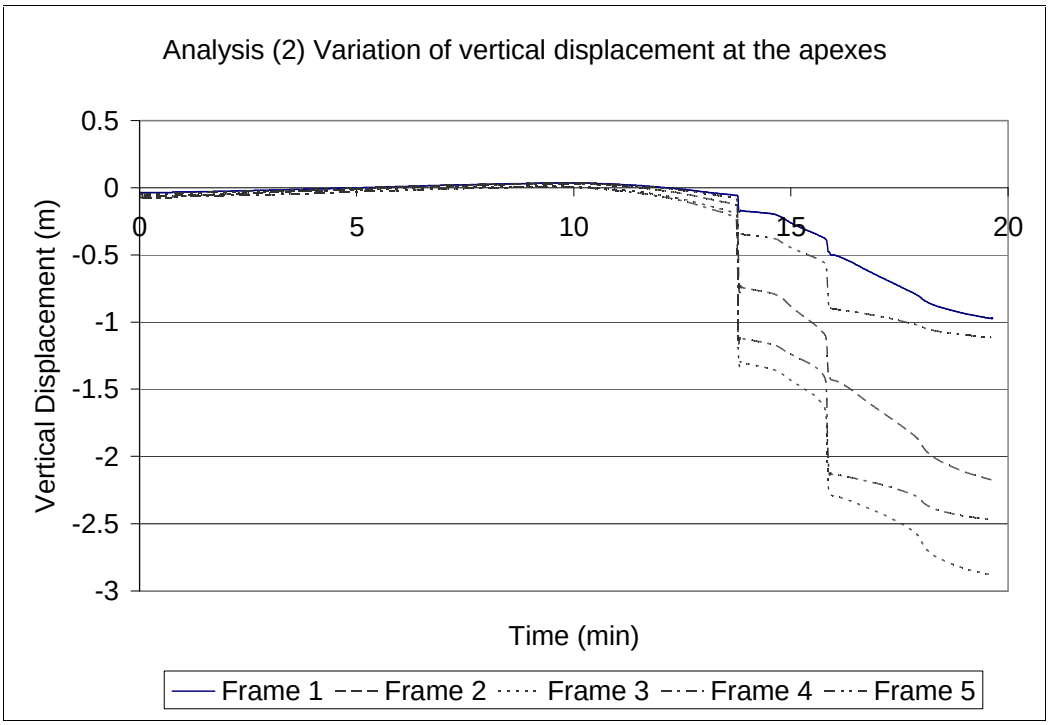

Figure 8-22 Variation of vertical displacement at the apexes in analysis (2)

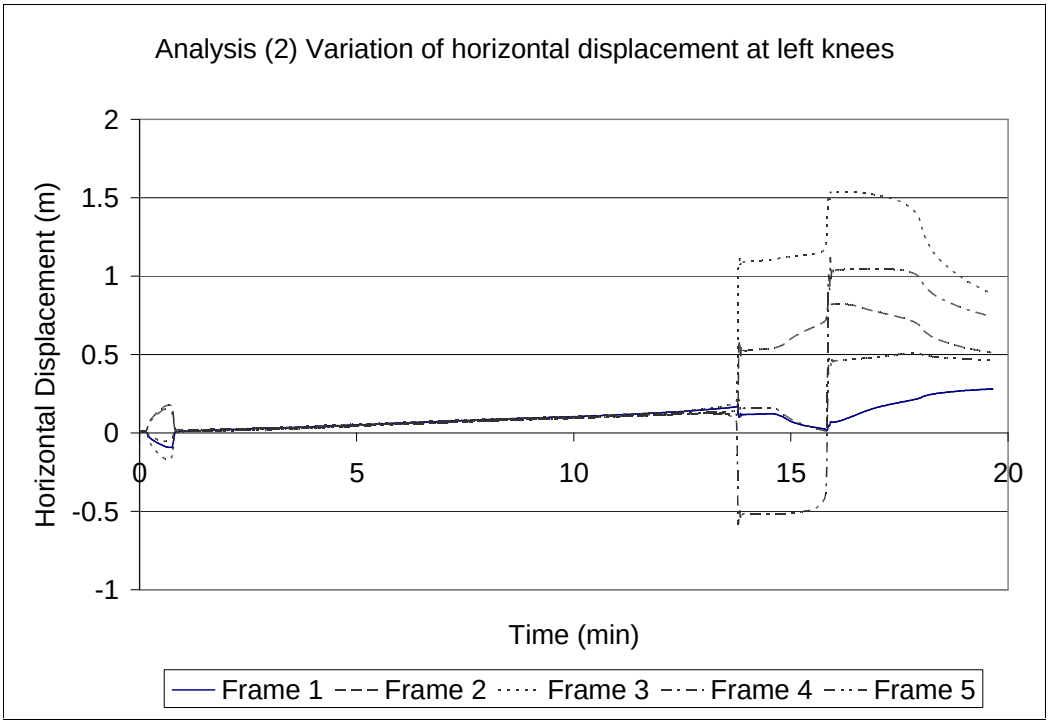

Figure 8-23 Variation of horizontal displacement at left knees in analysis (2)

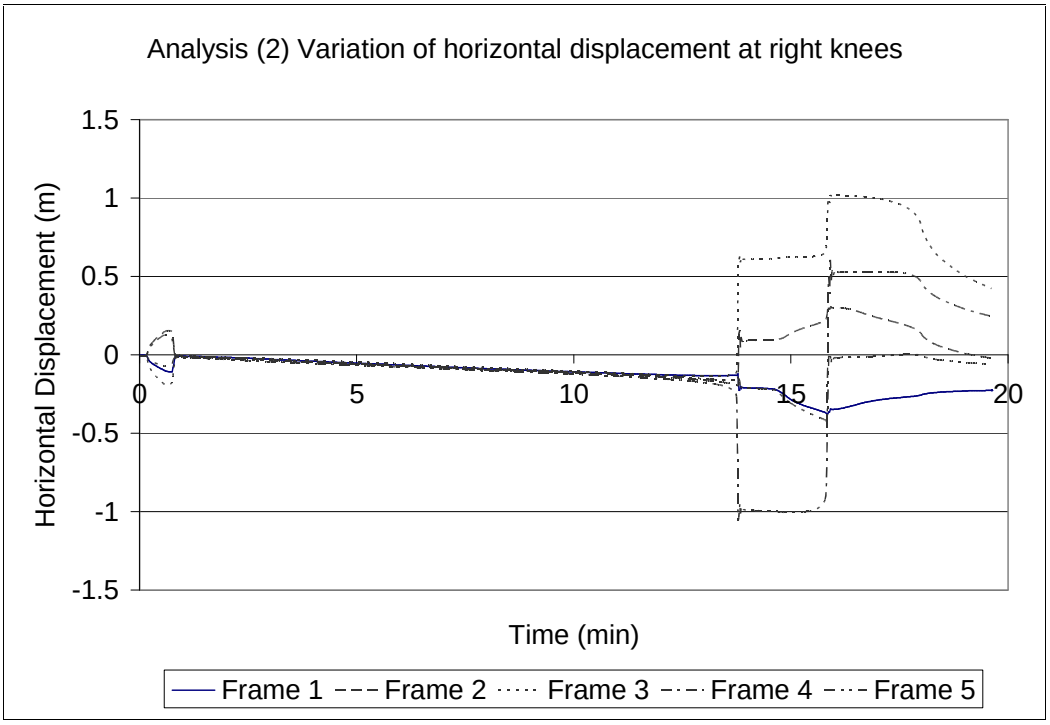

Figure 8-24 Variation of horizontal displacement at right knees in analysis (2)

Overall Structural Behaviour

During the initial stages of the fire, thermal expansion of the steel columns and rafters causes the roof structure to deflect upwards (Figure 8-22). The steel frames have been observed to sway sideways during the first 45 seconds (Figure 8-25 (a)). Out-of-plane local buckling of purlins also occurs due to thermal expansion of these purlins being resisted by the purlin axial restraints imposed by the end wall boundary conditions. The whole structure stabilises itself by concentrating the out-of-plane buckling in the purlins in bay 4 (Figure 8-25 (b)). This stabilising phenomenon has also been observed in analysis (1) with frames fully fixed at the column bases.

This deformed shape of the structure is observed until about 14 minutes of ISO fire exposure (Figure 8-26 (a)), where the roof structure in the vicinity of bays 2, 3 and 4 sags down relatively quickly and deforms into a catenary (Figure 8-26 (b)). Significant sway of frames 3 and 4 also occurs simultaneously and interestingly, these two frames sway in the opposite direction to each other (Figure 8-23 and Figure 8-24). The structure continues to deform in a relatively steady manner until approximately 16 minutes, the roof structure in bay 5 shows rapid sag and the steel

purlins are now in the form of catenary shape, holding the roofing between the restraints imposed by the end walls (Figure 8-26 (c)). It should be noted that although the structure also deforms into a catenary as in the fixed support case, it has been identified as the sway mode of failure in Table 8-3.

The sagging of this portion of the roof causes frame 4 to sway in the positive global x axis, which pulls the right column of frame 4 inwards and consequently pushes the left column outwards considerably. The roof structure continues to deform downwards due to decreasing strength and stiffness of the steel members until SAFIR stopped iterating to the next time step at 20 minutes. The final deflected shape is shown in Figure 8-27.

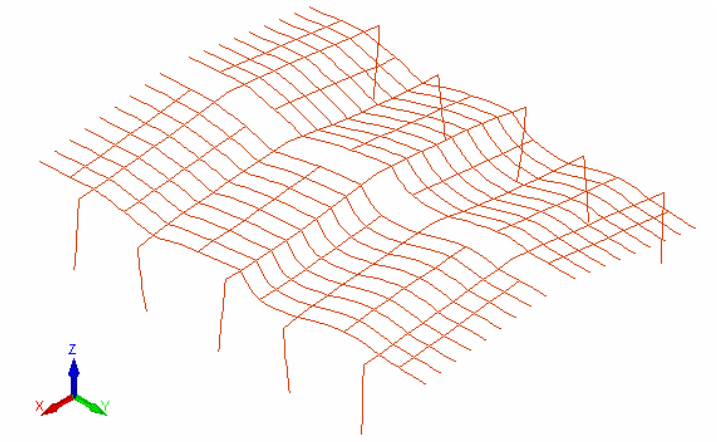

(a) Time = 45 seconds

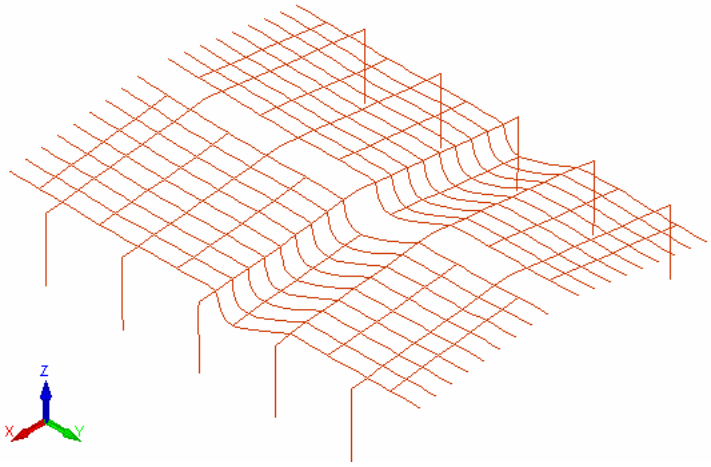

(b) Time = 50 seconds

Scale factor = 5x

Figure 8-25 Initial deformations in analysis (2)

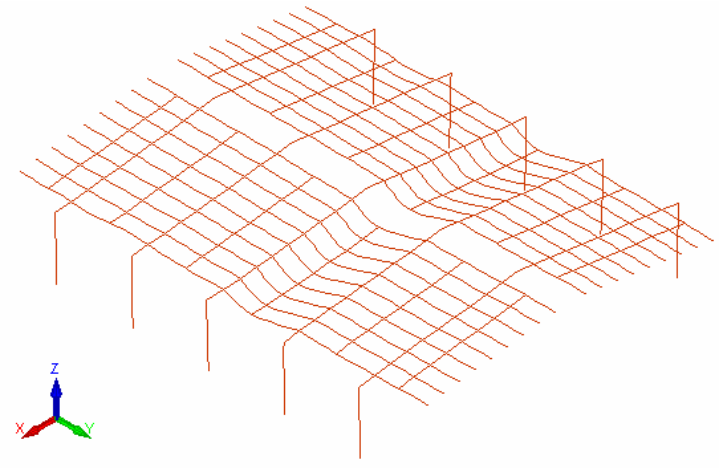

(a) Time = 13.8 minutes

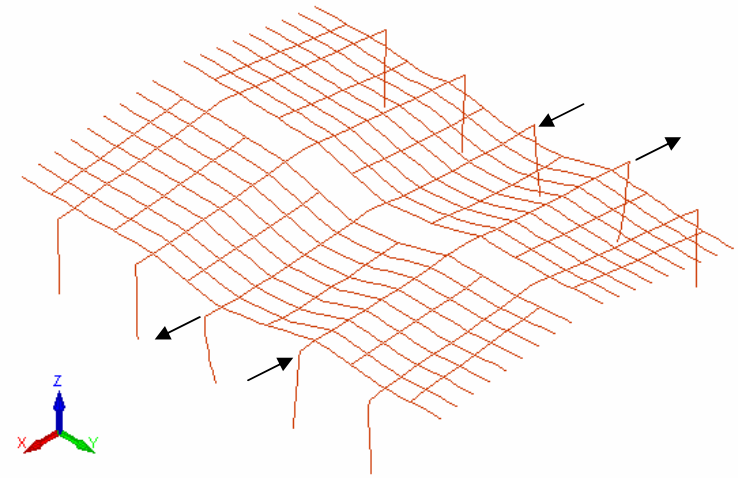

(b) Time = 13.9 minutes

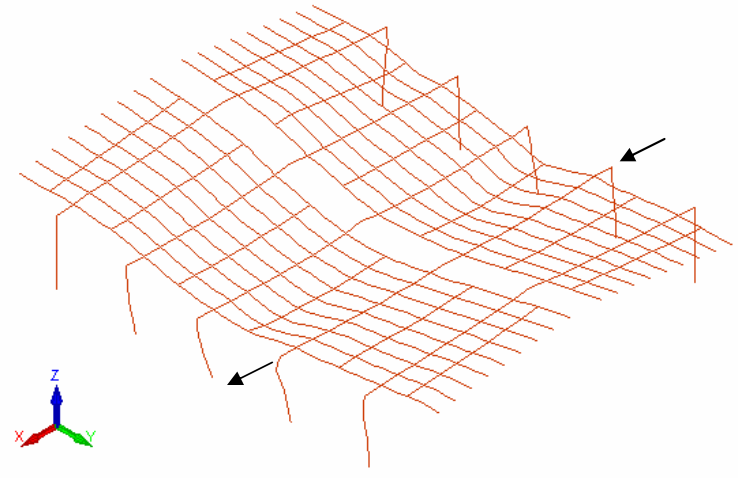

(c) Time = 16.0 minutes

Scale factor = 1x

Figure 8-26 Deflected shapes immediately before and after the rapid sagging of roof (analysis (2))

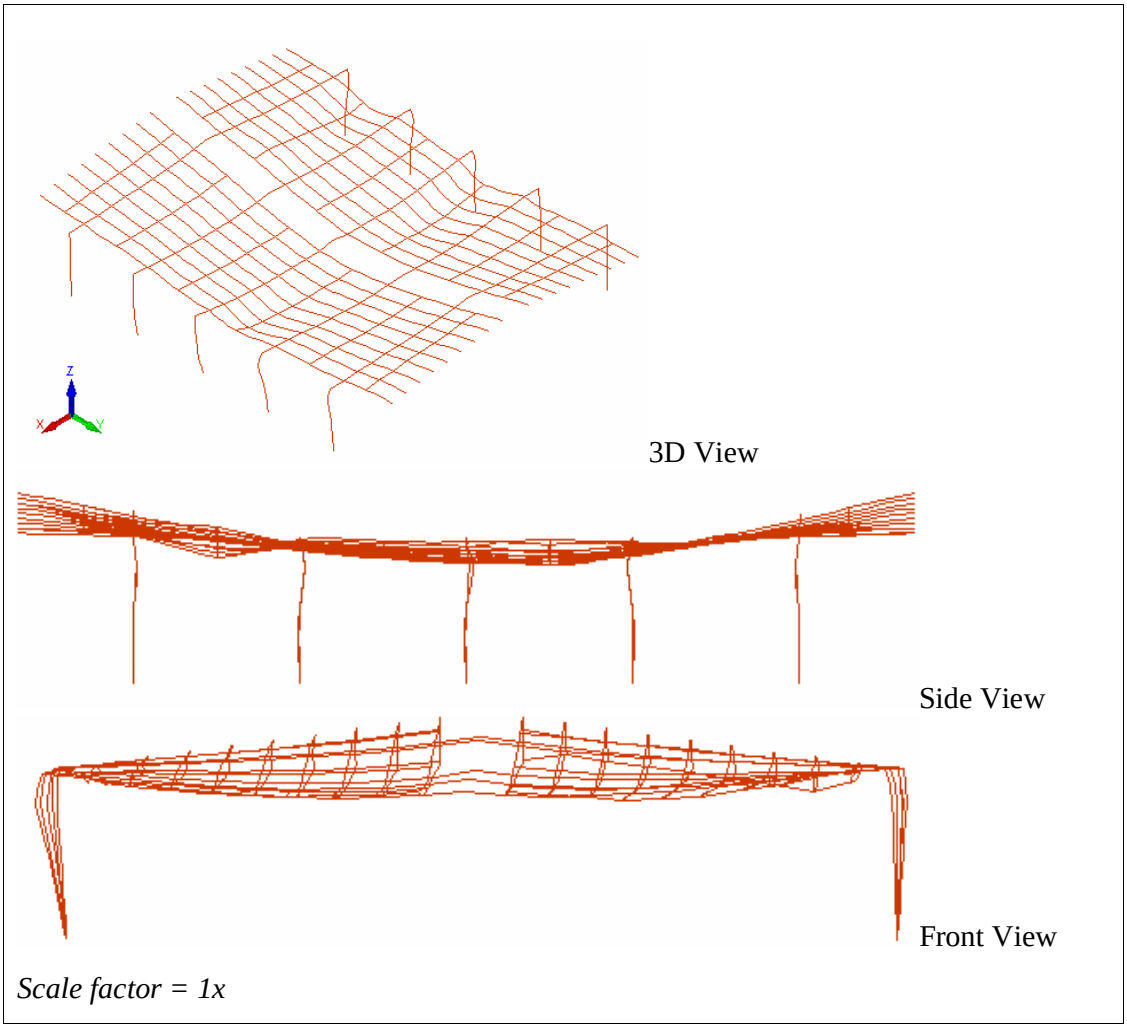

Figure 8-27 Final deflected shape from SAFIR (analysis (2))

Figure 8-22 shows that during the initial stages of the fire, the roof shows an upwards thrust due to the thermal expansion of the steel frames. The upwards deformation peaks at 10 minutes and the roof starts to deform downwards due to decreasing strength and stiffness of the frames. The rapid sagging of the roof structure at 14 and 16 minutes is clearly shown in the figure. It should be noted that the sagging of the roof structure occurs earlier when compared to analysis (1) with columns fixed at the bases. Frame 3 shows the largest downwards deflections of 2.9 m at the end of the simulation.

Figure 8-23 and Figure 8-24 show the horizontal deflection plots at the knees. The initial sway of frames before stabilisation occurs at 45 seconds is shown in the figures. After that, thermal expansion of the rafters causes the columns to deflect

outwards at a constant rate. The sway of the frames at 14 minutes results in 1.1 m of horizontal deflection at the left knee of frame 3 (Figure 8-23). Interestingly, the relative horizontal deflection between frame 3 and frame 4 is 2.1 m. At this instant, it is questionable if the joint connections holding the panels between these two frames would be strong enough to hold the panels as a complete unit and the walls are still attached to the frames instead of falling outwards. Furthermore, one or more frames may also collapse outwards due to the P-delta effects of the self-weight of the side wall panels. At 16 minutes, frame 3 sways further and increases the horizontal deflection up to as much as 1.5 m. As time increases, the roof continues to sag and this consequently pulls the knees inwards. Figure 8-23 and Figure 8-24 also show that frame 4 first sways to the right (negative global x axis) and then to the left (positive global x axis) at 14 and 16 minutes respectively.

Results from Analyses (3) and (4):

Analysis (3) - Fixed support frames with purlin axial restraints imposed by the end walls, localised fire near centre of building

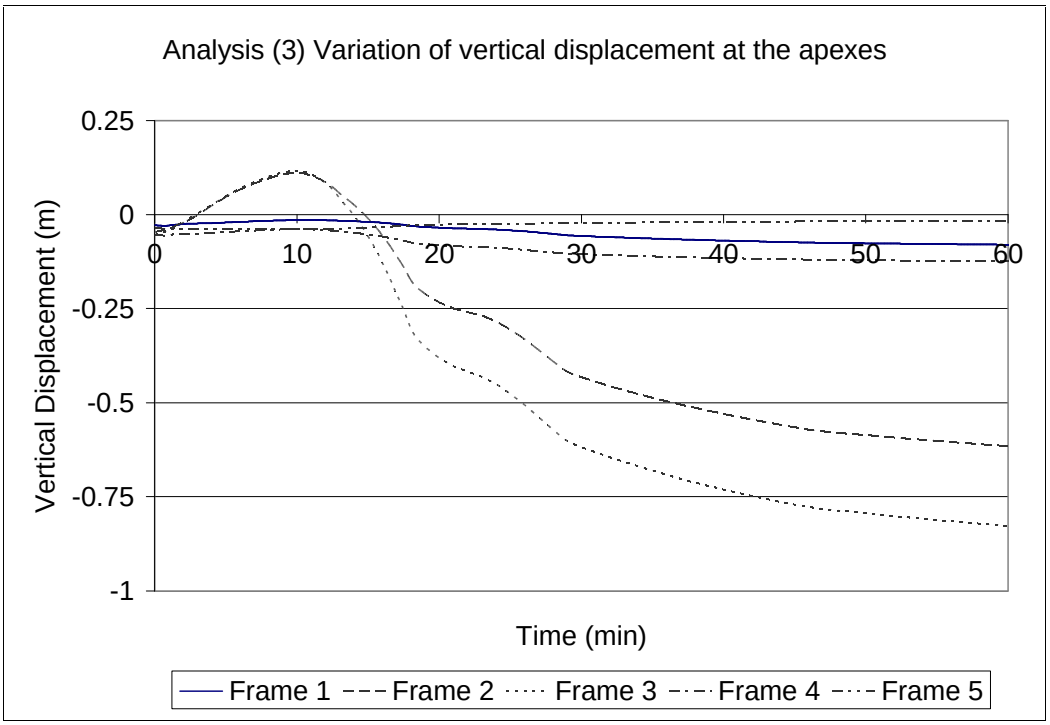

Figure 8-28 Variation of vertical displacement at the apexes in analysis (3)

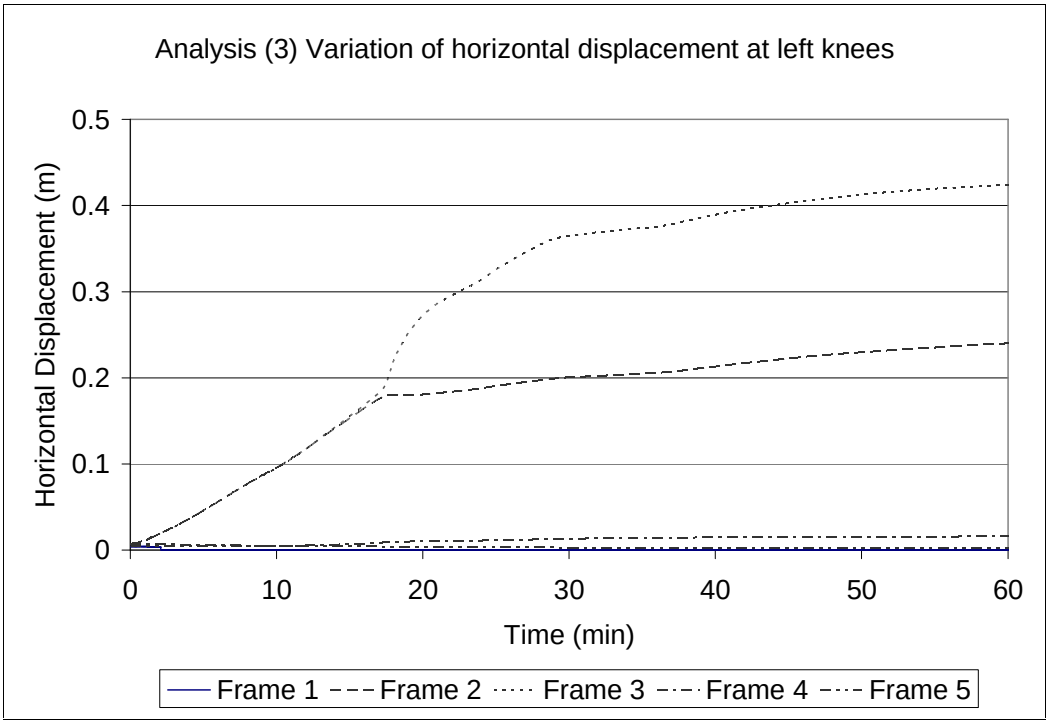

Figure 8-29 Variation of horizontal displacement at left knees in analysis (3)

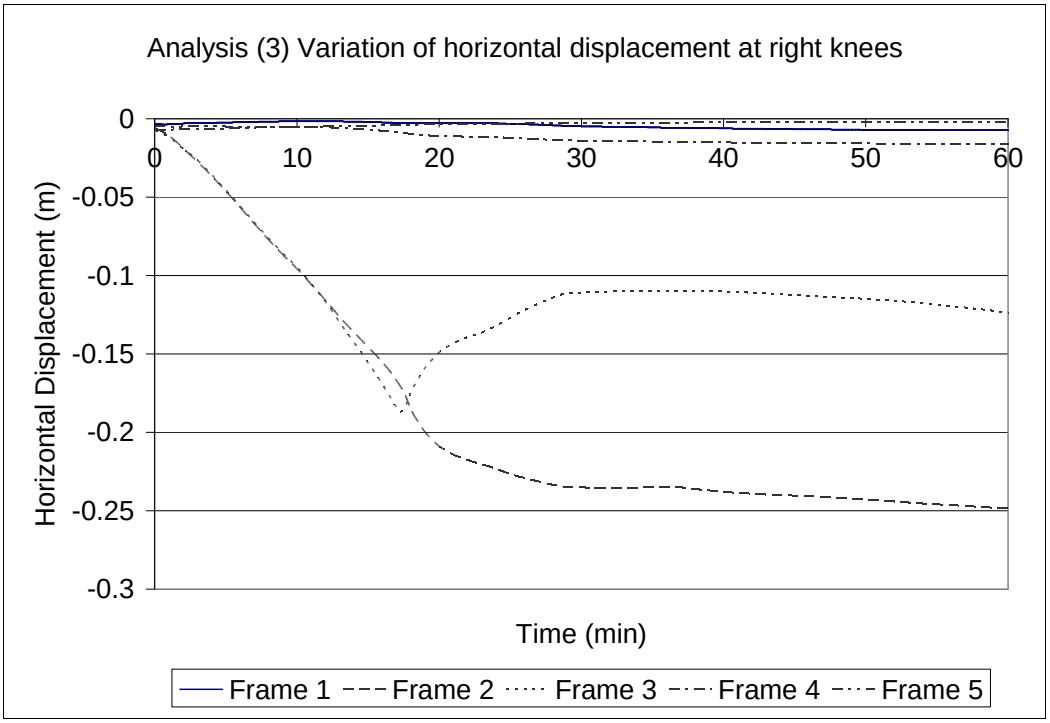

Figure 8-30 Variation of horizontal displacement at right knees in analysis (3)

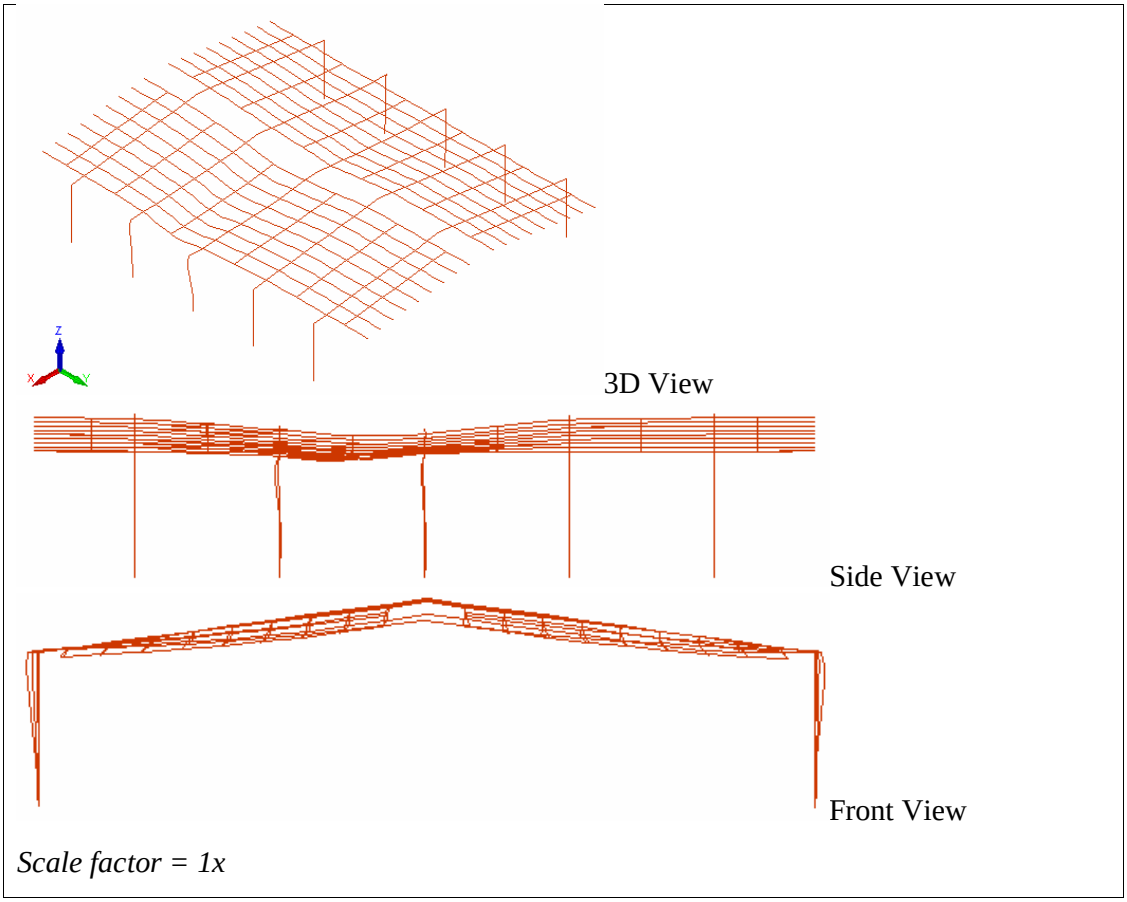

Figure 8-31 Final deflected shape from SAFIR (analysis (3))

Analysis (4) - Pinned support frames with purlin axial restraints imposed by the end walls, localised fire near centre of building

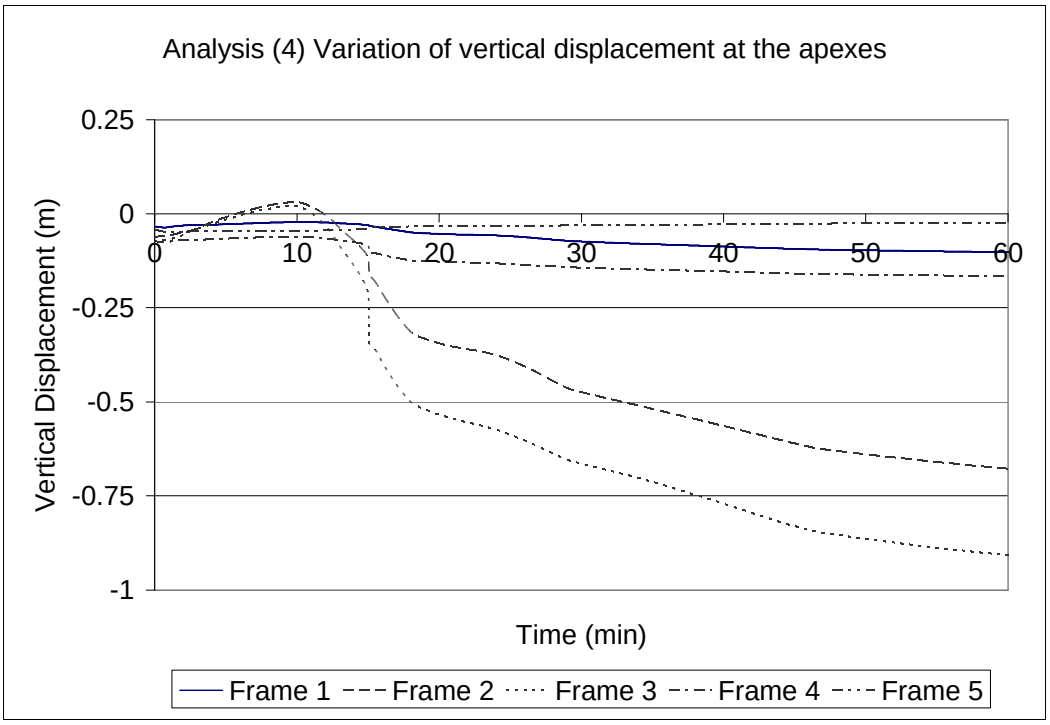

Figure 8-32 Variation of vertical displacement at the apexes in analysis (4)

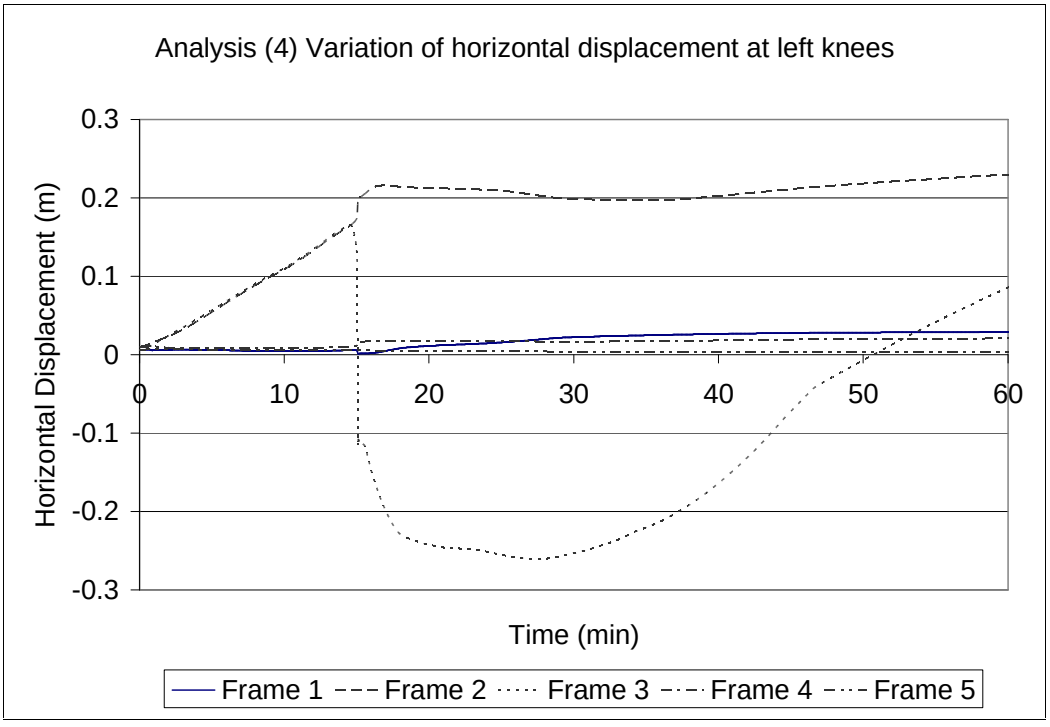

Figure 8-33 Variation of horizontal displacement at left knees in analysis (4)

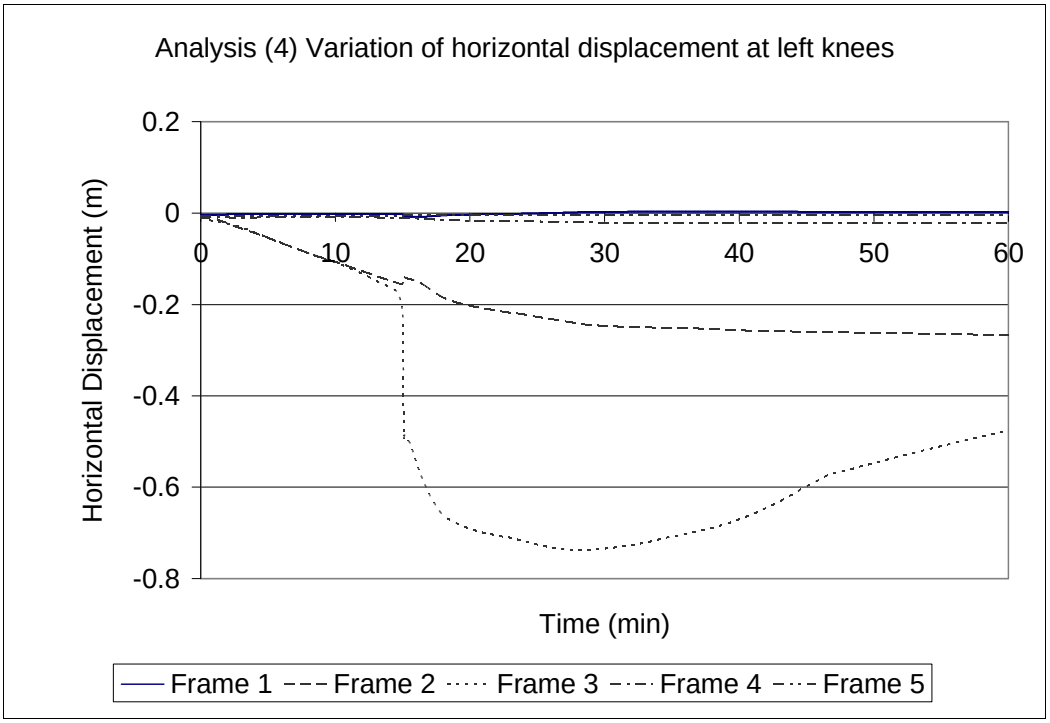

Figure 8-34 Variation of horizontal displacement at right knees in analysis (4)

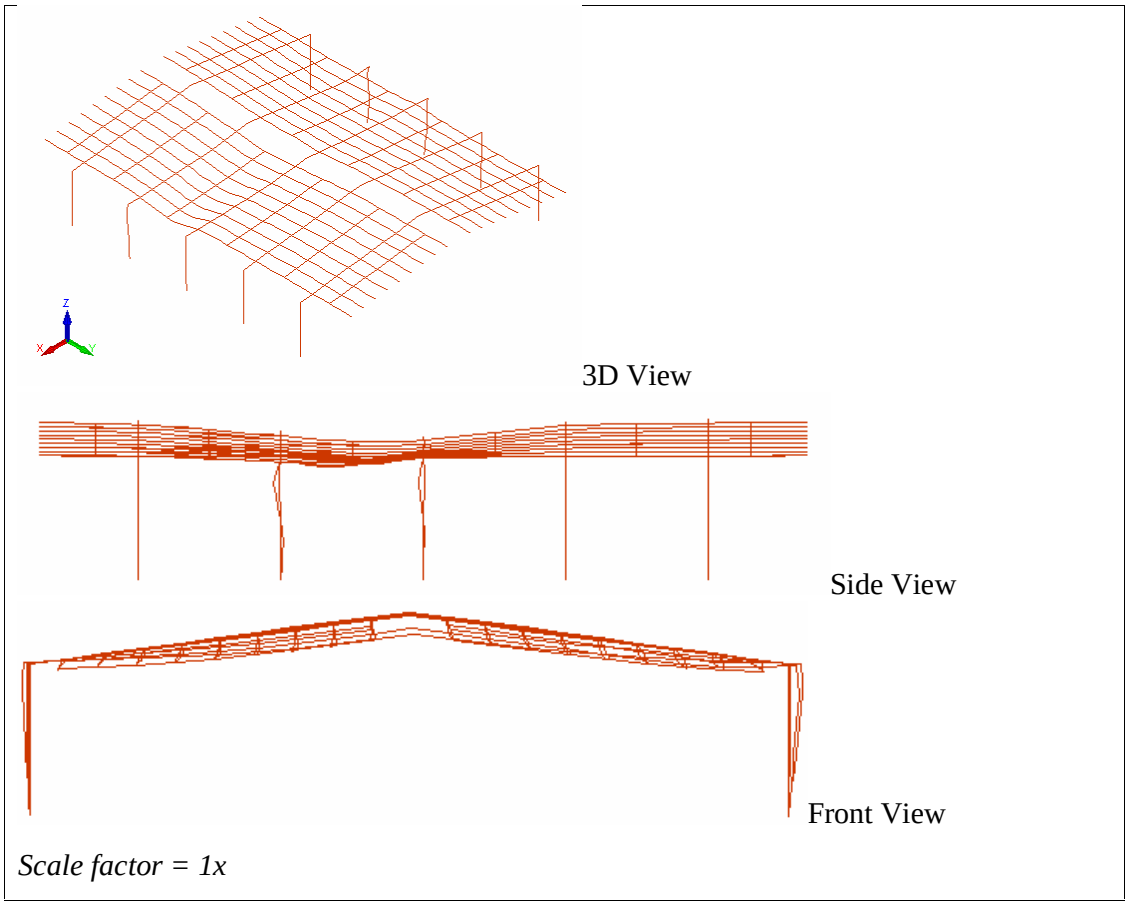

Figure 8-35 Final deflected shape from SAFIR (analysis (4))

The deflection mechanisms observed in the previous analyses are also applicable to the particular fire scenarios in analyses (3) and (4). The heated frames cause the roof structure in the heated region to deflect upwards due to thermal effects, and as heating continues, the decreasing strength and stiffness of the frames consequently result in downwards deformations (Figure 8-28 and Figure 8-32).

When the roof structure deforms downwards relatively quickly, the heated frames with pinned support conditions sway sideways (Figure 8-33 and Figure 8-34) and the fire-affected roof structure deforms into a catenary (i.e. this is defined as the sway mode failure). This implies the possibility of outwards collapse of the attached pre-cast concrete walls. The structure with fixed support conditions does not show the sway mode of failure mechanism and the deformation is also vertical. Similarly, the fire-affected bay deforms into a catenary shape (i.e. catenary mode failure). However, a horizontal deflection outwards of 0.42 m has been obtained at the end of the simulation (Figure 8-29) and the connections must be designed to accommodate this level of displacement to avoid outwards collapse of the walls.

During the fire, thermal expansions of the heated purlins are restrained by the adjacent frames and the purlin axial restraints imposed at the locations of the end walls. Sagging and out-of-plane buckling of these purlins are observed throughout the duration of the simulation. At the end of the simulation, the heated columns buckle out-of-plane and are stabilised at the locations of out-of-plane restraints imposed to represent the high stiffness of the side walls (see Side Views on Figure 8-31 and Figure 8-35).

Figure 8-28 and Figure 8-32 show the variation of vertical deflection at the apexes of all five frames. Frame 3 shows the greatest vertical deflection at the end of the simulation and frame 2 follows the similar deflection trend as frame 3 with less displacement. In addition, the frames adjacent to the heated bay show similar displacement trends although the frames remained at ambient temperature. This is because of load-sharing between the heated frames and the unheated frames and is described later.

Figure 8-29 and Figure 8-30 show the horizontal deflection plots at the top of the columns with fixed support conditions. It should be noted that the horizontal thrusts are caused by the combined effects of the reducing strength and stiffness of the heated columns, and the expansion and sagging of the heated rafter. During the first 16 minutes, similar deflection trends as in the previous analyses can be seen in the figures, where thermal expansion and sagging of the rafters push the heated columns outwards. However, in the later stages of the fire, the right knee of frame 3 deflects inwards due to the sagging of the roof structure up until 30 minutes when the continuous sagging of the roof structure causes it to deform outwards again. While this is happening, the sagging of the roof has also slowed the outwards deformation of the left column of frame 2. In general, larger outwards deformation has been achieved for frame 3 due to its greater distance from the end wall restraints (i.e. points of rigidity).

For the portal frame structure with pinned support conditions, the horizontal deflections occurring at the top of the columns (Figure 8-33 and Figure 8-34) are larger when compared to the case with fixed support conditions. This is because of the sidesway of the heated frames. Interestingly, the unheated part of the structure has provided some lateral restraint in preventing the heated frames from swaying and collapsing outwards.

The results from both analyses have shown that the heated frames can be seen to approach a stable state at the end of the simulation. This means that the cooler parts of the structure are capable of providing adequate restraint to the heated bay and may allow it to deform further in a steady manner for a long period of time.

Figure 8-36 shows the bending moment diagram for the whole building with fixed support conditions (analysis (3)) at various times and it is clear that the frames exposed to the fire have very low strength at the end of the simulation. Although the temperatures of the heated frames are increasing according to the ISO fire curve, the heated frames do not show a complete collapse after 1 hour of fire exposure. This is because the collapse of the heated bay (bay 3) is being prevented by the purlins in bays 2 and 4, which are in turn supported on the adjacent frames. The figure shows that the loads are being transferred to the adjacent frames.

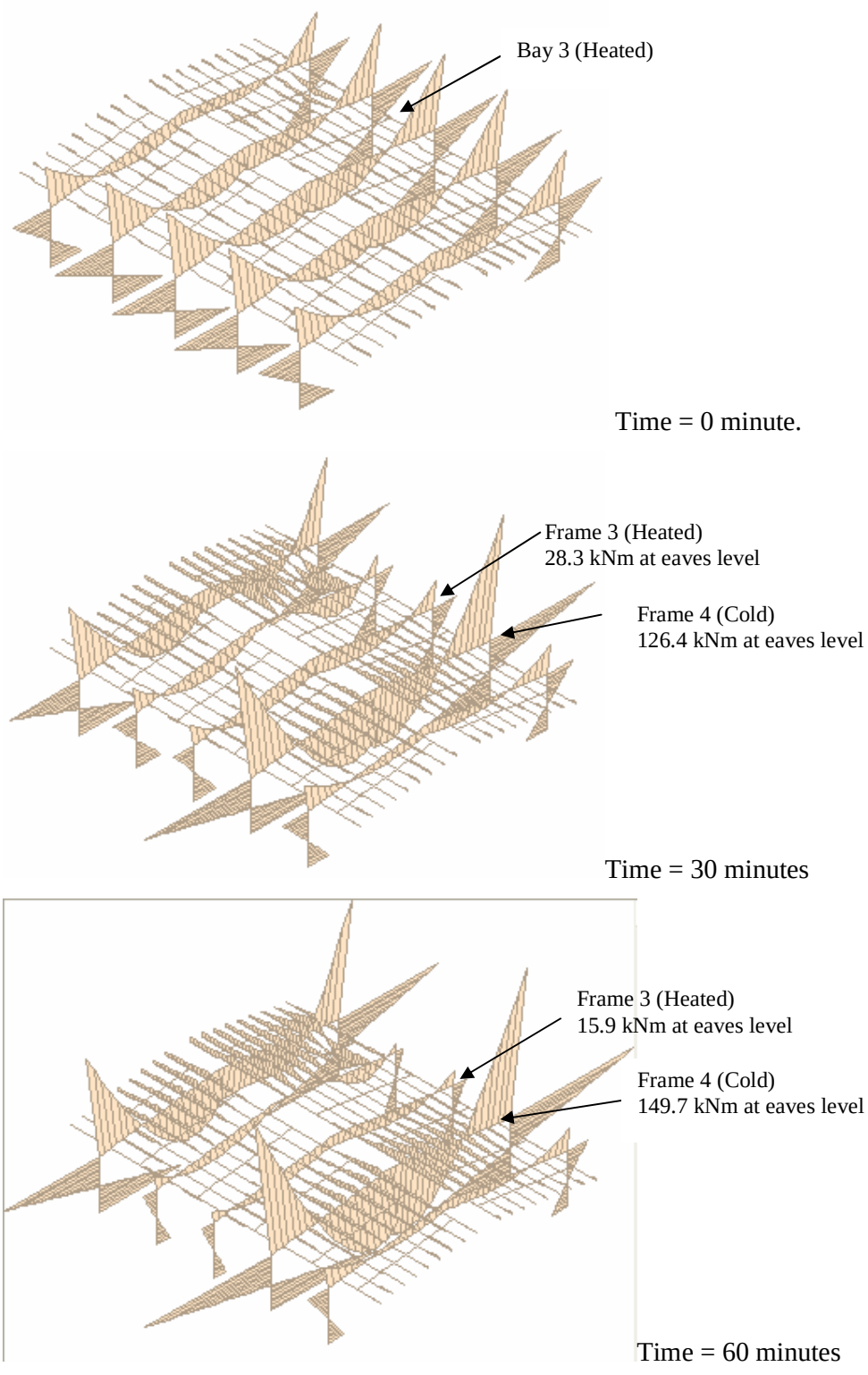

Figure 8-36 Variation of bending moment during the first hour of fire exposure (analysis (3))

Results from Analyses (7):

Fixed support frames without purlin axial restraint imposed by the end walls, fully developed fire

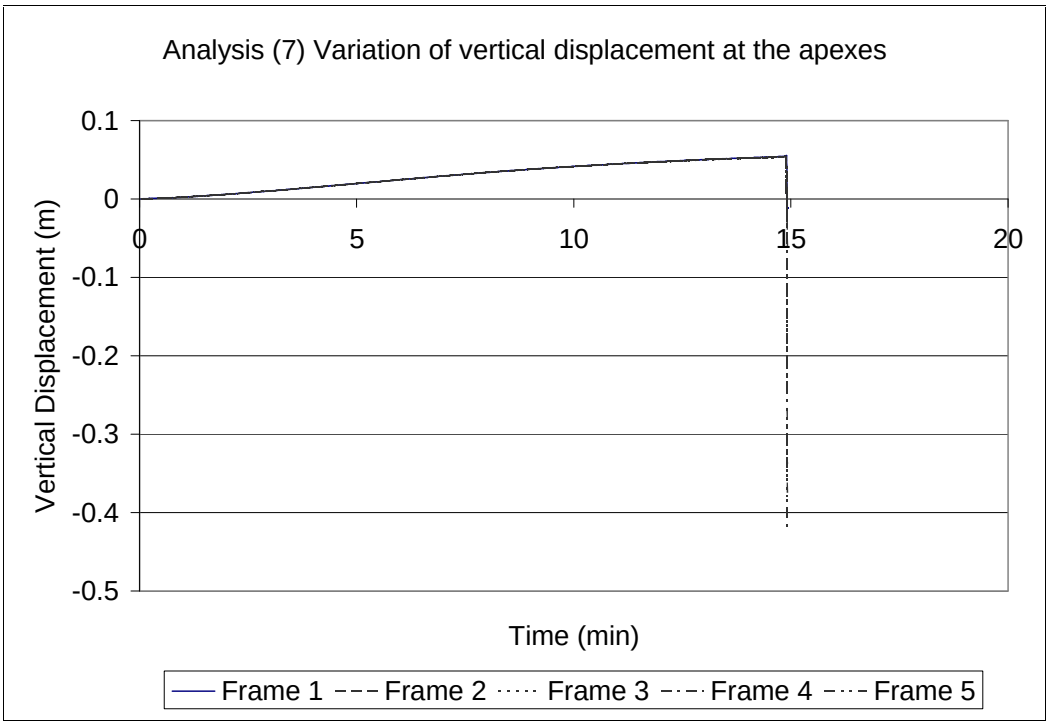

Figure 8-37 Variation of vertical displacement at the apexes in analysis (7)

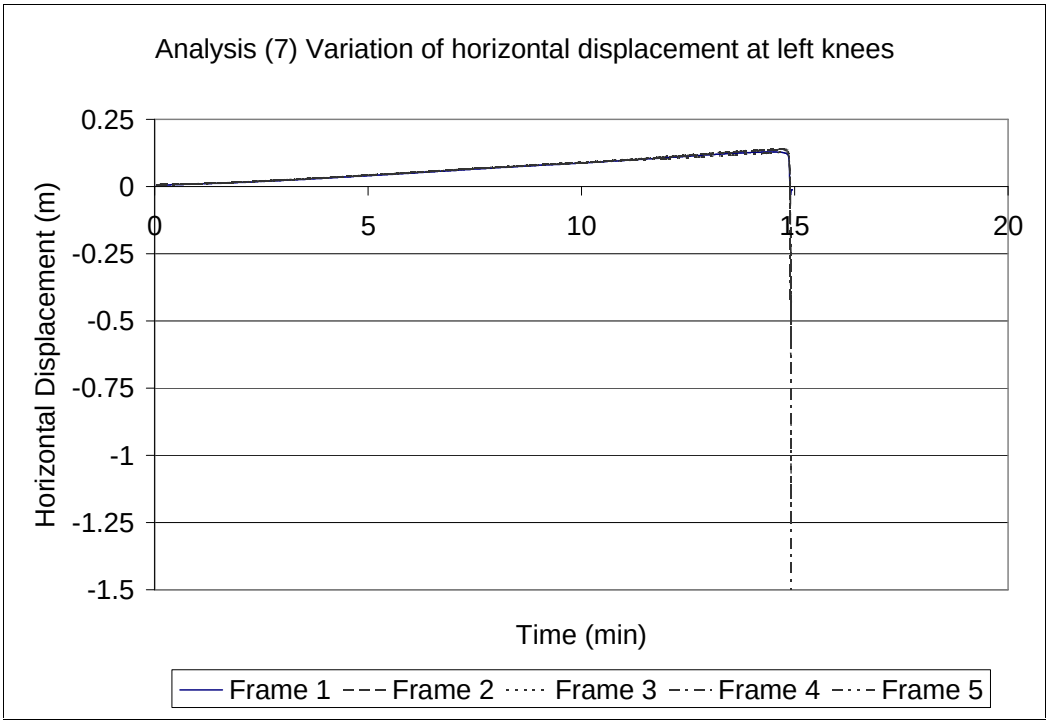

Figure 8-38 Variation of horizontal displacement at left knees in analysis (7)

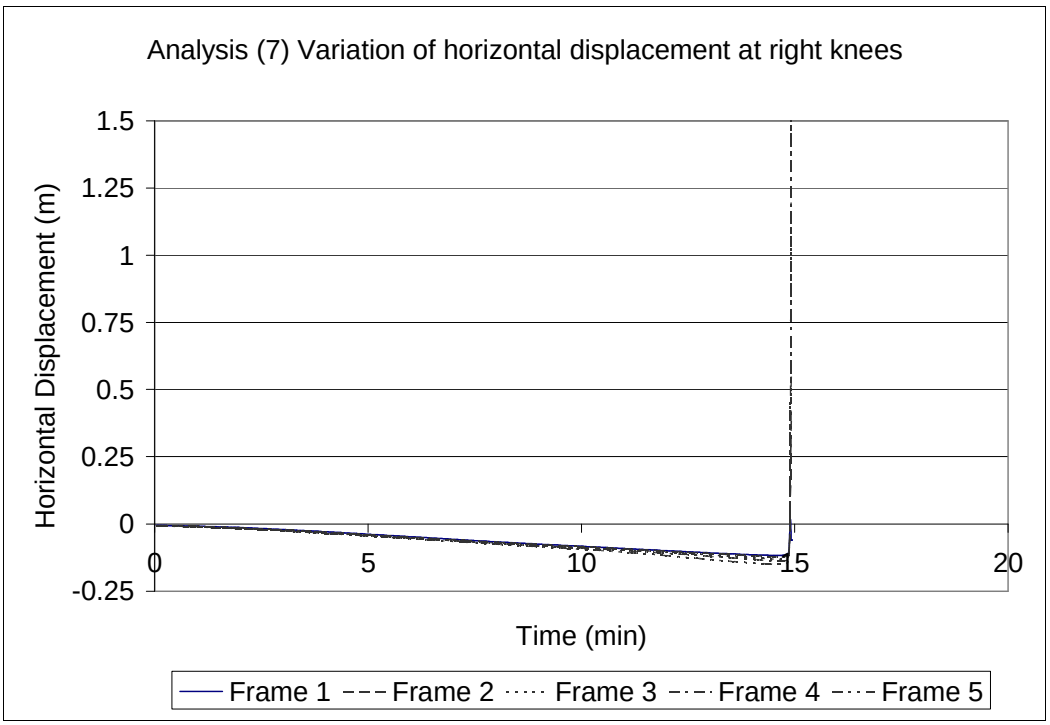

Figure 8-39 Variation of horizontal displacement at right knees in analysis (7)

During the initial stages of the fire, large out-of-plane local buckling of purlins does not occur since no purlin axial restraint is imposed by the end walls. The purlins are able to elongate freely in their longitudinal axes due to the thermal effects. Apart from this, the fire performance of the structure is similar to the previous analyses in that the roof structure deforms upwards (Figure 8-37) and the columns deflect outwards at a constant rate (Figure 8-38 and Figure 8-39) due to thermal expansions of the frames. However, the roof structure suddenly collapses to the ground at about 15 minutes, pulling the columns inwards (Figure 8-38 and Figure 8-39). This inwards collapse failure mode is due to the formation of plastic hinges at the knees of the frames, allowing large rotations to occur and the roof to undergo a snap-through failure mechanism. This failure mechanism can be clearly seen from the outputs of SAFIR (Figure 8-40) and is acceptable as the walls attached to the supporting frames will be pulled inwards and collapse into the building, assuming that the connections do not fail. The inwards collapse of the walls will either put the fire out underneath the collapsed walls or increase the separating distance between the building and the boundary sites.

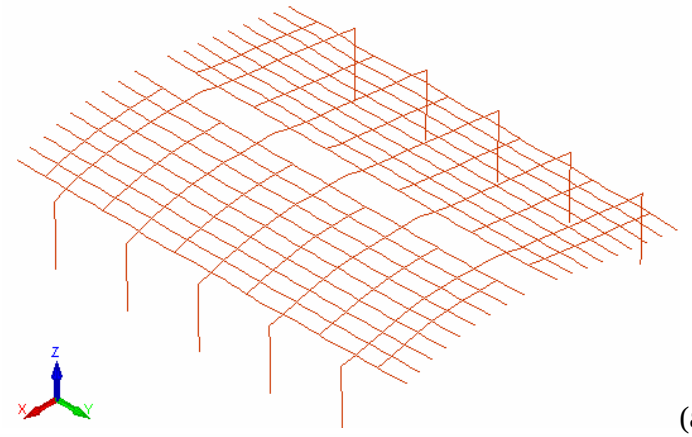

(a) Time = 14.87 minutes

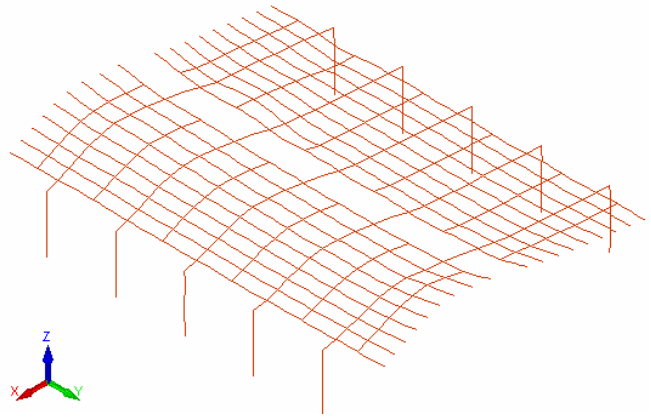

(b) Time = 14.90 minutes

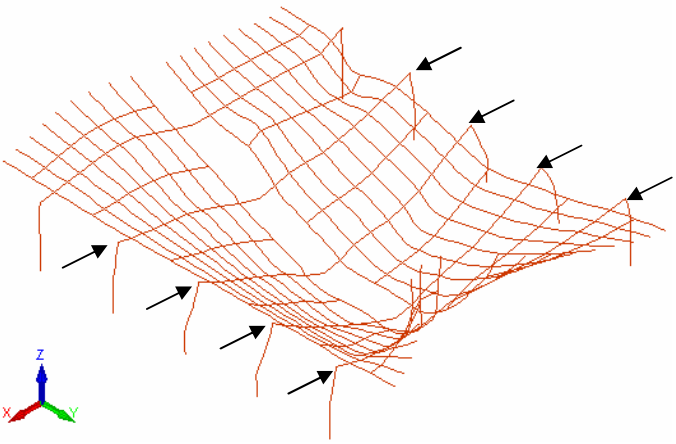

(c) Time = 14.92 minutes

Scale factor = 1x

Figure 8-40 Inwards collapse of the fixed support structure without purlin axial restraint imposed by the end walls and fully involved in the fire (analysis (7))

Results from Analyses (8):

Pinned support frames without purlin axial restraint imposed by the end walls, fully developed fire

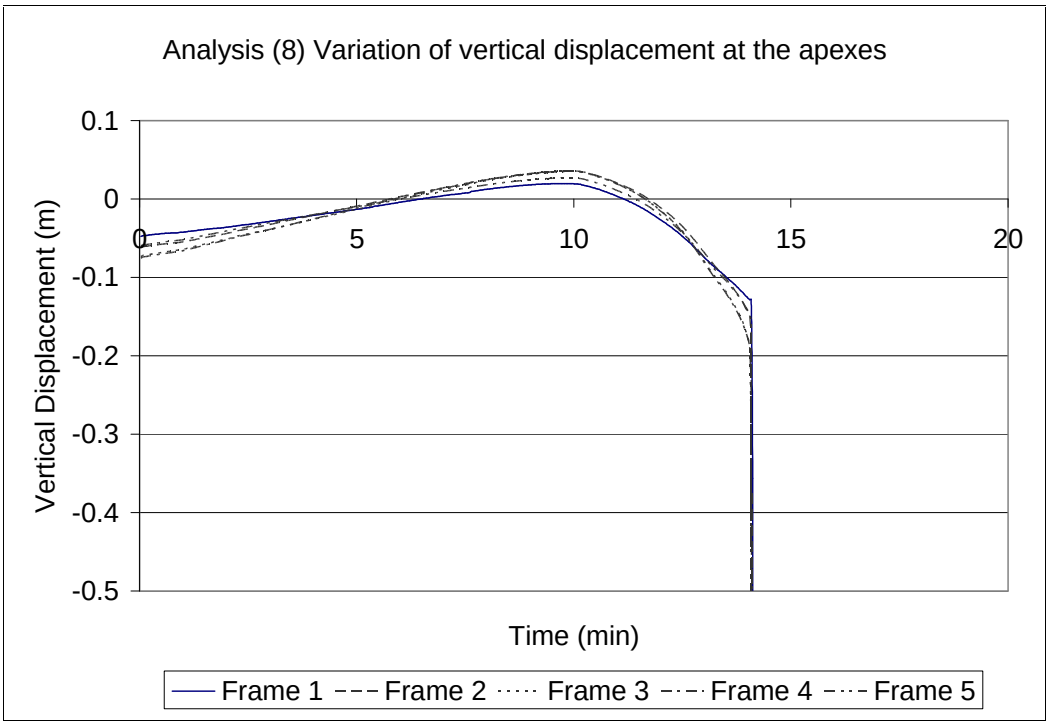

Figure 8-41 Variation of vertical displacement at the apexes in analysis (8)

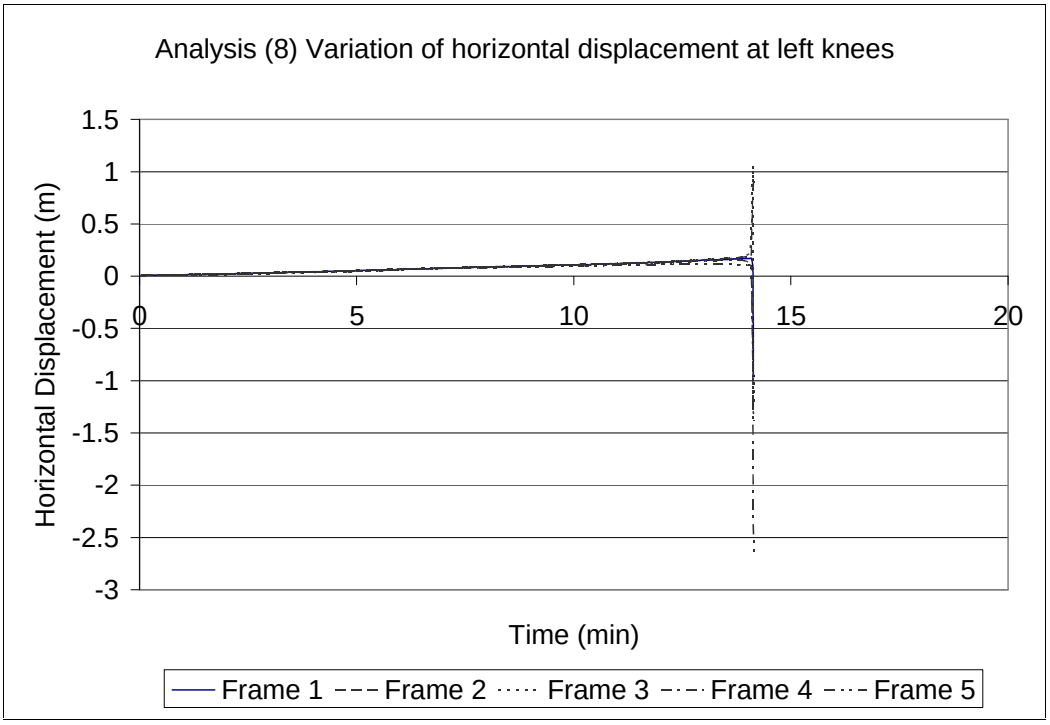

Figure 8-42 Variation of horizontal displacement at left knees in analysis (8)

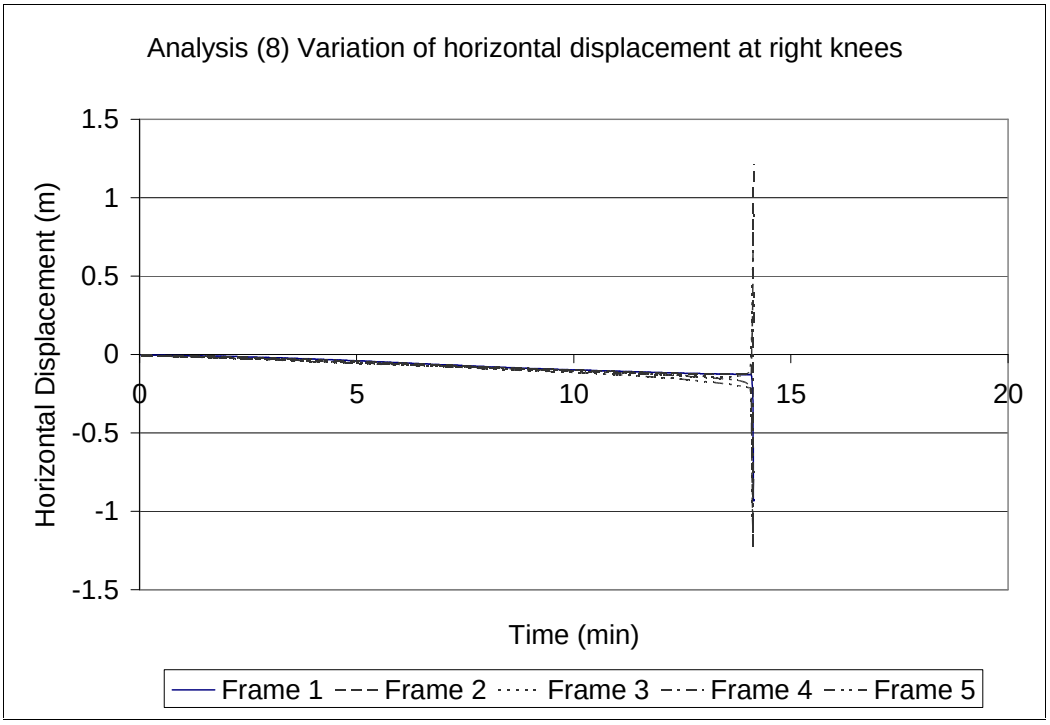

Figure 8-43 Variation of horizontal displacement at right knees in analysis (8)

Figure 8-41 shows that the vertical deflections at the apex reach a plateau at approximately 10 minutes of fire exposure, followed by a downwards trend and lastly, a sudden collapse of the structure. Without any purlin axial restraint from the end walls, noticeable out-of-plane local buckling of the purlins does not occur. The collapse of the structure occurs at 14.1 minutes, which is slightly earlier when compared to the fixed support structure at 14.9 minutes due to its higher load ratio and thus lower fire resistance (refer to Section 7.4.1.3). When the roof structure starts to collapse due to the formation of plastic hinges at the knees, significant sidesway of the frames occurs (Figure 8-44 (b)) which results in outwards horizontal deflections in excess of 1 metre (Figure 8-42 and Figure 8-43). Interestingly, as the roof structure collapses further to the ground, the columns are being pulled inwards as in the fixed support case (frames 3, 4 and 5 in Figure 8-44 (c)). Although SAFIR could not show the complete sequence of collapse of the structure, it is believed that as the roof structure collapses to the ground, all the columns will be pulled inwards.

This type of collapse mechanism has been classified as the sway mode of failure in Table 8-3 and is unacceptable according to the New Zealand Building Code (Section

2.2.1). The sidesway of the frames could cause one or more frames to collapse outwards due to the P-delta effects of the self weight of the walls and the large lateral deflections to one side. The wall panels could also collapse outwards along with the frames and cause fire spread to adjacent property or threaten the lives of fire-fighters standing close to the building while attending the fire.

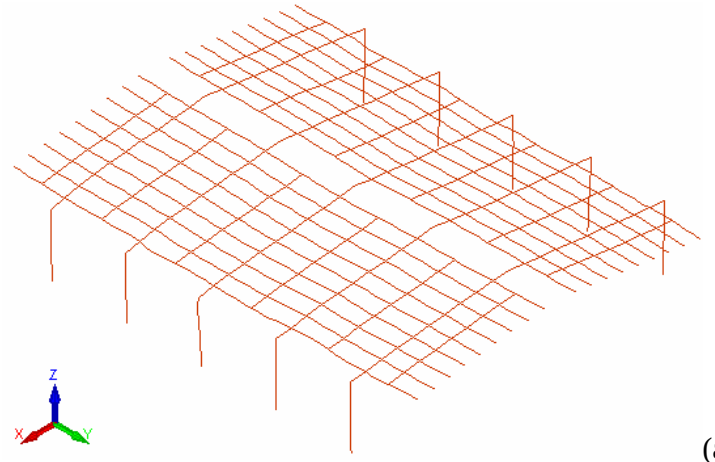

(a) Time = 14.08 minutes

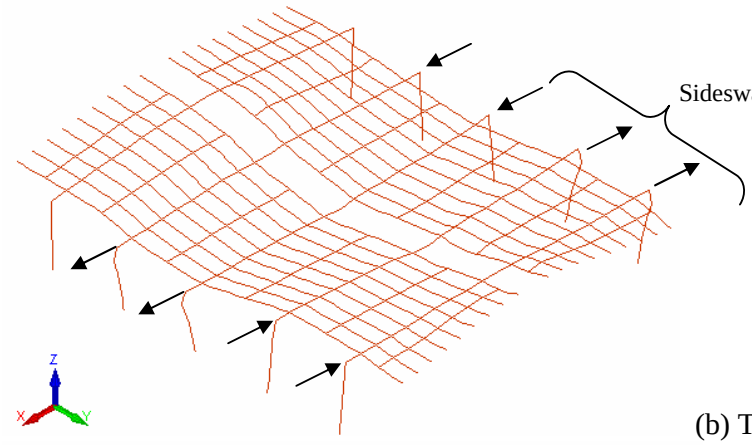

(b) Time = 14.12 minutes

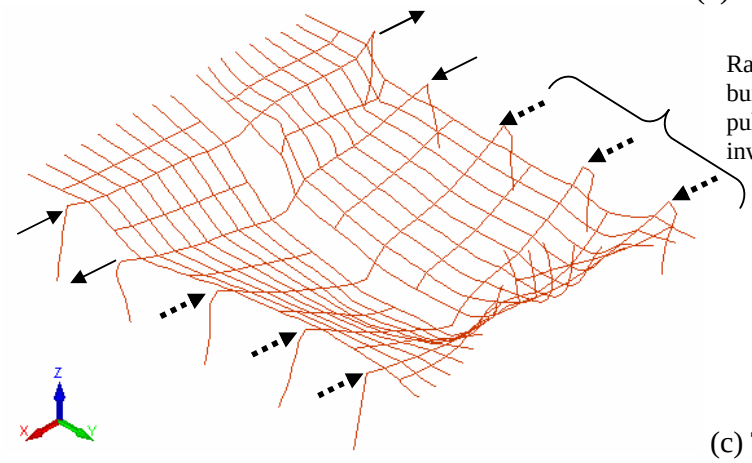

(c) Time = 14.13 minutes

Scale factor = 1x

Figure 8-44 Sideways collapse of the pinned support structure without purlin axial restraint imposed by the end walls and fully involved in the fire (analysis (8)).

8.3.2 Discussion

Localised Fires

If a fire occurs near the centre of the building and is confined in size (i.e. affecting a small number of structural elements in terms of strength and stiffness), load transfer can occur between the fire-affected and unaffected areas and it has been shown that the unaffected parts of the structure can provide adequate restraint to the heated area and the structure may deform in a steady manner for a long period of time.

The above phenomenon has also been observed in the case when the fire occurs near the end walls and the structure has purlin axial restraints provided by the end walls (i.e. load transfer can take place). However, when the purlin axial restraints are removed, the heated frame supporting the purlins in the end bay collapses because load-sharing cannot take place.

The results show that regardless of whether load transfer will occur or not, portal frames with fully fixed supports will fail in an acceptable way whereas portal frames with fully pinned supports will fail in an unacceptable manner. This is further described in more detail below (refer to the discussions on fully developed fires).

O'Meagher *et al*. (1992) suggest that the collapse of the heated frames which are located close to the point of fire origin will act as "anchors" to the rest of the building (Figure 4-26, reproduced here for clarity) causing it to collapse in an acceptable mode (refer to Section 4.4.2). The results of the analyses suggest that this inwards collapse will only occur when the purlins adjacent to the heated frames are not axially restrained. It should be noted that the purlins themselves can still have high tensile strength at elevated temperatures and the "anchors" deformations may not be achieved easily in practice. In addition, to achieve an effective inwards collapse, some level of fixity is required at the column bases or else the heated frames will sway sideways before collapsing inwards due to the collapsing rafter. This is further explained below.

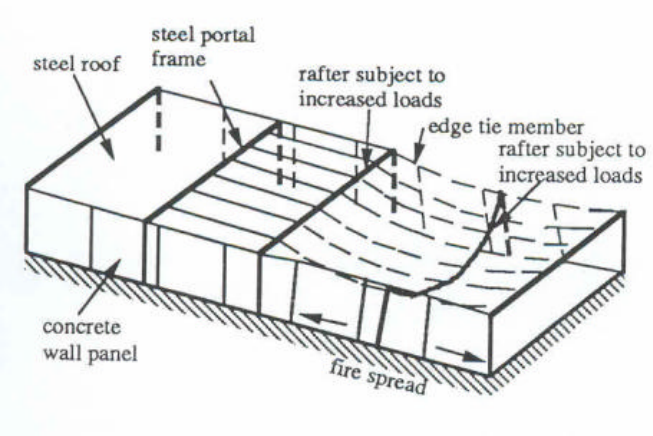

Figure 8-45 Heated frames acting as "anchors" (O'Meagher *et al*., 1992)

Fully Developed Fires

For fully developed fires in which all the structural elements are exposed to elevated temperatures, the structural fire behaviour is very dependent on the presence of purlin axial restraints imposed by the end wall boundary conditions (i.e. purlins connected to the end concrete walls are assumed to be translationally fixed in the longitudinal direction at the bolted connections) . With purlin axial restraints, the roof structure (steel rafters, purlins and brace channels) will deform into a catenary and without purlin axial restraint, the roof structure and the columns will collapse into the building. The intermediate failure mechanisms before getting to the final failure modes are in turn dependent on the type of support conditions at the base of the frames and are described in detail below.

Fixed Support Conditions

For the steel portal frame structure with bases fully fixed to the foundation, the deformation due to elevated temperatures is almost vertical and the roof structure will either collapse into the building and to the ground (no purlin axial restraint), or deform into a catenary shape (with purlin axial restraints). These types of failure mode are acceptable providing the connections between the walls and the supporting frames do not fail. For the inwards collapse mode, the side walls will be pulled inwards along with the collapsing rafters and reduce the risks of fire spread to adjacent property by increasing the fire separating distance to boundary sites and they may even extinguish the fire underneath the collapsed walls. For the catenary mode of failure, the walls must be held in outwards inclined positions to avoid outwards

collapse. This is very important in terms of the steel connections between the walls and the supporting frames. The self-weight of the concrete walls (i.e. P-delta effects) and also the reduced strength of steel at elevated temperatures must be taken into account in designing the connections.

Further analyses taking into account the different combinations of locations and severities of fires (i.e. two, three bays affected by the fire) were also carried out for the steel portal frame structure with ideally fixed support conditions and it was found that the largest possible horizontal deflection at the eaves level is 520 mm. This means that for this particular structure with fully fixed column bases, the connections to the panels must be designed to sustain a relative outwards displacement of 520 mm between the top and bottom of the column.

Pinned Support Conditions

The failure mechanisms for the steel portal frame building with pinned bases differ considerably when compared to the steel portal frame building with fixed bases. Due to the nature of ideally pinned connections at the bases of the columns, large rotations are possible at about any global axis and this is why significant sidesway of frames has been observed to occur when the roof structure starts to fail. The sidesway of frames can result in very large outwards horizontal deflections at the eaves levels (i.e. in excess of 1 metre). After that, the structure will deform into a catenary held in place by the purlin axial restraints imposed by the end walls, or in the scenario where purlin axial restraints are not provided by the end walls, the roof structure will collapse to the ground and the collapsing rafters will subsequently pull the frames inwards. These types of failure are unacceptable because the large lateral deflections to one side could cause a sideways collapse of one or more frames due to the P-delta effects of the self weight of the walls. In addition, the sidesway of the frames occurs without any warning when the roof structure deforms downwards and may threaten the lives of fire-fighters in close vicinity to the building.

8.4 Eurocode External Fire

Previous analyses have shown that if only a small number of the building elements are heated, structural failure may not be observed (Table 8-3). For consistency, the analyses carried out in this section and similarly in the subsequent sections assume that the whole building is fully involved in the fire at the first time step until the simulation stops (refer to Figure 8-10). The analyses in this section are performed using the Eurocode External fire curve which is commonly used to simulate well-ventilated fires, for example, after the collapse of the roof sheeting. The maximum temperature of the External fire curve is taken as 660^{o}C and either stays constant thereafter or decays linearly at 30 minutes (see Figure 8-46 and refer to Section 7.2.2 for more detail). The analyses in this section are tabulated in Table 8-4.

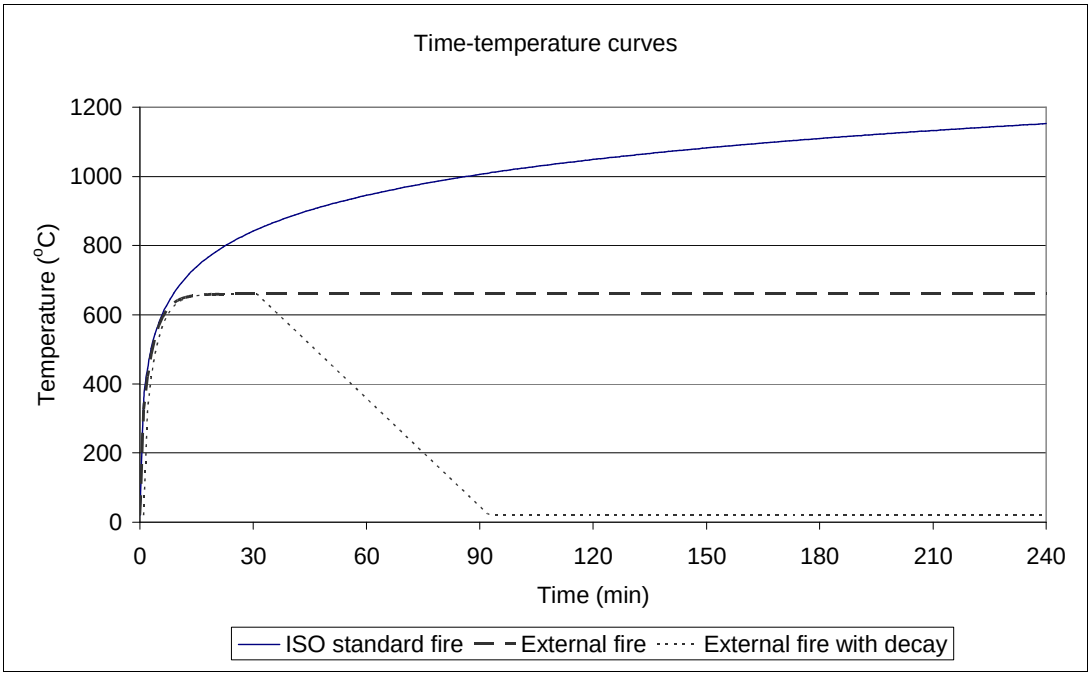

Figure 8-46 Time-temperature curves for the External fire with and without a decay phase

Table 8-4 Fire analyses in Section 8.4 – Eurocode External Fire

Analysis number	Description of the fire	Support conditions	Purlin Axial Restraints
(13) & (17)	External fire without decay phase	Fixed	Yes & No
(14) & (18)		Pinned	Yes & No
(15)	External fire with decay phase	Fixed	Yes
(16)		Pinned	Yes

8.4.1 Results of Analyses

The results of the analyses are summarised in Table 8-5. The analyses without a decay phase in the fire and purlin axial restraint provided by the end wall boundary conditions were not carried out because structural collapse occurred before the onset of the decay phase (analyses (18) and (19)) which was introduced in the External fire curve at 30 minutes.

Table 8-5 Results of analyses in Section 8.4 – Eurocode External Fire

Analysis number	Description of the fire	Support conditions	Purlin Axial Restraints	Mode of Failure	Simulation End Time (minutes)
(13)	External fire without decay phase	Fixed	Yes	Catenary	60.0*
(14)		Pinned	Yes	Sway	60.0*
(15)	External fire with decay phase	Fixed	Yes	No failure	120.0*
(16)		Pinned	Yes	No failure	120.0*
(17)	External fire without decay phase	Fixed	No	Inwards	26.9
(18)		Pinned	No	Sway	18.4

**Note: The maximum time limit of 60 or 120 minutes (arbitrarily chosen) was reached in SAFIR.*

The results of the analyses (13) to (16) are described below. SAFIR numerically iterated the deformations of the structure up until the specified maximum time limits were reached in these analyses. The results of the analyses without any purlin axial restraint from the end walls (analyses (17) and (18)) are not described in detail here as they show the inwards snap-through collapse for the fixed support portal frame structure (Figure 8-63) and the sway mode collapse for the pinned support portal frame structure (Figure 8-64), which were commonly observed in the previous analyses. It should be noted that the failure times for the last two analyses were significantly larger when compared to similar analyses performed with the ISO fire curve (i.e. 26.9 minutes compared to 14.9 minutes for the fixed support portal frame structure; 18.4 minutes compared to 14.1 minutes for the pinned support portal frame structure)

Results from Analysis (13):

Fixed support frames with purlin axial restraints imposed by the end walls, External fire without decay phase

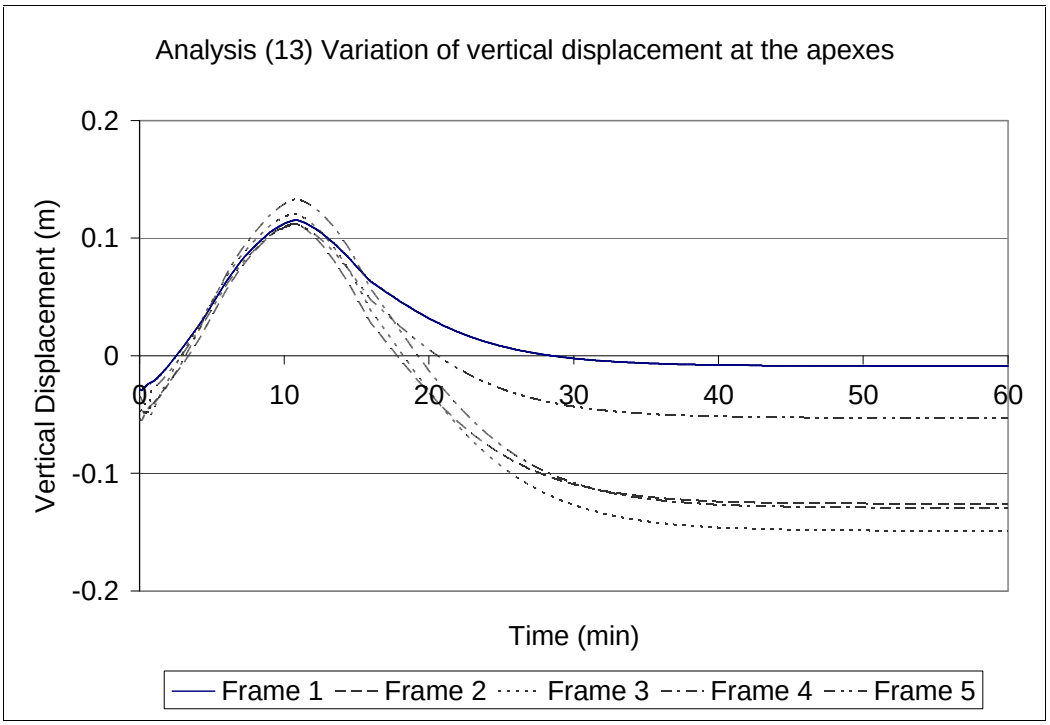

Figure 8-47 Variation of vertical displacement at the apexes in analysis (13)

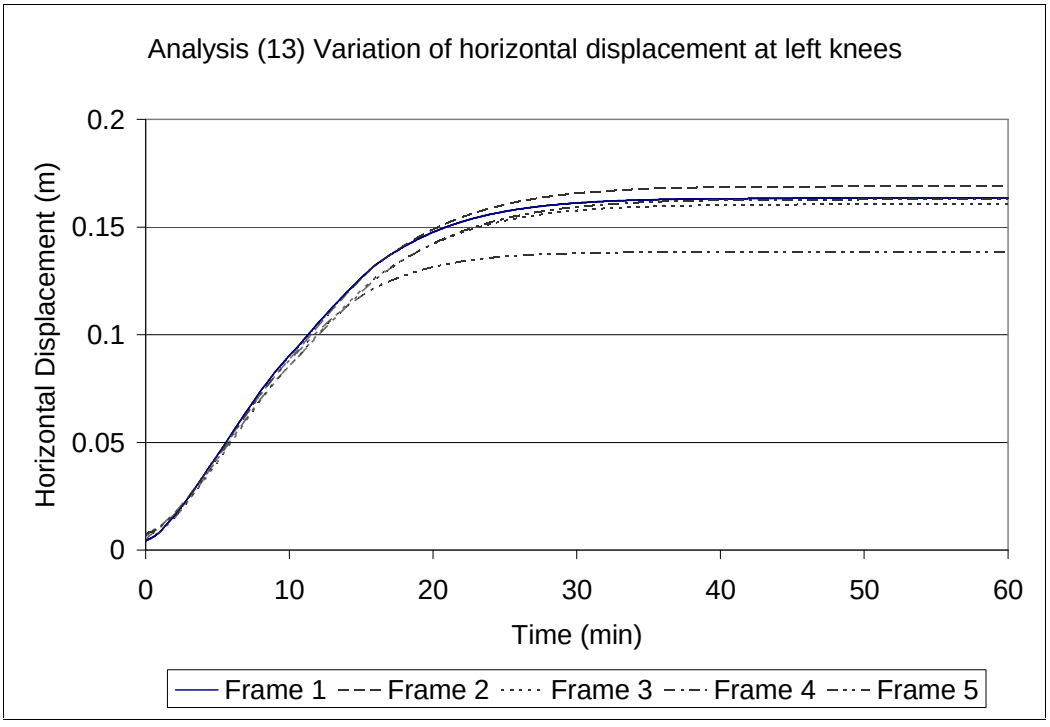

Figure 8-48 Variation of horizontal displacement at left knees in analysis (13)

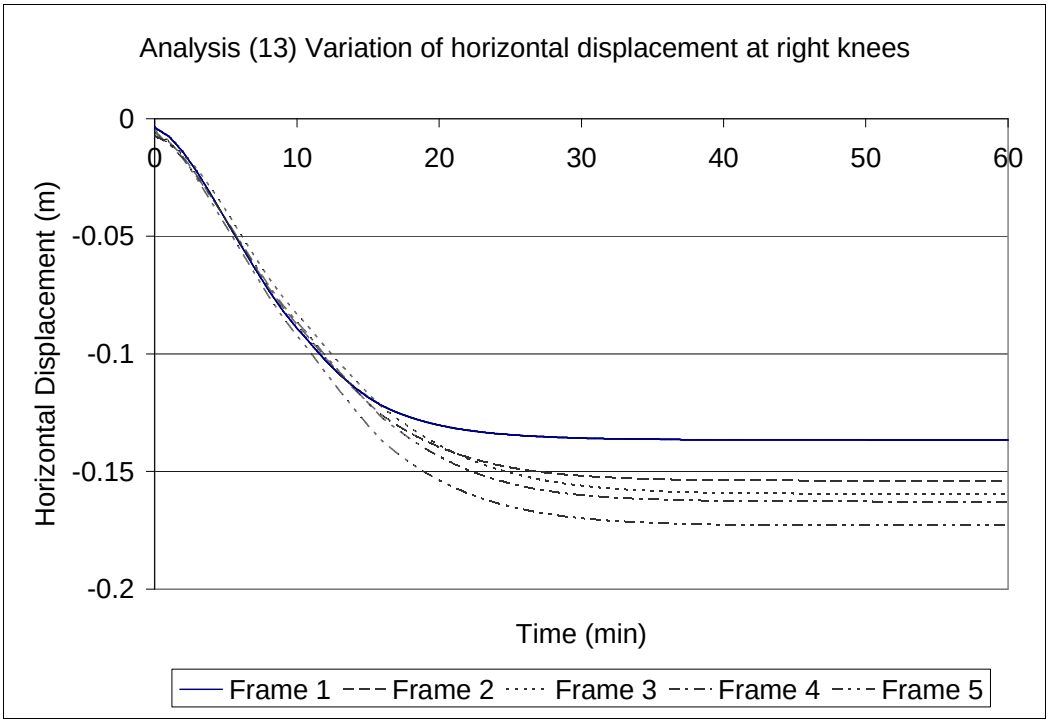

Figure 8-49 Variation of horizontal displacement at right knees in analysis (13)

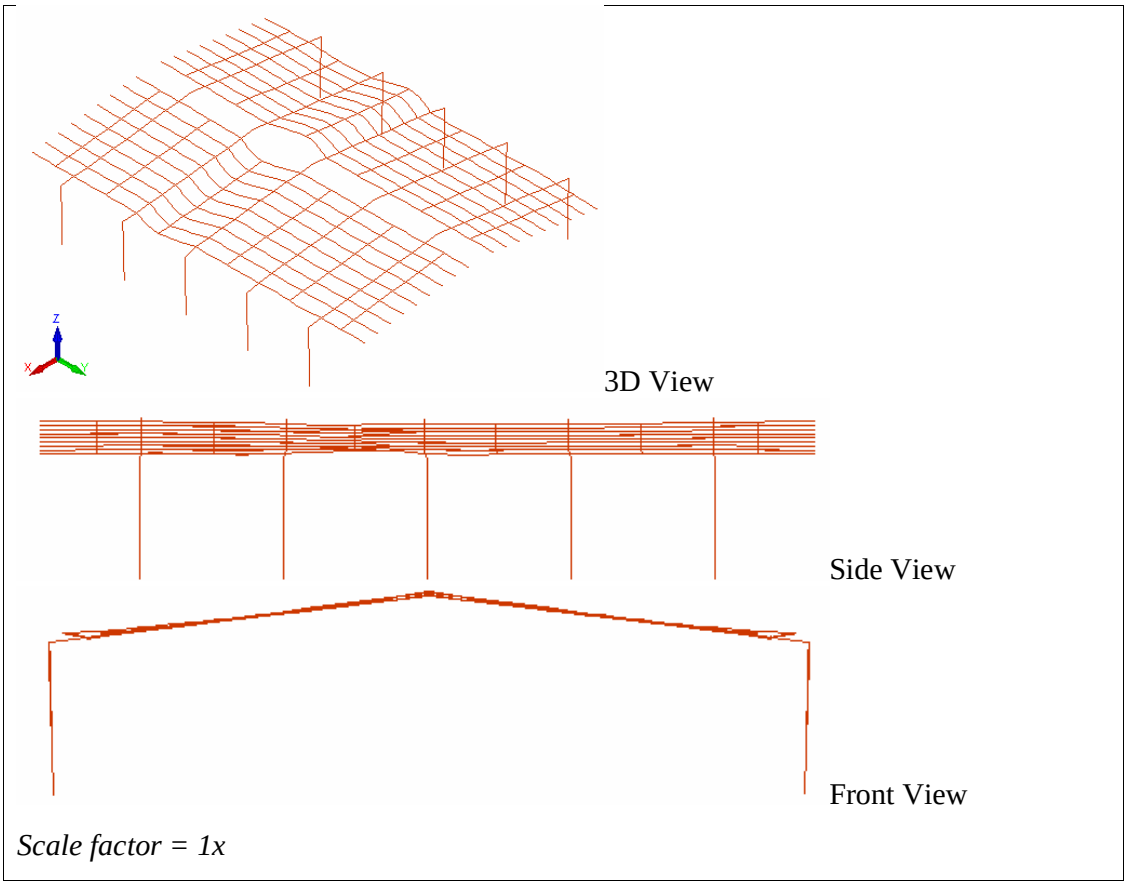

Figure 8-50 Final deflected shape from SAFIR (analysis (13))

Initially, the roof structure deforms upwards due to thermal expansion of the columns and the rafters. Since the time temperature curves of the ISO fire and the External fire coincide with each other for the first 7 minutes (Figure 8-46), out-of-plane local buckling of the pulins also occurs in the first 40 seconds of fire exposure. Similarly, the structure stabilises itself by concentrating the out-of-plane buckling in the purlins in bay 3. This deformed shape of the structure is observed throughout the duration of the simulation (60 minutes) and no sudden sag of the roof structure occurs during this period.

Figure 8-47 shows the vertical deflection at the apexes of all five frames. The upwards deformation of the roof structure peaks at approximately 10 minutes. The roof structure then deflects downwards due to the decreasing strength and stiffness of the steel members. The downwards deflections of the roof start to level off after 30 minutes, and frame 3 shows the largest vertical deflection of 0.15 m after one hour of External fire exposure to all the structural steel elements. The structure has reached a stable stage and collapse would not occur unless there is any temperature rise in the structural elements.

Figure 8-48 and Figure 8-49 show the horizontal deflection plots at the knees of the steel portal frames. The upwards deformation and sagging of the roof structure causes horizontal thrusts to the top of the steel columns, resulting in increasing outwards deflections for all the columns. The figures show that the outwards deflections start to level off after 30 minutes. The right knee of frame 5 shows the largest horizontal deflection of 0.17 m after 1 hour of External fire exposure. However, this is less than the maximum probable horizontal deflection of 0.52 m for a fixed support portal frame structure as stated in Section 8.3.2. Similarly, the displacement plots show that the deformations of the structure are less than those obtained using the ISO fire (Figure 8-47 to Figure 8-49 compared to Figure 8-13 to Figure 8-15).

In terms of outwards collapse of the concrete walls, the forces in the steel connections to the panels may still increase after the structure reaches a stable state due to the low conductivity of concrete material and the thermal bowing effects caused by the steep thermal gradient across the thickness. This is outside the scope of this research and will require a more sophisticated analytical model incorporating the thermal bowing

of the walls, the structural fire behaviour of the steel members and the steel connections in order to investigate this issue further. Future work on this will be mentioned in Chapter 9.

Results from Analysis (14):

Pinned support frames with purlin axial restraints imposed by the end walls, External fire without decay phase

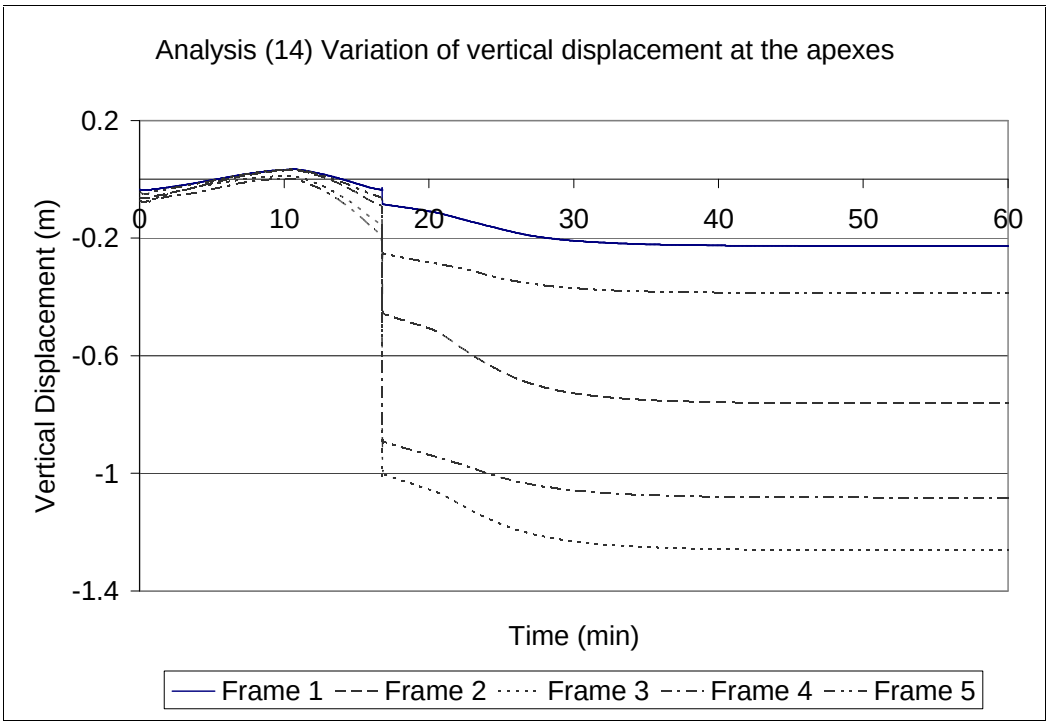

Figure 8-51 Variation of vertical displacement at the apexes in analysis (14)

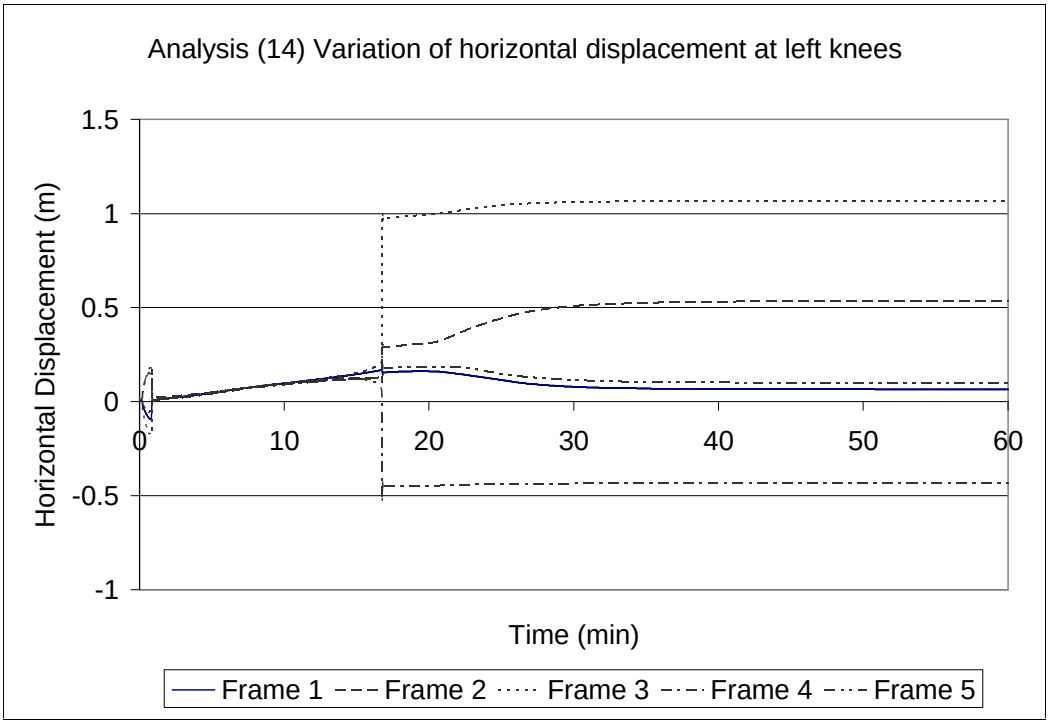

Figure 8-52 Variation of horizontal displacement at left knees in analysis (14)

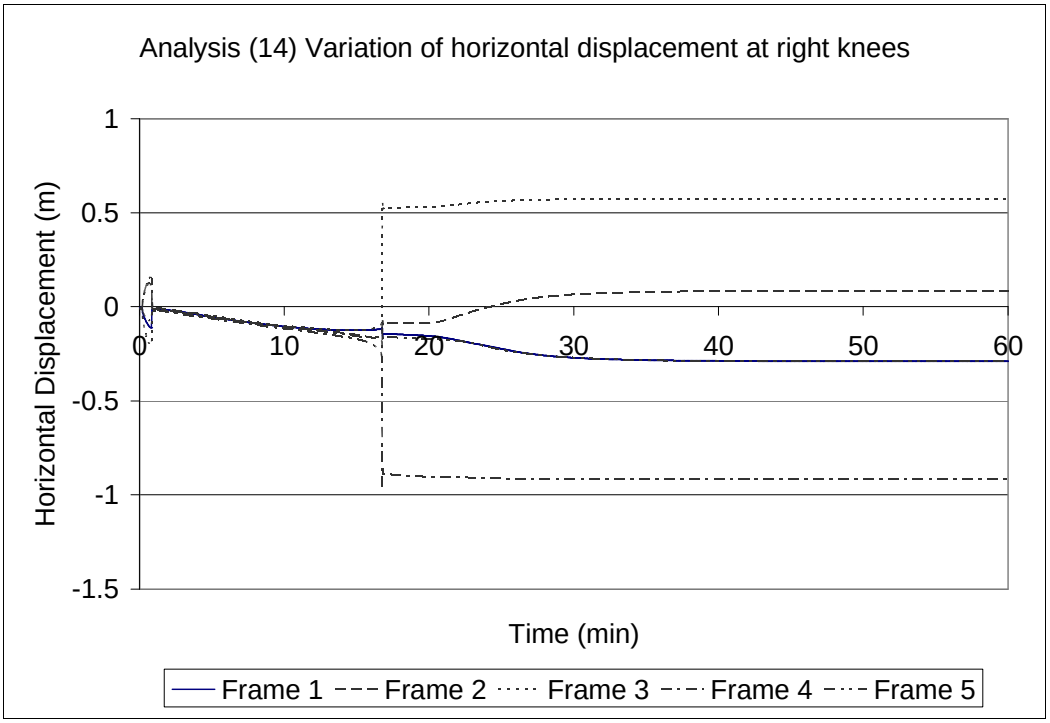

Figure 8-53 Variation of horizontal displacement at right knees in analysis (14)

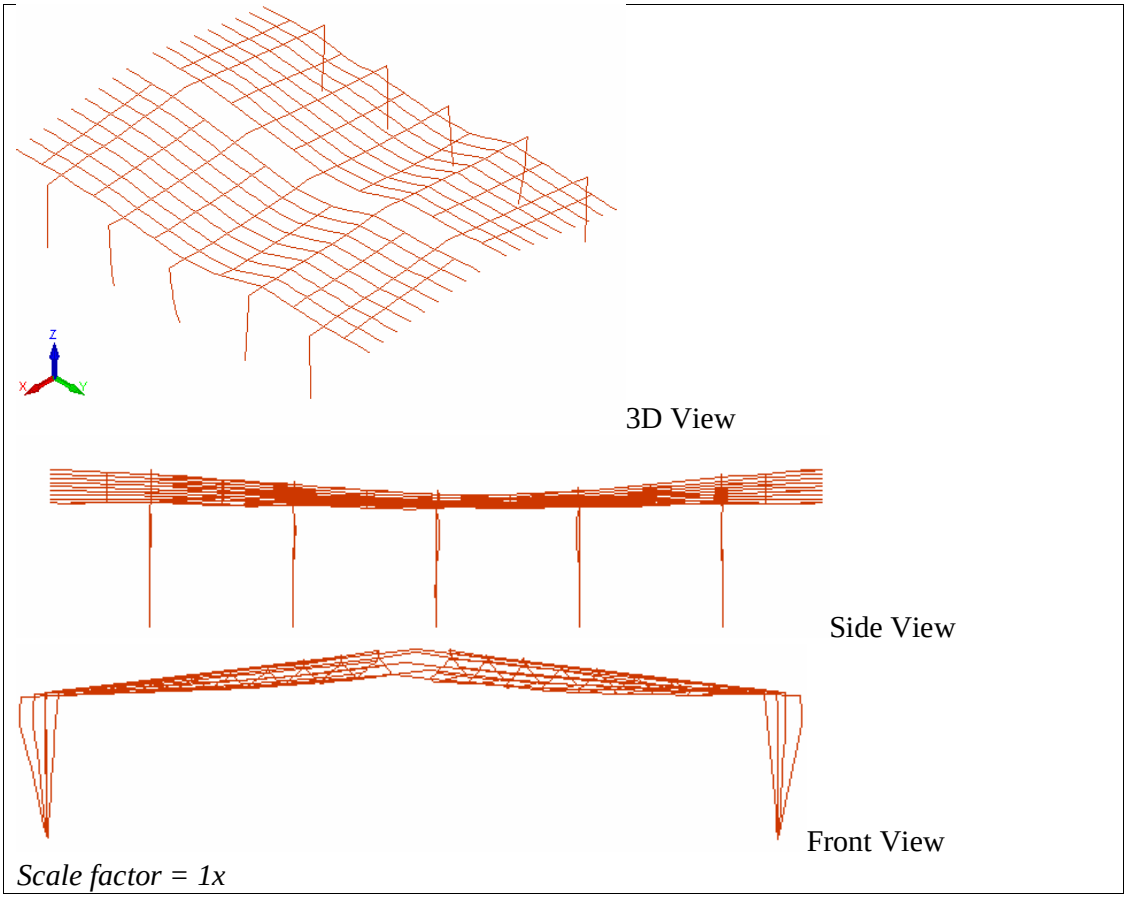

Figure 8-54 Final deflected shape from SAFIR (analysis (14))

The structural fire behaviour of the portal frame building is similar to the building which was exposed to an ISO fire (analysis (2) in Section 8.3). During the first 50 seconds, the steel frames sway sideways and the purlins buckle out-of-plane locally due to thermal expansion. After that, the whole structure stabilises itself by concentrating the out-of-plane deflection in the purlins in bay 4. This deformed shape is observed until approximately 17 minutes of fire exposure and the roof structure in the vicinity of bays 3 and 4 sags down rapidly and deform into a catenary. In the mean time, frames 3 and 4 also sway sideways in the opposite direction to each other. The roof structure continues to deform downwards and no further mechanisms such as rapid sagging of roof and sidesway of frames occur. The whole building reaches a steady state shortly after 30 minutes.

Figure 8-51 shows the vertical deflection at the apexes of the frames. Similarly, the upwards deformation peaks at 10 minutes and the roof deflects downwards due to the decreasing strength and stiffness of the frame. Frame 3 shows the largest downwards deflections of 1.3 m at the end of the simulation. This is considerable higher when compared to the fixed support portal frame structure (analysis (13)) and is due to the sidesway of the heated frame.

Figure 8-52 and Figure 8-53 show the horizontal deflection plots at the knees. Thermal expansion of the rafters causes all the columns to deflect outwards at a constant rate. The sway of frames at 17 minutes results in horizontal deflection of nearly 1.0 m at the top of the left column of frame 3 (refer to Figure 8-52). The horizontal deformation of the column continues to a small extent until the whole structure reaches its steady state at 30 minutes.

In general, the displacement plots show that the deformations of the structure are less than that obtained from similar analytical models carried out with the ISO fire (Figure 8-51 to Figure 8-53 compared to Figure 8-22 and Figure 8-24).

Results from Analysis (15):

Fixed support frames with purlin axial restraints imposed by the end walls, External fire with decay phase

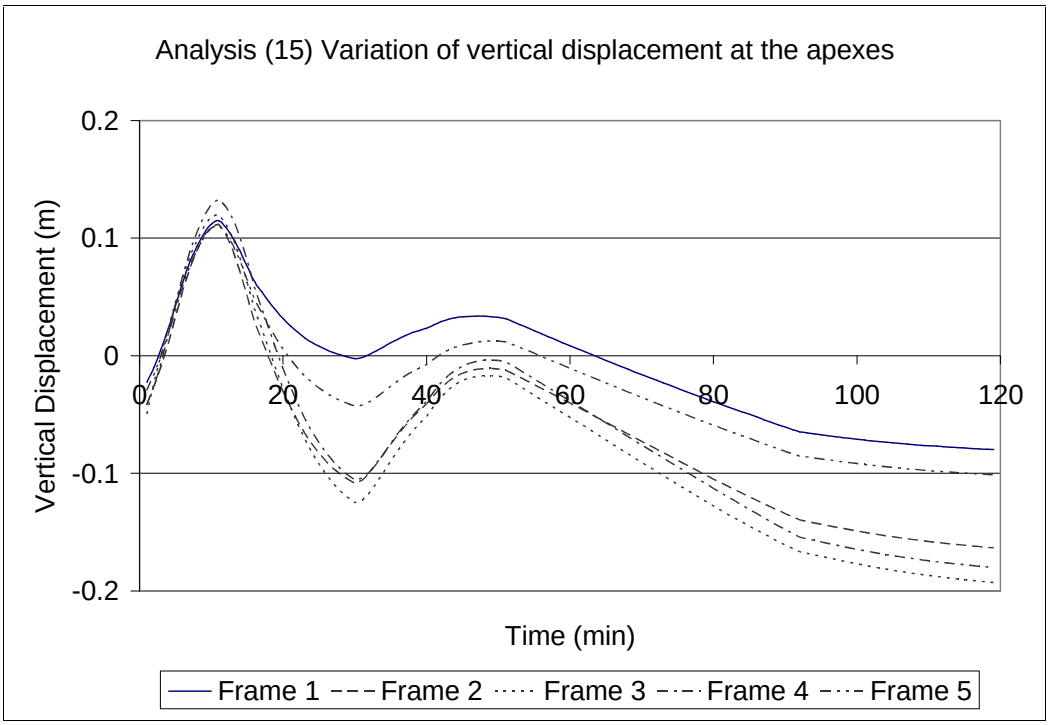

Figure 8-55 Variation of vertical displacement at the apexes in analysis (15)

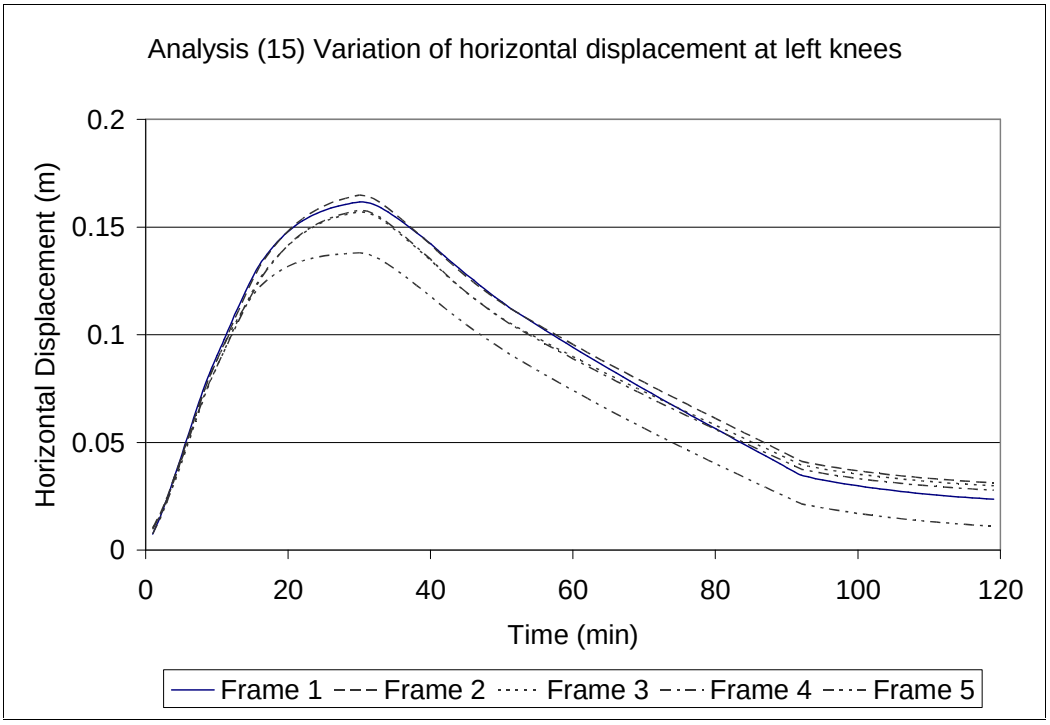

Figure 8-56 Variation of horizontal displacement at left knees in analysis (15)

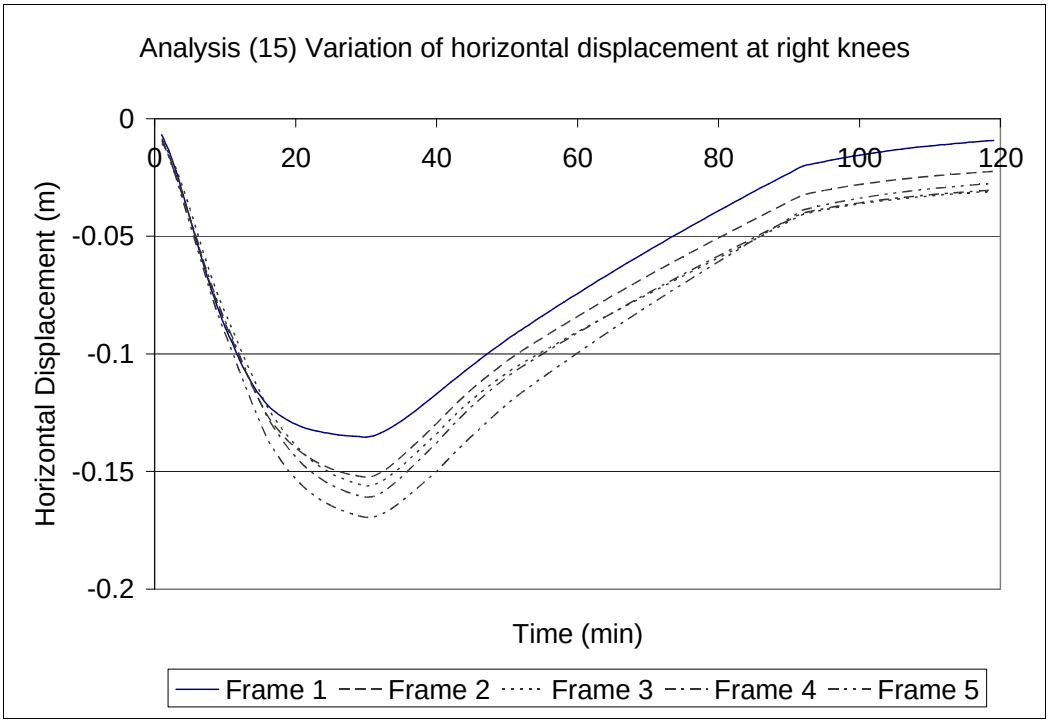

Figure 8-57 Variation of horizontal displacement at right knees in analysis (15)

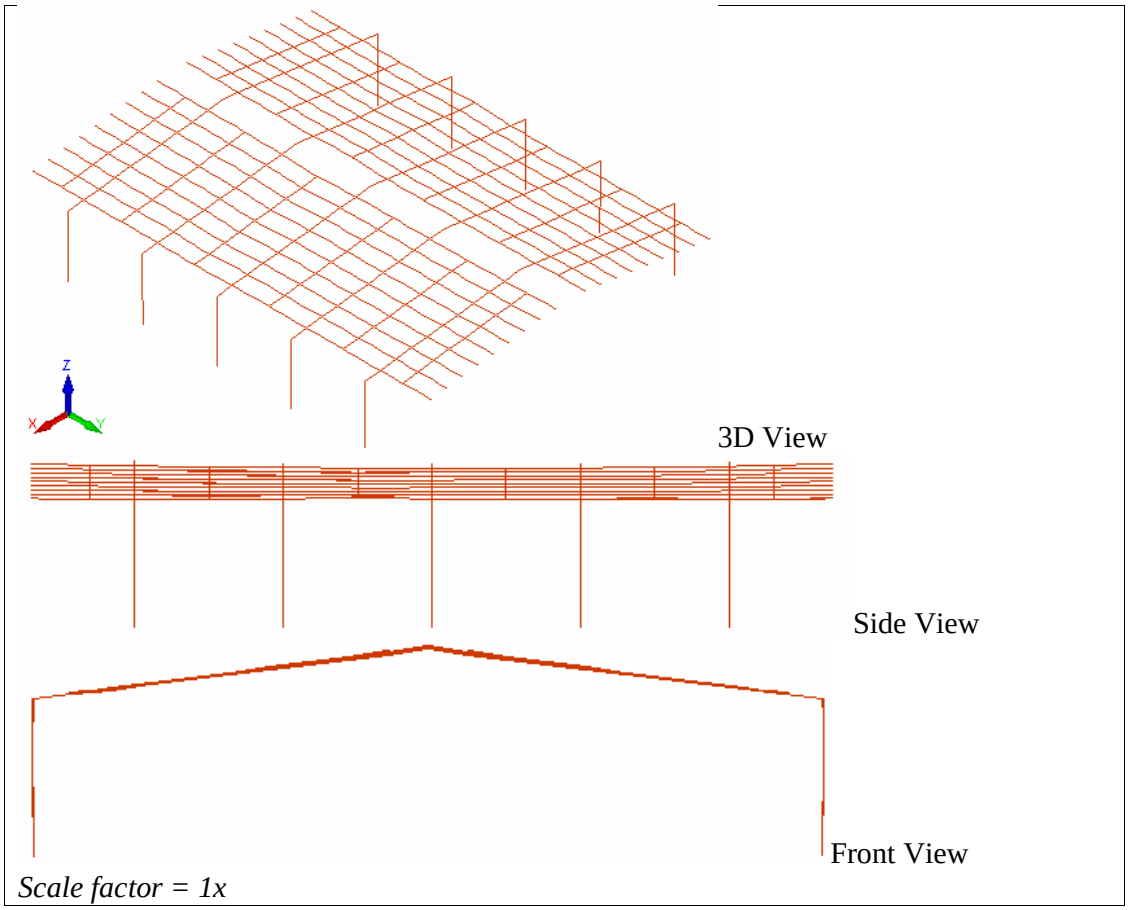

Figure 8-58 Final deflected shape from SAFIR (analysis (15))

In the early stages of the fire, the behaviour of the structure is similar to that observed in the structure which was exposed to the ISO fire (analysis (1)) and the External fire without a decay phase (analysis (13)). Local out-of-plane buckling concentrates in the purlins in bay 3 as the structure stabilises itself thus releasing the thermal strains built up in the early stages. As heating continues, the roof structure deforms upwards and then sags down before the decay phase. During the decay phase of the fire, the roof has been observed to deform in the similar pattern to that before the decay phase, in which it deforms upwards and reaches a second peak at 50 minutes, and deflects downwards again.

Figure 8-55 to Figure 8-57 show that all the frames have suffered minor permanent deformations at the end of the simulation. Interestingly, the columns have been observed to deform almost back towards their original positions after the onset of the decay phase (Figure 8-56 and Figure 8-57). This has an effect on the reduction of the forces in the steel connections due to lower P-delta effects from the self weight of the walls and is beneficial in terms of the outwards collapse of the concrete walls.

Results from Analysis (16):

Pinned support frames with purlin axial restraints imposed by the end walls, External fire with decay phase

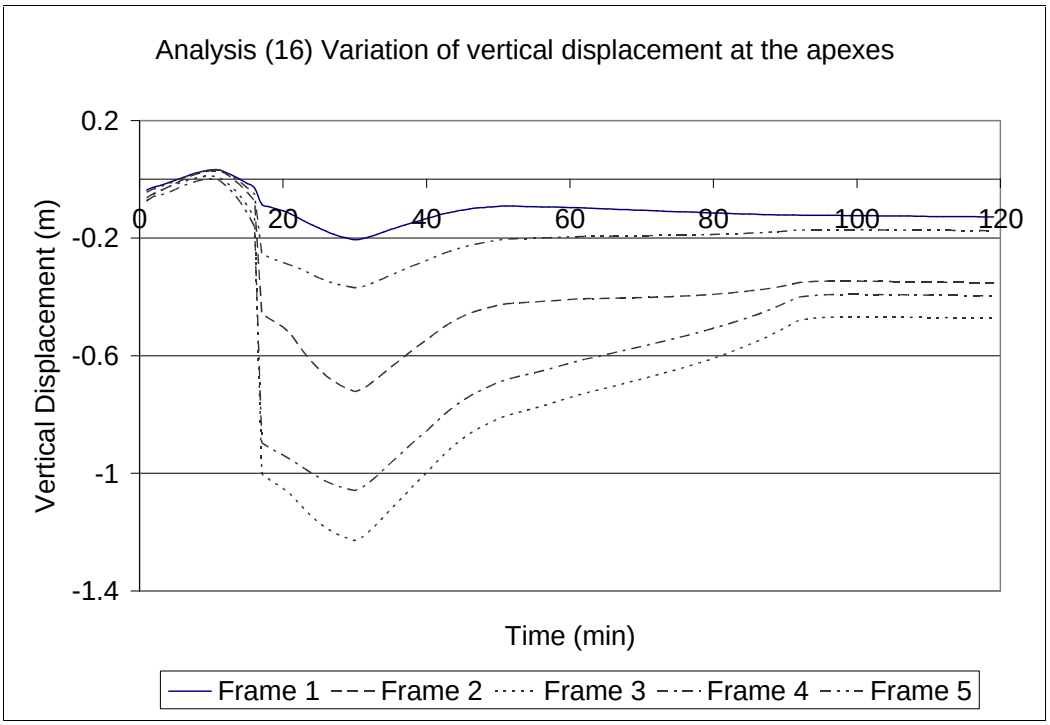

Figure 8-59 Variation of vertical displacement at the apexes in analysis (16)

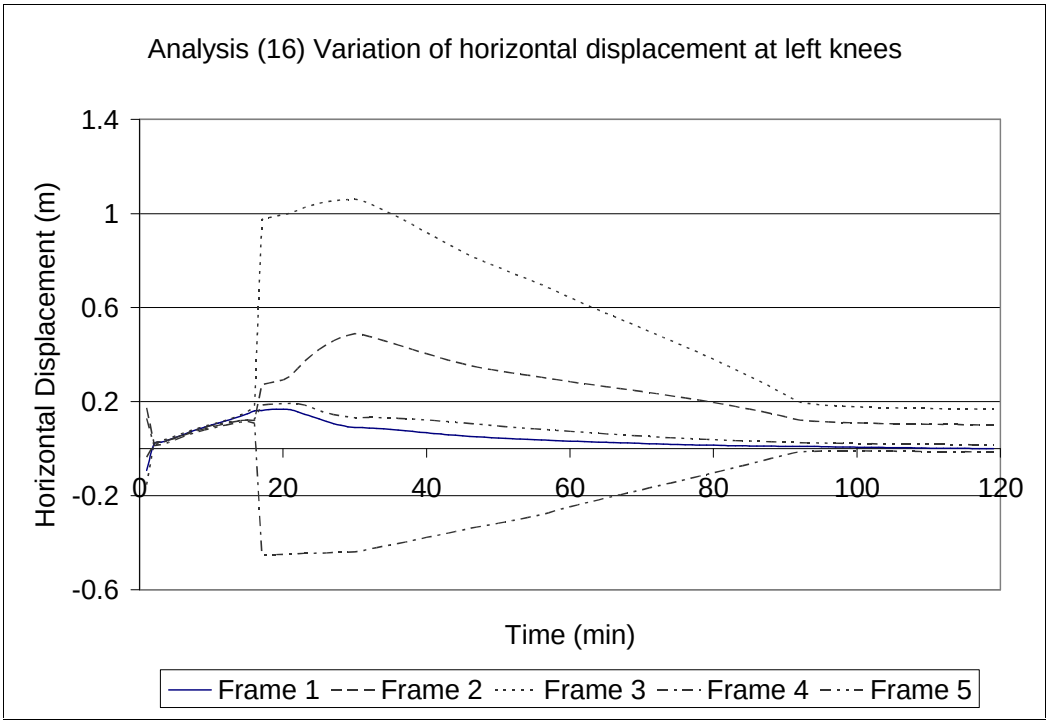

Figure 8-60 Variation of horizontal displacement at left knees in analysis (16)

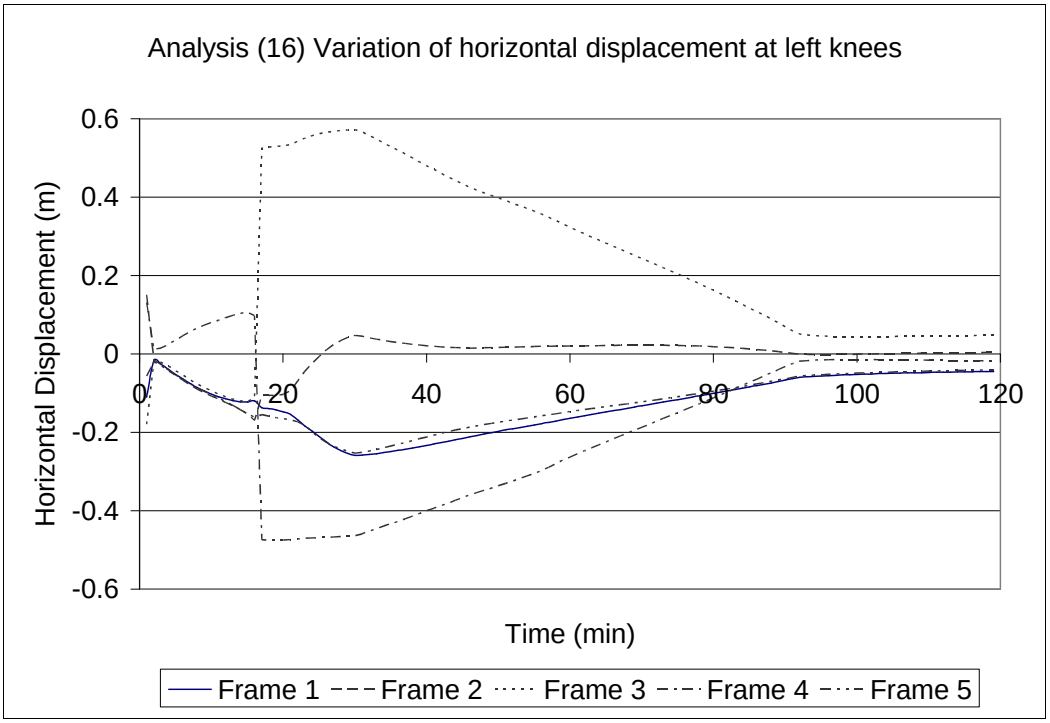

Figure 8-61 Variation of horizontal displacement at right knees in analysis (16)

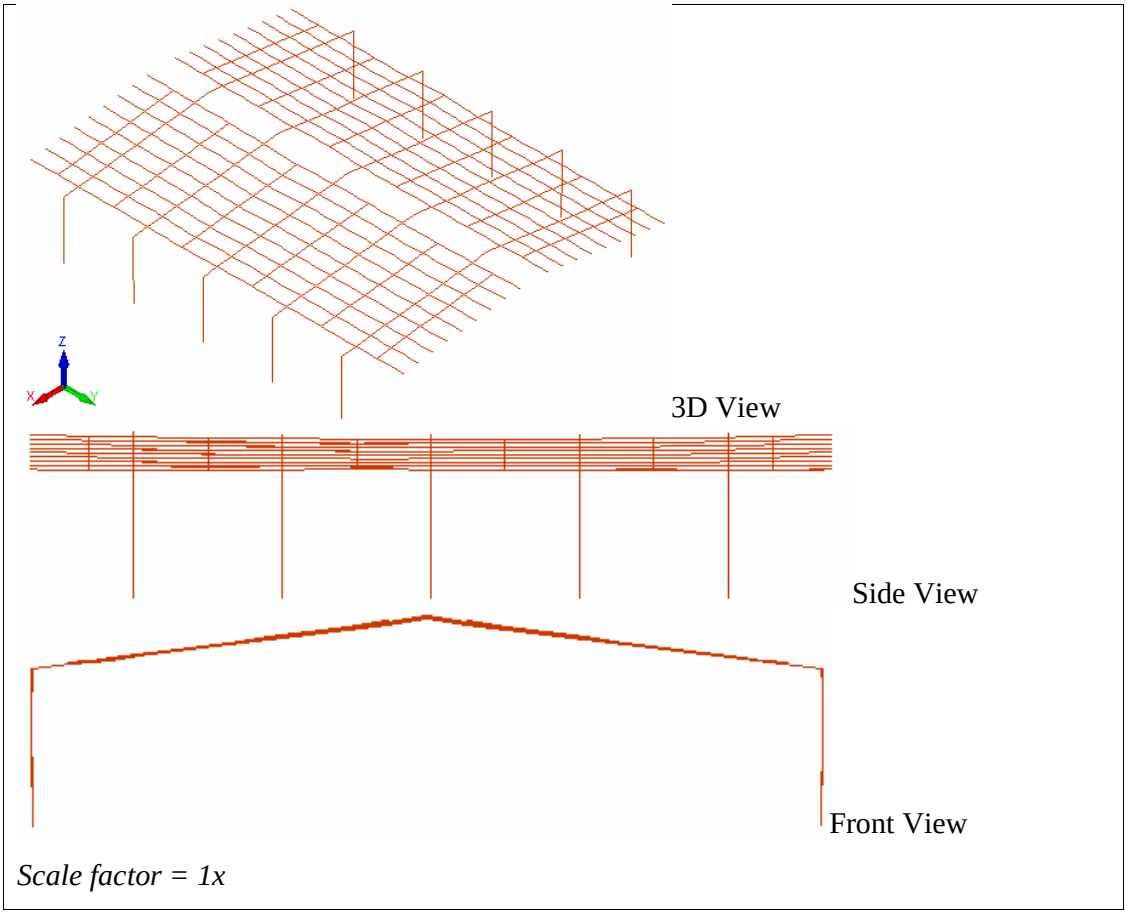

Figure 8-62 Final deflected shape from SAFIR (analysis (16))

During the early stages of the fire, the behaviour of the structure is similar to that observed in the structure which was exposed to the ISO fire (analysis (2)) and the External fire without decay phase (analysis (14)). The steel frames were observed to sway sideways and the purlins buckle in the first minute of the fire exposure. The structure stabilises itself by concentrating the out-of-plane buckling in the purlins in bay 4. Rapid sagging of the roof and sidesway of frames occur after 17 minutes of fire exposure and the roof structure is observed to deform into a catenary shape. The roof structure continues to deform downwards until 30 minutes when the fire reaches its decay phase. During the decay phase of the fire, the structure tries to deflect back towards its original form (Figure 8-62). However, the building suffers minor permanent deformations at the end (Figure 8-59 and Figure 8-61).

Results from Analysis (17):

Fixed support frames without purlin axial restraint imposed by the end walls, External fire without decay phase

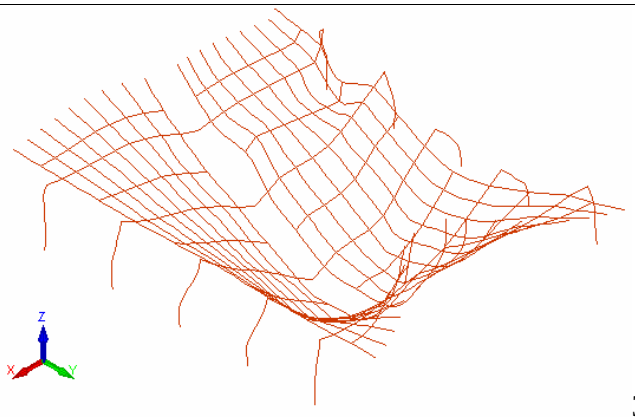

3D View

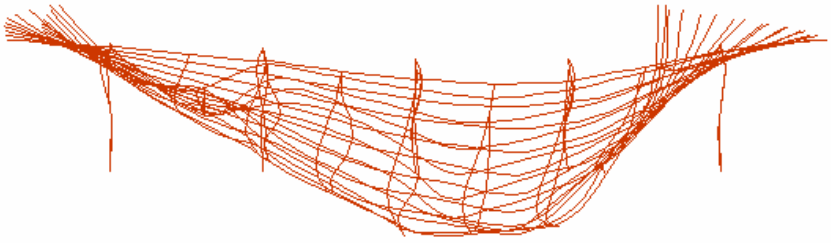

Side View

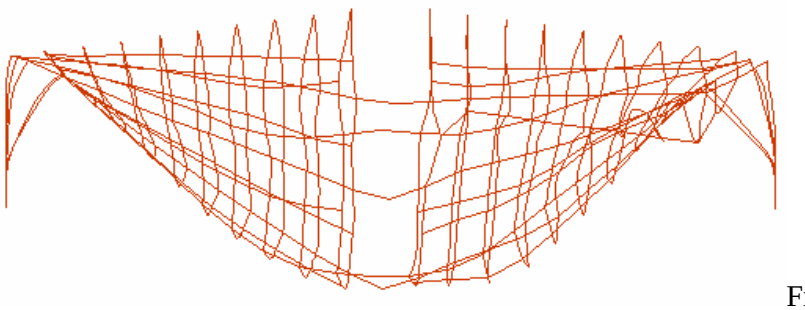

Front View

Scale factor = 1x

Figure 8-63 Final deflected shape at 26.9 minutes from SAFIR (analysis (17)

The fixed support steel portal frame structure exposed to the Eurocode External fire fails in the inwards collapse mode at 26.9 minutes. The collapse mode is similar to that obtained using the ISO fire but the collapse time is almost doubled (i.e. 26.9 minutes compared to 14.9 minutes obtained from using the ISO fire, refer to Table 8-3 – analysis (7)).

Results from Analysis (18):

Pinned support frames without puriln axial restraint imposed by the end walls, External fire without decay phase

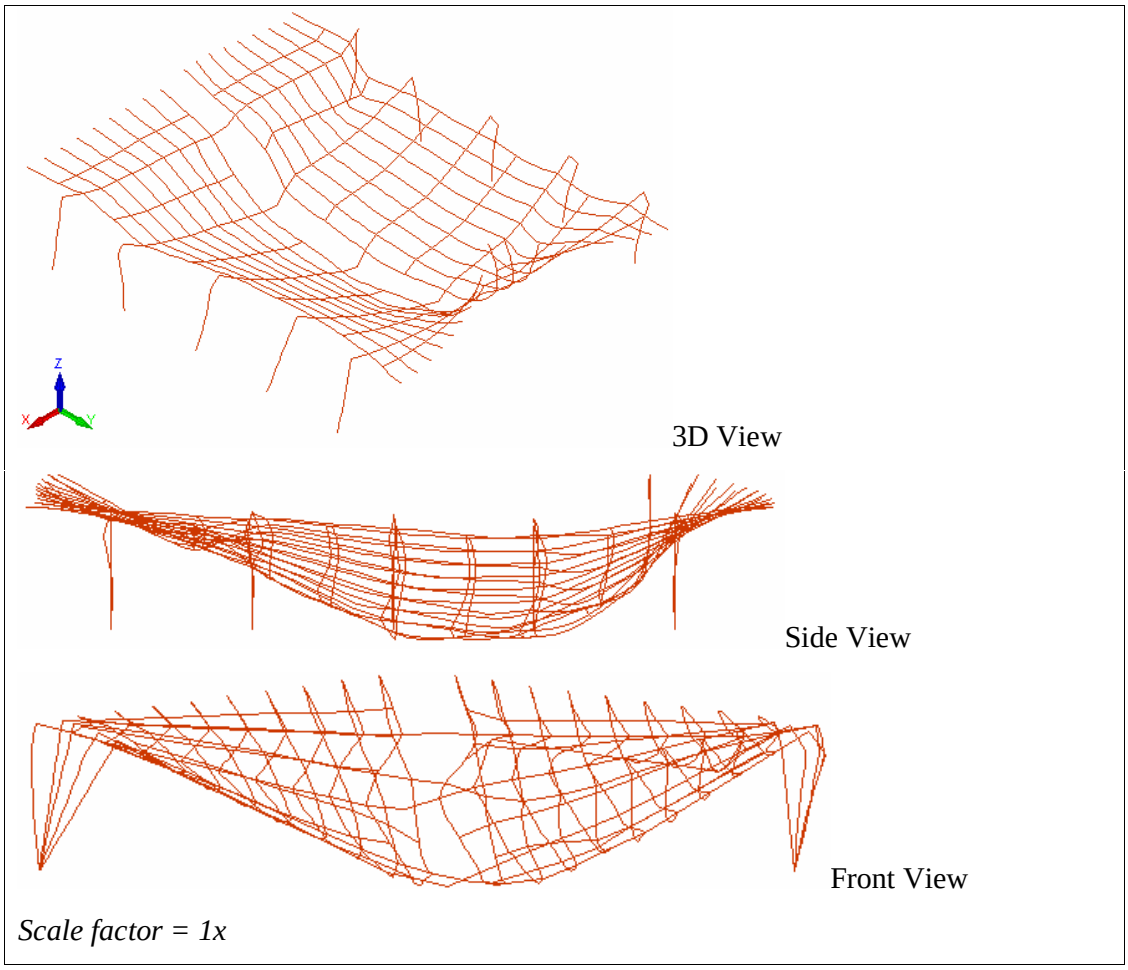

Figure 8-64 Final deflected shape at 18.4 minutes from SAFIR (analysis (18)

The pinned support steel portal frame structure exposed to the Eurocode External fire fails in the sidesways failure mode at 18.4 minutes. The collapse mode is similar to that obtained using the ISO fire but the collapse time is slightly increased (i.e. 18.4 minutes compared to 14.1 minutes obtained from using the ISO fire, refer to Table 8-3 – analysis (8)).

8.4.2 Discussion

The displacement trends for all the analyses during the first 10 minutes are similar for both fire curves. This is due to the same temperatures of the fire curves during that period as seen in Figure 8-46. In general, the deformations of the structure due to the External fire are smaller than in the ISO fire. This is because the temperatures in the External fire are lower than the ISO fire in the later stages of the fires. Therefore, the reduction of strength and stiffness of the structure exposed to the External fire is less.

No Decay Phase

Without the decay phase in fire, similar failure modes are obtained. With the presence of purlin axial restraints which are imposed by the end wall boundary conditions, the roof structure deforms into a catenary for the fixed support portal frame structure, whereas the frames sway sideways excessively for the pinned support portal frame structure. The structure has also been observed to reach a steady state some time in the later stages of the fire. Without the purlin axial restraint from the end wall boundary conditions, the frames either collapse inwards for the fixed support portal frame structure or sway excessively before collapsing into the building for the pinned support portal frame structure. The latter mode of failure (sidesways failure mode) is considered unacceptable according to the building codes. As expected, the analytical models without purlin axial restraint and decay phase show complete collapse of the structure later when compared to the similar models performed with the ISO fire.

With Decay Phase

The introduction of the decay phase to the External fire results in regaining of strength and stiffness of the structure. The structure has been observed to deflect back towards its original form and sustain a small level of permanent set at the end of the simulation. The permanent set is due to the irrecoverable plastic deformation (yielding) of the steel material. The decay phase is beneficial in terms of the steel connections to the panels because the rebound of the deformations will reduce the forces in these connections due to smaller P-delta effects from the self weight the walls. However, the forces may still increase due to the continuing thermal bowing of the walls after the decay phase and this has not been investigated here and is outside the scope of the project.

8.5 Out-of-plane Restraints to Columns

As mentioned in Section 8.2, the connections to the side walls may fail at high temperatures and the columns may deform excessively about the minor axis (i.e. weak axis). Similarly, providing out-of-plane restraints along the length of the columns to prevent out-of-plane deformations may alter the fire performance of the structure. Figure 8-65 and Figure 8-66 show the column boundary conditions without any out-of-plane restraint and with full out-of-plane restraints to the columns, respectively, in replacement of the out-of-plane restraints imposed at the top and mid-height of the columns to simulate the effects from the side walls panels as shown in Figure 8-5. These two scenarios serve as the extreme cases in terms of wall stiffness and connections to the columns and are investigated in this section. Out-of-plane restraints were previously provided at the top and mid-height of the columns and were fixed in space, meaning that they were not movable throughout the duration of the simulation and this applies to the analyses with full out-of-plane column restraints. The analyses in this section are tabulated in Table 8-6 and the whole building is exposed to the fire.

Table 8-6 Fire analyses in Section 8.5 – Out-of-plane Restraints to Columns

Analysis number	Description of the out-of-plane restraint	Support conditions	Purlin Axial Restraints
(19) & (23)	No out-of-plane restraint	Fixed	Yes & No
(20) & (24)		Pinned	Yes & No
(21) & (25)	Full out-of-plane restraints	Fixed	Yes & No
(22) & (26)		Pinned	Yes & No

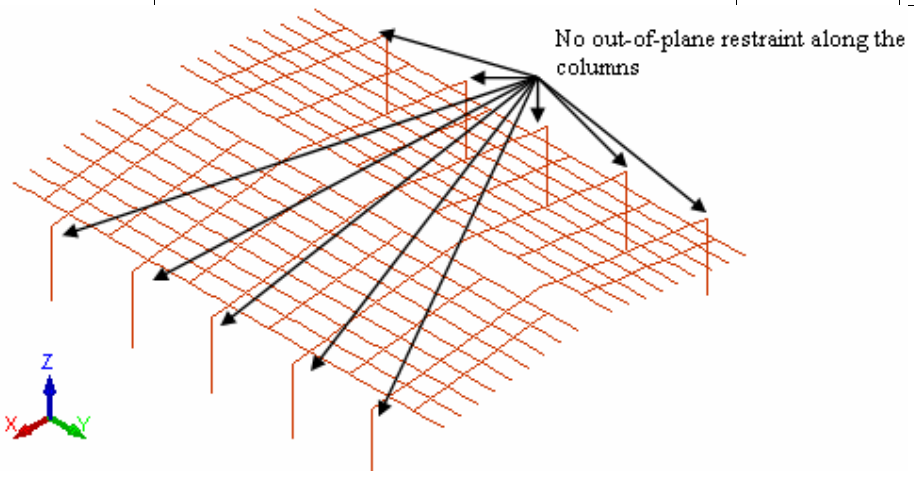

Figure 8-65 No out-of-plane restraint provided to the columns

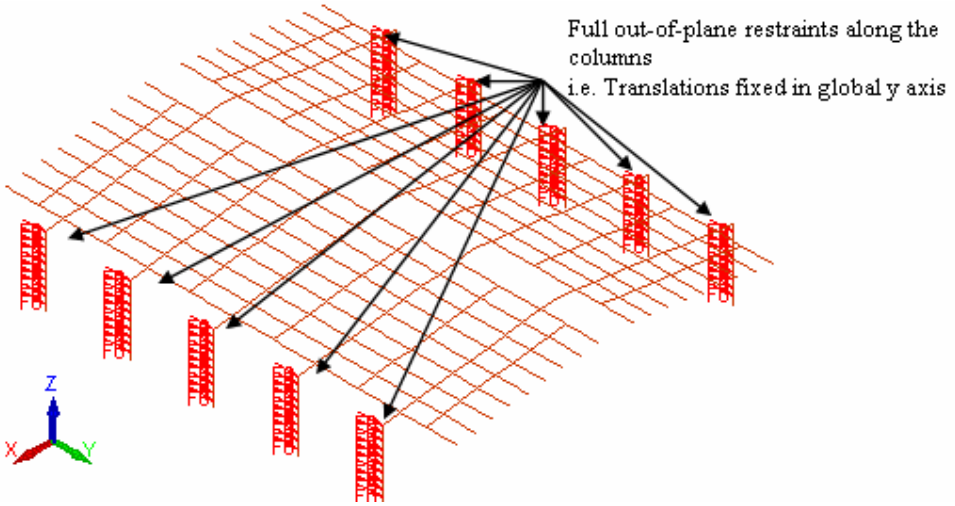

Figure 8-66 Full out-of-plane restraints along the length of the columns

8.5.1 Results of Analyses

The results of the analyses are summarised in Table 8-7.

Table 8-7 Results of analyses in Section 8.5 – Out-of-plane Restraints to Columns

Analysis number	Description of the out-of-plane restraint	Support conditions	Purlin Axial Restraints	Mode of Failure	Simulation End Time* (minutes)
(19)	No out-of-plane restraint	Fixed	Yes	Catenary	15.8
(20)		Pinned	Yes	Sway	13.3
(21)	Full out-of-plane restraints	Fixed	Yes	Catenary	17.1
(22)		Pinned	Yes	Sway	15.2
(23)	No out-of-plane restraint	Fixed	No	Weak-axis	11.3
(24)		Pinned	No	Weak-axis	0.2
(25)	Full out-of-plane restraints	Fixed	No	Inwards	14.9
(26)		Pinned	No	Sway	14.9

**Note: The simulation end times were obtained when SAFIR was unable to converge to a solution.*

With Purlin Axial Restraints

The analyses with purlin axial restraints imposed by the end walls (analyses (19) to (22)) show similar failure modes to those found with out-of-plane restraints provided at top and mid-height of columns. For frames fixed at the base, the deformation is approximately vertical and the roof structure deforms into a catenary (i.e. catenary mode of failure); for frames pinned at the base, they sway sideways when the roof starts to deform into a catenary shape (i.e. sway mode of failure).

The main discrepancy is the deformation or buckling about the weak axis of the columns. With no out-of-plane column restraint (analyses (19) and (20)), the columns deform about the weak axis along the length in the later stages of the fire and are more significant when the roof deforms into a catenary (Figure 8-67 and Figure 8-68). For the analyses with full out-of-plane column restraints (analyses (21) and (22)), no deformation about the minor axis of the steel columns occurs and this is expected due to the full restraints provided (Figure 8-69 and Figure 8-70).

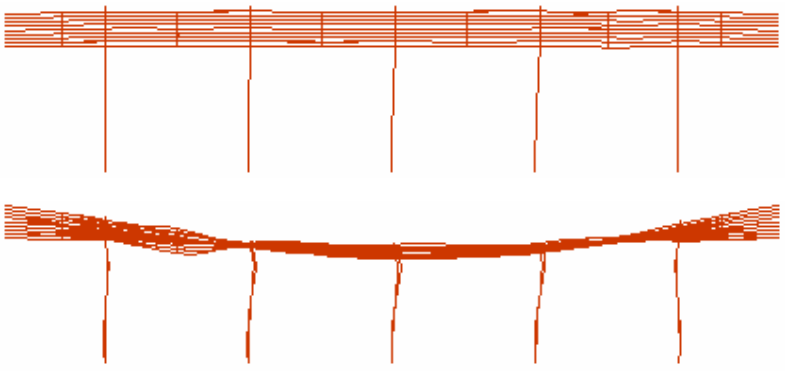

Figure 8-67 Deformation about the weak axis of the steel columns at 10 and 15.8 (final time step) minutes in analysis (19) – Fix-fix supported frames with no out-of-plane column restraint (Scale = 1x)

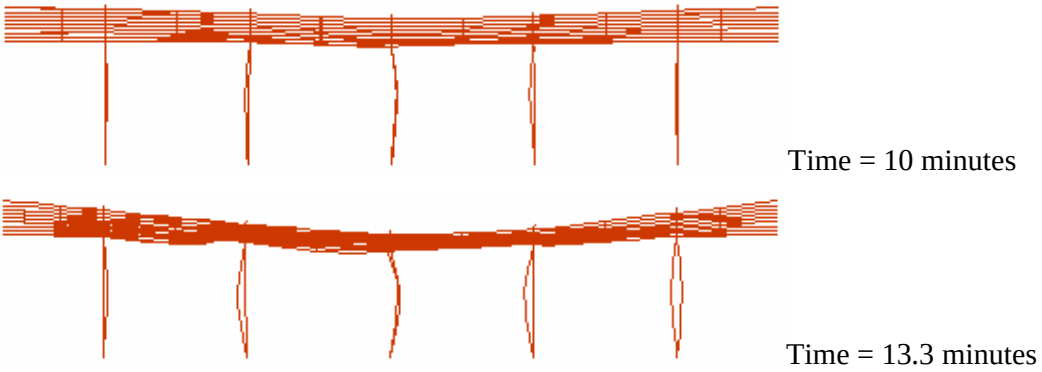

Figure 8-68 Deformation about the weak axis of the steel columns at 10 and 13.3 (final time step) minutes in analysis (20) – Pin-pin supported frames with no out-of-plane column restraint (Scale = 1x)

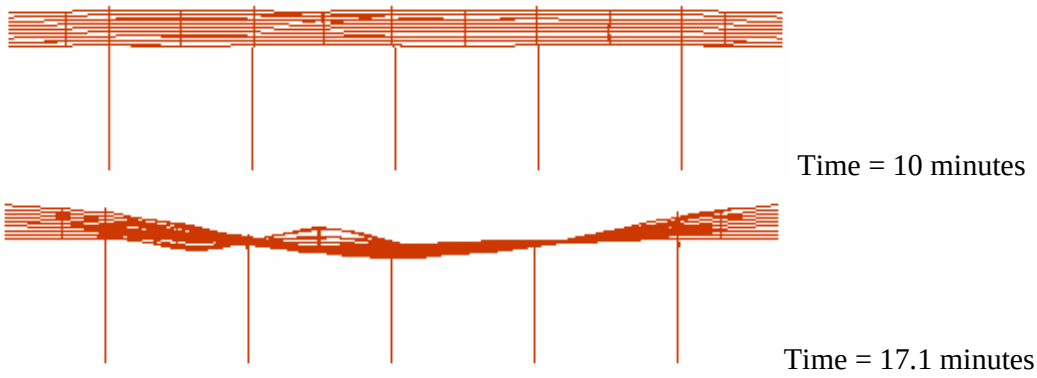

Figure 8-69 No deformation about the weak axis of the steel columns throughout the simulation in analysis (21) – Fix-fix supported frames with full out-of-plane column restraints (Scale = 1x)

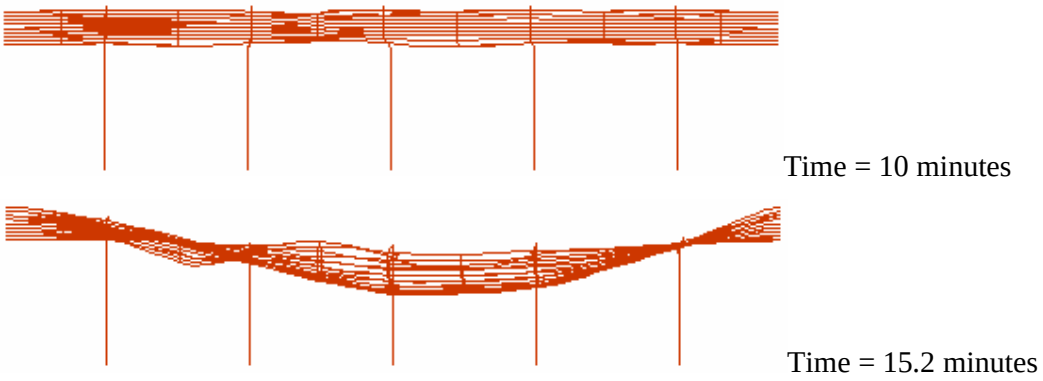

Figure 8-70 No deformation about the weak axis of the steel columns throughout the simulation in analysis (22) – Pin-pin supported frames with full out-of-plane column restraints (Scale = 1x)

Without Purlin Axial Restraint

The analyses without purlin axial restraint from the end wall boundary conditions and out-of-plane column restraint (analyses (23) and (24)) show that the steel portal frame structure fails in the weak-direction of the frame and the frames collapse towards the end walls. The portal frame structure with fixed supports (analyses (23)) does not show any distinct deformations during the first 10 minutes of the fire (Figure 8-71 (a)). After that, it fails in the weak direction when the roof collapses at 11.2 minutes (Figure 8-71 (b) and (c)). The portal frame structure with pinned supports (analysis (24)) is very unstable because there is no longitudinal stiffness provided to resist the deformations in the weak direction and the structure collapses during the first 13 seconds of the fire (Figure 8-72).

With the provision of full out-of-plane restraints to the columns (analyses (25) and (26)), the collapse modes are similar to the analyses without any purlin axial restraint imposed by the end walls and with the common out-of-plane restraints provided at the top and mid-height of the columns (Figure 8-73 and Figure 8-74). In addition, the collapse times of the structure with full out-of-plane column restraints (analysis (25) and (26)) are very close to the similar analyses with the common out-of-plane column restraints (analysis (7) and (8)), all of which fail between 14 and 15 minutes. This means that the provision of full out-of-plane restraints to the columns will not improve the fire resistance of the structure.

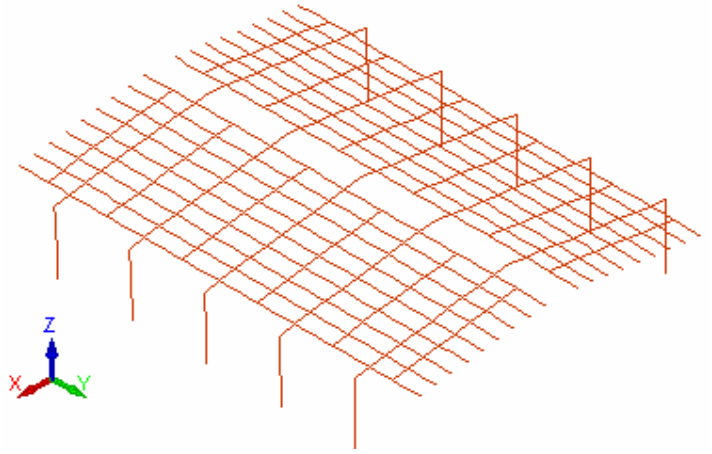

(a) Time = 10 minutes

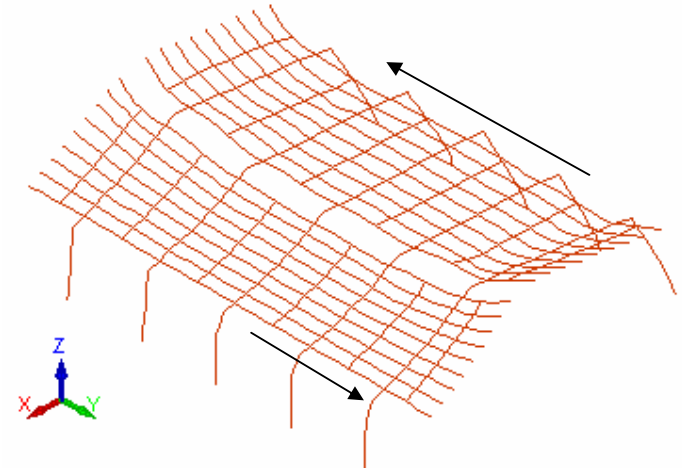

(b) Time = 11.2 minutes

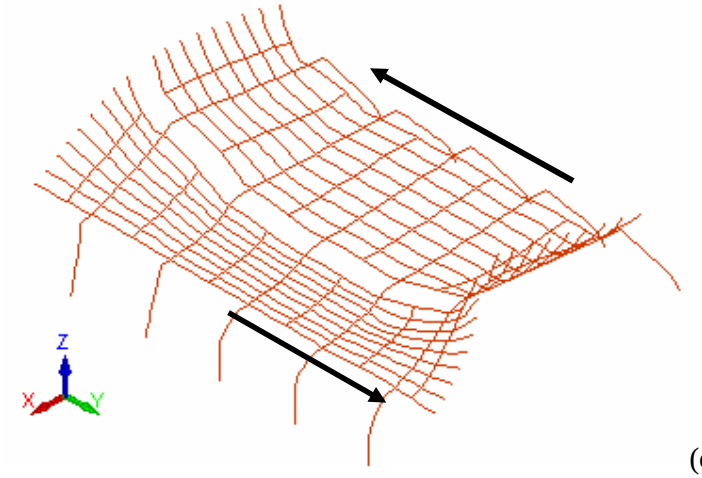

(c) Time = 11.3 minutes

Scale factor = 1x

Figure 8-71 Collapse of fix-fix supported steel portal frame structure in the weak direction of the frame (analysis (23) – Fix–Fix supported frames with no out-of-plane column and purlin axial restraints)

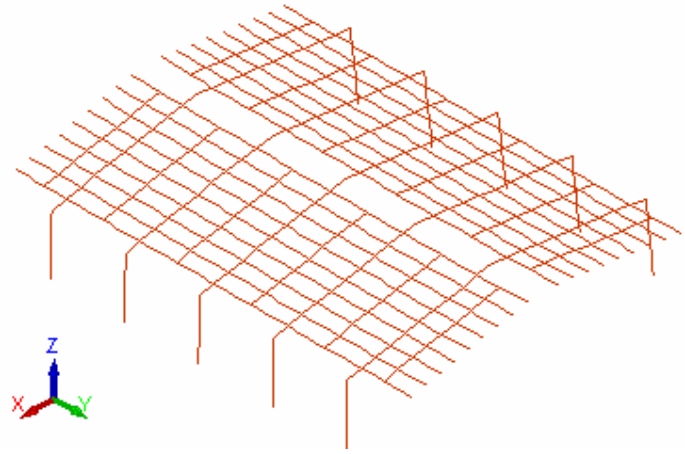

(a) Time = 10 seconds

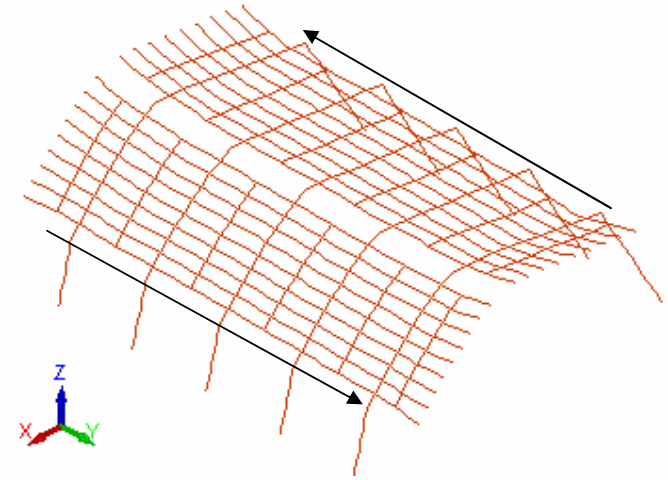

(b) Time = 12 seconds

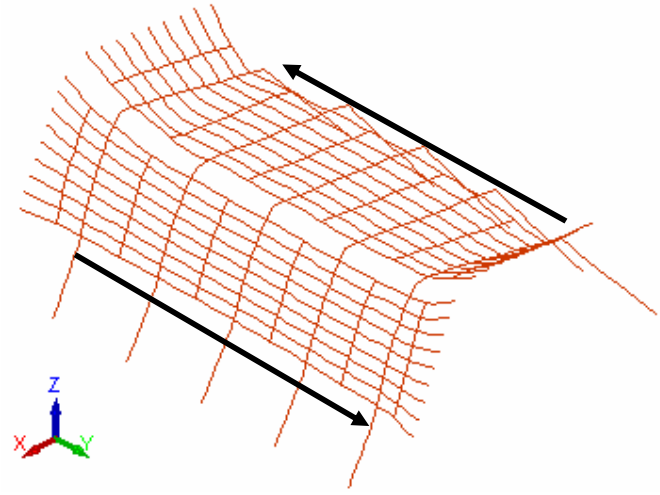

(c) Time = 13 seconds

Scale factor = 1x

Figure 8-72 Collapse of pin-pin supported steel portal frame structure in the weak direction of the frame (analysis (24) – Pin–Pin supported frames with no out-of-plane column and purlin axial restraints)

Results from Analysis (25):

Fixed support frames without purlin axial restraint imposed by the end walls, full out-of-plane restraints along the columns

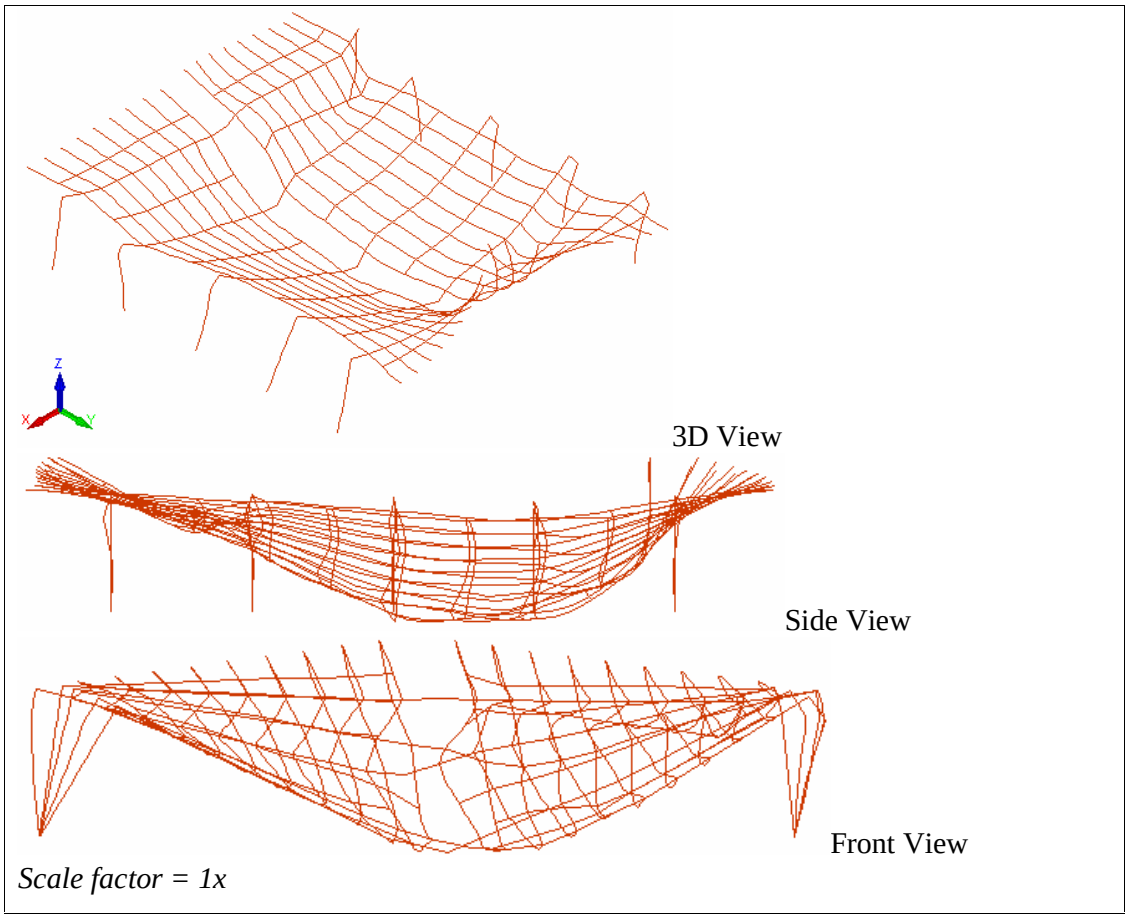

Figure 8-73 Final deflected shape at 14.9 minutes from SAFIR (analysis (25))

Results from Analysis (26):

Pinned support frames without purlin axial restraint imposed by the end walls, full out-of-plane restraints along the columns

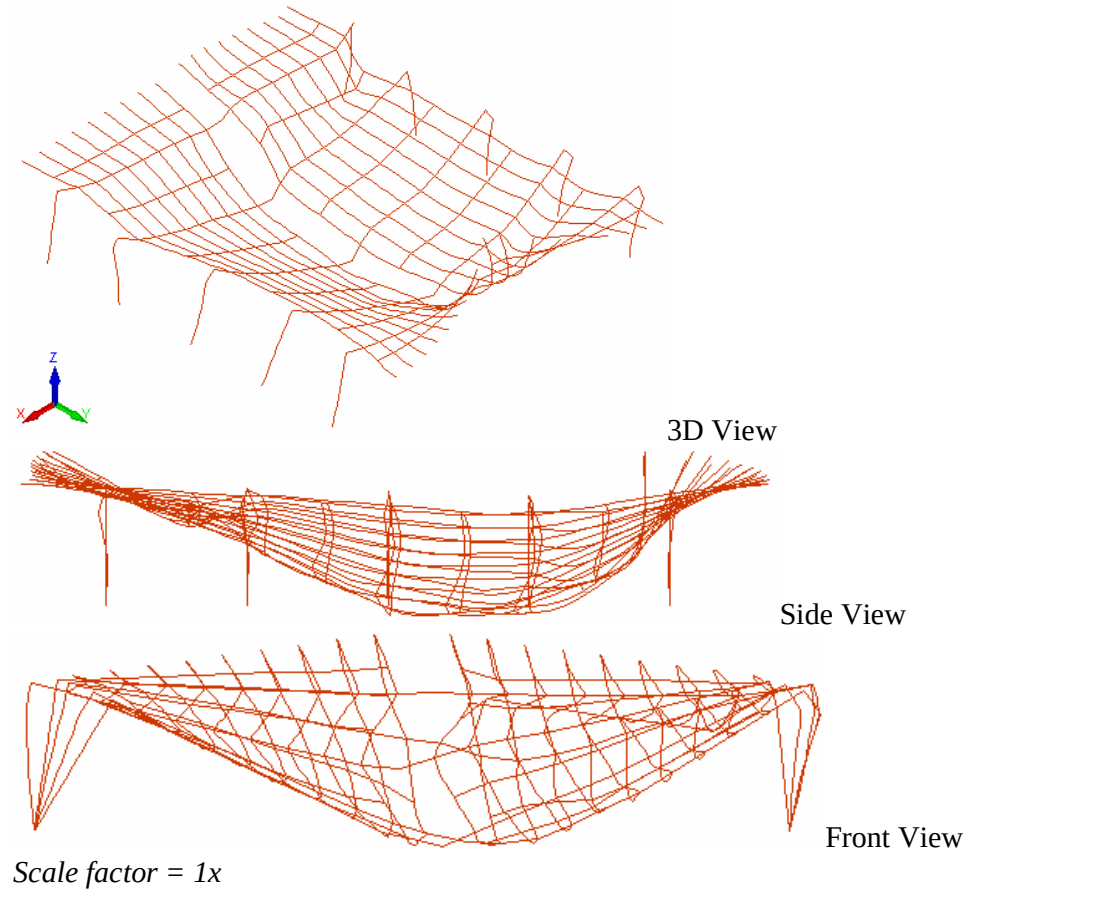

Figure 8-74 Final deflected shape at 14.9 minutes from SAFIR (analysis (26))

8.5.2 Discussion

The analyses with different levels of out-of-plane restraint to the columns have again shown that a steel portal frame structure with fixed support conditions at the base will perform in the acceptable manner whereas a steel portal frame structure with ideally pinned support conditions will fail in a sidesway mode which is not acceptable. In addition, providing full out-of-plane restraints to the columns will not improve the fire resistance of the structure. The analyses with no purlin axial and out-of-plane column restraints show that the structure collapses in the weak direction of the frames. This type of collapse mode is not likely happen in real fires as steel portal frame structures will always have some stiffness in the longitudinal direction to resist wind and earthquake loads in the longitudinal direction

8.6 Passive Fire Protection to Columns

In practice, it is common to fire protect all or part of the steel portal frame column legs with concrete encasement to provide additional fire resistance. However, concrete encasement may fall off when exposed to very high temperatures (Figure 4-67) or when the steel portal frame deforms excessively. In addition, when the concrete panels are trying to bow away from the supporting structures as they are exposed high temperatures on one side, the forces developed in the connections between the steel frames and the attached concrete panels will be larger due to the higher strength and stiffness of the protected steel columns (refer to Section 4.6). If these connections fail, the walls could collapse outwards and cause spread of fire to adjacent property or threaten the lives of fire-fighters standing close to the building. The advantage of providing this additional fire protection is questionable for many designers.

In this section, analytical models with steel columns protected with cast *in-situ* concrete to either full (Figure 8-75) or two-thirds (Figure 8-76) of the height are analysed. The analyses with columns fully encased in concrete serves as the upper bound in terms of concrete protection to the column legs. The analyses assume that the building is fully involved in the fire and the ISO fire curve is used in the thermal analysis.

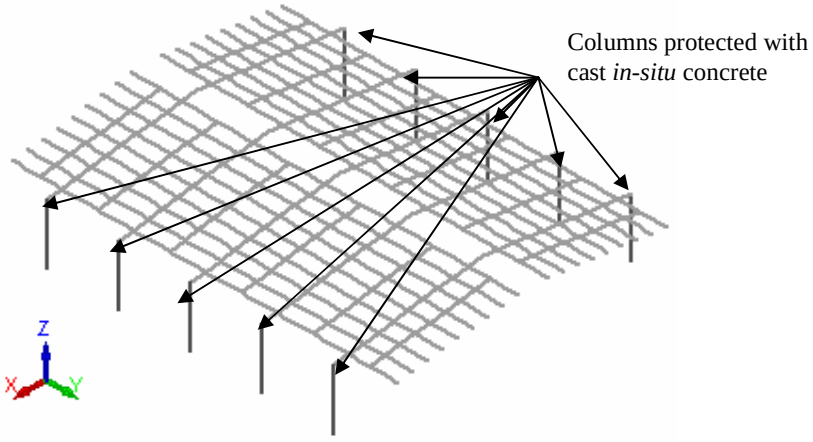

Figure 8-75 Steel columns protected with cast *in-situ* concrete

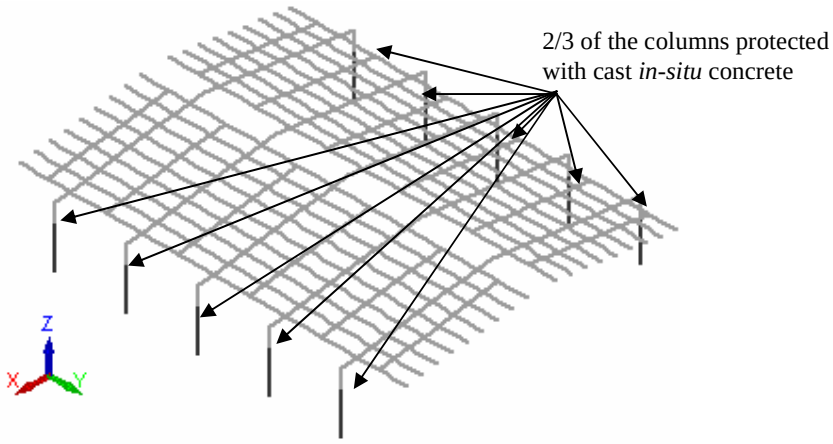

Figure 8-76 Steel columns protected with cast *in-situ* concrete to two-thirds of the full height

The cross-section of the steel column encased in concrete is shown in Figure 8-77 (a) and the discretisation of the section in SAFIR is shown in Figure 8-77 (b). Figure 8-78 shows the thermal boundaries of the concrete encased section and it is assumed that the boundary attached to the precast wall panels is not thermally exposed to the ISO fire curve. Two concrete models are available in SAFIR, and they are siliceous and calcareous concrete models. The siliceous concrete model is used in both thermal and structural analysis in SAFIR as siliceous concrete is commonly used in the construction of concrete structures in New Zealand.

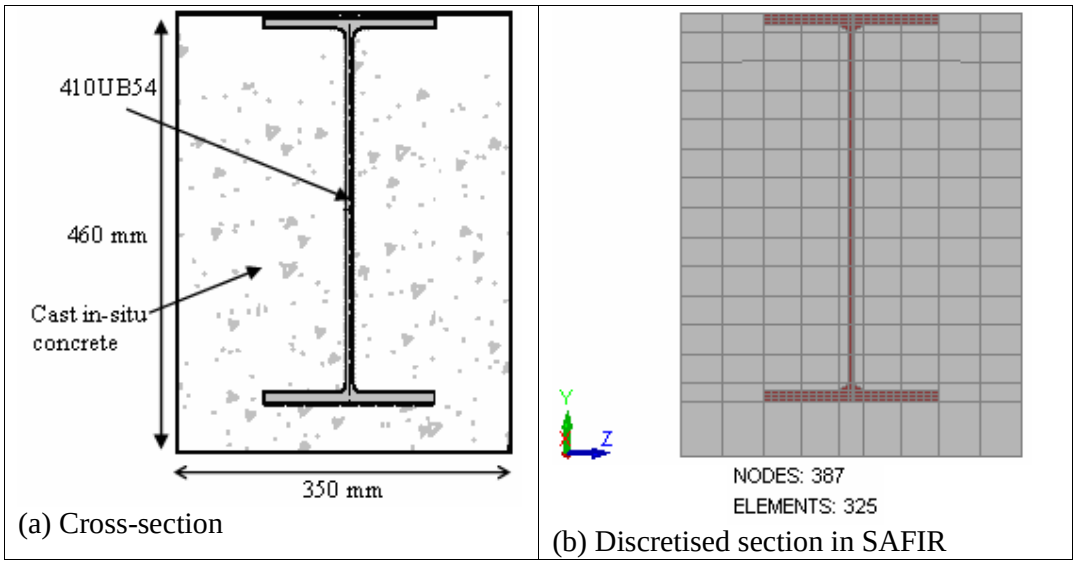

Figure 8-77 Cross-section and discretisation of steel columns encased in concrete

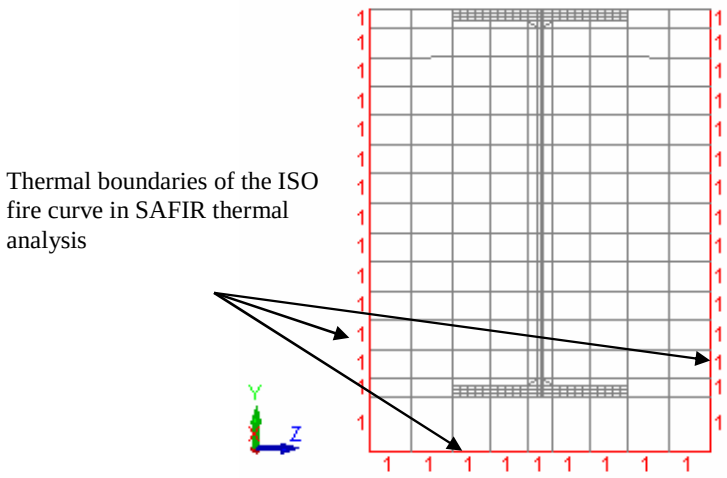

Figure 8-78 Thermal boundaries of the concrete encased section

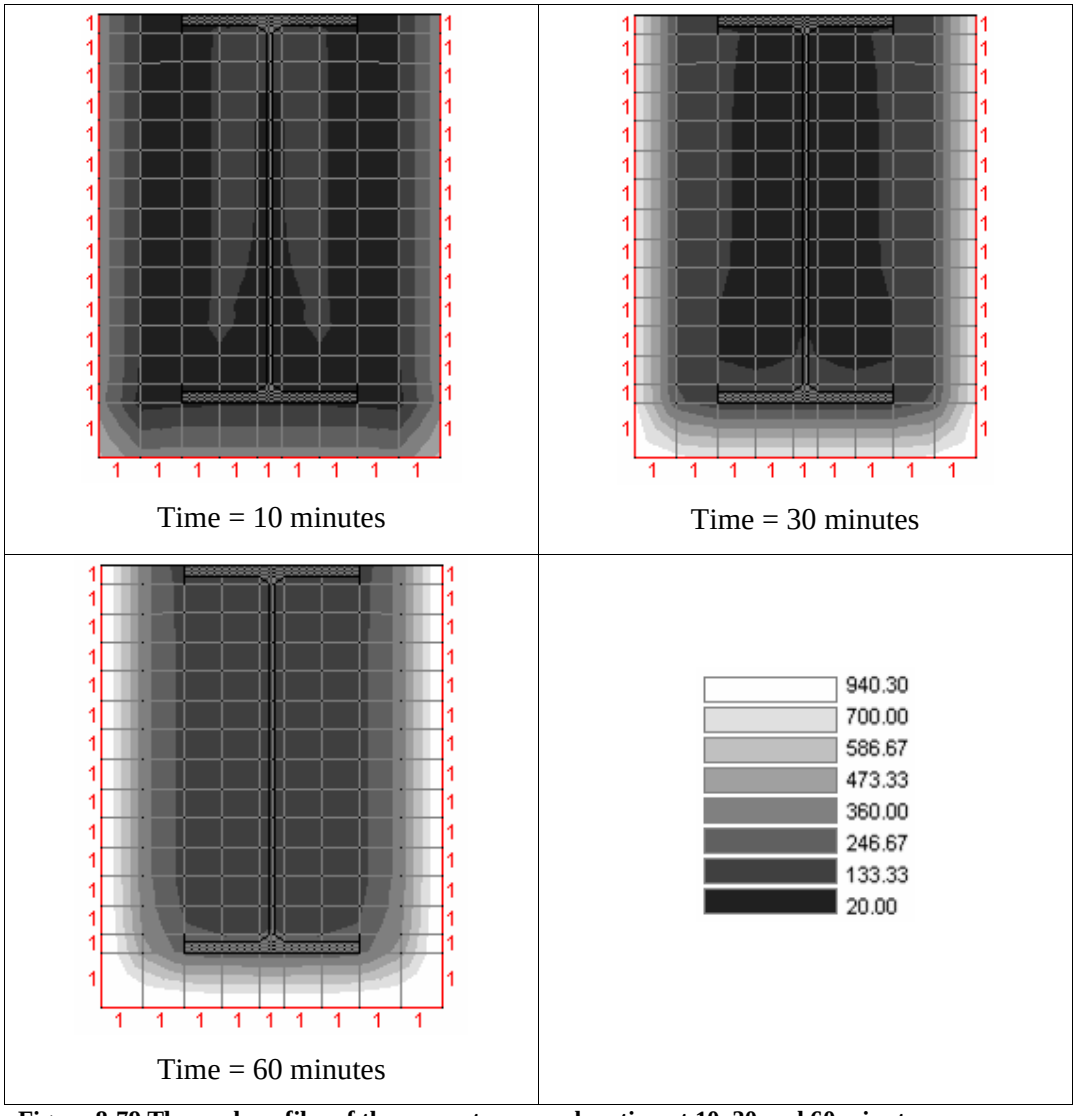

Figure 8-79 Thermal profiles of the concrete encased section at 10, 30 and 60 minutes

Figure 8-79 shows the temperature profiles of the concrete encased section at 10, 30 and 60 minutes, respectively. The figure shows that after 10 minutes of fire exposure, the steel column still remains near the ambient temperature of 20 ^{o}C. At 30 minutes, the maximum temperature occurs in the lower flange (inner flange) of the column and reaches about 50 ^{o}C. The concrete encasement can be seen to effectively reduce the temperature of the steel column by a considerable amount.

The analyses in this section are tabulated in Table 8-8. As mentioned above, concrete encasement may fall off during fire. Therefore, it has been conservatively assumed that the concrete has negligible strength (i.e. no tensile and compressive strength) in the structural analysis and it was added solely for the thermal analysis to determine the temperature profiles of the steel columns.

Table 8-8 Fire analyses in Section 8.6 – Passive Fire Protection to Columns

Analysis number	Description of passive fire protection to columns	Support conditions	Purlin Axial Restraints
(27) & (31)	Full concrete encasement along the length	Fixed	Yes & No
(28) & (32)		Pinned	Yes & No
(29) & (33)	2/3 concrete encasement of the full length	Fixed	Yes & No
(30) & (34)		Pinned	Yes & No

8.6.1 Results of Analyses

The results of the analyses are summarised in Table 8-9.

Table 8-9 Results of analyses in Section 8.6 - Passive Fire Protection to Columns

Analysis number	Description of passive fire protection to Columns	Support conditions	Purlin Axial Restraints	Mode of Failure	Simulation End Time* (minutes)
(27)	Full encasement	Fixed	Yes	Catenary	19.6
(28)		Pinned	Yes	Sway	17.2
(29)	2/3 encasement	Fixed	Yes	Catenary	17.1
(30)		Pinned	Yes	Sway	16.7
(31)	Full encasement	Fixed	No	Upright	14.7
(32)		Pinned	No	Sway	15.9
(33)	2/3 encasement	Fixed	No	Upright	14.2
(34)		Pinned	No	Sway	15.0

**Note: The simulation end times were obtained when SAFIR was unable to converge to a solution.*

With Purlin Axial Restraints

The analyses with purlin axial restraints imposed by the end wall boundary conditions (analyses (27) to (30)) show similar failure modes to those obtained without concrete encasement to the steel columns. For the steel portal frame building with fixed base connections, the structure deforms in an acceptable manner (i.e. catenary failure mode); for the steel portal frame building with pinned base connections, the frames sway sideways when the roof structure starts to deform into a catenary shape. The main difference is that the part protected with concrete stays relatively straight until SAFIR detected numerical instability in the stiffness matrix and stopped iterating to the next time step. The only exception is the analysis with fix-fix supported frames protected with 2/3 of concrete encasement (analysis (29)) and the columns deform similarly to that without any fire protection (analysis (1) as shown in Figure 8-18). Figure 8-80 to Figure 8-83 shows the front views of the final deflected shapes obtained from SAFIR.

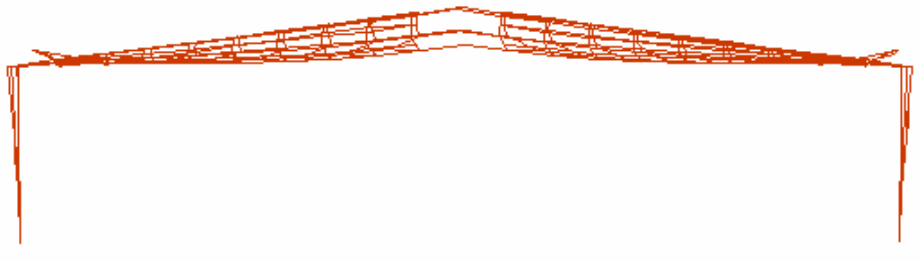

Time = 19.6 minutes

Figure 8-80 Front view of the final deflected shape at 19.6 minutes in analysis (27) - Fix-fix supported frames with full concrete encasement to column legs (Scale = 1x)

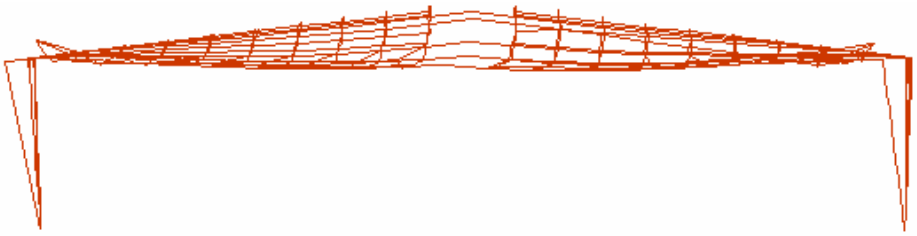

Time = 17.2 minutes

Figure 8-81 Front view of the final deflected shape at 17.2 minutes in analysis (28) – Pin-pin supported frames with full concrete encasement to column legs (Scale = 1x)

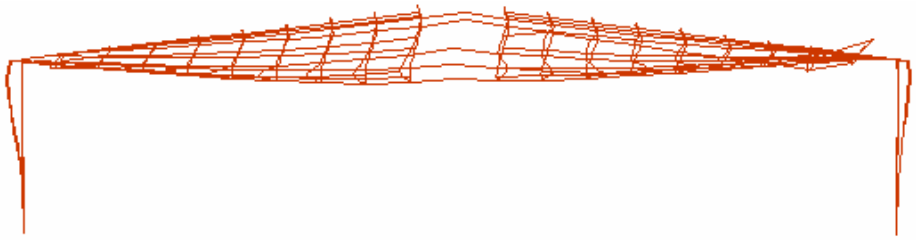

Time = 17.1 minutes

Figure 8-82 Front view of the final deflected shape at 17.1 minutes in analysis (29) – Fix-fix supported frames with 2/3 concrete encasement to column legs (Scale = 1x)

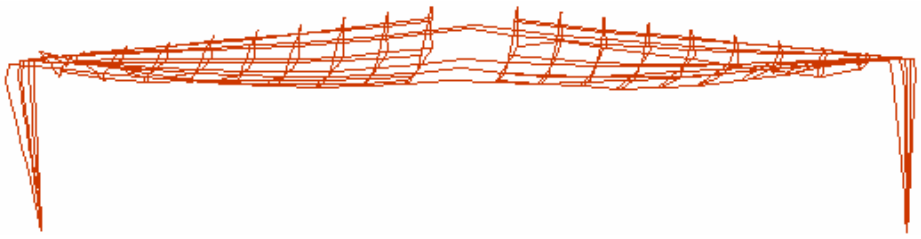

Time = 16.7 minutes

Figure 8-83 Front view of the final deflected shape at 16.7 minutes in analysis (30) – Pin-pin supported frames with 2/3 concrete encasement to column legs (Scale = 1x)

Without Purlin Axial Restraint

Without the provision of any purlin axial restraint from the end walls, SAFIR was able to obtain the behaviour up until the roof structure collapses into the building and down to the ground. The analyses (analyses (31) to (34)) have again shown that the part of the columns protected with concrete encasement stays relatively straight until the end of the simulation. For the columns protected to two-thirds of the full height, the top unprotected part can be seen to be pulled inwards due to the collapsing rafter (Figure 8-86 and Figure 8-87).

For the steel portal frame structure with pinned supports at the base, the frames with protected columns sway sideways significantly when the roof starts to deform downwards and they subsequently collapse into the building along with the collapsing rafters. This type of failure mechanism is similar to the previous analyses without concrete encasement and is not acceptable (i.e. sway mode of failure).

However, for the portal frame structure with fixed supports at the base, the protected part of the columns is still relatively straight and upright when the roof structure collapses and this suggests that inwards collapse of the walls may not occur (i.e. this is defined as the upright failure mode in Table 8-8). The walls would remain standing upright along with the columns assuming that they did not collapse due to the initial outwards thrusts caused by thermal expansion in the initial stages of the fire.

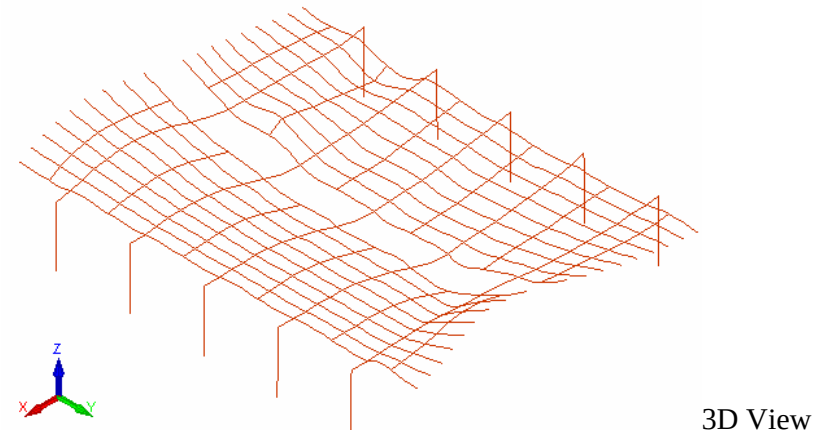

Figure 8-84 Final deflected shape at 14.7 minutes from SAFIR in analysis (31) – Fix-fix supported frames with full concrete encasement to column legs (Scale = 1x)

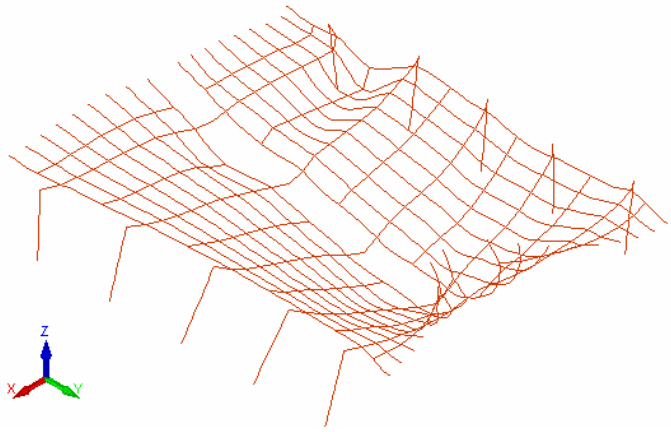

3D View

Figure 8-85 Final deflected shape at 15.9 minutes from SAFIR in analysis (32) – Pin-pin supported frames with full concrete encasement to column legs (Scale = 1x)

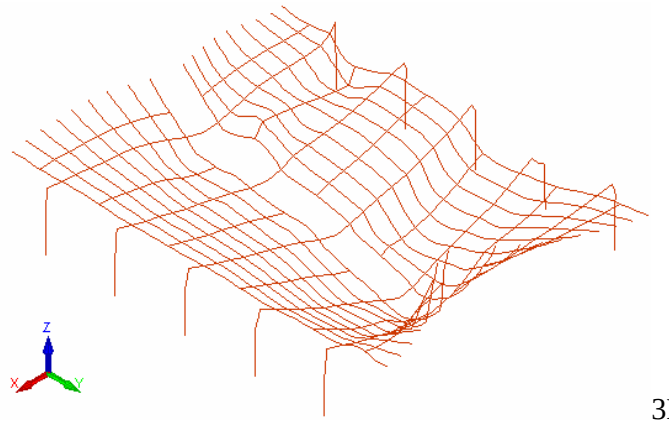

3D View

Figure 8-86 Final deflected shape at 14.2 minutes from SAFIR in analysis (33) – Fix-fix supported frames with 2/3 concrete encasement to column legs (Scale = 1x)

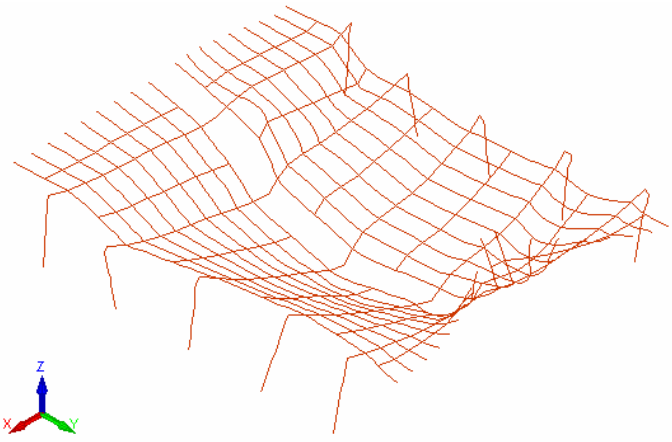

3D View

Figure 8-87 Final deflected shape at 15.0 minutes from SAFIR in analysis (34) – Pin-pin supported frames with 2/3 concrete encasement to column legs (Scale = 1x)

8.6.2 Discussion

The analyses with concrete encasement show that the parts of the columns protected do not deform excessively and are relatively straight during the period of simulation. It has also been shown that applying concrete encasement to columns with pinned connections at the base does not improve the structural performance, and the steel portal frames will deform in an unacceptable way such that they sway sideways and one or more frames could fall outwards due to P-delta effects of the self-weight of the concrete walls.

For the fixed support structure without any purlin axial restraint from the end walls, the protected part of the columns is relatively straight and upright when the roof shows a runaway displacement trend and collapses to the ground. This is because the strength and stiffness of the concrete encased part of the steel columns are largely unaffected and the stability of the columns has not been affected. If the connections between the supporting frames and wall panels do not fail, the walls will be attached to the frames and remain standing during the fire. This type of failure mechanism has been observed in real fire incidents (refer to Section 4.8.1 and Figure 4-58). This is acceptable providing the walls do not collapse outwards during and after the fire and this design approach has been adopted by some design engineers. The stability of the walls after the fire becomes an issue and the walls must resist wind loads as outwards collapse after the fire is also unacceptable.

It should be noted that the concrete part of the columns was added solely for the purpose of thermal analysis and had no strength and stiffness in the structural analysis (i.e. structural behaviour during the fire). In reality, the protected columns will be stiffer than the unprotected columns providing the concrete does not fall off. In terms of outwards collapse of the concrete walls, the forces in the steel connections to the panels may be higher due to the higher degree of restraint imposed by the protected columns. This is because during the fire, the walls will tend to bow away from the fire and if the columns are fire protected, this outwards movement of the walls will be restricted resulting in higher forces in the connections. This is outside the scope of this research and is not discussed further here. Future work on this issue will be recommended in Chapter 9.

8.7 Partially Fixed Frames

For most practical portal frames designed with pinned bases, the real base connections and foundations can actually provide some degree of fixity and rotation stiffness to the column bases. Four holding-down bolts are normally used to secure the bases of the steel portal frames to the foundation, and it is believed that this can provide a certain amount of fixity which enables portal frames to perform better in fire than the idealisation of pinned connections.

In this section, analytical models with partially fixed frames are analysed. The supporting nodes of the frames are assumed to be fully fixed as shown in Figure 8-3. However, the adjacent elements connecting the nodes which represent the supports (i.e. where the fully fixed boundary conditions are imposed) are assumed to have only half the actual yield strength and modulus of elasticity (i.e. fy = 160 MPa and G =105 GPa instead of F_y = 320 MPa and G = 210 GPa as shown in Table 3-1). It should be noted that the reduced properties of the supporting elements do not represent 50% fixity at the base as the actual fixity is depending upon the length of these elements.

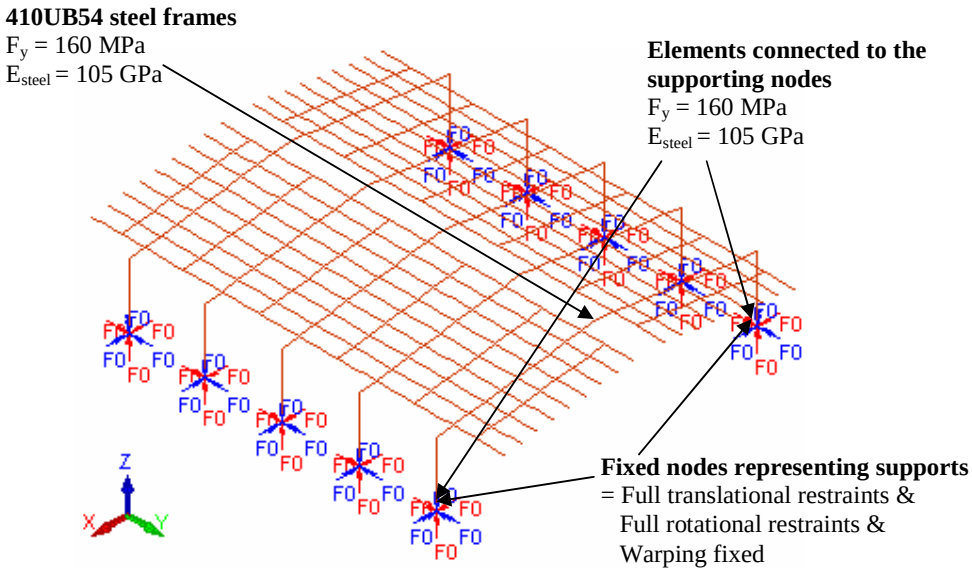

Figure 8-88 Partially fixed steel portal frame structure (Note: Arrows shown are applicable to all five frames)

It is assumed that the whole building is involved in a fire equivalent to an ISO 834 standard fire, and the heating includes the supporting elements having half the actual yield strength and modulus of elasticity (i.e. partial properties of the supporting elements reduce as the temperature of the steel columns increases). In practice, it is common to fire protect the columns located close to neighbouring property while keeping the rest of them unprotected. The analyses in this section cover both an unprotected steel portal frame structure and a portal frame structure with only the right hand side columns encased in concrete to two-thirds of the full height (Figure 8-89). The dimensions of the concrete encasement, discretised section and the thermal boundaries are similar to those found in Section 8.6 (Figure 8-77 and Figure 8-78). The analyses in this section are tabulated in Table 8-10 below.

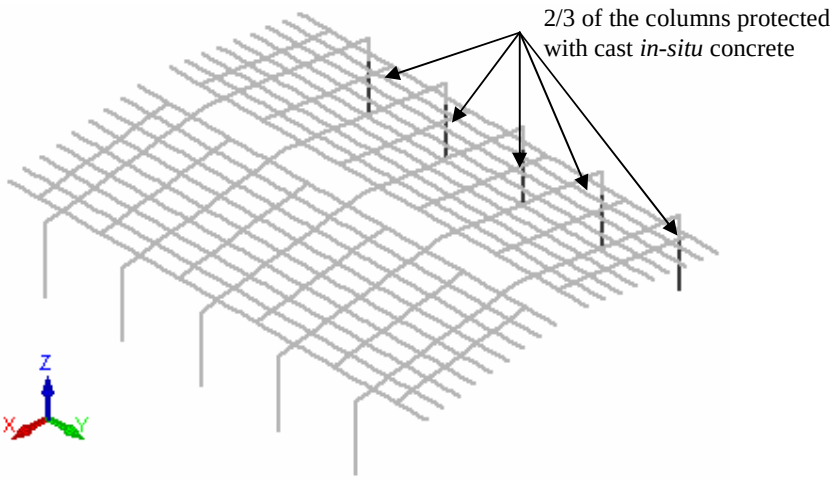

Figure 8-89 The columns on the right are protected with concrete encasement to 2/3 of the full height

Table 8-10 Fire analyses in Section 8.7 – Partially Fixed Frames

Analysis number	Description of passive fire protection to columns	Support conditions	Purlin Axial Restraints
(35) & (36)	No passive fire protection	Partially fixed	Yes & No
(37) & (38)	2/3 concrete encasement to the right columns	Partially fixed	Yes & No

8.7.1 Results of Analyses

The results of the analyses are summarised in the following table.

Table 8-11 Results of analyses in Section 8.7- Partially Fixed Frames

Analysis number	Description of passive fire protection to columns	Support conditions	Purlin Axial Restraints	Mode of Failure	Simulation End Time* (minutes)
(35)	No protection	Partially fixed	Yes	Catenary	15.9
(36)			No	Inwards	15.6
(37)	2/3 encasement to right columns	Partially fixed	Yes	Catenary	16.0
(38)			No	Inwards & Upright	15.2

**Note: The simulation end times were obtained when SAFIR was unable to converge to a solution.*

With Purlin Axial Restraints

The analyses with purlin axial restraints imposed by the end walls (analyses (35) and (37)) show that when the roof shows the runaway displacement trend, it deforms into a catenary shape until SAFIR fails to iterate to the next time step. This type of failure mechanism is similar to the previous analyses with the column bases of the steel portal frames fully fixed to the foundation. No significant sidesway occurred given that the supporting elements had reduced strength and stiffness. The final deflected shapes obtained from SAFIR are shown in Figure 8-90 and Figure 8-91. Figure 8-91 shows that the part of the columns protected with concrete encasement is still intact when the roof fails.

Without Purlin Axial Restraint

The outputs from analysis (36) show that the columns are pulled inwards when the rafters collapse to the ground (Figure 8-92). This is similar to the analysis with frames ideally fixed at the base. This is in contrast to the analysis with the right columns protected to two-thirds of the height (analysis (38)). When the roof shows the runaway trend and collapses to the ground, the protected columns are not being pulled inwards whereas the unprotected columns collapse inwards as expected due to the collapsing rafters (see Figure 8-93, this is defined as the inward & upright failure mode in Table 8-11).

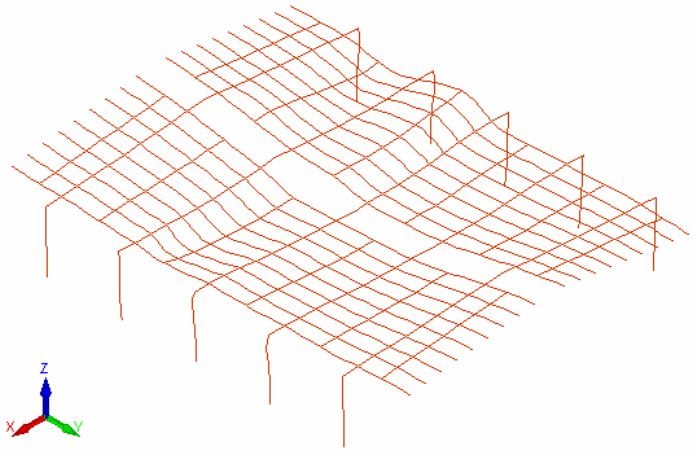

Figure 8-90 Final deflected shape at 15.9 minutes from SAFIR in analysis (35) – Partially fixed frames without fire protection to column legs (Scale = 1x)

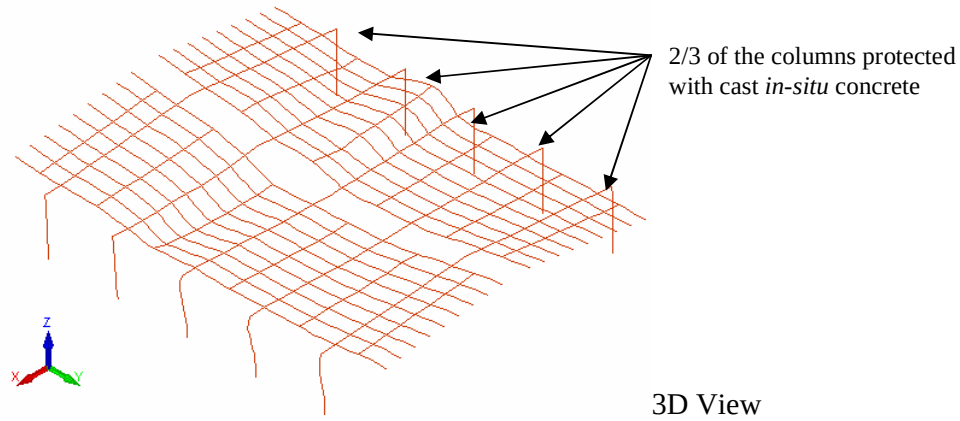

Figure 8-91 Final deflected shape at 16.0 minutes from SAFIR in analysis (37) – Partially fixed frames with 2/3 concrete encasement to right column legs (Scale = 1x)

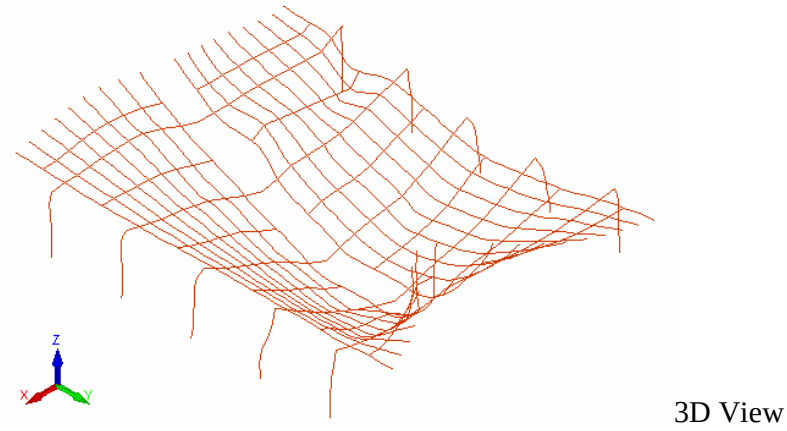

Figure 8-92 Final deflected shape at 15.6 minutes from SAFIR in analysis (36) – Partially fixed frames without fire protection to column legs (Scale = 1x)

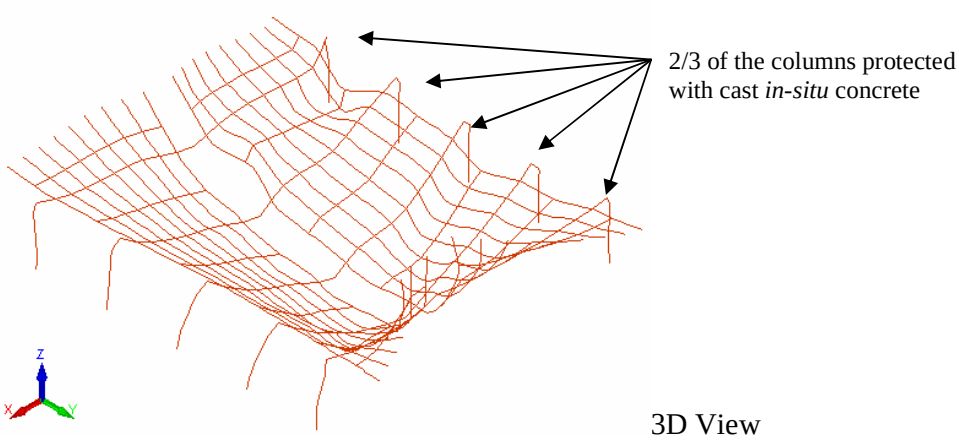

Figure 8-93 Final deflected shape at 15.2 minutes from SAFIR in analysis (38) – Partially fixed frames with 2/3 concrete encasement to right column legs (Scale = 1x)

8.7.2 Discussion

The analyses have shown that the structure with partially fixed supports will perform in a satisfactory way during fire. With purlin axial restraints imposed by the end walls, the structure will deform into a catenary. Without purlin axial restraint imposed by the end walls, the unprotected columns will collapse inwards with the collapsing rafters whereas the protected columns will be standing upright. If columns are protected with concrete encasement, the connections to the panels must be carefully detailed considering the forces resulting from thermal bowing of the walls due to the steep thermal gradient across the thickness and P-delta effects of the self weight of the walls due to outwards deformations of the frames.

It is expected that for similar types of steel portal frame building, a certain level of fixity is required at the base such that the building will not fail in the sidesway mode during the fire. The actual amount of fixity provided is not well known in the analytical models with the supporting elements having reduced properties. Future work will be recommended on the least amount of fixity required at the column base for different sizes of steel portal frames and with different building geometries and different loading conditions.

8.8.2 Half of the Building exposed to the fire

It is possible that only half of the building will be exposed to the fire and the other half of the structure remains at lower temperatures such that the stability of the structure is not severely affected. In this section, the fire-affected members are exposed to the ISO fire while the unaffected members are assumed to remain at ambient temperature.

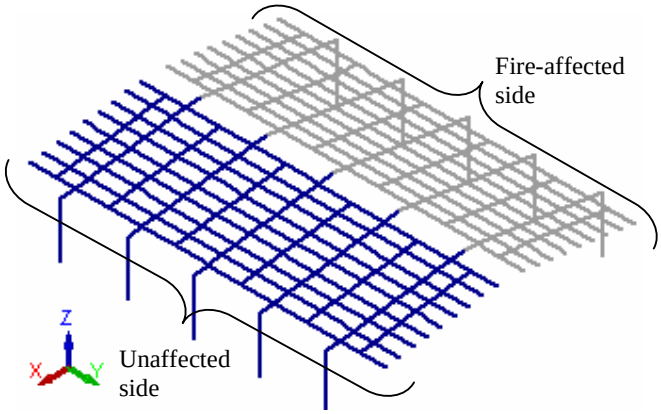

Figure 8-95 Half of the building exposed to the ISO fire

The results of the analyses are tabulated in the following table. With purlin axial restraints provided by the end wall boundary conditions (analyses (39) and (40)), SAFIR was able to obtain the behaviour up until 40 minutes when the stiffness matrix became negative. The fire-affected roof deformed steadily into a catenary and interestingly, no sidesway of frames occurred for the structure with pinned support conditions at the column bases (Figure 8-96 and Figure 8-97). This is because the cold part of the structure and the purlin axial restraints imposed by the end walls were able to provide enough lateral resistance to prevent the sideway of the frames.

Without any purlin axial restraint provided from the end walls, the analysis with fixed support conditions (analysis (41)) shows that the fire-affected columns were starting to collapse inwards due to the collapsing rafters. For the pinned support structure (analysis (42)), the frames were observed to sway sideways significantly when the roof showed the runaway displacement trend. The final deflected shapes at the point of numerical failure are shown in Figure 8-98 and Figure 8-99.

Analysis number	Description of analysis	Support conditions	Purlin Axial Restraints	Failure Mode	Simulation End Time* (minutes)
(39)	Half of the building exposed to the fire	Fixed	Yes	Catenary	39.7
(40)		Pinned	Yes	Catenary	39.2
(41)	Half of the building exposed to the fire	Fixed	No	Inwards	31.2
(42)		Pinned	No	Sway	15.1

**Note: The simulation end times were obtained when SAFIR was unable to converge to a solution.*

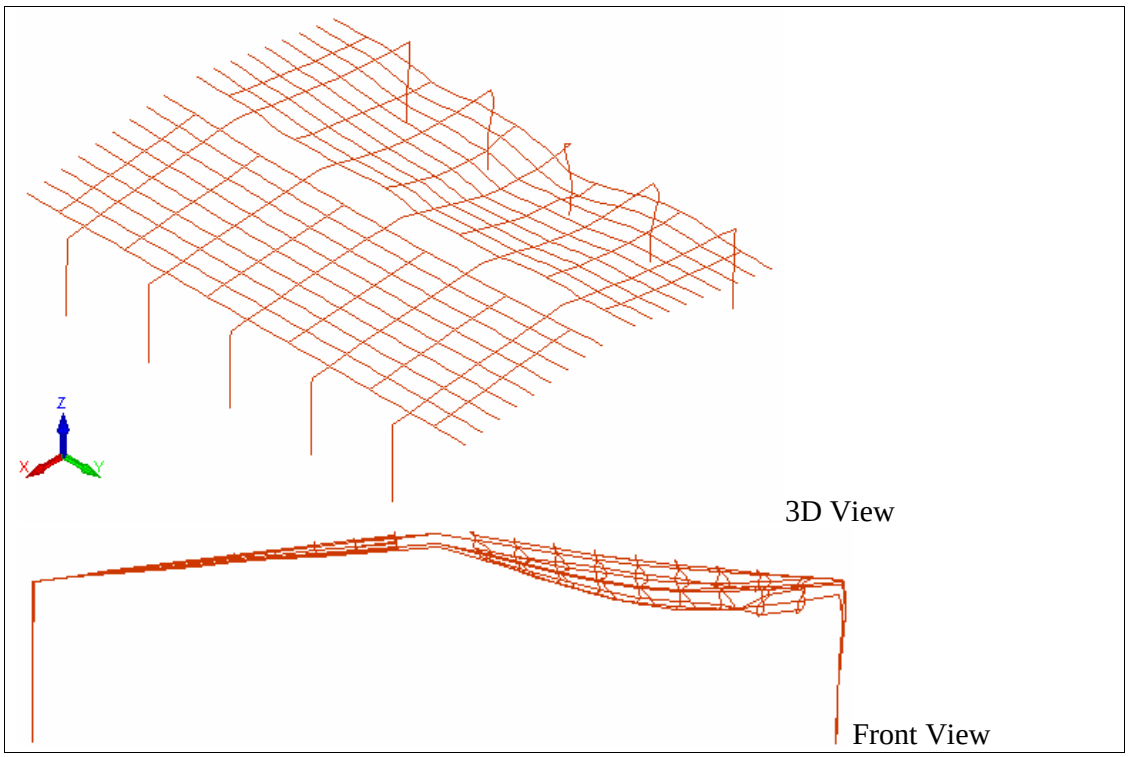

Figure 8-96 Final deflected shape at 39.7 minutes from SAFIR in analysis (39) – Fully fixed frames with purlin axial restraints imposed by the end walls (Scale = 1x)

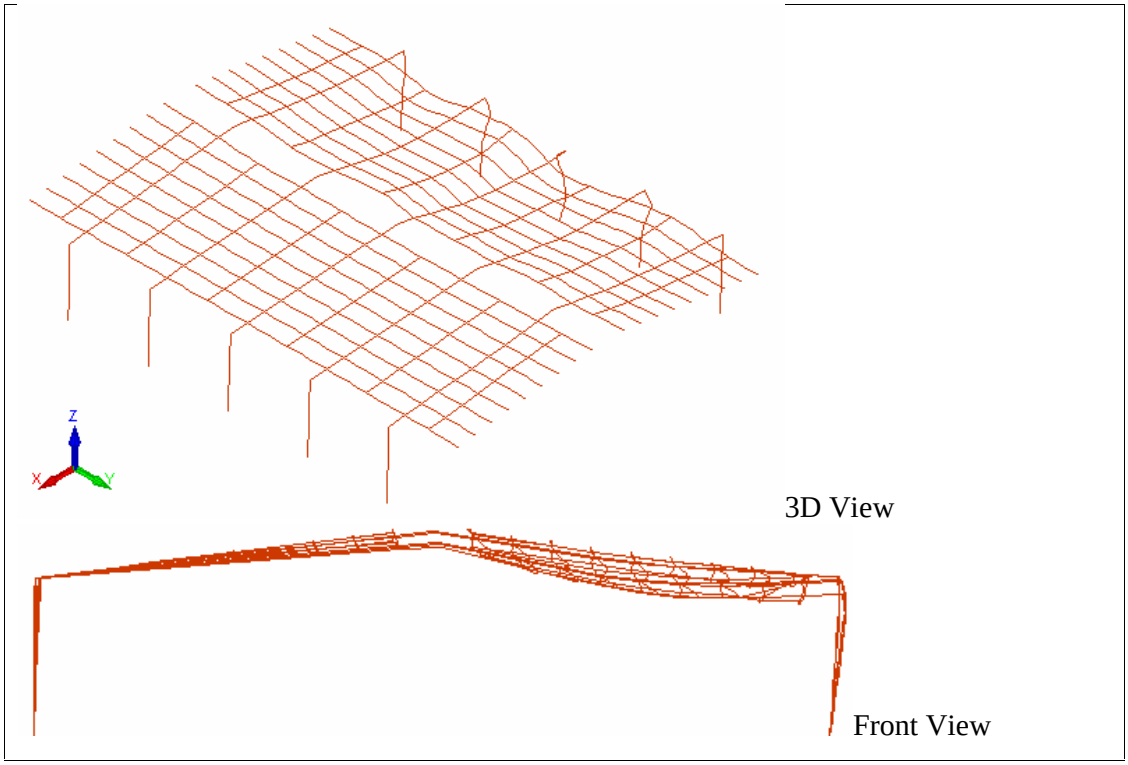

Figure 8-97 Final deflected shape at 39.2 minutes from SAFIR in analysis (40) – Fully pinned frames with purlin axial restraints imposed by the end walls (Scale = 1x)

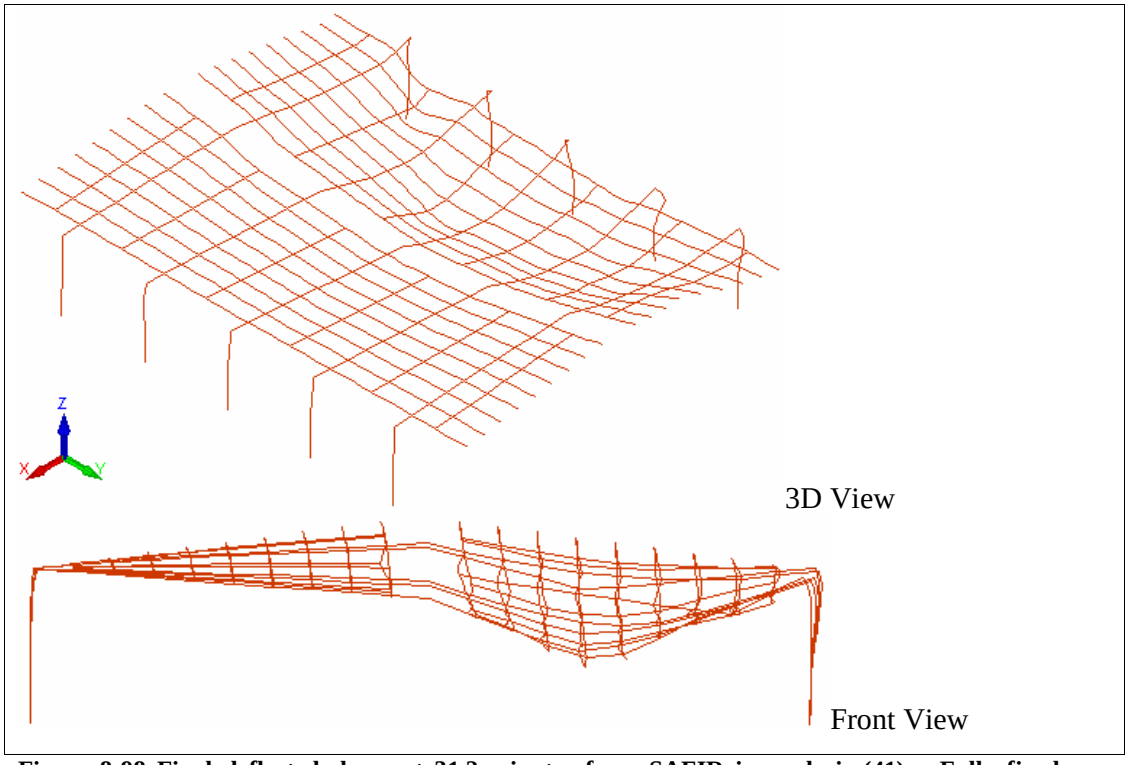

Figure 8-98 Final deflected shape at 31.2 minutes from SAFIR in analysis (41) – Fully fixed frames without purlin axial restraint imposed by the end walls (Scale = 1x)

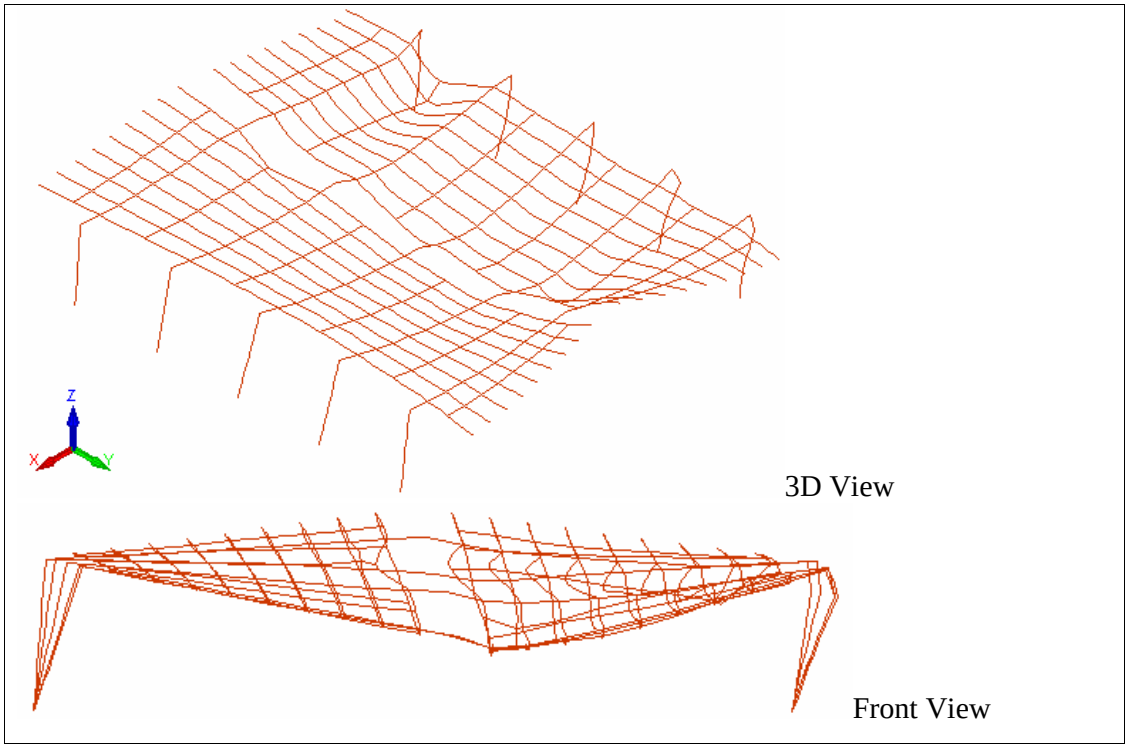

Figure 8-99 Final deflected shape at 15.1 minutes from SAFIR in analysis (42) – Fully pinned frames without purlin axial restraint imposed by the end walls (Scale = 1x)

Redistribution of Bending Moment

For the purpose of understanding the redistribution of bending moment in the structure, the results of analysis (40) is described. Figure 8-100 shows the variation of bending moment diagram for the whole building with pinned support conditions and with purlin axial restraints imposed by the end wall panels (analysis (40)) at various times. The figure shows clearly the redistribution of bending moment from the fire-affected members to the unaffected members. The figure also shows that the members exposed to the fire have very low strength at the end of the simulation when SAFIR failed to iterate to the next time step. The largest bending moment at the knees is recorded as 105.6 kN/m (Figure 8-100 (c)) and this is significantly lower than the plastic section capacity of a 410UB54 section of 339 kNm (i.e. Mp = S x f_y). This means that plastic hinges did not occur at the unaffected knees during the duration of the simulation.

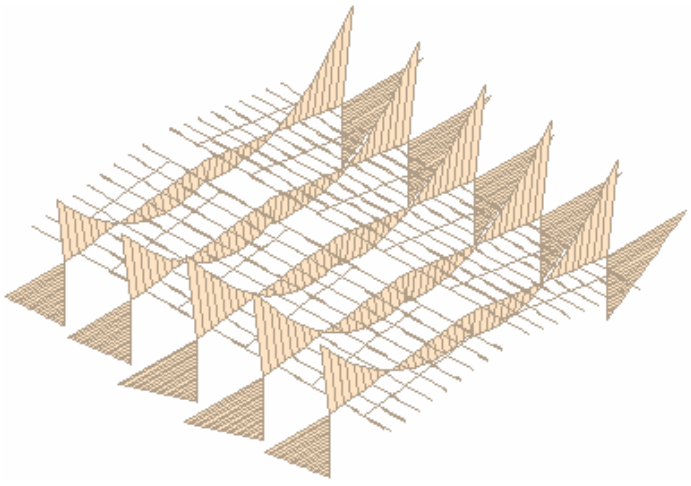

(a) Time = 10 minutes

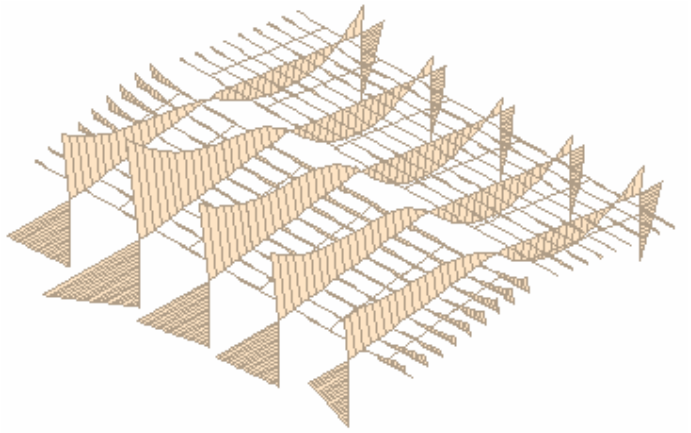

(b) Time = 30 minutes

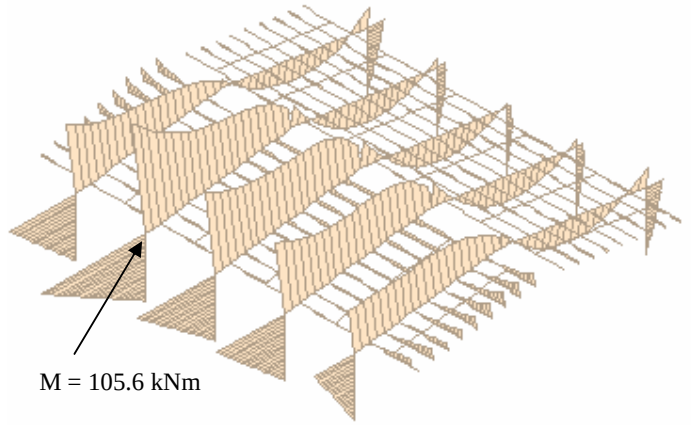

(c) Time = 39.2 minutes
(End of simulation)

Figure 8-100 Variation of bending moment in analysis (40) – Fully pinned frames with purlin axial restraints imposed by the end walls

8.8 Other Analyses

8.8.1 Geometrical Imperfection

Previous analyses assumed that there was no geometrical imperfection in the structure. The analyses have shown that a pinned support steel portal frame structure will fail in the sidesway mode whereas a fixed support steel portal frame structure will collapse inwards without the provision of any purlin axial restraint by the end walls. Geometrical imperfection is now considered and the following analyses are carried out with a horizontal force of 12.7 N (i.e. approximately 1% of the resulting UDL on the rafter) applied at each of the left eaves (Figure 7-16). The collapse times and the runaway deformations of the structure match exactly with the analyses without geometrical imperfection (analyses (7) and (8)) and the results are not discussed further here.

Description of analysis	Support conditions	Purlin Axial Restraints	Failure Mode	Collapse Time (minutes)
Fully developed fire with geometrical imperfection	Fixed	No	Inwards	14.9
	Pinned	No	Sway	14.1

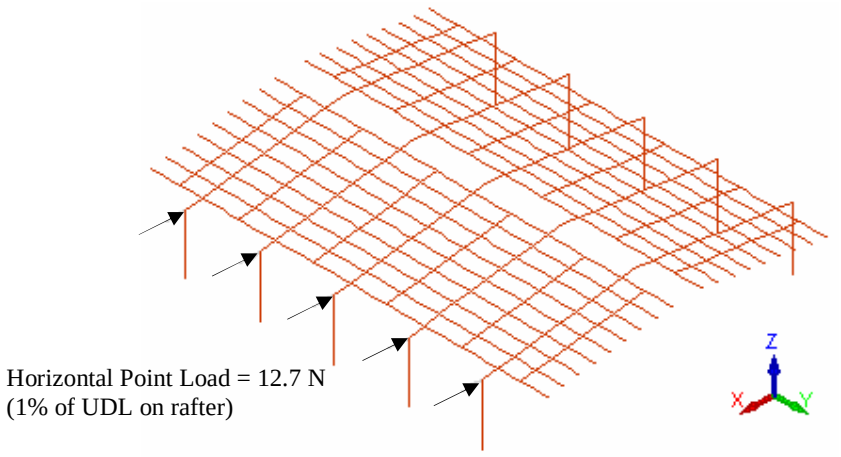

Figure 8-94 A horizontal force of 12.7 N applied to each frame to simulate geometrical imperfection

8.9 Further Discussion on the Steel Connections between the Side walls and the Supporting Frames

It has been assumed that full fixity can be practically achieved at the joints between the columns and the rafters (refer to Section 7.4.2). The analyses have shown that the rapid sagging of the roof structure has resulted in larger horizontal deflections below the eaves level (refer to Figure 8-18, Figure 8-27, Figure 8-31, Figure 8-35, Figure 8-44, etc). The top connections holding the walls to the supporting columns are very likely to fail due to high pull-out forces (Figure 8-101) as a result of this relative horizontal deflection. This could possibly cause outwards collapse of the concrete walls if flexural capacity is not provided at the base, such as occurs with 'pinned' base walls. This suggests that there should be more connections between the top and bottom of the wall such that if the top connection failed due to a pull-out mechanism, the additional connections would be beneficial in preventing the outwards collapse of the walls. The additional connections should not be located close to the eaves of the frames where high pull-out forces may be induced in the connections.

If the columns are protected with concrete encasement to half or two-thirds of the full height, this will make the protected part of the column stronger and it is unlikely that the columns will deform excessively during the fire. However, when the unprotected roof structure sags down relatively quickly in a runaway mode, the unprotected upper part of the columns will be pulled inwards assuming this part is exposed to high temperatures and is flexible enough, and similarly the top connections are very likely to fail due to a pull-out mechanism (Figure 8-102). This again emphasises that there should be more than one connection between the side walls and the supporting columns.

The above findings are only applicable to walls which are pinned at the base and are allowed to deform laterally along with the deformation of the frames due to the fire, as assumed in all the analyses in this project. If the side walls were included in the analytical models as beam elements and were assumed to be pinned to the supporting columns (i.e. by master-slave relationship in the SAFIR input file), this would make the columns very stiff due to the stiffness of the concrete walls. Consequently, the columns would not deform excessively about their strong axes and thus the deformed

shapes as shown in Figure 8-101 and Figure 8-102 might not occur. Therefore, the findings on the pull-out failures of the steel connections located near the top of the columns could have been missed.

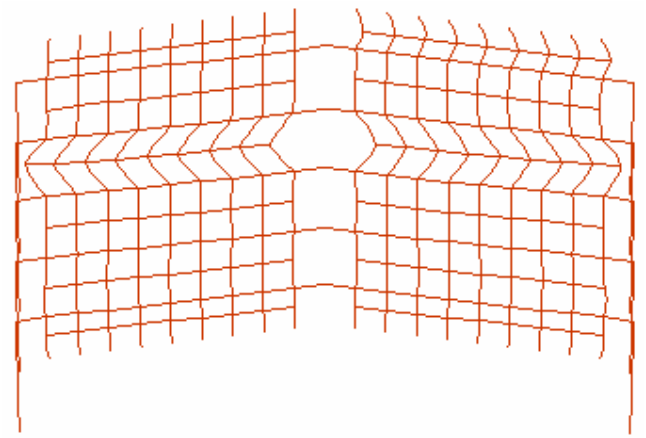

(a) Deflected shape immediately before rapid sag of roof

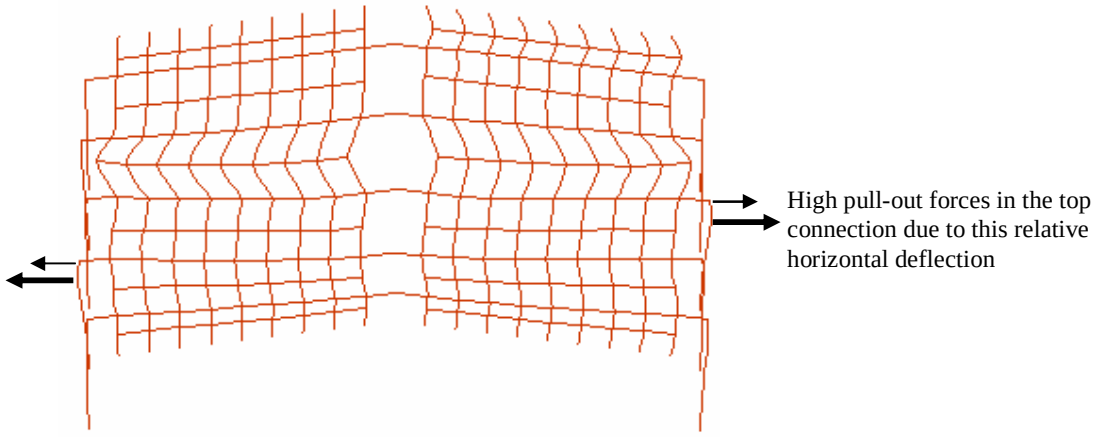

(b) Deflected shape immediately after rapid sag of roof

Figure 8-101 Failure of top connection due to a pull-out mechanism (figures from analysis (1) - Fully fixed frames with no concrete encasement (Scale = 1x))

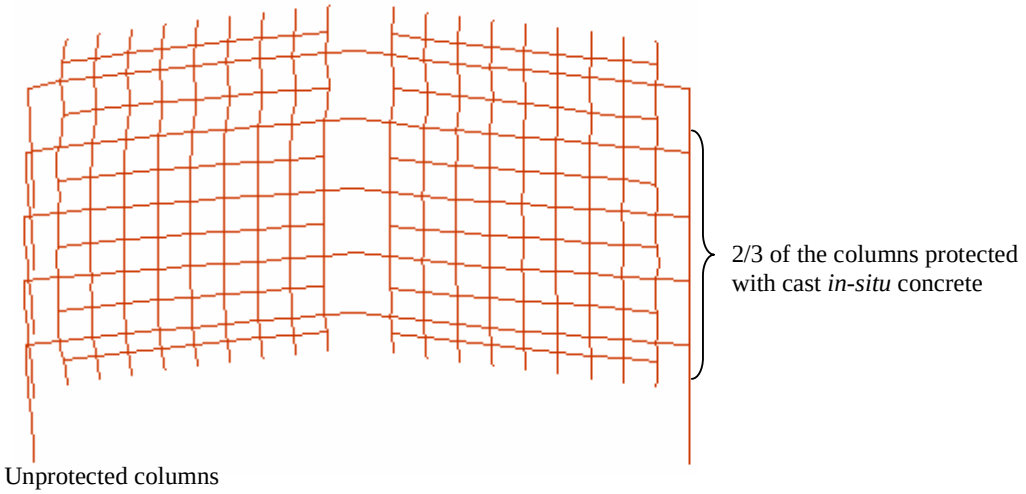

(a) Deflected shape immediately before rapid sag of roof

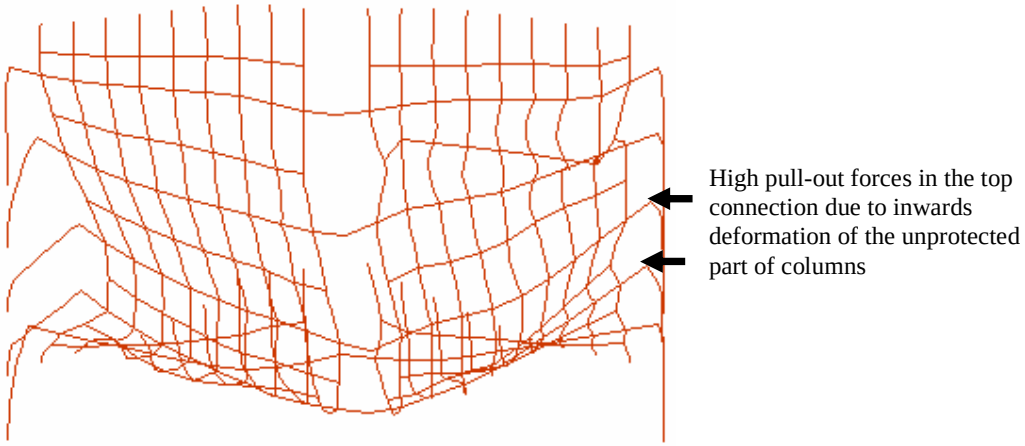

(b) Deflected shape immediately after rapid sag of roof

Figure 8-102 Failure of top connection due to a pull-out mechanism (figures from analysis (38) - Partially fixed frames with 2/3 concrete encasement to right column legs (Scale = 1x))

8.10 Summary

The following tables summarise the failure times and collapse modes from analyses carried out in this chapter.

Fire (no decay)		ISO	External	ISO	ISO	ISO
Fire size		100%	100%	100%	100%	50%
Column protection		None	None	2/3 height	Full height	None
Column out-of-plane restraint		Top & Mid-height	Top & Mid-height	Top & Mid-height	Top & Mid-height	Top & Mid-height
	Purlin axial restraint					
FIX BASE	No	14.9 Inwards	26.9 Inwards	14.2 Upright	14.7 Upright	31.2 Inwards
PIN BASE	No	14.1 Sway	18.4 Sway	15.0 Sway	15.9 Sway	15.1 Sway
PARTIAL FIXITY	No	15.6 Inwards	-	15.2* Inwards & Upright	-	-
FIX BASE	Yes	18.5 Catenary	60 Catenary	17.1 Catenary	19.6 Catenary	39.7 Catenary
PIN BASE	Yes	19.6 Sway	60 Sway	16.7 Sway	17.2 Sway	39.2 Catenary
PARTIAL FIXITY	Yes	15.9 Catenary	-	16.0* Catenary	-	-
Ref pages		174, 243	206	236, 243	236	248

** Note: 2/3 concrete encasement applied to the right columns only*

Fire (no decay)		ISO	ISO	External[3]	ISO	ISO
Fire size		18%[1]	18%[2]	100%	100%	100%
Column protection		None	None	None	None	None
Column out-of-plane restraint		Top & Mid-height	Top & Mid-height	Top & Mid-height	None	Full height
	Purlin axial restraint					
FIX BASE	No	60 Catenary	20.5 Inwards	-[4]	11.3 Weak-axis	14.9 Inward
PIN BASE	No	60 Sway	18.5 Sway	-[4]	0.2 Weak-axis	14.9 Sway
PARTIAL FIXITY	No	-	-	-	-	-
FIX BASE	Yes	60 Catenary	60 Catenary	120 No failure	15.8 Catenary	17.1 Catenary
PIN BASE	Yes	60 Sway	60 Sway	120 No failure	13.3 Sway	15.2 Sway
PARTIAL FIXITY	Yes	-	-	-	-	-
Ref pages		174	174	206	224	224

[1] *Localised fire occurred near the centre of the building*

[2] *Localised fire occurred near the end of the building*

[3] *External fire with a linear decay phase*

[4] *Structural failure occurred before the decay phase*

8.11 Conclusions

As noted in separate discussion sections of this chapter, the following conclusions can be drawn:

- Most pin based frames fail in a sidesway mode.
- All partially fix based frames have the same failure mode as fully fix based ones.
- For the most common case of an ISO fire occupying the whole building, without strong axial restraint of the purlins and with common column out-of-plane restraints provided by the side wall panels, structural collapse occurs at about 15 minutes.
- External fire is less severe on the structure than an ISO fire, and the main structure may not collapse in short duration fires.
- Fire in half of the building doubles the time before collapse, and for a building with column bases pinned at the foundation, the cooler parts of the building may prevent significant side sway from occurring.
- Fire in a smaller part of the building gives even less likelihood of collapse.
- Full or partial base fixity, with column protection, gives good after-fire stability, with columns remaining vertical (hence much better repairability).
- Providing concrete encasement to columns gives no benefit if the column bases are fully pinned.
- The level of axial restraint provided by the steel purlins is much less important than providing some degree of flexural fixity at the bases of the portal frame columns to ensure the structure deforms in an accepetable manner.

9 CONCLUSIONS AND RECOMMENDATIONS

9.1 Introduction

This research project was conducted to analyse the fire performance of steel portal frame structures in industrial buildings. The analysis in this project was conducted with SAFIR, a non-linear finite element programme. The scope of the analysis covered various locations and severities of fires in the building, different support conditions at the column bases, the presence of axial restraints in the purlins provided by the surrounding structure (i.e. adjacent frames or the end walls), different levels of out-of-plane restraint to the columns, and the effect of concrete encasement of the columns.

9.2 The Building

The structure studied in this project is an industrial building formed by five parallel steel portal frames composed of a 410UB54 section as the major framing elements. The roof structure consists of 410UB54 rafters, DHS250/15 purlins and DB89/10 brace channels, and the steel purlins and brace channels are produced by Dimond Industries. The structure measures 40 metres long by 30 metres wide and the roof is inclined at 7.9^{o}. The steel frames have a span of 30 metres and are spaced at 7.2 metres. The columns are 6 metres high and the distance from ground level to the apex of the frame is 8 metres. The purlins are spaced equally at about 1.5 metres and span between the steel frames. The steel sheeting has been ignored in the analytical structure but the self-weight has been included in the analysis. The precast concrete panels on the side walls are attached to the steel portal frames and those on the end walls are supported on steel or reinforced concrete cantilever columns. The conclusions below refer to steel portal frame buildings of this size and type of structure.

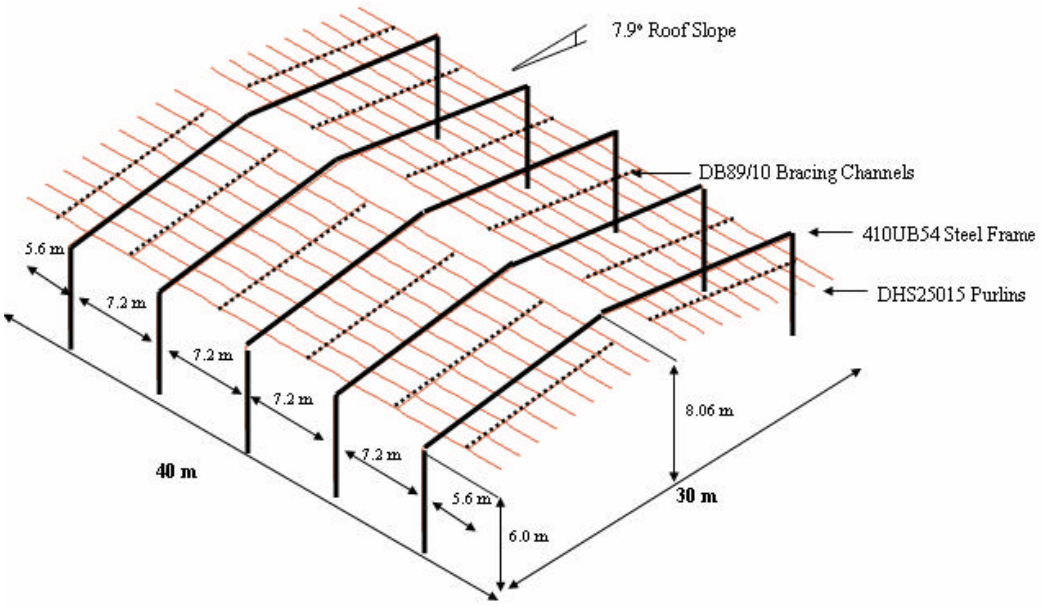

Figure 9-1 Dimensions and structural elements of the analytical structure

9.3 SAFIR

SAFIR uses a step-by-step iterative procedure to evaluate the fire behaviour of structures with respect to time. The material properties are generally those in the Eurocodes 2 and 3 (EC2, 1995 and EC3, 1995). The analysis of a structure exposed to fire consists of three main steps in SAFIR. The first step is to perform thermal analysis on the structural members. The second step is the torsional analysis of 3D beam elements whereby a section is subjected to warping and where the warping function and torsional stiffness of the cross section are required to predict the behaviour at elevated temperatures. The last part of the analysis is the structural analysis, and is carried out for determining the response of the structure due to applied loads and thermal distribution evaluated from the thermal analysis.

The procedure repeats itself in every time step and stops when the specified final time is reached or numerical failure occurs, whichever occurs first. In the previous versions of SAFIR, analysis of structures submitted to fire is performed by a succession of subsequent static analyses of the structure taking into account the variations of the displacement and the temperature profile in the structure from one time step to the next. The new version of SAFIR (*SAFIR 2004*) has the dynamic algorithm implemented to cope with partial or local failure commonly encountered during the

unstable states of the structure. With the dynamic algorithm in SAFIR, the simulation can be performed for substantially larger displacements and gives a much better insight into the failure mode and allows, in certain cases, to judge the possibility of progressive collapse.

The analyses in this project have shown that in most cases, the dynamic algorithm in SAFIR is capable of analysing three dimensional steel portal frame structures exposed to elevated temperatures, until the time that failure modes can be clearly identified and meaningful results are obtained.

9.4 Fire Analysis of the Whole Building

The analyses in this report have shown that the structural fire behaviour of the building is very sensitive to the support conditions at the column bases and the axial restraints provided in the steel purlins by the surrounding structure.

9.4.1 Axial Restraint of Purlins

Axial restraints can be provided in the steel purlins by the surrounding structure, provided that the bolted end connections have sufficient axial load capacity. This restraint is translational fixity in the longitudinal direction of the purlins. The surrounding structure providing the restraint can either be the adjacent frames or the restraint conditions imposed by the end walls.

In a real building, it is impossible to know the precise level of axial restraint which will be provided, but it will certainly be somewhere between the two extremes of zero and fully restrained which were modelled in this project.

The degree of axial restraint may depend on the fire growth and severity, because steel purlins have been observed to fall to the ground in a very hot fire, but they have also been observed to remain in place, even though severely damaged, in many other fires.

It has been shown in this study that the degree of axial restraint of the purlins is much less important than providing some degree of flexural fixity at the bases of the portal frame columns.

9.4.2 Support Conditions at the column base

Fixed Support Conditions

For a steel portal frame structure with bases fully fixed to the foundation, the deformation of the fire-affected roof structure (steel rafters, purlins and brace channels) is almost vertical. Immediately after the fire-affected roof structure starts to fail, the fire-affected frames will collapse inwards if the adjacent purlins are not axially restrained, or the fire-affected roof structure will deform into a catenary if the adjacent purlins are axially restrained by the surrounding structure. These failure modes are acceptable providing that the connections between the side walls and the supporting frames do not fail.

For the inwards collapse mode (no axial restraint to purlins), the initial outwards deformations of the steel columns are less than 200 mm at the top of the column and are solely due to the thermal expansion of the steel portal frame. When the fire-affected roof structure shows a snap-through failure mechanism and collapses to the ground, the columns will be pulled inwards along with the collapsing rafters. Therefore, the side walls will collapse inwards and this will not only reduce the risks of fire spread to neighbouring property but also prevent the lives of the fire-fighters from being endangered due to the outwards collapse of the walls.

For the catenary mode of failure (axially restrained purlins), the sagging of the fire-affected roof structure into the catenary shape will push the top portions of the columns outwards to some extent (i.e. up to 520 mm at the top of the column). Providing the connections to the walls panels do not fail, the walls can still be attached to the supporting frames and held in outwards inclined positions. This is acceptable according to the codes.

Pinned Support Conditions

For a steel portal frame structure with pinned base connections, significant sidesway of the fire-affected frames will occur when the fire-affected roof structure (steel rafters, purlins and brace channels) begins to fail and the sway of the fire-affected frames will result in very large horizontal deflections at the top of the columns (i.e. possibly in excess of 1 metre). After that, the fire-affected roof structure will deform into a catenary if the adjacent purlins are axially restrained, or in the case where the purlins are not axially restrained, the roof structure will collapse to the ground and the analyses have shown that the collapsing rafters will subsequently pull the frames inwards. These failure modes are unacceptable because the large lateral deflections to one side could cause a side-sway collapse of one or more frames due to the P-delta effects of the self weight of the walls.

Partially Fixed Support Conditions

Most real buildings are designed and built with partially fixed portal frame bases. The collapse mechanisms of a structure with portal frames partially fixed at the base are similar to the structure with fully fixed support conditions. The partially fixed supports were modelled by having half the actual yield strength and modulus of elasticity in the elements adjacent to the supports. If the purlins fixed to the fire-affected steel frames are axially restrained by the surrounding structure, the structure will deform into a catenary; without axial restraint in the purlins, the portal frame columns and the attached wall panels will collapse inwards when the roof structure collapses to the ground.

9.4.3 Location and Severity of Fire

Fire occupying whole building

The conclusions in Section 9.4.2 are for a fully developed fire occupying the whole building. Some analyses were also carried out for localised fires.

Localised Fires

For localised fires in the building, load sharing can occur between the fire-affected and unaffected structural members. If the adjacent parts of the structure remain at relatively low temperatures such that structural stability is not significantly reduced,

these cooler parts can provide adequate restraint and stiffness to the heated area and the structure may deform in a steady manner for a long period of time. However, structural collapse will occur if load transfer cannot take place. Regardless of whether load sharing or load transfer will occur or not, portal frames with fully fixed supports will perform in an acceptable way whereas portal frames with fully pinned supports will perform in an unacceptable manner as described above (see Section 9.4.2).

9.4.4 Out-of-plane Restraints to Columns

Providing full out-of-plane restraints along the length of the columns to prevent out-of-plane deformations will not improve the fire resistance of the structure. In contrast, if the portal frame does not have any out-of-plane stiffness, collapse in the weak direction can occur. However, out-of-plane stiffness always exists in this type of building to resist wind and earthquake loads in the longitudinal direction either by roof bracing to transfer the loads to the side wall panels or by the end walls acting as cantilevers. Therefore, the weak-axis collapse as observed in the analyses without any out-of-plane restraint is unlikely to occur.

9.4.5 Passive Fire Protection

This section refers to steel columns encased in concrete for some or all of their height to provide fire protection. For protected columns which are not pinned at the base and some fixity is provided by the support connections, the concrete encased part of the columns will not deform excessively and will remain relatively straight during the fire. If the rafters collapse to the ground, the protected columns will not collapse inwards along with them and can still be standing after the fire. This is acceptable as long as the walls do not collapse outwards after the fire due to failure of the connections between the panels and the columns. The forthcoming New Zealand Concrete Structures Standard NZS 3101:2005 will require that the connections be designed for a face load of 0.5 kPa applied to the concrete walls during the fire.

This study has shown that applying concrete encasement to columns which are fully pinned at the base will not improve the fire behaviour of the structure and sidesway of frames will occur resulting in outwards collapse of the columns and hence the walls.

9.4.6 Eurocode External Fire

The above conclusions refer to the behaviour of the building exposed to the ISO 834 standard fire with no decay period. A lower severity and shorter duration fire is the Eurocode External Fire, which is commonly used to simulate well-ventilated fires and was used in the analysis to investigate the fire behaviour of the structure exposed to such fires.

This analysis is based on an assumption that the roof sheeting collapsed and the plastic skylights melted in the very early stages of the fire and most of the heat was vented straight into the atmosphere resulting in a maximum temperature of 660 ^{o}C in the steel members. In general, the deformations of the structure due to the External Fire are smaller than in the ISO standard fire and structural collapse times are increased. If the fire starts to decay due to burnout of fuel before the collapse of the frames occurs, the structure can regain its strength and stiffness and deflect back towards its original form, with minor permanent deformations due to irrecoverable plastic deformation of the steel materials.

In conclusion, steel portal frame structures will perform better in well-ventilated fires than in the ISO standard fire, in terms of deflection and structural stability. For some short duration fires the main structure will not collapse during or after the fire.

9.5 Design Recommendations

Support connections of the steel portal frames

The portal frame support connections must be detailed and designed to provide some level of rotational restraint, in order to prevent the sidesway of frames and outwards collapse of wall panels.

Passive fire protection to the column legs

Assuming that the recommendation of some base fixity will always be followed, providing fire protection such as concrete encasement to the columns can ensure that the columns will remain standing during and after the fire. If this design approach is adopted, stability of the external walls can be maintained in the post-fire condition,

which may be desirable in many situations although not required by the codes. This benefit does not apply if the portal frames have fully pinned supports.

Connections between the wall panels and the supporting frames

The wall panels must always be well connected to the supporting frames so that the outwards collapse of the panels, due to both thermal bowing of the concrete walls and outwards movement of the columns, can be prevented. This is regardless of whether or not the steel columns are fire protected. The forthcoming New Zealand Concrete Structures Standard NZS 3101:2005 will require at least two upper strong and well designed connections to the panels to ensure that the wall panels are well attached to the supporting columns. The connections near the top of the columns will have to withstand very high pullout forces. Apart from the top connections, additional connections should be located near the mid-height of the columns.

If multiple panels are used between the supporting frames, the panels must be well connected to each other such that they act as a complete unit. An eaves tie member is recommended to keep all the walls panels connected during a fire and the connections to the walls and supporting columns should be carefully detailed and designed to prevent outwards collapse of the individual panels.

9.6 Recommendations for future research

It is recommended that future research should include:

- Finite element structural analysis with more realistic fire curves. This may require the use of a computational fluid dynamics computer programme to determine the temperature profiles for each of the structural elements. In particular, developing fires where cooling and heating can occur at the same time at different locations should be considered.
- More sophisticated finite element models incorporating the roof sheeting, boundary concrete walls and all the steel elements of the portal frame structure. The collapse of the roof sheeting, the forces in the steel connections, the deformation of the steel elements, and thermal bowing of the concrete walls should be taken into account in the models.

- Fire resistance of the connections between the concrete wall panels and the steel or cast *in-situ* columns.
- Determination of the minimum amount of fixity required at the supports of the steel portal frames to ensure the building will not fail in a sidesway mode. The analysis should consider different sizes of steel portal frames, purlins, brace channels and also different building geometries and different loading conditions.
- Experimental verification of the fire behaviour of steel portal frame structures.
- Analysis of the effects of unsymmetrical steel portal frame structures, also partial loading conditions and geometrical imperfections.
- Analysis of connection forces for walls connected to each other at right angles using shell elements in SAFIR. Large forces will develop at the connections holding the corner walls when the walls try to deform outwards due to thermal bowing effects.

10 REFERENCES

ABAQUS - Finite Element Analysis Programme, Hibbitt, Karlsson and Sorensen Inc, 1988.

AISC (1994), Design Capacity Tables for Structural Steel, Volume 1: Open Sections, Second Edition, Australian Institute of Steel Construction, NSW, Australia.

Anderberg, Y. (1976), Fire exposed hyperstatic concrete structures – An experimental and theoretical study, Lund Institute of Technology, Division of Structural Mechanics and Concrete Construction, Bulletin 55, Sweden.

Australian Building Codes Board (2004), BCA: Building Code of Australia, Canberra, A.C.T.: CanPrint Communications, Australia.

Bennetts, I.D. and O'Meagher, A.J. (1995), Single Storey Steel-framed Buildings: Support of External Walls in Fire, BHP Structural Steel Development Group, Technical Note No.1, Australia.

Bennetts, I.D. and Poh, K.W. (2000), Steel Portal Frame Buildings – Support of External Concrete Wall Panels, Fire Design Note No.1, OneSteel Manufacturing Pty Ltd, Australia.

Bennetts, I.D. (1981), Elevated temperature behaviour of concrete and reinforcing steel, Melbourne Research Laboratories of BHP, Australia.

Bernhart, I.D. (2004). The Effect of Support Conditions on the Fire Resistance of a Reinforced Concrete Beam, Fire Engineering Research Report 04/5, Department of Civil Engineering, University of Canterbury, Christchurch, New Zealand.

Buchanan, A.H. *Editor* (1994), Fire Engineering Design Guide: Report of a Study Group of the New Zealand Structural Engineering Society and the New Zealand Fire

Protection Association, Centre for Advanced Engineering, University of Canterbury, Christchurch, New Zealand.

Buchanan, A.H. *Editor* (1999). Timber Design Guide, Second Edition, New Zealand Timber Industry Federation, Wellington, New Zealand.

Buchanan, A.H. (2001), Structural Design for Fire Safety, John Wiley & Sons, U.K.

Building Industry Authority (2000), Approved Document for New Zealand Building Code: Fire Safety Clauses, Standards New Zealand, Wellington, New Zealand.

Clifton, G.C. and Forrest, E. (1996), Notes Prepared for a Seminar on the Design of Steel Buildings for Fire Emergency Conditions, HERA Report R4-91, Manukau City, New Zealand.

Cooke, G.M.E. (1987), Fire engineering of tall fire separating walls. Part 1 and Part 2. Fire Surveyor, Vol. 16, pp 13-29 (No.3) and 19-29 (No.4).

Cooke, G.M.E. and Morgan, P.B.E. (1988), Thermal bowing in fire and how it affects building design, Building Research Establishment Information Paper, December, UK.

Cooke, G.M.E., Virdi, K.S. and Jeyarupalingam, N. (1996), The thermal bowing of brick walls exposed to fire on one side. *Proc. Interflam' 96*, 915-919, Interscience, London.

Cosgrove, B.W. (1996), Fire design of single storey industrial buildings, Fire Engineering Research Report No.96/3, University of Canterbury, Christchurch, New Zealand.

Dimond Industries (1995), Hi-Span Design Manual, Manual No.9 in the Dimond Design Information Series, New Zealand.

EC1 (1994), Eurocode 1: Basis of Design and Designs Actions on Structures. ENV1992: Part 2.2: Actions on Structures Exposed to Fire, European Committee for Standardization, Brussels, Belgium.

EC2, (1995), Eurocode 2: Design of concrete structures. ENV 1992: Part 1.2: General rules - Structural fire design, European Committee for Standardization, Brussels, Belgium.

EC2, (2002), Eurocode 2: Design of concrete structures. prEN 1992: Part 1.2: General rules - Structural fire design, European Committee for Standardization, Brussels, Belgium.

EC3, (1995), Eurocode 3: Design of steel structures. ENV 1993: Part 1.2: General rules - Structural fire design, European Committee for Standardization, Brussels, Belgium.

EC3, (2002), Eurocode 3: Design of steel structures. DRAFT prEN 1993: Part 1.2: General rules - Structural fire design, European Committee for Standardization, Brussels, Belgium.

Franssen, J.M. and Gens, F. (2004), Dynamic analysis used to cope with partial and temporary failures. Paper S6-3, pp 297-310, Third International Workshop on Structures in Fire, Ottawa, Canada.

Franssen, J.M., Kodur, V.K.R. and Mason, J. (2002), Elements of Theory for SAFIR 2002: A computer program for analysis of structures subjected to fire, Department of Civil Engineering, University of Liege, Belgium.

Franssen, J.M., Kodur, V.K.R. and Mason, J. (2004), User manual for SAFIR 2004: A computer program for analysis of structures subjected to fire. Department of Civil Engineering, University of Liege, Belgium.

Gorenc, B.E., Tinyou, R. and Syam, A. (1996), The steel designer's handbook, 6th Edition, University of New South Wales Press, Sydney, Australia.

Harmathy, T.Z. (1967), A Comprehensive creep model. *Transactions*, American Society of Mechanical Engineers, *Journal of Basic Engineering*, 89.

Harmathy, T.Z. (1993), Fire Safety Design and Concrete. Concrete Design and Construction Series. Longman Scientific and Technical, UK.

Hisley, B.W. (2003), Storage Occupancies, Fire Protection Handbook, Section 13, Chapter 15, 19th Edition, National Fire Protection Association, Quincy, Massachusetts.

Institution of Structural Engineers (1975), Fire resistance of concrete structures. Report of a Joint Committee of the Institution of Structural Engineers and the Concrete Society, London, UK.

Institution of Structural Engineers (1978), Design and Detailing of Concrete Structures for Fire Resistance. The Institution of Structural Engineers, London, UK.

International organisation for Standardisation 834 (1985), Fire-resistance Tests – Elements of Building Construction, 1st Ed.

Jansson, R. and Bostrom, L. (2004), Spalling of concrete for tunnels. Interflam 2004, Proceedings of the tenth international conference, Vol. 1, Interscience Communications Limited, London, UK.

Karlsson, B. and Quintiere, J.G. (2000), Enclosure Fire Dynamics, CRC Press, Boca Raton, Florida, USA.

Kirby, B.R. and Preston, R.R. (1988), High temperature properties of hot-rolled structural steels for use in fire engineering design studies. *Fire Safety Journal*, 13, 27-37.

Kitchen, A. (2004), Concrete ideas, *Fire Prevention and Fire Engineers Journal, The International Journal for Fire Professionals, October 2004,* Fire Protection Association and The Institution of Fire Engineers, London, UK.

Kodur, V.K.R. (1997), Studies on the fire resistance of high strength concrete at the National Research Council of Canada, Proceedings of the International Workshop on Fire Performance of High Strength Concrete, pp 75-86, NIST Special Publication 919. National Institute of Standards and Technology, USA.

Lim, L. and Buchanan, A.H. (2003), Stability of Precast Concrete Tilt Panels in Fire, *SESOC Journal: Journal of the New Zealand Structural Engineering Society*, Volume 16, No.2, September, New Zealand.

Lim, L., Buchanan, A., Moss, P. and Franssen, J.M. (2004), Numerical modelling of two-way reinforced concrete slabs in fire, Engineering Structures, Vol. 26, No. 8, pp 1081-1091, Elsevier.

Lim, L.C.S. (2000), Stability of Precast Concrete Tilt Panels in Fire, Fire Engineering Research Report 00/8, University of Canterbury, Christchurch, New Zealand.

Malhotra, H.L. (1984), Spalling of concrete in fires, *Technical Note No.118*, Construction Industrial Research and Information Association (CIRIA), London, UK.

McMenamin, A. (1999), The Performance of Slender Precast Reinforced Cantilever Walls with Roof Level Lateral Displacement Restraint under Simulated In-plane Seismic Loading, Civil Engineering Research Report 99/4, Department of Civil Engineering, University of Canterbury, Christchurch, New Zealand.

Munukutla, R. (1989), Modelling Fire Performance of Concrete alls, Research Report No.89/5, Department of Civil Engineering, University of Canterbury, Christchurch, New Zealand.

Newman, G.M. (1990), Fire and steel construction: The Behaviour of Steel Portal Frames in Boundary Conditions, Second Edition, The Steel Construction Institute, UK.

Nwosu, D. and Kodur, V.K.R. (1998), Behaviour of steel frames under fire conditions, *Canadian Journal of Civil Engineering*, 26, 156-167

O'Meagher, A.J. and Bennetts, I.D. (1987), Behaviour of concrete walls in fire. Proceedings of First National Structural Engineering Conference, pp 438-445, Melbourne, Australia.

O'Meagher, A.J. (1994), Behaviour of concrete walls, industrial buildings and composite columns in fire. PhD thesis, University of Melbourne, Australia.

O'Meagher, A.J. and Bennetts, I.D. (1991), Modelling of concrete walls in fire. *Fire Safety Journal*, Vol. 17, pp 315 – 335,

O'Meagher, A.J., Bennetts, I.D., Dayawansa, P.H., and Thomas, I.R and BHP Research Melbourne Laboratories (1992), Design of Single Storey Industrial Buildings for Fire Resistance, *Journal of Australian Institute of Steel Construction*, Vol. 26, No.2, Australia.

Potter, R.J. (1994), Real Concrete Buildings in Fire, Paper presented at the 'Fire and Concrete: Understanding the Behaviour of Concrete Buildings in Fire' Seminar, 18p., 28 April, Sydney, Australia,

Reick, M. (2001), Brandverhalten von Befestigungen mit großem Randabstand in Beton bei zentrischer Zugbeanspruchung (In German), PhD Thesis, University of Stuttgart, Germany.

Restrepo, J.I., Chrisafulli, F.J. and Park, R. (1996), Seismic Design Aspects for Tilt-up Buildings, *SESOC Journal: Journal of the New Zealand Structural Engineering Society*, Volume 9, No.2, December, New Zealand.

Standards New Zealand (2005a), Concrete Structures Standard: Post Public Comment Draft 1a, Draft Number: DZ 3101.1 PPPC1a, Wellington, New Zealand.

Standards New Zealand (2005b), Concrete Structures Commentary: Post Public Comment Draft 1a, Draft Number: DZ 3101.2 PPPC1a, Wellington, New Zealand.

Vassart, O., Cajot, L.G., O'Connor, M., Shenkai, Y., Fraud, C., Zhao, B., De la Quintana, J., Martinez de Aragon, J., Franssen, J.M. and Gens, F. (2004), 3D simulation of Industrial Hall in case of fire. Benchmark between ABAQUS, ANSYS and SAFIR. Interflam 2004, Proceedings of the tenth international conference, Vol. 2, Interscience Communications Limited., London, UK.

Welsh, R. (2001), 2-D Analysis of Composite Steel-Concrete Beams in Fire, Department of Civil Engineering, University of Canterbury, Christchurch, New Zealand.

Wickström, U. (1979), TASEF-2, a computer program for temperature analysis of structures exposed to fire. Report No.79-2, 1979, Lund Institute of Technology, Sweden.

Wickström, U. (1986), A very simple method for estimating temperatures in fire exposed structures, pp 186-194, New Technology to Reduce Fire Losses and Costs, Elsevier Applied Science, London.

Wong, S.Y. (2001), The Structural Response of Industrial Portal Frame Structures in Fire, PhD Thesis, University of Sheffield, UK.

Wong, S.Y., Burgess, I.W. and Plank, R.J. (2000), Simplified Estimation of Critical Temperatures of Portal Frames in Fire, Paper 09.03, Proc. International Conference on Steel Structures of the 2000s, Istanbul.

Woolcock, S.T., Kitipornchai, S. and Bradford, M.A. (1993), Limit State Design of Portal Frame Buildings, Australian Institute of Steel Construction, Second Edition, Sydney, Australia.

APPENDIX

Appendix A Bending Moment Diagrams

BMD for Load Case No.1

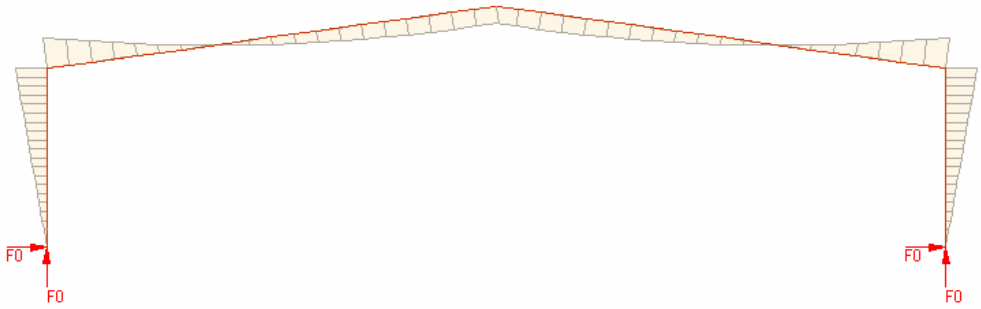

BMD for Load Case No.2*

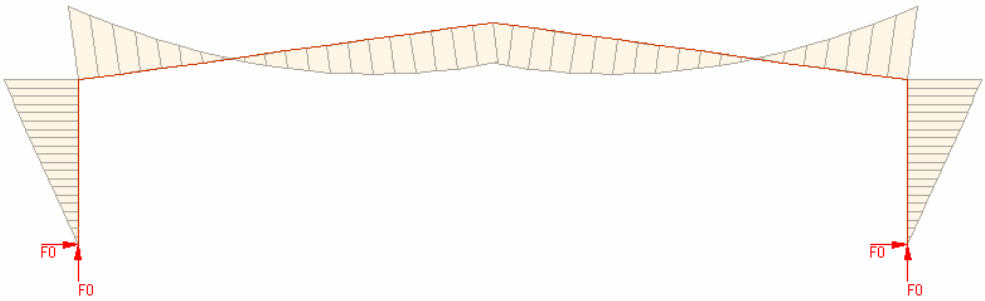

BMD for Load Case No.3 with W_u1

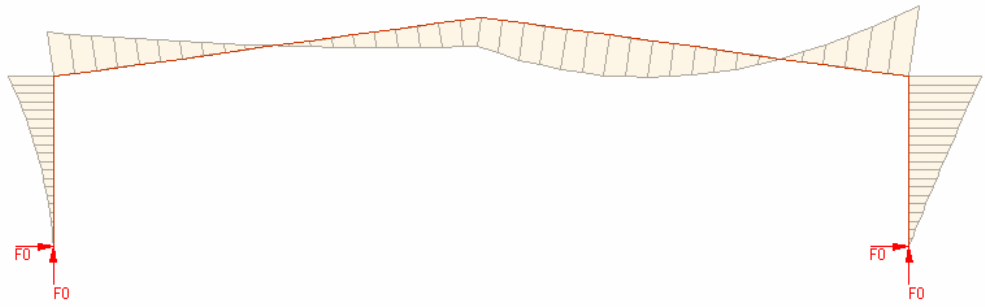

BMD for Load Case No.3 with W_u2

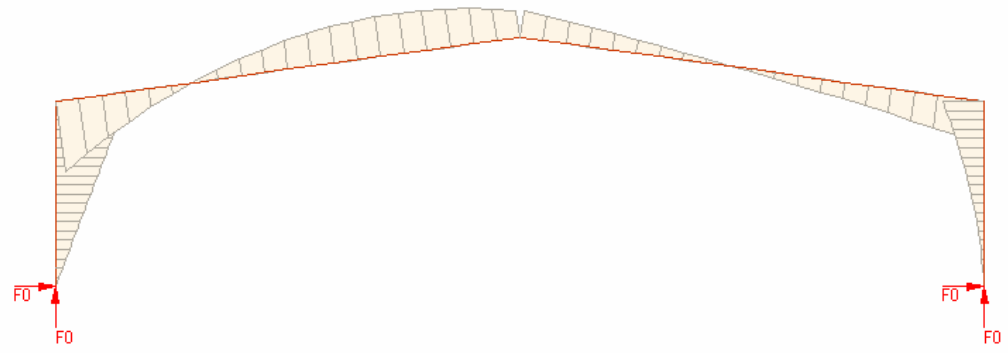

BMD for Load Case No.3 with W_u3

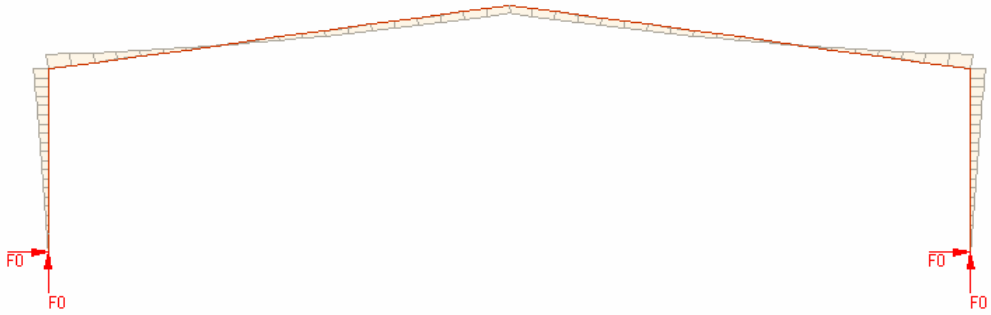

BMD for Load Case No.3 with W_u4

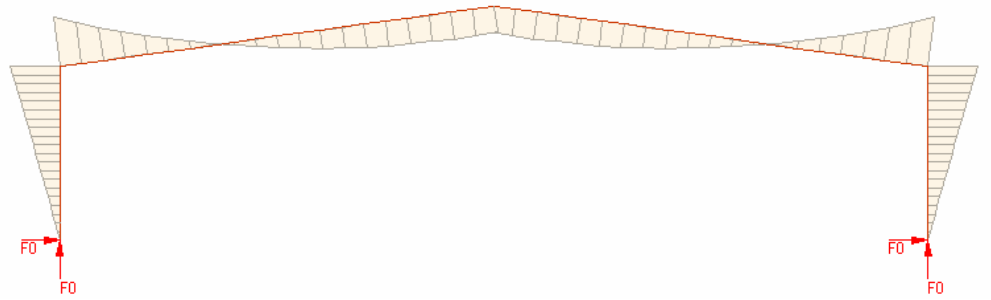

BMD for Load Case No.3 with W_u5

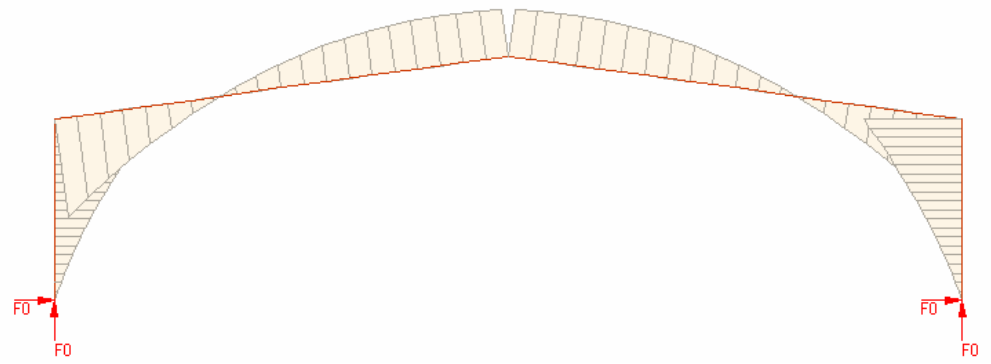

BMD for Load Case No.3 with W_u6

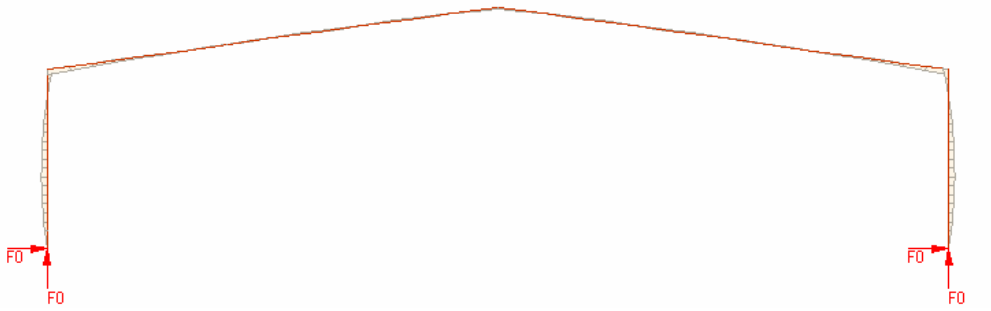

BMD for Load Case No.4 with W_u1

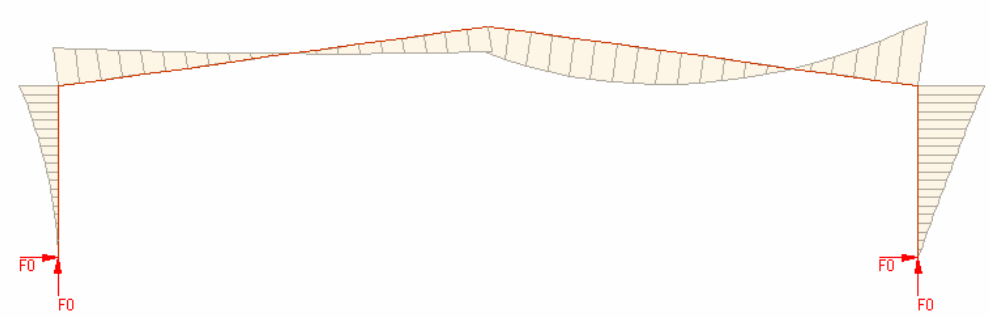

BMD for Load Case No.4 with W_u2

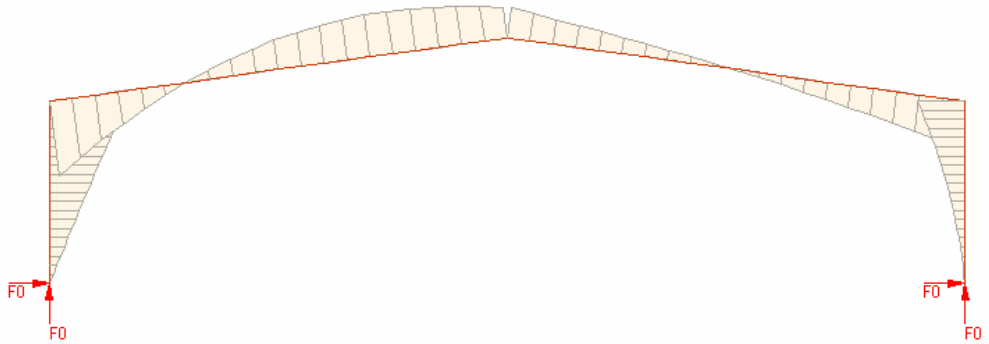

BMD for Load Case No.4 with W_u3

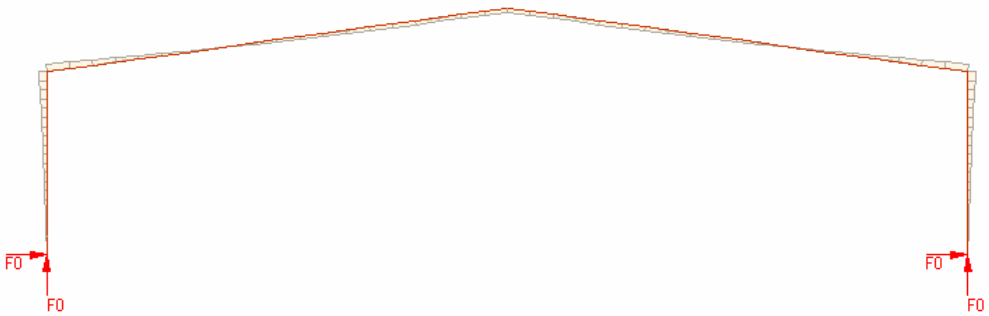

BMD for Load Case No.4 with W_u4

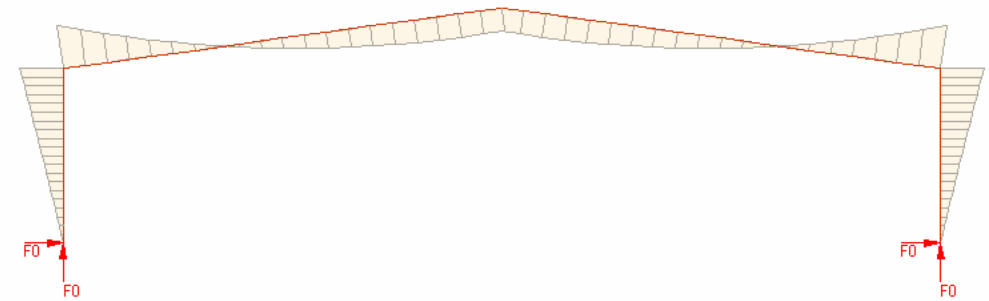

BMD for Load Case No.4 with W_u5**

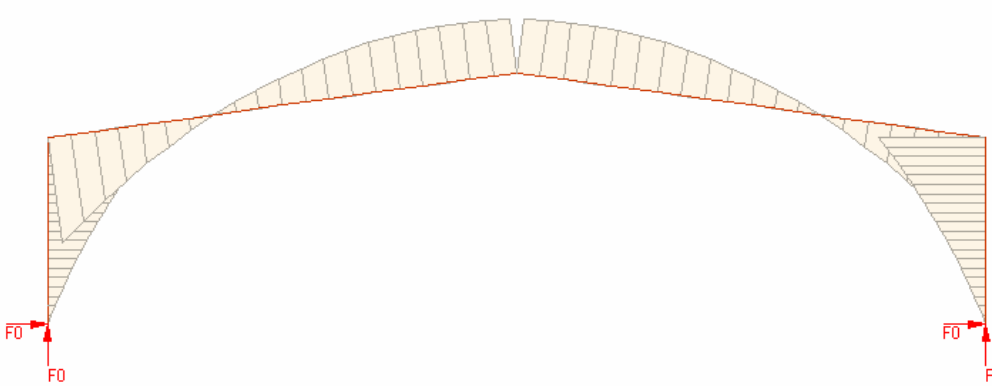

BMD for Load Case No.4 with W_u6

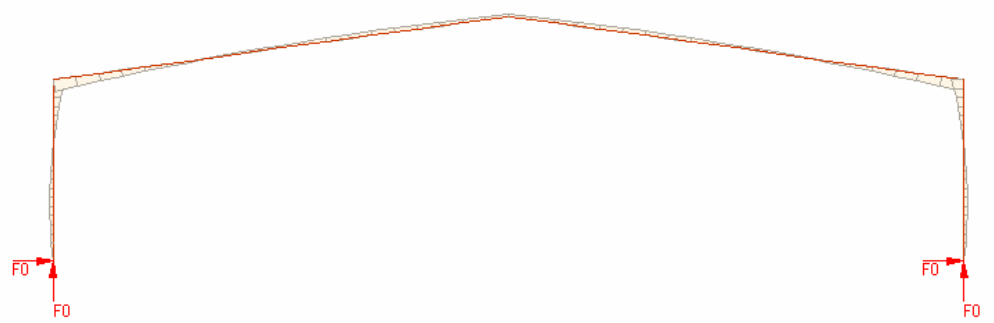

BMD for Load Case No.5

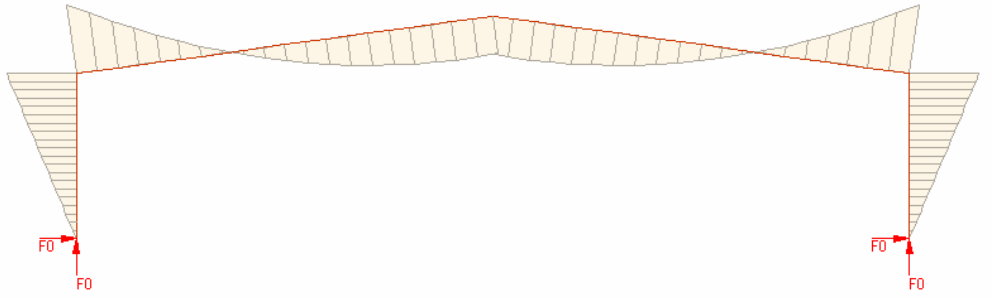

Appendix B Axial Force Diagrams

Axial Force Diagram for Load Case No.1

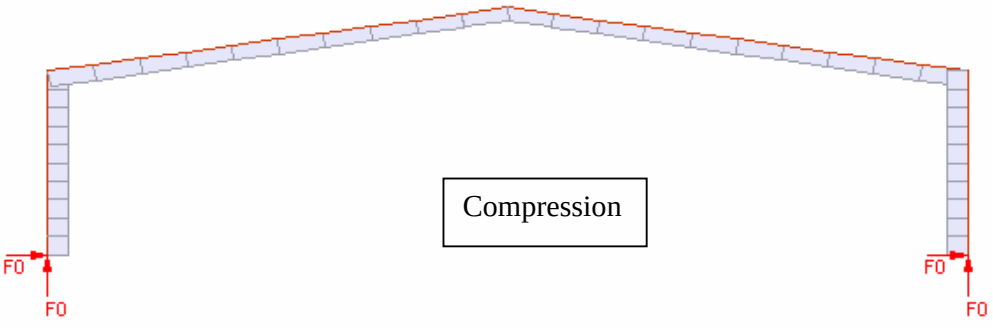

Axial Force Diagram for Load Case No.2*

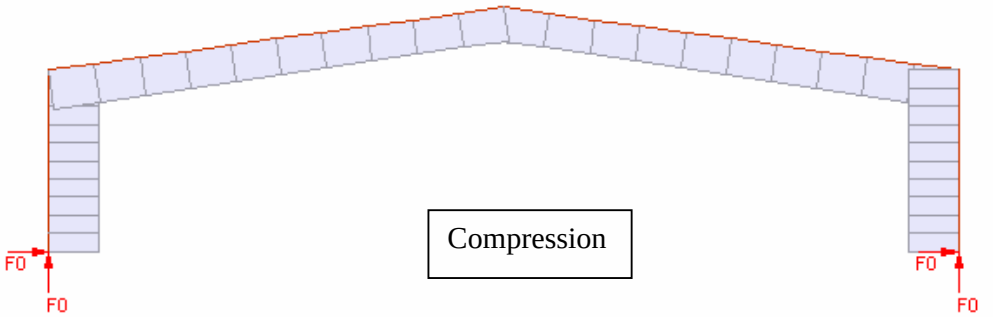

Axial Force Diagram for Load Case No.3 with W_u1

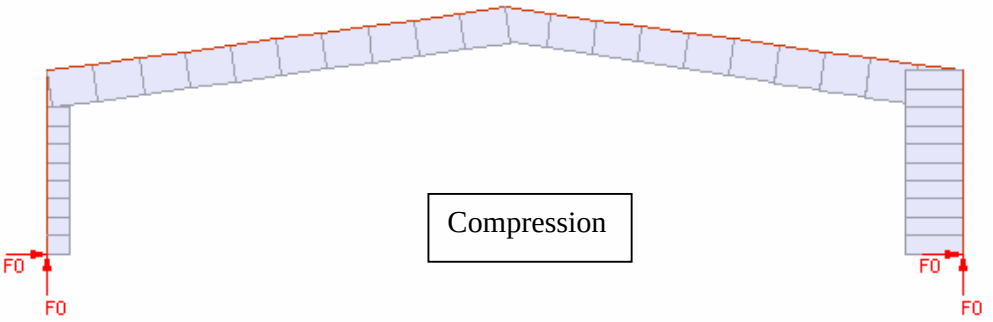

Axial Force Diagram for Load Case No.3 with W_u2

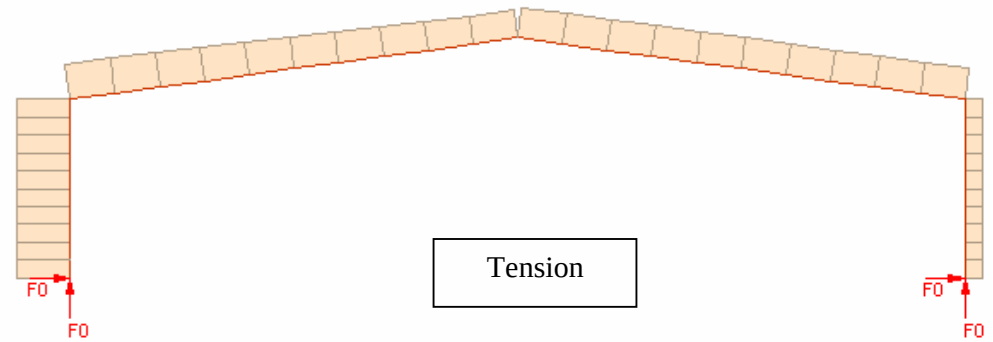

Axial Force Diagram for Load Case No.3 with W_u3

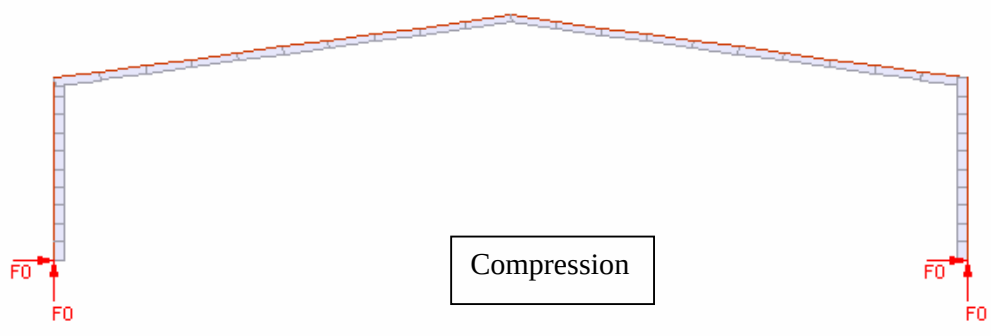

Axial Force Diagram for Load Case No.3 with W_u4

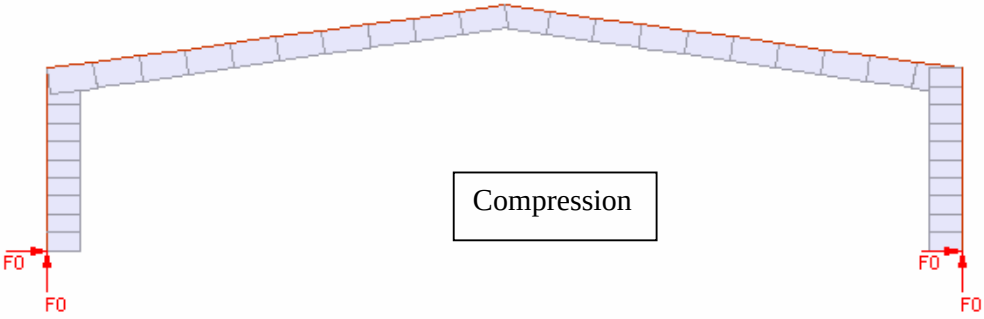

Axial Force Diagram for Load Case No.3 with W_u5

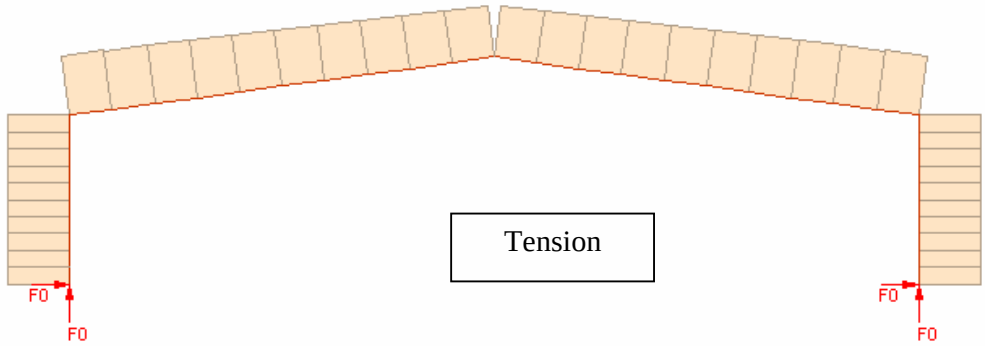

Axial Force Diagram for Load Case No.3 with W_u6

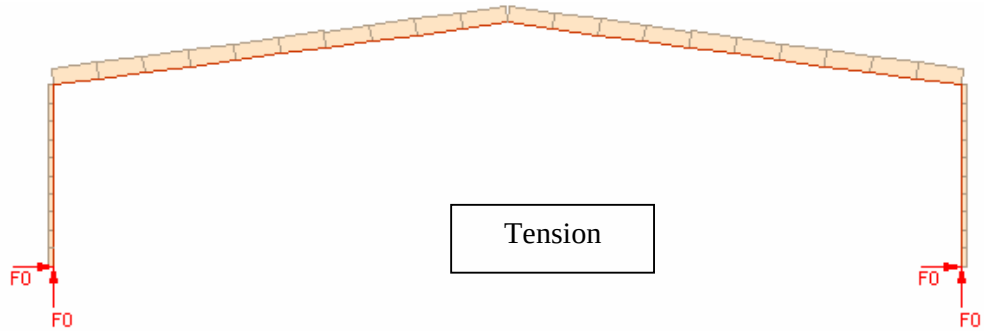

Axial Force Diagram for Load Case No.4 with W_u1

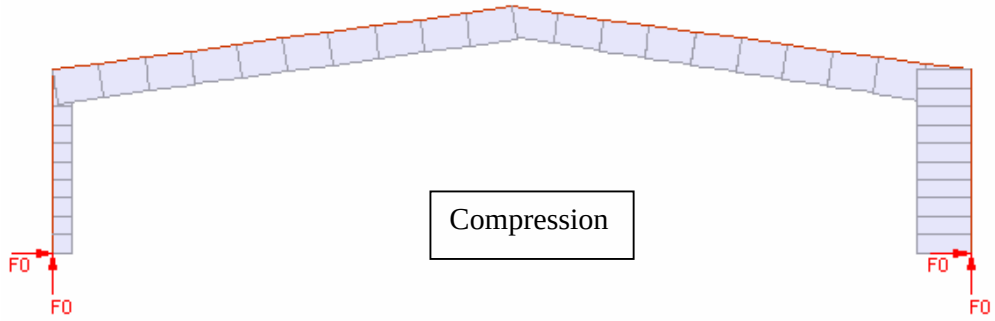

Axial Force Diagram for Load Case No.4 with W_u2

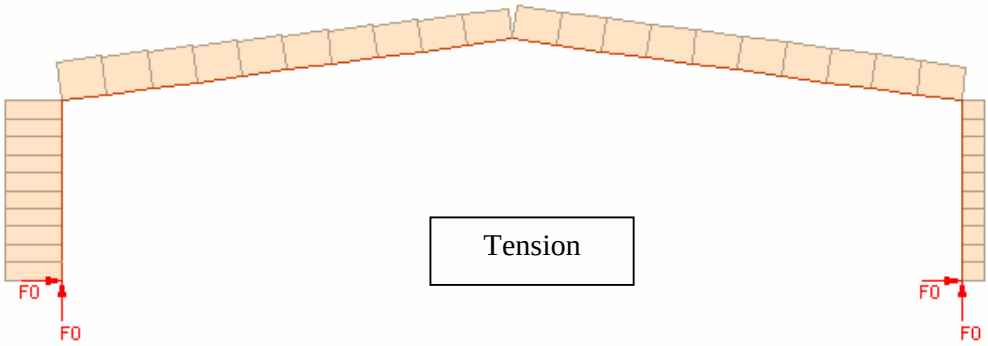

Axial Force Diagram for Load Case No.4 with W_u3

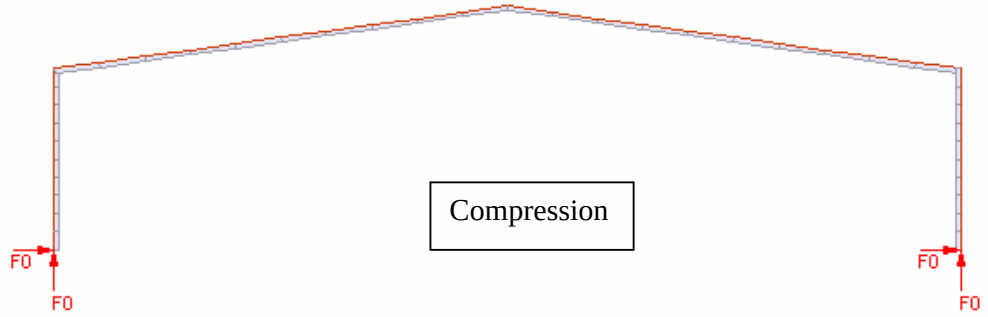

Axial Force Diagram for Load Case No.4 with W_u4

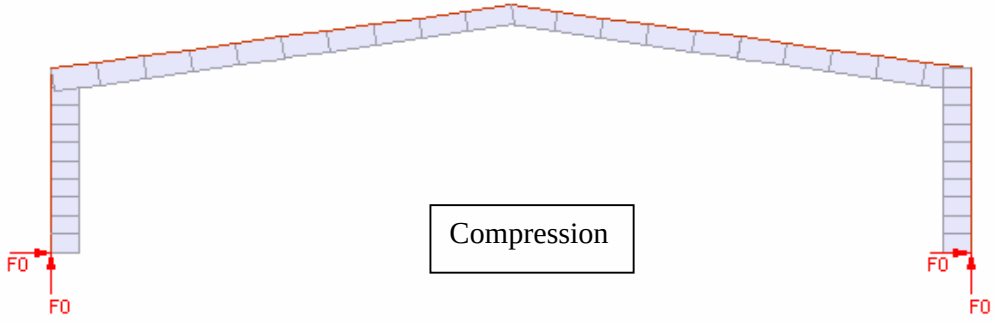

Axial Force Diagram for Load Case No.4 with W_u5

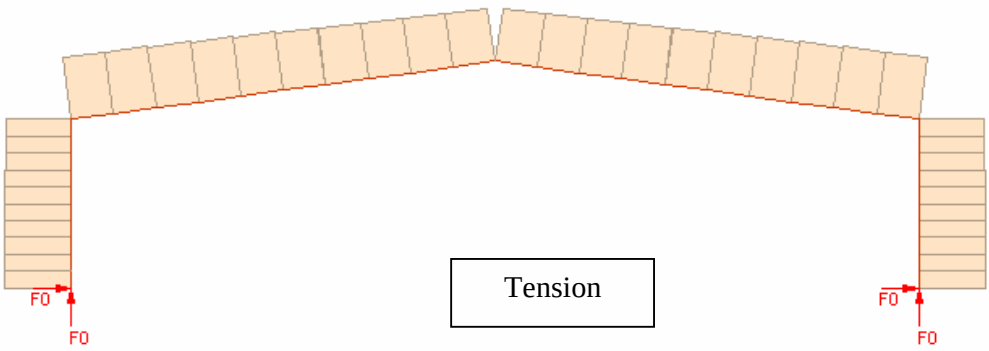

Axial Force Diagram for Load Case No.4 with W_u6

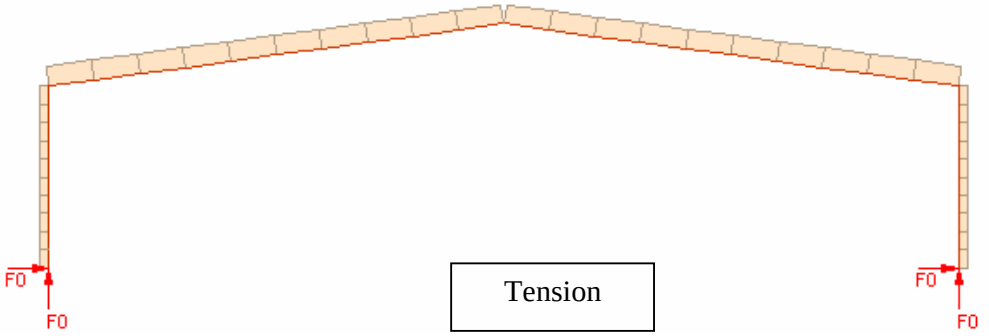

Axial Force Diagram for Load Case No.5

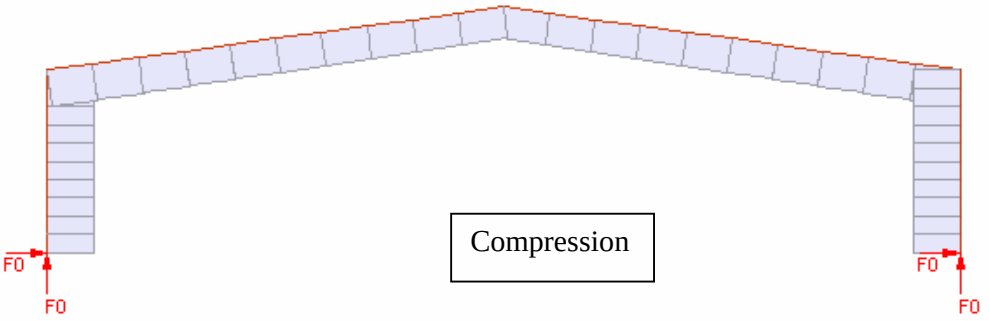

Appendix C Load-displacement curves for Purlin without lateral restraint under cold conditions

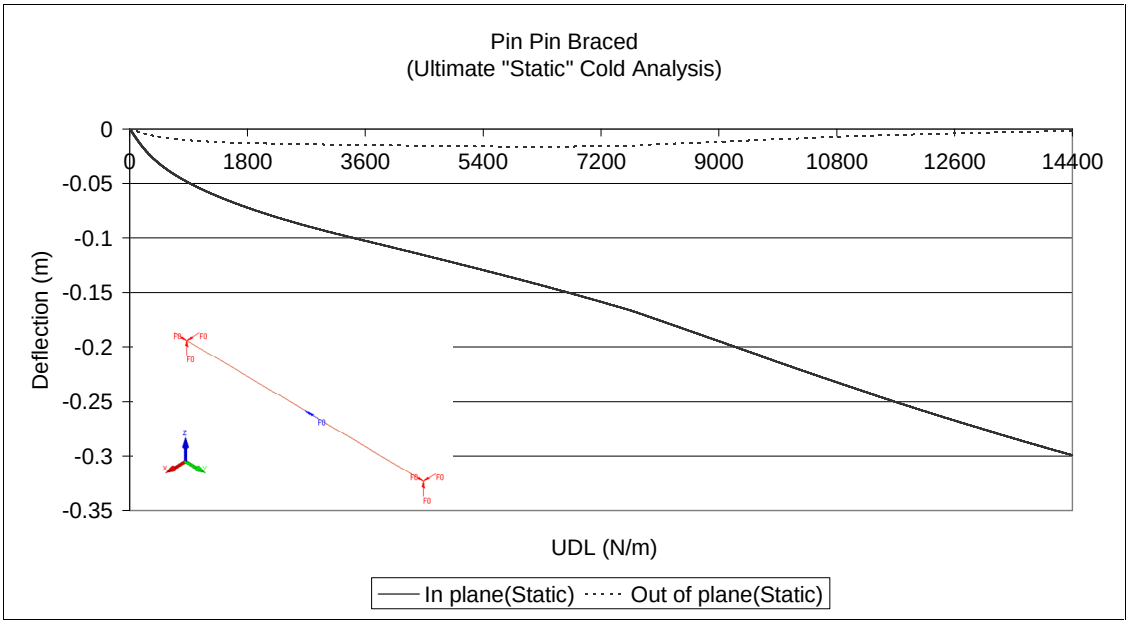

Midspan in-plane and out-of-plane displacements plotted against load for 'Pin Pin Braced' purlin under "static" analysis

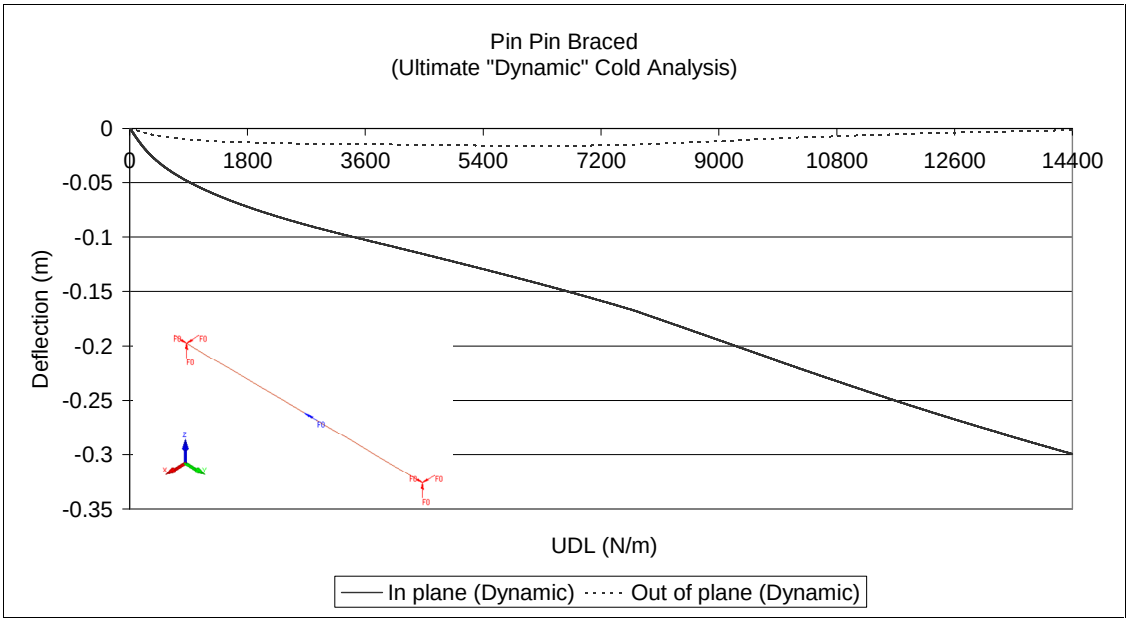

Midspan in-plane and out-of-plane displacements plotted against load for 'Pin Pin Braced' purlin under "dynamic" analysis

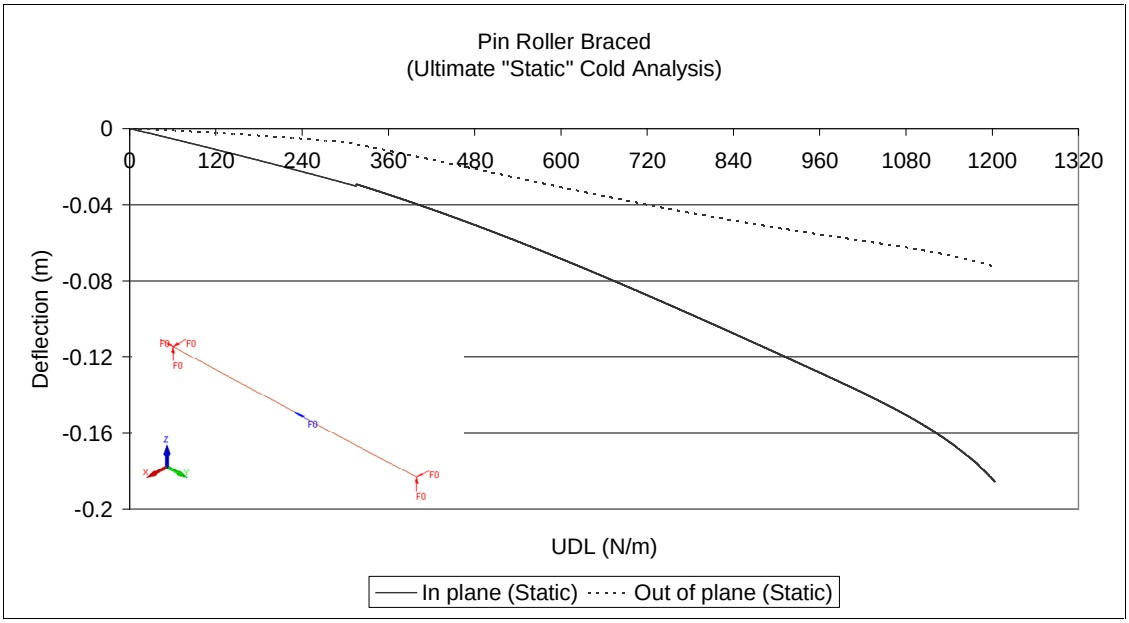

Midspan in-plane and out-of-plane displacements plotted against load for ‘Pin Roller Braced’ purlin under “static” analysis

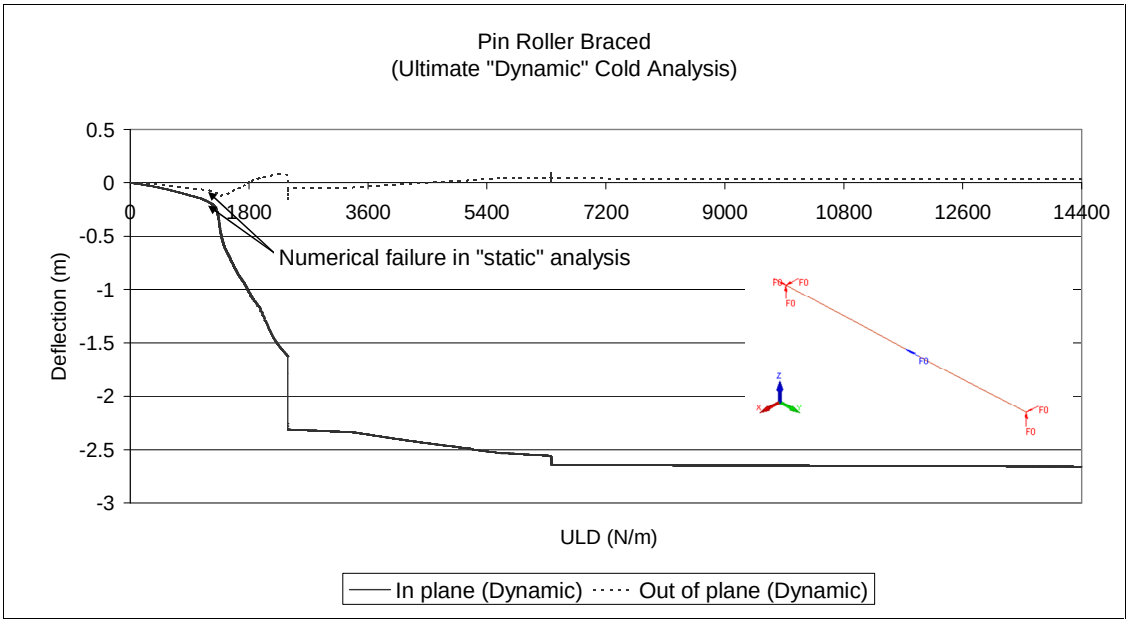

Midspan in-plane and out-of-plane displacements plotted against load for ‘Pin Roller Braced’ purlin under “dynamic” analysis

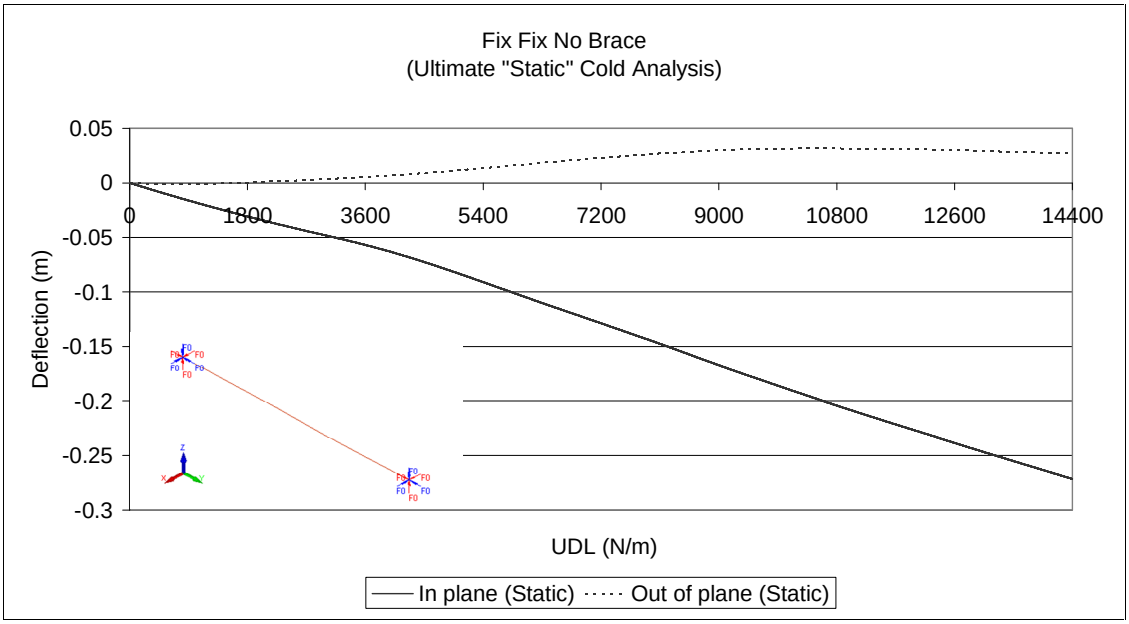

Midspan in-plane and out-of-plane displacements plotted against load for 'Fully Fixed end supports' purlin under "static" analysis

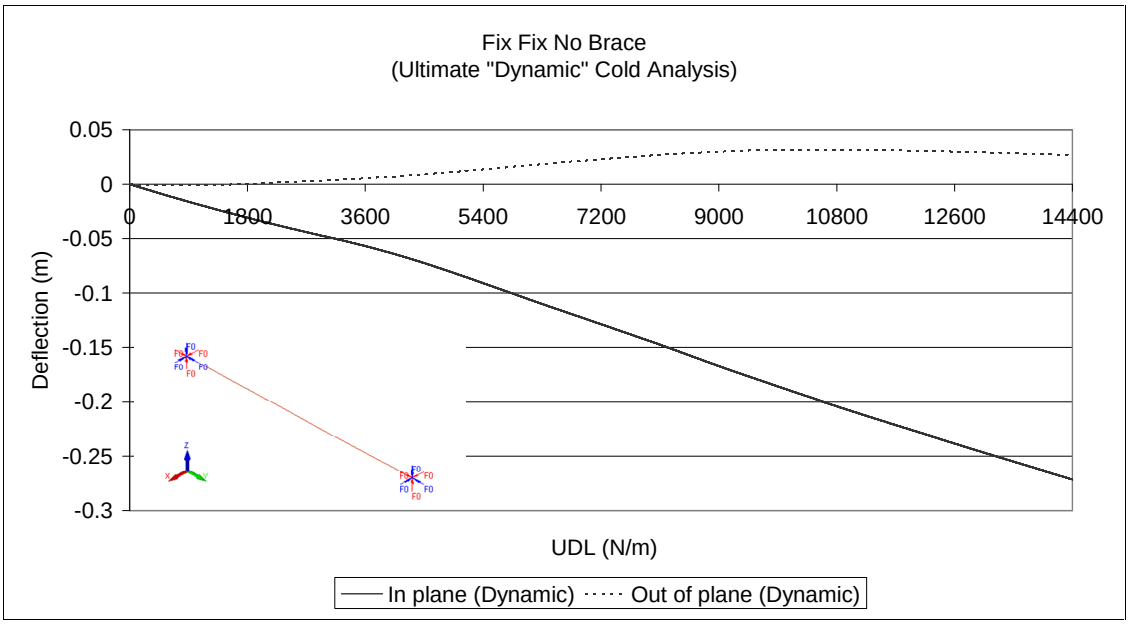

Midspan in-plane and out-of-plane displacements plotted against load for 'Fully Fixed end supports' purlin under "dynamic" analysis

Appendix D Load-displacement curves for Purlin without lateral restraint under hot conditions

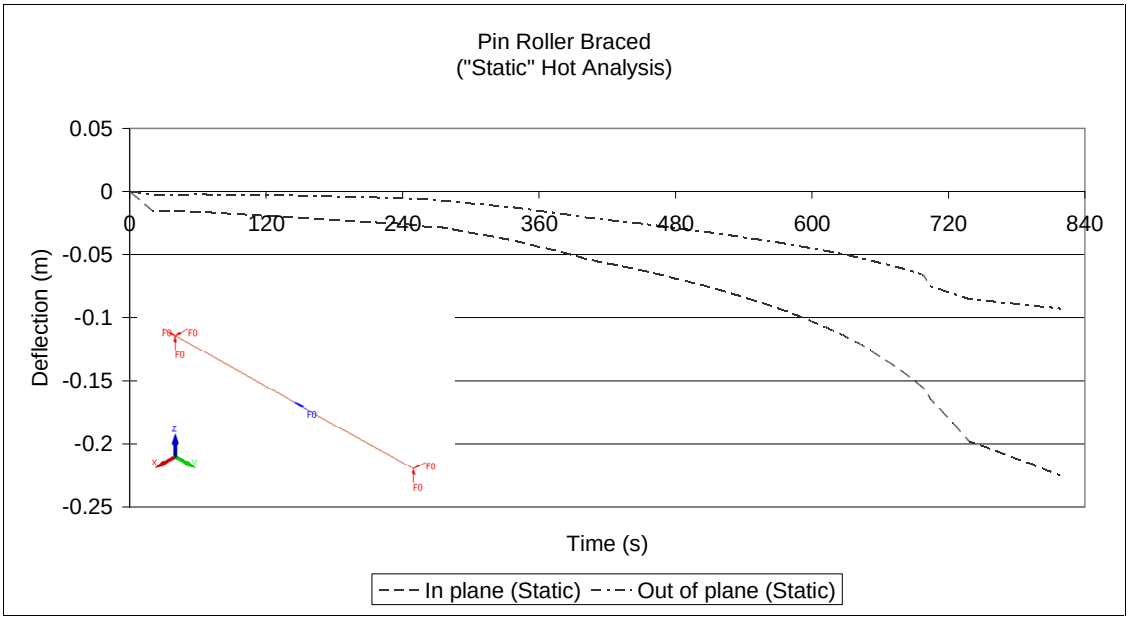

Midspan in-plane and out-of-plane displacements plotted against load for 'Pin Roller Braced' purlin under "static" analysis

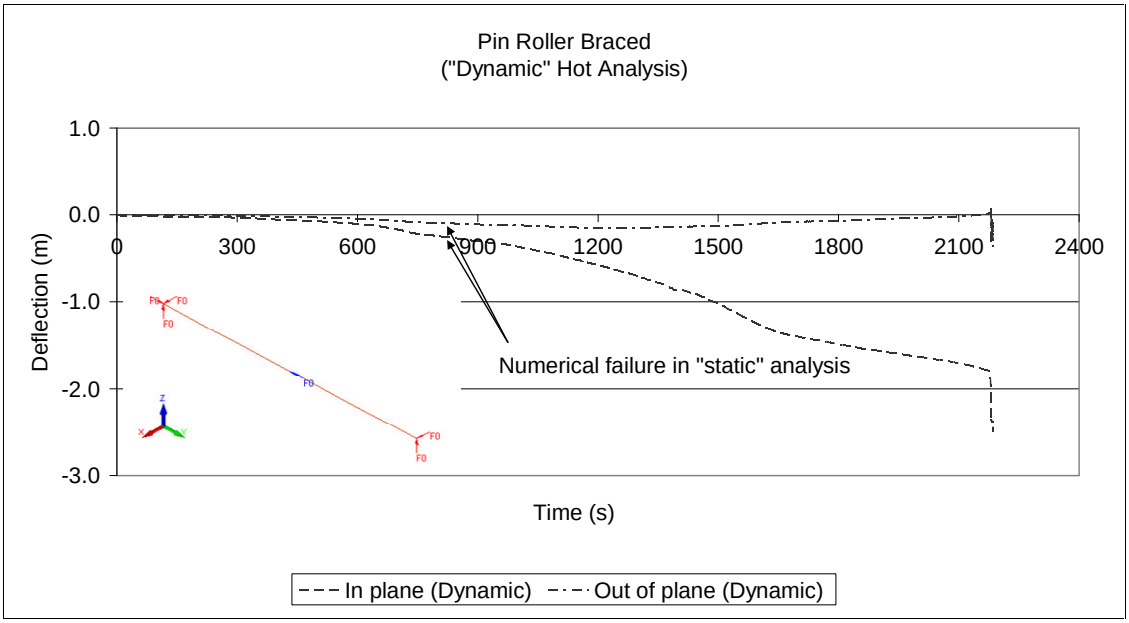

Midspan in-plane and out-of-plane displacements plotted against load for 'Pin Roller Brace' purlin under "dynamic" analysis

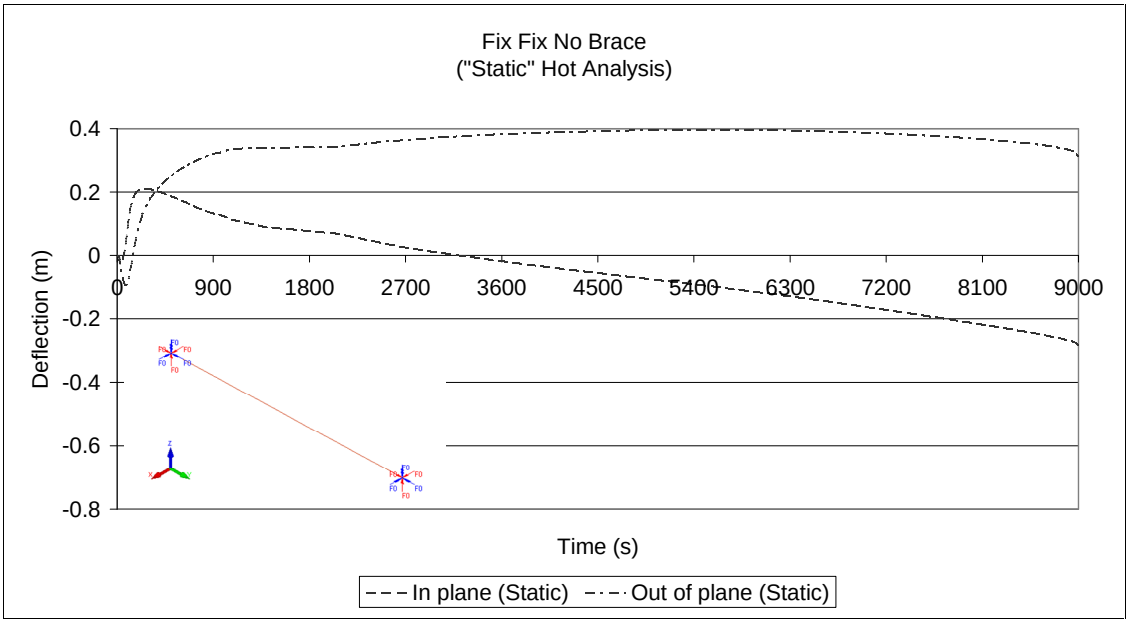

Midspan in-plane and out-of-plane displacements plotted against load for 'Fully Fixed end supports' purlin under "static" analysis

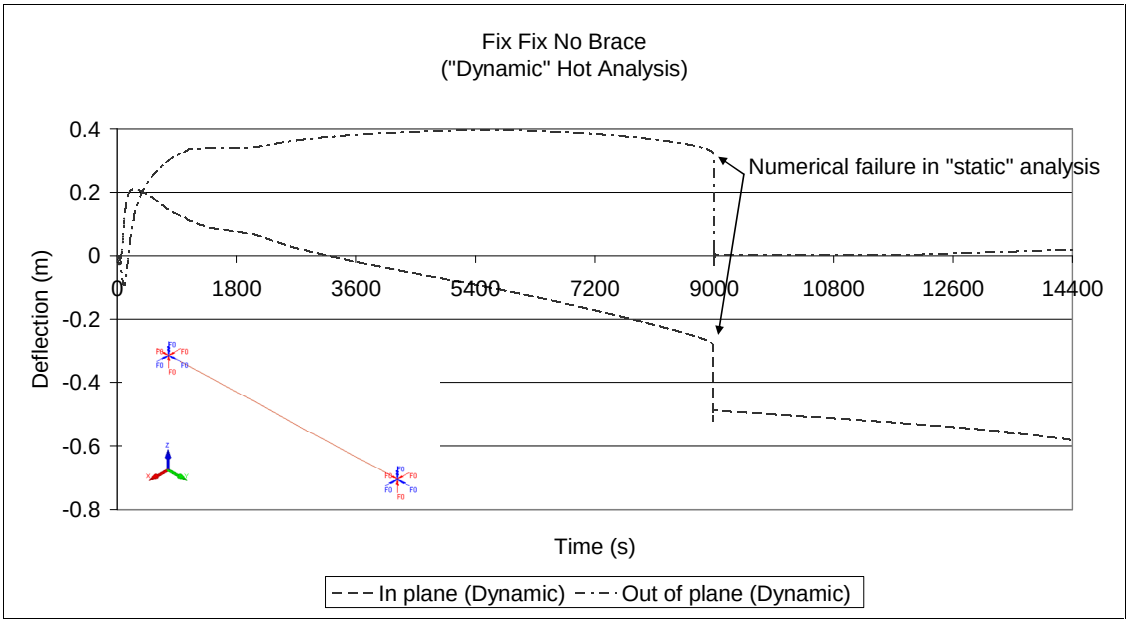

Midspan in-plane and out-of-plane displacements plotted against load for 'Fully Fixed end supports' purlin under "dynamic" analysis